1-1-2002

Synthesis, characterization, and crystallization of model semi-crystalline polymers : influence of hydrogen-bonding.

Robin L. McKiernan
University of Massachusetts Amherst

SYNTHESIS, CHARACTERIZATION, AND CRYSTALLIZATION OF MODEL, SEMI-CRYSTALLINE POLYMERS: INFLUENCE OF HYDROGEN-BONDING

A Dissertation Presented

by

ROBIN L. MCKIERNAN

Submitted to the Graduate School
of the University of Massachusetts Amherst in partial fulfillment
of the requirements for the degree of

DOCTOR OF PHILOSOPHY

September 2002

Polymer Science and Engineering

SYNTHESIS, CHARACTERIZATION, AND CRYSTALLIZATION OF MODEL, SEMI-CRYSTALLINE POLYMERS: INFLUENCE OF HYDROGEN-BONDING

A Dissertation Presented

by

ROBIN L. MCKIERNAN

Approved as to style and content by:

Jacques Penelle, Co-Chair

Samuel P. Gido, Co-Chair

Paul M. Lahti, Member

Thomas J. McCarthy, Department Head
Polymer Science and Engineering

DEDICATION

In memory of my father Samuel David Gittleson.

ACKNOWLEDGMENTS

I would like to thank all of the people (faculty members, departmental staff, and students) in the Polymer Science and Engineering Department who have been like a second family to me during my graduate studies. I am particularly indebted to my co-advisors Dr. Jacques Penelle and Dr. Sam Gido. I am truly grateful to have found not one, but two research advisors who are encouraging, patient, and resourceful. Dr. Penelle has been extremely supportive of both my research and my future. During my first year here, he went as far as to set up a study group to work out chemistry-related questions in preparation for the cumulative exams. Dr. Gido has challenged me and allowed me the opportunity to look at my project and results from a non-chemist perspective. I would also like to thank Dr. Paul Lahti, who as the final member of my committee has offered me valuable advice and thoughts regarding this research project.

This project has had support from numerous researchers, and I would like to acknowledge each of them. Amy Heintz under the supervision of Dr. Shaw Ling Hsu has been instrumental in employing infrared and Raman spectroscopy to examine the crystallization behavior and kinetics of the polymers in this study. Dr. Ted Atkins and his student Pawel Sikorski (University of Bristol) provided valuable help regarding the crystal structure, diffraction pattern, and unit cell determination of hydrogen-bonded polymers. The heteroatom-containing diols used in this study were synthesized by Grégoire Cardoen (Ecole Nationale Supérieure de Chimie de Montpellier) under the supervision of Dr. Bernard Boutevin and Dr. Bruno Améduri, an expert in the synthesis

of telechelic diols. The self-organization of the long-chain α,ω-diols was examined by Dr. David Padowitz (Amherst College).

All of the Penelle and Gido group members, both past and present, have been wonderful to work with and contributed to a productive and helpful work environment. As the predecessors of this project, Cedric and Joel were especially supportive of me when I first began my research and were both great resources for information regarding diol synthesis and polymer characterization. I have also enjoyed useful conversations with the next generation researchers of this project, Gabi and Benoit. I am also thankful for the friendship of my fellow classmates, particularly my fellow study group members (Didem, Cheryl, Dan, and Buddy).

The university and departmental facilities are first rate, and much of that is due to the incredible staff. I am grateful for the training provided by and expertise of Gregory Dabkowski (Microanalysis Laboratory), Charles Dickinson (Nuclear Magnetic Resonance Laboratory), Stephen Eyles (Molecular Weight Characterization Laboratory), Louis Raboin (W. M. Keck Polymer Morphology Laboratory), and Alan Waddon (X-ray Diffraction and Scattering Laboratory). Additionally, I would like to thank Andre Mel'cuk for his assistance in my computer dilemmas. I am also tremendously in debt to the departmental secretarial staff (Eileen, Eleanor, Sophie, and Ann) who help keep this department running, as well as Susan who has single-handedly organized the Gido group.

I would not have gotten this far in life without the never-ending support of my family. I am grateful for the encouragement and love of my mother, sister, husband, and his entire family (grandmother, parents, and sister). I would like to dedicate this work to my father, Samuel Gittleson, who passed away two years ago. His pride in my

accomplishments and support of my continuing education were instrumental in the pursuit of my Ph.D.

ABSTRACT

SYNTHESIS, CHARACTERIZATION, AND CRYSTALLIZATION

OF MODEL, SEMI-CRYSTALLINE POLYMERS:

INFLUENCE OF HYDROGEN-BONDING

SEPTEMBER 2002

ROBIN L. MCKIERNAN, B.S., COLLEGE OF WILLIAM & MARY

Ph.D., UNIVERSITY OF MASSACHUSETTS AMHERST

Directed by: Professors Jacques Penelle and Samuel P. Gido

In order to better understand structure-property relationships, semi-crystalline polymers were synthesized, and the influence of hydrogen-bonds, heteroatoms, and uniformed lamellar thickness were examined. Literature procedures were modified, optimized, and then used to synthesize long-chain α,ω-diols containing up to 46 consecutive methylene groups. Melt polyadditions of these diols with short, aliphatic α,ω-diisocyanates produced a series of polyethylene-like polyurethanes whose hydrogen-bonding densities were systematically decreased. The hydrogen-bonds (or perturbations) were located at regular and controlled distances. These model, polyethylene-like polymers were characterized in order to determine the influence of the perturbations to the aliphatic backbone on the physical, thermal, and morphological properties of these polymers. The increasingly long-chain polyurethanes displayed physical and thermal characteristics (including melting point, lamellar stacking periodicity, and solubility) typical of polyethylene despite the presence of hydrogen-bonding. Crystallization studies showed that, although diluted, hydrogen-bonding still controlled the crystallization

process of these polyethylene-like polymers. This resulted in analogous crystal structures and morphologies as polyamides and polyurethanes containing higher hydrogen-bonding densities. The effect of further perturbations, caused by heteroatoms on the aliphatic backbone, where also investigated with an emphasis on the resulting thermal properties of the polymers. The heteroatoms (oxygen and sulfur) caused a decrease in the melting temperature of the polymers without affecting the decomposition temperature or crystal structure. Ongoing research focuses on chemically controlling the lamellar thickness in order to engineer polyethylene-like crystals with hydrogen-bonding sites on the surface.

TABLE OF CONTENTS

LIST OF TABLES

LIST OF FIGURES

LIST OF SCHEMES

LIST OF ABBREVIATIONS, ACRONYMS, AND SYMBOLS

α ..... unit cell angle of *bc* plane

a ..... unit cell length

A ..... ampere

Å ..... angstrom

ADMET ..... acyclic diene metathesis

Anal. Calc. ..... calculated analysis

aq ..... aqueous

Ar ..... argon

atm ..... atmosphere

AU ..... arbitrary unit

β ..... unit cell angle of *ac* plane

b ..... broad (spectra)

b ..... unit cell length

b.p ..... boiling point

c ..... centi (10^{-2})

c ..... speed of light

c ..... unit cell length

C ..... C-face centered

°C ..... degree Celsius

C_6D_6 ..... deuterated benzene

$CDCl_3$ ..... deuterated chloroform

CD_3OD ..... deuterated methanol

δ ..... NMR chemical shift in parts per million downfield from tetramethylsilane

Δ ..... change

Δ ..... heat

ΔT ..... undercooling

d ..... day

d ..... deuteron (NMR solvent)

d ..... doublet (spectra)

d ..... spacing (X-ray)

D ..... degradation

DBO ..... 1,4-dizabicyclo[2.2.2]octane

DBTDL ..... dibutyltin dilaurate

DMF ..... *N,N*-dimethylformamide

$DMSO\text{-}d_6$ ..... deuterated dimethylsulfoxide

dn/dc ..... refractive index increment

DPPA ..... diphenyl phosphoryl azide

DSC ..... differential scanning calorimeter

E ..... elastic modulus

e.g. ..... for example

Eq ..... equation

et al ..... and others

FT ..... Fourier transform

FTS ..... Fourier transform spectroscopy

γ ..... unit cell angle of *ab* plane

g ..... gram

G ..... Gibbs free energy

GPC ..... gel permeation chromatography

h ..... hour

h ..... crystallographic index (*hkl*)

H ..... enthalpy

HDPE ..... high-density polyethylene

H_f ..... enthalpy of fusion

HPLC ..... high-pressure liquid chromatography

Hz ..... hertz

I ..... insolubility

i.e ..... that is

IR ..... infrared

J ..... joule

J ..... coupling constant (NMR)

k ..... kilo (10^3)

k ..... crystallographic index (*hkl*)

K ..... kelvin

Kα ..... spectral line

K_{eg} ..... equilibrium constant

l ..... crystal thickness

l ..... crystallographic index (*hkl*)

L ..... liter

LAM ..... longitudinal acoustic (or accordion) mode

LCB ..... long-chain branch

LDPE ..... low-density polyethylene

lit ..... literature

LLDPE ..... linear, low-density polyethylene

LSP ..... lamellar stacking periodicity

μ ..... micro (10^{-6})

m ..... medium (spectra)

m ..... meter

m ..... mode order

m ..... milli (10^{-3})

m ..... multiplet (spectra)

m ..... meta

M ..... mega (10^{6})

MAXS ..... medium-angle X-ray scattering

MCT ..... mercury cadmium telluride

MD ..... molecular dynamic

min ..... minute

mol ..... mole

m.p ..... melting point

M_w ..... weight-average molecular weight

ν ..... frequency

n.....nano (10^{-9})

n.....normal

N_2.....nitrogen

NMR.....nuclear magnetic resonance

o.....ortho

%.....percent

p.....pico (10^{-12})

p.....progressive shearing

p.....para

p-TSOH.....*p*-toluenesulfonic acid

P.....primitive

PDI.....polydispersity index

pH.....negative logarithm of hydrogen ion concentration

PL.....Polymer Laboratory

ppm.....parts per million

q.....quartet (spectra)

q.....scattering vector

ρ.....density

R.....gas constant

RI.....refractive index

RT.....room temperature

σ_e.....fold surface free energy

s.....second

s ..... singlet (spectra)

s ..... strong (spectra)

S ..... entropy

SAM ..... self-assembled monolayer

SAXS ..... small-angle X-ray scattering

SCB ..... short-chain branch

S_N2 ..... second-order nucleophilic substitution

STM ..... scanning tunneling microscope

t ..... triplet (spectra)

t ..... tertiary

T ..... thermodynamic temperature

TA ..... Thermal Analysis

T_c ..... crystallization temperature

T_d ..... decomposition temperature

TEM ..... transmission electron microscope

T_g ..... glass transition temperature

TGA ..... thermogravimetric analysis

THF ..... tetrahydrofuran

THP ..... tetrahydropyran

T_m ..... melting temperature

T_t ..... transition temperature

UV-vis ..... ultraviolet-visible

V ..... volt

vs ..... very strong (spectra)

W .....watt

WAXS.....wide-angle X-ray scattering

w/v.....weight per volume

))).....sonication

CHAPTER 1. INTRODUCTION AND BACKGROUND

1.1 Overview

Understanding structure-property relationships is a fundamental issue in the design of polymers for commercial purposes. Since the majority (by volume) of commercialized polymers are semi-crystalline (e.g. polyethylene, polypropylene, poly(vinyl chloride), poly(vinyl alcohol), polytetrafluoroethylene, polyesters, polyamides, and polyurethanes), a detailed knowledge of the crystallization behavior of semi-crystalline polymers is of vital importance. There has been extensive research into comprehending the crystallization process through both experimentation and theoretical models, and the results have been thoroughly reviewed in the literature.[1-6] However, to date, there still exists differences in the scientific community[7-9] concerning the specific details of these models.

Progress in the understanding of polymer crystallization is hampered by the fact that existing systems have already been extensively studied. In order to further the knowledge in this field and to support existing theories with experimental results, new polymers with well-defined architectures are desired. This research project hopes to contribute to the debate through the synthesis and examination of some novel, semi-crystalline polymers based on a polyethylene-like backbone with perturbations or "defects" located at controlled and regular distances. Investigation of these polymers will allow for an understanding between the influence of the chemical nature (including type, position, and amount) and the resulting crystallization behavior and structure (in addition to the physical and thermal properties).

1.2 Crystallization of Semi-Crystalline Polymers

1.2.1 Overview

The description of the structure of a semi-crystalline homopolymer can include the chemical repeat, molecular architecture (e.g. presence of branches), and stereochemistry (e.g. tacticity). These structural variables along with the crystallization conditions (e.g. cooling rate, melting temperature, pressure, presence of orientation, and additives) influence the percent crystallinity, size of the crystals, and crystal packing of the resulting polymer, as well as whether the polymer will crystallize at all. The structural and physical variables influence the crystallization of polymers because the polymers are kinetically trapped, and therefore the crystallization process is not under thermodynamic control (minimization of the Gibbs free energy, see Section 1.2.3). The resulting crystalline properties in turn influence the physical, thermal, and mechanical properties (e.g. transparency, solvent resistance, melting temperature, flexibility, and strength) of the polymer.

1.2.2 Microstructure at Different Length Scales

On the atomic scale, the individual atoms of a polymer crystal are held together by covalent bonds, which form helical stems that in order to maximize intermolecular forces (e.g. van der Waals forces) pack laterally (Figure 4.1) in the chain direction forming a 3-dimensional array. The tacticity and branching of the polymer as well as the secondary forces between chain segments all influence the way the polymer packs.

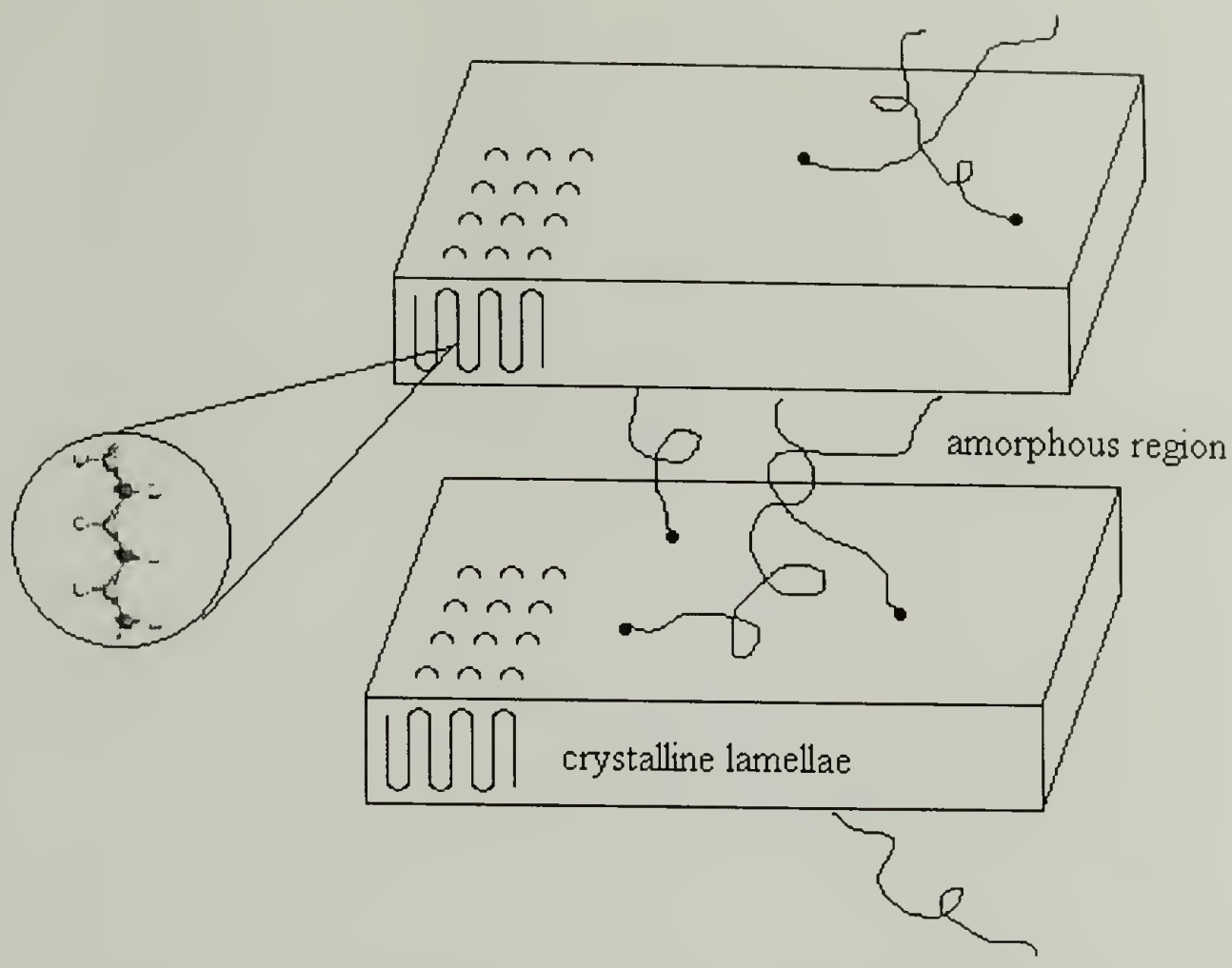

Figure 1.1. Packing of Chains to Form Polymer Crystals.

The repetitive unit of the regular array of atoms in the polymer crystal is defined as the unit cell. The unit cell (Figure 1.2) has a size and shape defined by the 3 lengths *a*, *b*, and *c* (in polymer science, *c* is defined by the chain axis) and the 3 angles (usually ≥ 90°, exceptions include polyamides) α, β, and γ. Space groups (e.g. P*nam* and C*m2m*) describe the 3-dimensional arrangement and symmetry (e.g. P = primitive and C = C-face centered) of the unit cell. The unit cell in turn describes the type of crystal lattice (Figure 1.3). The orientation of planes in the crystal lattice is represented by the Miller indices (*hkl*), which index the planes by the fractional intercept the plane makes with the crystallographic axes. The number of polymer chains per unit cell and the unit cell dimensions determine the density of the resulting crystal.

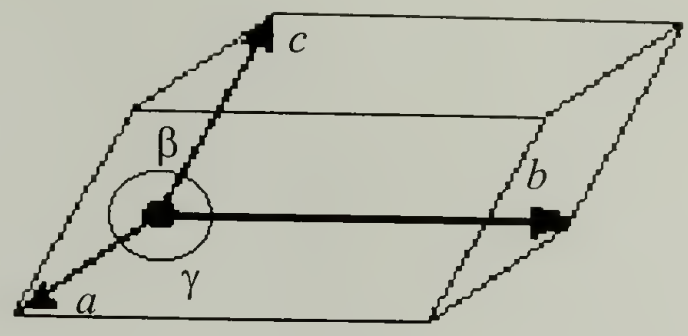

Figure 1.2. Unit Cell with Dimensions *a*, *b*, and *c* and Angles α, β, and γ.

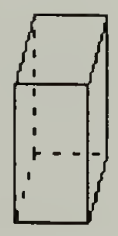

Tetragonal:
$a = b \neq c$
$\alpha = \beta = \gamma = 90°$

Orthorhombic:
$a \neq b \neq c$
$\alpha = \beta = \gamma = 90°$

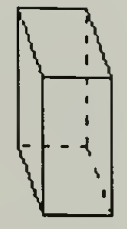

Hexagonal:
$a = b \neq c$
$\alpha = \beta = 90°, \gamma = 120°$

Monoclinic:
$a \neq b \neq c$
$\alpha = \beta = 90°, \gamma > 120°$

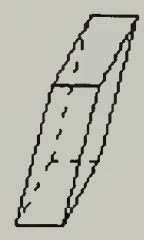

Triclinic:
$a \neq b \neq c$
$\alpha \neq \beta \neq \gamma \neq 90°$

Figure 1.3. Most Common Crystal Lattices Found for Polymer Crystals.

At the next hierarchical level, the polymer chains fold to form crystalline lamellae separated by amorphous regions (Figure 1.1). Proof that the polymer chains are folded came from observing single polymer crystals grown from dilute solution.[10,11] Using electron microscopy, thin, plate-like lamellae were observed. By applying shadowing

techniques, it was determined that the crystal sheets were ~ 100 Å thick. Since the polymer chains were more than an order of magnitude longer, it was concluded that the polymer chains must be folded back and forth to form the lamellae. Diffraction patterns revealed that the polymer chains were aligned more or less perpendicularly to the crystal surface.[12] Keller suggested that the chain-folds were regular with the polymer chains forming hairpin turns at the crystal surface and then re-entering the crystal at an adjacent position (Figure 1.4).[11] This theory of adjacent re-entry is supported by the work of Wittmann et al.[13] and Patil et al.[14] on dilute solution crystallization.

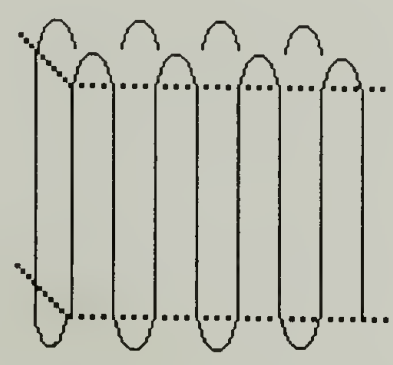

Figure 1.4. Regular Re-Entry Chain-Folding Model.

When either the concentration of the polymer in solution is increased or the polymer is crystallized from the melt, the polymer chains are no longer isolated from each other, and they entangle. A switchboard model of chain-folding was proposed for these polymers. In this model, the polymer chains can form variously sized loops that re-enter the same crystal. Additionally, some of the polymer chains do not re-enter the same crystal, but either reside in the amorphous region or enter another crystal (Figure 1.5).[15] The exact nature of the chain-folds depends on the solvent, concentration, temperature, cooling rate, molecular weight, chain flexibility, and defects (such as branches).

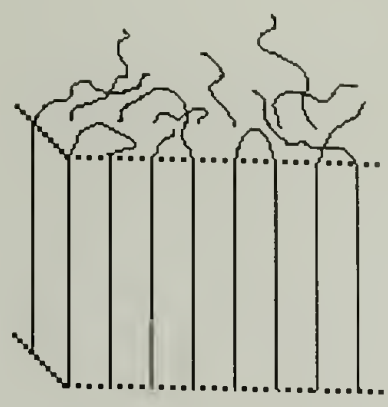

Figure 1.5. Switchboard Chain-Folding Model.

Crystallization from the melt often results in the aggregation of crystals (e.g. to form spherulites). Spherulites (Figure 1.6) start from a center (nucleus) with the polymer molecules aligned tangentially, and then the lamellae grow radially outwards until the spherulite impinges on an adjacent spherulite. During their growth, the lamellae can branch, twist, and splay. The resulting spherulites have dimensions on the order of several micrometers, and therefore can be viewed using an optical microscope under crossed polars.

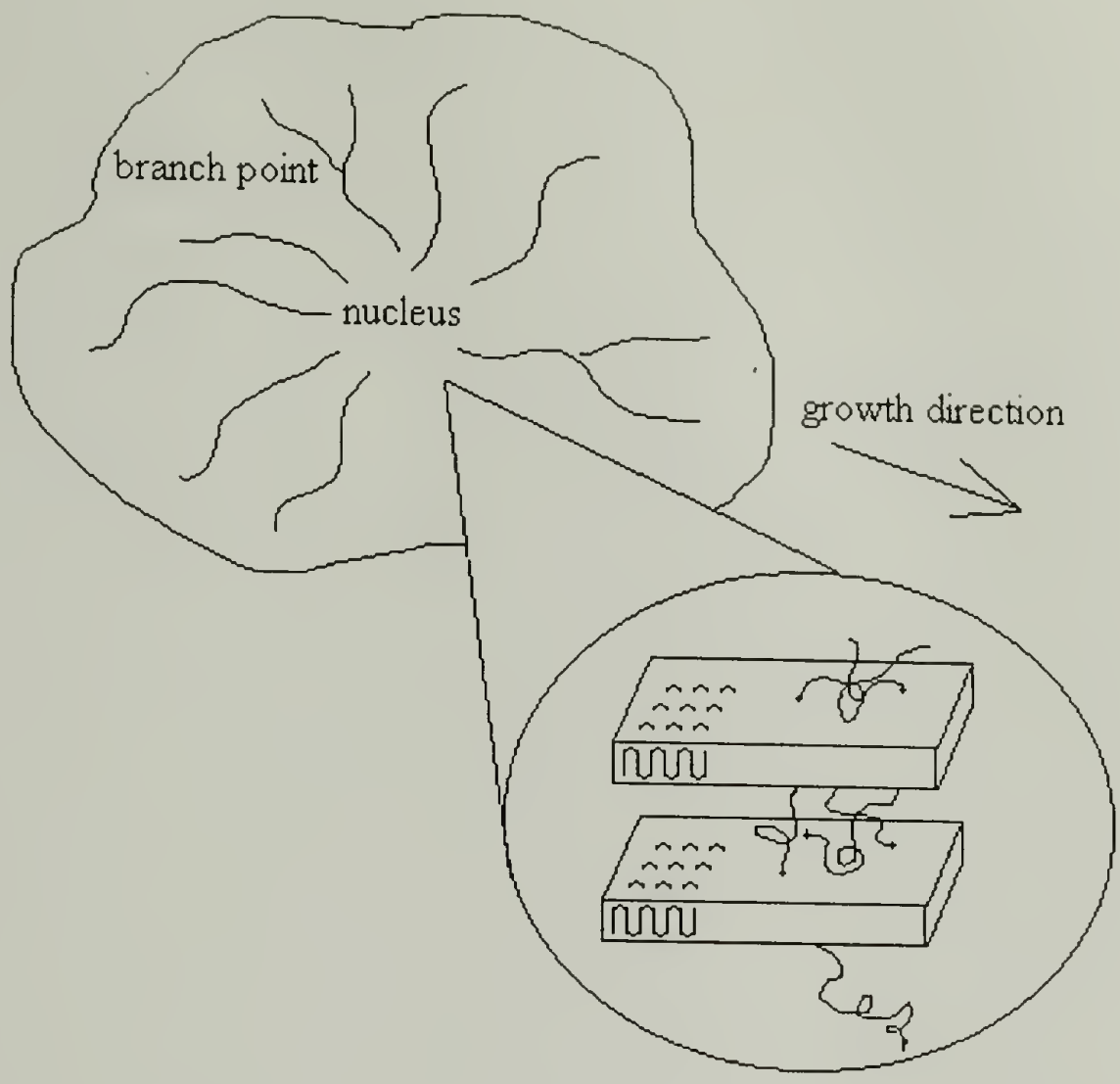

Figure 1.6. Model of Spherulite with Lamellae Growing Radially Outwards.

1.2.2 Thermodynamics and Kinetics of Crystallization

The crystallization of polymers is thermodynamically favored when the change in the Gibbs free energy ΔG is less than zero. ΔG is defined by Equation 1.1, where ΔH = change in enthalpy, T = thermodynamic temperature, and ΔS = change in entropy.

$$\Delta G = \Delta H - T \cdot \Delta S \qquad \text{(Eq. 1.1)}$$

Due to the increase in order found in a crystal (compared to the melt or solution), there is always an entropic penalty for a polymer to crystallize. At low enough temperatures, the large decrease in enthalpy overcomes this penalty.

However, the thermodynamic theory does not account for chain-folding. The most thermodynamically favored polymer crystal (the one of the lowest free energy) is the fully extended chain. In almost all cases (an exception includes the crystallization of polyethylene at high pressure),[5] the crystallization of polymers is under kinetic control, and the polymers undergo chain-folding. Based on the kinetic theory of polymer crystallization proposed in 1960 by Lauritzen and Hoffman,[16] a polymer will fold when the energy penalty for forming the fold is compensated by the energy gain from the enthalpy of fusion. The resulting crystal thickness l (Equation 1.2) is dependent on the fold surface free energy σ_e, melting temperature T_m, the change in the enthalpy of fusion ΔH_f, and the undercooling $\Delta T = T_m - T_c$, where T_c = crystallization temperature.

$$l = 2\sigma_e \cdot T_m \cdot (\Delta H_f \cdot \Delta T)^{-1} + \delta l \qquad \text{(Eq. 1.2)}$$

As shown in Equation 1.2, the thickness l of a polymer crystal depends not on the absolute temperature at which the crystals are grown, but rather on the undercooling. At lower T_c values, crystals form rapidly and as a result are thin (thus having a lower T_m value). At low enough T_c, the rate of crystallization is slowed down due to the lower mobility of the polymer chains near their glass transition temperature T_g. The crystal thickness of some polymers (e.g. polyethylene) can be increased by annealing the polymer at temperatures between their T_m and T_g. Annealing results in a decrease in the surface area of the crystal and reduces G.

The Lauritzen and Hoffman theory provides a simplified model as to why polymers crystallized from dilute solution fold and includes several assumptions[5] (e.g.

completely flat crystal surfaces, infinite substrate on which the crystal grows, crystal thickness fixed by first stem, only 1 polymer chain crystallizes on a surface at a time). Modifications to this theory have been made by numerous scientists.[17-29] In addition, many other theories exist and have been reviewed by Armistead and Goldbeck-Wood[30] as well as Ungar and Zeng.[31] To date, although current crystallization theories are all based on a kinetic treatment, the scientific community still disagrees on the exact details of these differing models.[7-9]

1.3 Goals and Objectives

1.3.1 Background

As mentioned in the beginning of this chapter, a further understanding of polymer crystallization and experimental evidence able to differentiate the various proposed crystallization models will be difficult to obtain from existing polymers investigated using traditional technologies. The problem with existing polymers is their imperfect nature (e.g. polydispersity in molecular weight, variable amount of structural defects, and random distribution of functionalities along the polymer backbone), which makes furnishing a generalization about their crystallization behavior difficult. Most studies (both theoretical and experimental) have focused on polyethylene $[CH_2\text{-}CH_2]_n$ due to the simple structure of the polymer. The goal of this research was to synthesize and examine model polymers, where defects of known and controllable chemistry were placed at periodic and controlled locations along a polyethylene-like backbone. These polymers should be useful in determining the influence of the chemical nature, amount, and

periodicity of a perturbation or defect on the crystallization of polymers, and they could be directly compared with the numerous theoretical and experimental studies on polyethylene and copolymers of ethylene and α-olefins.

Since the propagating segment does not feel the rest of the polymer chain, a chain-type polymerization is not a realistic synthetic option to make these model polymers. A step-growth polymerization based on α,ω-monomers that already contain the desired structural information provides a more desirable method to synthesize model polymers containing defects at a regular periodicity. Acyclic diene metathesis (ADMET) polycondensation (Scheme 1.1) has been employed by Wagener and co-workers to produce and study polymers that are regularly substituted with functionalities. His research group has synthesized and characterized polyethylene-like polymers containing regularly spaced methyl branches,[32,33] copolymers of ethylene and vinyl alcohol,[34] and polyalkenylenes containing regularly spaced functionalities.[35-41] Currently, the distance between side groups (as demonstrated with their polyethylene with methyl branches systematically placed on every ninth to twenty-first carbon atom resulting in very low T_m values ranging from -14 to 62 °C)[32,33] is lower than that needed for the polymers to self-organize and crystallize. ADMET polycondensation is clearly a reasonable way to achieve the objective of synthesizing model polymers. However, there still exists a need for a method to synthesize monomers with longer aliphatic segments. Previous work in the Penelle group by Cedric Le Fevere de Ten Hove[42] and Joel Schall[43] has focused on employing traditional step-growth polymerizations (e.g. polyesterifications) to synthesize long-chain, polyethylene-like polymers where the defects were systematically placed on every thirteenth to forty-fifth carbon atom (Figure 1.7).

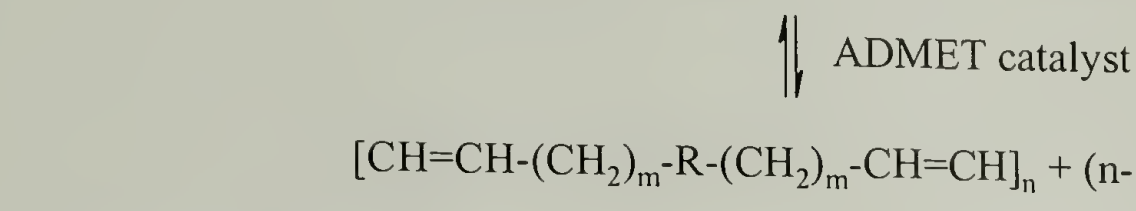

Scheme 1.1. Scheme Showing the Synthesis of Polymers Regularly Substituted with Functionalities (R) via ADMET Polycondensation.

(a) $[O-(CH_2)_x-O-C(O)-(CH_2)_{y-2}-C(O)]_n$

(b) $[O-(CH_2)_x-O-C(O)-(CF_2)_{y-2}-C(O)]_n$

Figure 1.7. Polymers Previously Examined: (a) by Le Fevere de Ten Hove,[42] with x = 12, 22, or 44 and y = 3 to 8 (b) by Schall,[43] with x = 12 or 22 and y = 4, 8, 10, or 12.

If the aliphatic segments of these polyethylene-like polymers are long enough to crystallize, and the defect is excluded from the crystalline region of the polymer, one could chemically engineer the crystal structure of the polymer. The resulting crystals would have controlled lamellar thickness and functionalized surfaces (Figure 1.8). Regularly spaced, short, aliphatic branches could be used to create a model linear, low-density polyethylene, where the location, size, and quantity of branches were precisely controlled. More exotic perturbations such as fluorinated segments or hydrogen-bonding groups could also be employed to synthesize polyethylene-like crystals with chemically different surfaces.

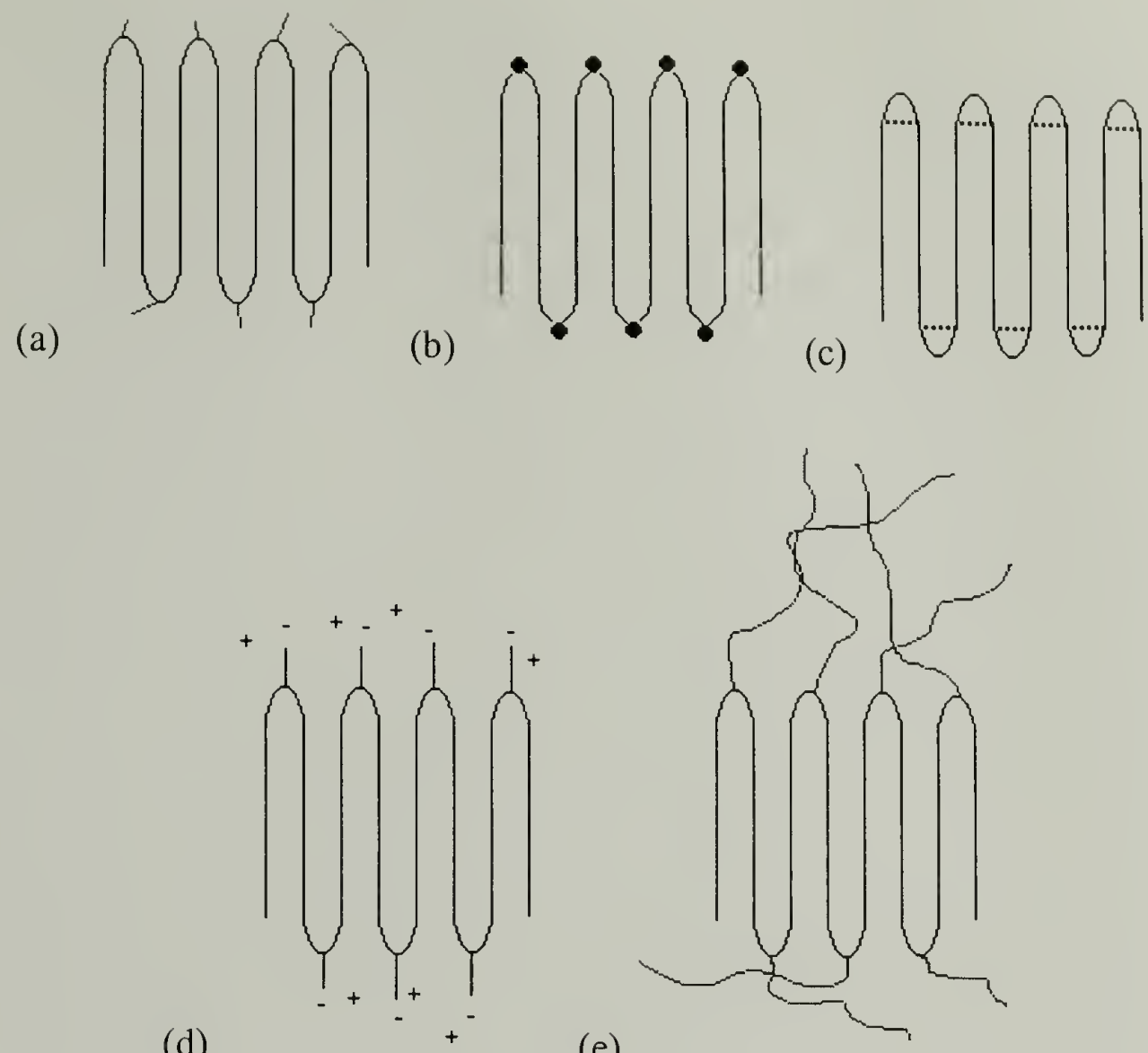

Figure 1.8. Model, Polyethylene-Like Polymers Containing Functionalized Surfaces of: (a) Short-Chain Branches, (b) Noncrystallizable Groups, (c) Hydrogen-Bonded Groups, (d) Ionic Groups, (e) Long-Chain Branches or Polymers, and (f) Crosslinkable Groups.

Previous work concerning the control of lamellar thickness in the Penelle group has focused on polyesters (Figure 1.9) containing defects or perturbations that could

theoretically force the polymers to chain-fold at exactly periodic locations. Le Fevere de Ten Hove[42] examined sterically hindered groups (e.g. propyl branches) and groups that mimic chain-folds (e.g. cyclic groups), while Schall[43] examined incompatible groups (e.g. perfluorinated segments) and sterically hindered groups (e.g. branches and ionomers). It was found that the introduction of propyl branches led to robust control of the lamellar thickness, and the preliminary results from the ionomer-containing polymers were also very promising.

(a) $[O\text{-}(CH_2)_x\text{-}O\text{-}C(O)\text{-}X\text{-}C(O)]_n$

(b) $[(CH_2)_y\text{-}CX_2]_n$

Figure 1.9. Perturbations Previously Examined: (a) by Le Fevere de Ten Hove,[42] with X = CH_2-CH(CH_2-CH_2-CH_3)-CH_2 or CH(CH_2)CH and (b) by Schall,[43] with X = C(O)-O-$(CF_2)_n$-CF_3 or C(O)-O^-.

1.3.2. Specific Objectives of this Research Project

This study expanded on the long-chain polyester work of Le Fevere de Ten Hove[42] and examined the influence of hydrogen-bonding on the properties of model, semi-crystalline m,n-polyurethanes of the general structure $[O\text{-}(CH_2)_m\text{-}O\text{-}C(O)\text{-}NH\text{-}(CH_2)_n\text{-}NH\text{-}C(O)]_n$. In these model polyurethanes, the carbamate esters O-C(O)-NH (non-aliphatic perturbation) are placed at controlled and regular distances on the aliphatic backbone (Figure 1.10). The synthesis of these polymers was accomplished by reacting equimolar amounts of long-chain, aliphatic α,ω-diols $HO\text{-}(CH_2)_m\text{-}OH$, where m = 12, 22, 32, or 46, with short-chain, aliphatic α,ω-diisocyanates $O{=}C{=}N\text{-}(CH_2)_n\text{-}N{=}C{=}O$, where n

= 4, 6, 8, or 12. The first section of this thesis (Chapter 2) deals with the synthesis and characterization of the long-chain, monodisperse, aliphatic α,ω-monomers.

Figure 1.10. Introduction of Backbone Functionalities (Perturbations) at Regular Distances to an Otherwise Aliphatic Polymer. ● = O-C(O)-NH-$(CH_2)_n$-NH-C(O)-O.

By systematically increasing the aliphatic segment derived from the diol, the amount of hydrogen-bonding C=O···H-N in the polymer was diluted. At long enough $(CH_2)_m$ lengths, the polymers resembled copolymers of polyethylene and carbamate esters. The second portion of this thesis (Chapters 3 and 4) deals with determining whether these "copolymers" behaved as polyethylene or polyurethane or somewhere in between. In particular, it was desired to determine what the minimum length of the $(CH_2)_m$ segment was for a transition from a polyurethane-like to a polyethylene-like behavior to occur. To examine this transition, the physical, chemical, and thermal properties of the long-chain polymers were examined. By relating these properties to the crystallization behavior and structure, a better understanding of structure-property relationships should be gained.

Schall[43] showed that aliphatic $(CH_2)_x$ and perfluorinated $(CF_2)_y$ segments could co-crystallize. The resulting polyesters (Figure 1.7b) had crystal structures dependent on

the length of both the aliphatic and the perfluorinated segments, interesting surface properties (e.g. non-wetting), but very low T_m values. In the third section of this thesis (Chapter 5), the results of adding a different perturbation to the aliphatic backbone is examined. In particular, it was desired to understand the influence of heteroatoms (oxygen and sulfur) on the thermal properties and crystal structure of polyurethanes of the general structure $[O\text{-}(CH_2)_{11}\text{-}S\text{-}(CH_2)_2\text{-}X\text{-}(CH_2)_2\text{-}S\text{-}(CH_2)_{11}\text{-}O\text{-}C(O)\text{-}NH\text{-}(CH_2)_6\text{-}NH\text{-}C(O)]_n$, where $X = CH_2$, O, or $O\text{-}(CH_2)_2\text{-}O$, and determine whether these polymers, which are easier to synthesize, might be affordable alternatives to the model, aliphatic m,n-polyurethanes.

Another aspect of interest was to determine whether perturbations could pre-organize the polymers to fold (Figure 1.11). While Le Fevere de Ten Hove[42] and Schall[43] used perturbations or defects that were excluded from the crystalline region (e.g. branching or crystallization mismatch), this study examined whether a perturbation (intramolecular hydrogen-bonding) could be used to pre-organize the polymers to fold (Figure 1.11). This proposed chain-folding is similar to the β-sheet folding of proteins,[44] although the analogy is somewhat limited since proteins are not crystallized from the melt. If both the chain-folds are formed and the aliphatic segments derived from the long-chain diols are long enough, polyethylene-like crystals with functionalized surfaces should be created (Figure 1.12). The last section of this thesis (Chapter 6) examines the attempts to chemically control the lamellar thickness of polyurethanes through hydrogen-bonding.

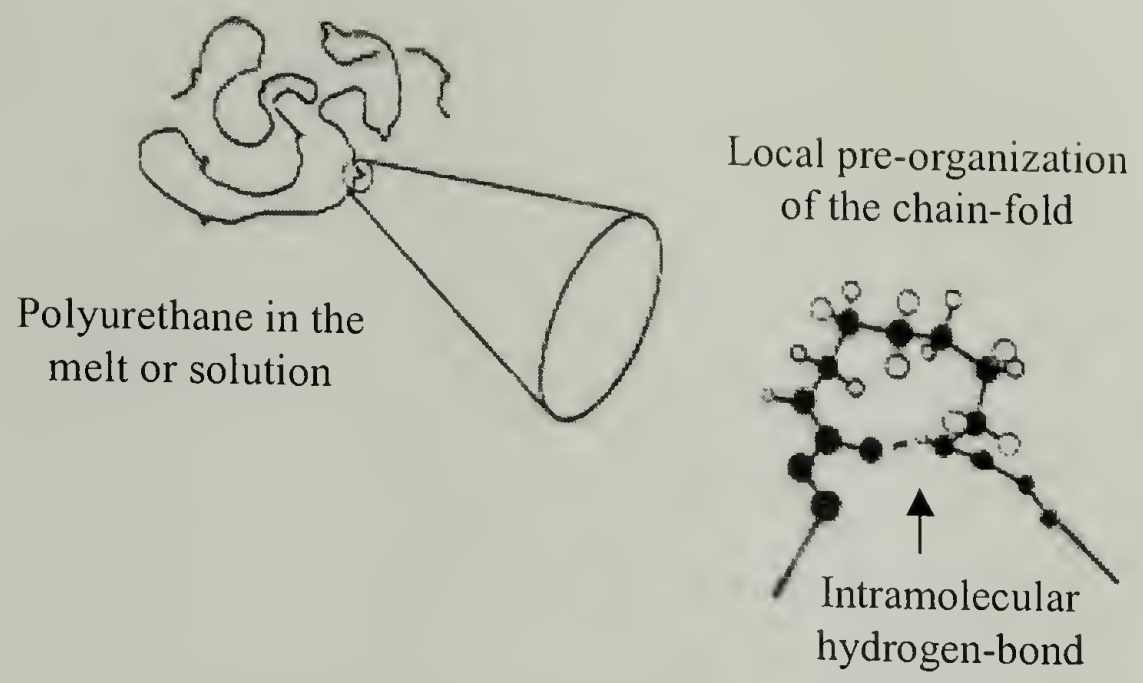

Figure 1.11. Intramolecular Hydrogen-Bonding in the Melt or Solution.

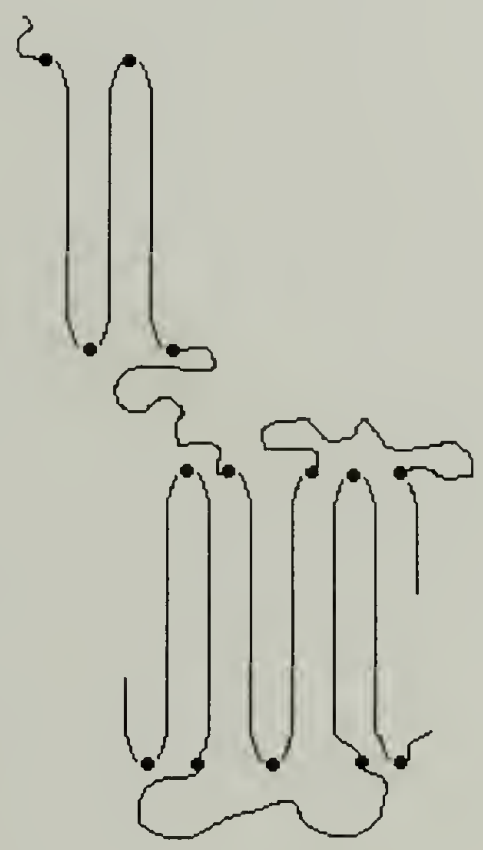

Figure 1.12. Introduction of Chain-Folding at Regular Distances Due to Perturbations in an Otherwise Aliphatic Polymer.

1.4 Synthetic Approach

In this work, long-chain polyurethanes (polyethylene-like structures containing carbamate esters periodically) were made by step-growth polyadditions of equimolar amounts of α,ω-diols and α,ω-diisocyanates. The α,ω-diols employed were long-chain, thus imparting a polyethylene-like structure to the final polymer. By increasing the aliphatic length of the α,ω-diols, the influence of the carbamate ester functionality could be systematically diluted. The α,ω-diisocyanates employed were much shorter in order to help form tight chain-folds.

Step-growth polymerizations are advantageous since they are performed under mild conditions, have few (and controllable) side-products, and produce polymers of relatively low PDI values (~ 2). By employing different α,ω-monomers, a variety of model polymers of different functionalities (e.g. amide, carbonate, ester, and urethane groups) can be examined. The length between functionalities (and thus the density of the functionality in the resulting polymer) can be controlled and systematically increased by methodically increasing the length of one or both of the monodisperse α,ω-monomers.

The long-chain, monodisperse, aliphatic α,ω-diols used ranged from 12 to 46 methylene units in length. Twenty or more methylene units are generally needed for an *n*-alkane to crystallize at room temperature.[45] Thus the 1,12-dodecanediol HO-$(CH_2)_{12}$-OH was below this critical crystallization length, the 1,22-docosanediol HO-$(CH_2)_{22}$-OH was right around this critical crystallization length, and the 1,32-dotriacontanediol HO-$(CH_2)_{32}$-OH and 1,46-hexatetracontanediol HO-$(CH_2)_{46}$-OH were both above this critical crystallization length. Heteroatom-containing diols HO-$(CH_2)_{11}$-S-$(CH_2)_2$-X-$(CH_2)_2$-S-$(CH_2)_{11}$-OH, where X = CH_2, O, and O-$(CH_2)_2$-O, (29 to 32 total methylene groups and

heteroatoms) were also employed and allowed for the examination of the influence of increased flexibility on the aliphatic chains.

The short-chain, monodisperse, aliphatic α,ω-diisocyanates used ranged from 4 to 12 methylene units in length. Six to eight carbon atoms are typically needed to make a tight chain-fold in polyethylene.[46] Thus the 1,4-diisocyanatobutane O=C=N-$(CH_2)_4$-N=C=O was below this critical fold length, the 1,6-diisocyanatohexane O=C=N-$(CH_2)_6$-N=C=O and 1,8-diisocyanatooctane O=C=N-$(CH_2)_8$-N=C=O) were right around this critical fold length, and the 1,12-diisocyanatododecane O=C=N-$(CH_2)_{12}$-N=C=O was clearly above this critical fold length. A stronger driving force than hydrogen-bonding was desired, and so the synthesis of the branched 1,1-dimethylisocyanatobutane $CH_3CH_2CH_2CH(CH_2\text{-}N=C=O)_2$, where the propyl branch was not expected to be accommodated into the crystalline region, was also examined.

1.5 Review of the Crystal Structure and Resulting Thermal and Morphological Properties of Semi-Crystalline Polymers Relevant to this Investigation

1.5.1 Polyethylene

At room temperature and pressure, polyethylene $[CH_2\text{-}CH_2]_n$ has an orthorhombic unit cell (Figure 1.13) and Pnam-D_{2h} space group. The unit cell contains 4 planar, zig-zag chains and has dimensions a = 7.40 Å, b = 4.93 Å, and c = 2.53 Å.[47] The wide-angle X-ray scattering (WAXS) pattern of orthorhombic polyethylene is comprised of 2 intense reflections at d-spacings of 4.1 Å (d_{110}) and 3.7 Å (d_{200})).[48] Monoclinic and hexagonal packing have been observed for polyethylene under more extreme conditions. Physical

deformation of polyethylene typically results in a monoclinic unit cell with dimensions a = 8.09 Å, b = 4.79 Å, and c = 2.53 Å and β = 107.9° and $C2m^{-1}$-C_{2h} space group.[49] High pressure (~ 73 kbar) transforms polyethylene into a hexagonal unit cell with dimensions a = 8.46 Å, b = 4.88 Å, and c = 2.45 Å.[50,51] The monoclinic and hexagonal structures are characterized by a WAXS reflection at a d-spacing of 4.6 Å (d_{001})[48,52] and a diffuse reflection at a d-spacing of 2.3 Å (d_{001}),[53] respectively.

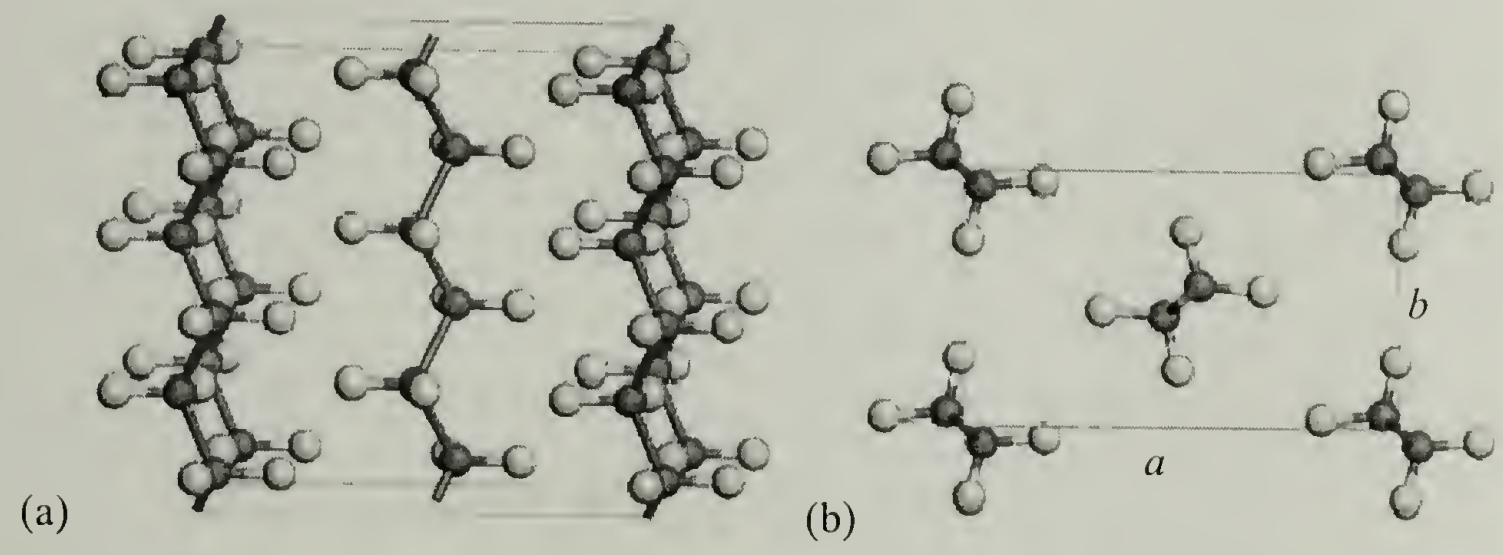

Figure 1.13. Crystal Structure of Orthorhombic Polyethylene: (a) General View and (b) Projection of the Unit Cell Parallel to the Chain Direction c. Carbon and Hydrogen Atoms are Gray and White, Respectively.

Polyethylene crystals are held together by weak van der Waals forces (~ 1 $kJ \cdot mol^{-1}$)[54] between neighboring chains. The resulting lamellae are typically of the order of 110 to 140 Å (~ 88 to 112 methylene units) long,[55] although values as high as 250 to 500 Å (~ 200 to 400 methylene units) have also been reported.[5] Branching can influence the lamellae thickness and has resulted in crystal thickness values as low as 40 Å (~ 32 methylene units).[56] Heating polyethylene crystals at temperatures above their T_c causes the lamellae to thicken (anneal) continuously with time (as observed by the increase in the lamellar stacking periodicity determined by small-angle X-ray scattering (SAXS)

and/or the T_m determined using differential scanning calorimeter (DSC)).[57] Based on the extrapolation of the melting temperatures of the *n*-alkane series, polyethylene has a theoretical T_m of 145 °C and enthalpy value of 4.14 kJ·mol^{-1}.[58,59] All experimental values of T_m and enthalpy have been lower for synthetic polyethylene (regardless of polymerization method) due to the chain-folded nature of the polymer (T_m = ~142 °C for fully extended polyethylene crystallized at 227 °C and 480 atm with weight-average molecular weight = 80,000 g·mol^{-1}, PDI = ~10, and extended chain length = 30,000 Å).[60]

Depending on the polymerization conditions, a variety of molecular architectures (Figure 1.14) can be obtained ranging from the highly branched, low-density polyethylene (LDPE) to the very linear, high-density polyethylene (HDPE). The long-chain branches (LCBs) and short-chain branches (SCBs) in LDPE, formed by intermolecular (hydrogen abstraction) and intramolecular (backbiting) chain transfer, respectively, can act as structural defects that are rejected from the crystal and forced into the amorphous regions. These defects or perturbations to the aliphatic chain influence the crystallinity, density, lamellar morphology, as well as the physical, thermal, and mechanical properties of the resulting polyethylene (Table 1.1).[61] The amount of branching as well as their length can be controlled to some extent by copolymerizing ethylene with α-olefins to synthesize linear, low-density polyethylene (LLDPE).

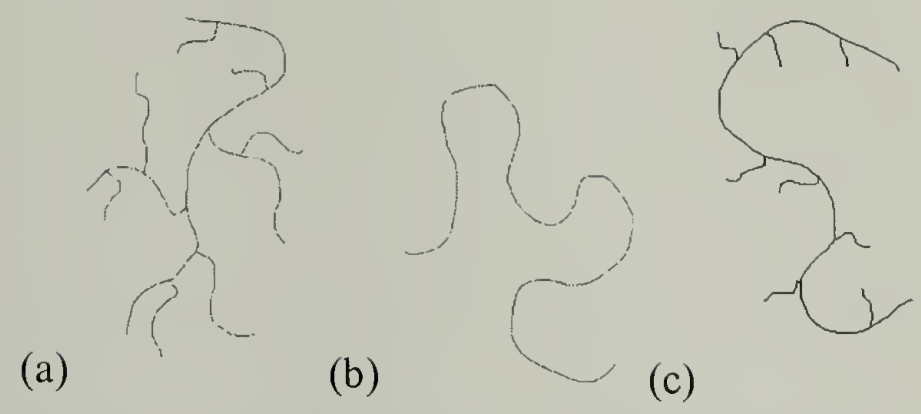

Figure 1.14. Influence of Branching on the Molecular Architecture of Polyethylene: (a) LDPE, (b) HDPE, and (c) LLDPE.

Table 1.1. Comparison of the Typical Structural, Physical, Thermal, and Morphological Properties[a] of LDPE, HDPE, and LLDPE.

Property	LDPE	HDPE	LLDPE – Ziegler-Natta	LLDPE – Metallocene
$M_w \cdot 10^{-4}$	2 to 40	5 to 25	5 to 20	4 to 11
PDI	3 to 20	1 to > 10	4 to 35	2 to 2.5
Density ($g \cdot cm^{-3}$)	0.91 to 0.93	0.94 to 0.96	0.91 to 0.93	0.89 to 0.94
Amount of Branching	15 to 30 CH_3 per 1000 C	0.5 to 3 CH_3 per 1000 C	2 to 4 mol %	0.5 to 7 mol %
Type of Branches	methyl, ethyl, butyl, amyl, and longer		ethyl, butyl, and hexyl	ethyl, butyl, and hexyl
% Crystallinity	40 to 60	70 to 90	33 to 53	33 to 53
T_m (°C)	105 to 115	133 to 138 (observed), 145 (theoretical)	121 to 125	90 to 125
Enthalpy ($kJ \cdot mol^{-1}$)	1.37 to 2.18	1.45 to 3.73 (observed), 4.14 (theoretical)	1.37 to 2.18	1.37 to 2.18
T_g (°C)	-103 to –133	-113 to –133		

a) See references 61-62 and 65-67.

In the highly branched LDPE, the presence of a large number of SCBs (~ 15 to 30 methyl branches per 1000 carbon atoms) lowers the T_m (105 to 115 °C), enthalpy (1.37 to 2.18 $kJ \cdot mol^{-1}$), density (0.91 to 0.93 $g \cdot cm^{-3}$) and degree of crystallinity (40 to 60%) from the theoretical values.[62] It has been reported that higher levels of methylene branching

(~ 150 or more methyl branches per 1000 carbon atoms) result in a completely amorphous polymer.[63,64] On the other hand, the highly linear HDPE, which has no LCBs and very few SCBs (~ 0.5 to 3 methyl branches per 1000 carbon atoms), has a higher T_m (133 to 138 °C), enthalpy (1.45 to 3.73 $kJ \cdot mol^{-1}$), density (0.94 to 0.96 $g \cdot cm^{-3}$), and degree of crystallinity (70 to 90%) than that of branched LDPE.[65] In between that of LDPE and HDPE, LLDPE has no LCBs and a controlled amount of SCBs. If a Ziegler-Natta type catalyst is used, the SCBs are predominately located in the lower molecular weight chains, while if a metallocene catalyst is used, the SCBs have a more homogeneous distribution (conditions can be identified to prevent the formation of dyads of branching). The T_m (90 to 125 °C), density (0.89 to 0.94 $g \cdot cm^{-3}$), and degree of crystallinity (33 to 53%) can range dramatically depending on the polymerization conditions (such as comonomer type and quantity as well as catalyst).[66,67] The introduction of methyl branches does not change the orthorhombic packing of polyethylene but does increase the *a* dimension of the unit cell.

1.5.2 Polyesters

In 1940, Fuller[68] first reported that AABB type, aliphatic polyesters of the general structure $[O\text{-}(CH_2)_x\text{-}O\text{-}C(O)\text{-}(CH_2)_{y\text{-}2}\text{-}C(O)]_n$ exhibit a polyethylene-like packing if the $(CH_2)_m$ sequences are long enough. The ester groups are sterically not large enough to introduce a large disruption in the *ab*-crystal plane. In the *c* direction, the ester groups on adjacent polymer chains form planes, which are inclined relative to the chain axis, in order to optimize dipole-dipole interactions. Generally, polyesters have orthorhombic, monoclinic, or triclinic packing (Figure 1.3) depending on the amount of gliding

(displacement of identical repeat units on adjacent polymer chains) the chains undergo.[69] In particular, aliphatic polyesters typically have orthorhombic or monoclinic packing if the number of carbon atoms in the repeat unit is odd or even, respectively.[1]

The introduction of polar ester groups O-C(O) to an otherwise hydrophobic, aliphatic backbone disrupts the packing of the resulting polyester chains resulting in a lower T_m (compared to polyethylene). Odd-even parity effects are observed, resulting in lower T_m values for polyesters containing an odd x or y value than for those containing even x and y values.[42,70] As the aliphatic length of the polyester is increased, the T_m increases towards that of polyethylene.[42,70] Lamellar thickening occurs when aliphatic polyesters are heated above their T_c and result in a continuous increase in their T_m values. The work of Cho and Lee[71] (30,30-polyester) and Le Fevere de Ten Hove[42] (12,4-, 12,5-, 12,6-, 12,8-, 22,4-, 22,5-, 22,6-, 22,8-, and 44,5-polyesters) on long-chain, aliphatic polyesters showed that these polymers had properties (e.g. physical, thermal, and morphological) intermediate of that of short-chain polyesters and HDPE.

1.5.3 Polyamides

Aliphatic polyamides can be divided into 6 categories: even (number of carbon atoms) or odd type AB nylons $[NH\text{-}(CH_2)_{m-1}\text{-}C(O)]_n$ and even-even, even-odd, odd-even, or odd-odd type AABB nylons $[NH\text{-}(CH_2)_m\text{-}NH\text{-}C(O)\text{-}(CH_2)_{n-2}\text{-}C(O)]_n$. The even-even polyamides are synchelphlic (head to head, tail to tail type polymerization) and have no polarity with respect to the chain direction. The crystal packing of the aliphatic polyamides is controlled by the formation and maximization of the hydrogen-bonds (energy gained, dependent on the hydrophobicity of the environment and mobility of

chains,[72] = ~ 10 to 40 kJ·mol^{-1})[54] between neighboring chains. The polyamide type (AB or AABB), length of the aliphatic segment(s), and whether the nylons are even or odd all influence the resulting crystal structure (typically monoclinic, triclinic, or pseudohexagonal (Figure 1.3)). The monoclinic, triclinic, and pseudohexagonal structures are characterized by WAXS reflections at *d*-spacings of 4.4 Å (d_{200}) and 3.7 Å (d_{020} and d_{220}),[73] 4.4 Å (d_{100}) and 3.7 Å (d_{010} and d_{110}),[55] and 4.2 (d_{200}),[74] respectively. Since the polyurethanes under examination in this study are even-even (Chapters 3 and 4) and odd-even (Chapter 5), only the even-even and even-odd (due to differences in nomenclature the odd-even m,n-polyurethanes [O-$(CH_2)_m$-O-C(O)-NH-$(CH_2)_{n-2}$-NH-C(O)]$_n$ are analogous to the even-odd nylons [NH-$(CH_2)_m$-NH-C(O)-$(CH_2)_{n-2}$-C(O)]$_n$) polyamides will be discussed.

At room temperature, most even-even polyamides have a triclinic unit cell (Figure 1.15) in order to maximize the amount of hydrogen-bonding. The fully extended, all *trans* chains form planar sheets through hydrogen-bonds. In order to form linear hydrogen-bonds, the chains are progressively sheared in the *c* direction. Additionally, the sheets are progressively sheared parallel to the sheet plane. Due to the progressive shearing of the chains (~ 42° tilt for nylon 6,6), the interchain distance of 4.8 Å results in a WAXS reflection at 4.4 Å (d_{100}).[73] The intersheet distance results in a WAXS reflection at 3.7 Å, which actually consists of two unresolved reflections (the 3.73 Å (d_{010}) and the slightly weaker 3.66 Å (d_{110})). Some 2N 2(N+1) nylons of very high hydrogen-bonding density (e.g. nylons 2,4, 4,6, and 6,8) have a monoclinic unit cell due to alternating shearing of the hydrogen-bonded sheets. The alternative shearing of sheets is believed to be less stable than the usual progressive shearing and forms only when the

aliphatic segments (originating from either the diacid or the diamine) are too short to form a chain-fold.[75]

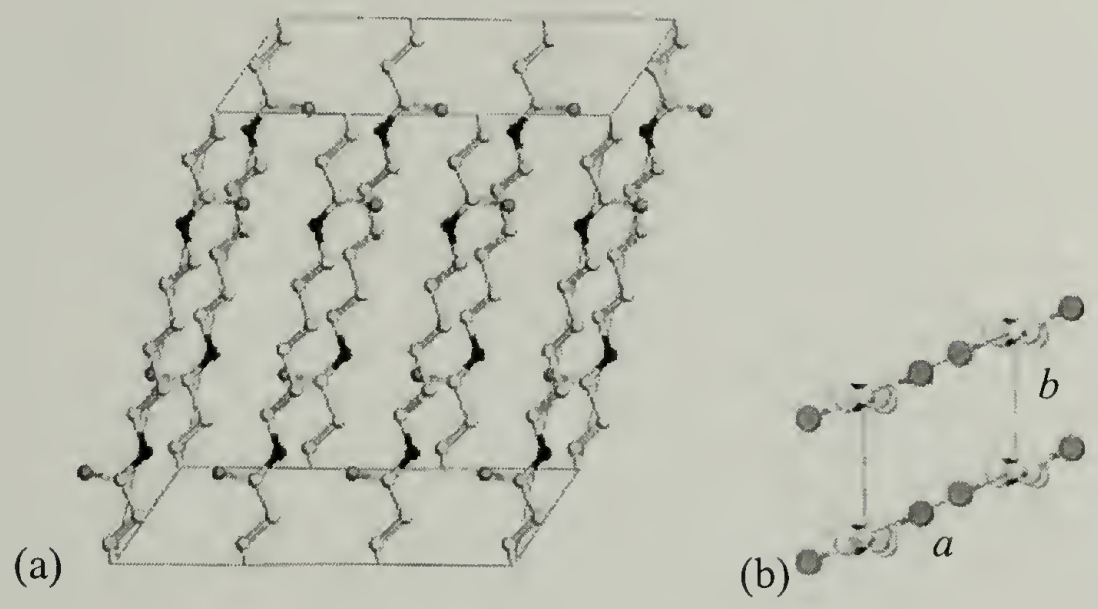

Figure 1.15. Crystal Structure of Triclinic Nylon 6,6 (α-Phase): (a) General View and (b) Projection of the Unit Cell Parallel to the Chain Direction *c*. Carbon, Nitrogen, and Oxygen Atoms are White, Black, and Gray, Respectively, and Hydrogen Atoms are Not Shown.

If the even-odd polyamides exhibited the same crystal packing as the even-even polyamides, all of the amide groups would not be hydrogen-bonded. The relatively lower T_m of the even-odd nylons was originally attributed to this theory of a lower amount of hydrogen-bonding.[76,77] However, Trifan and Trenzi[78] reported that there were no free NH groups observable in the IR. In order for all of the amide groups to be hydrogen-bonded, it has been proposed that consecutive amide groups form alternate hydrogen-bonding between 2 crystallographic planes.[79-82] The even-odd polyamides have been assigned a monoclinic unit cell with fully extended, planar chains.

Under certain conditions, the triclinic and monoclinic packing of polyamides can be converted to a pseudohexagonal packing. These conditions include the use of a solvent or a swelling agent,[83-85] rate of fiber-spinning,[86] and temperature.[87] The

relationship between crystal packing and temperature was first reported by Brill, who observed the merging of the 3.7 and 4.4 Å WAXS reflections to a single reflection at 4.2 Å upon heating nylon 6,6.[87] For some polyamides, both triclinic or monoclinic packing and pseudohexagonal packing can exist simultaneously at room temperature. Ramesh and co-workers[88] recently showed that nylon 6,6 grows in a pseudohexagonal form and switches to the triclinic form upon cooling.

Similar to ester groups, amide groups C(O)-NH, which undergo hydrogen-bonding, are polar in nature. However, unlike the ester groups, the amide groups introduce very strong intermolecular interactions to the resulting aliphatic polyamide chains resulting in a higher T_m (compared to polyethylene). Odd-even parity effects are observed, resulting in lower T_m values for polyamides containing an odd number of methylene groups than for those containing an even number of methylene groups (Figure 1.16).[89,90] AB type polyamides usually exhibit a lower T_m than the corresponding AABB type polyamides (Figure 1.16).[89,90] As the aliphatic length of the polyamide is increased, the T_m decreases towards that of polyethylene (Figure 1.17).[91]

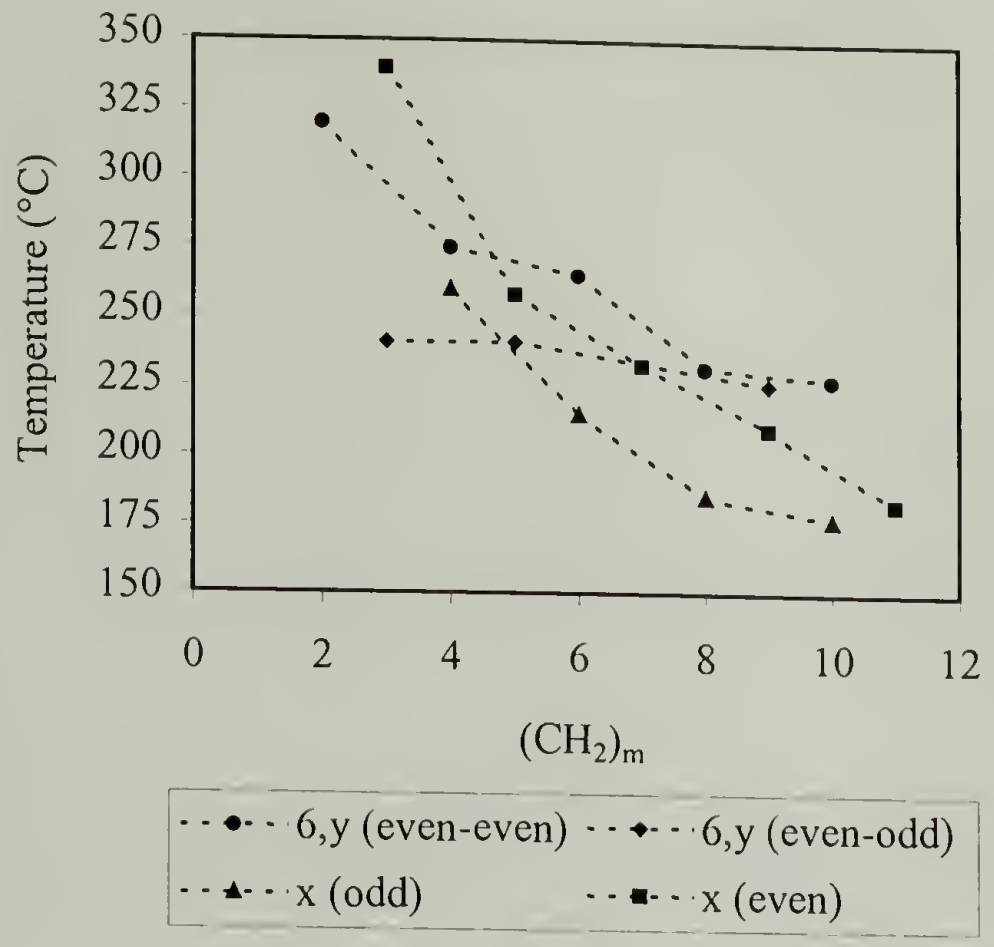

Figure 1.16. T_m of the Aliphatic Polyamides of the Type AABB $[NH\text{-}(CH_2)_x\text{-}NH\text{-}C(O)\text{-}(CH_2)_{y\text{-}2}\text{-}C(O)]_n$ and Type AB $[NH\text{-}(CH_2)_{x\text{-}1}\text{-}C(O)]_n$ (See References 89 and 90).

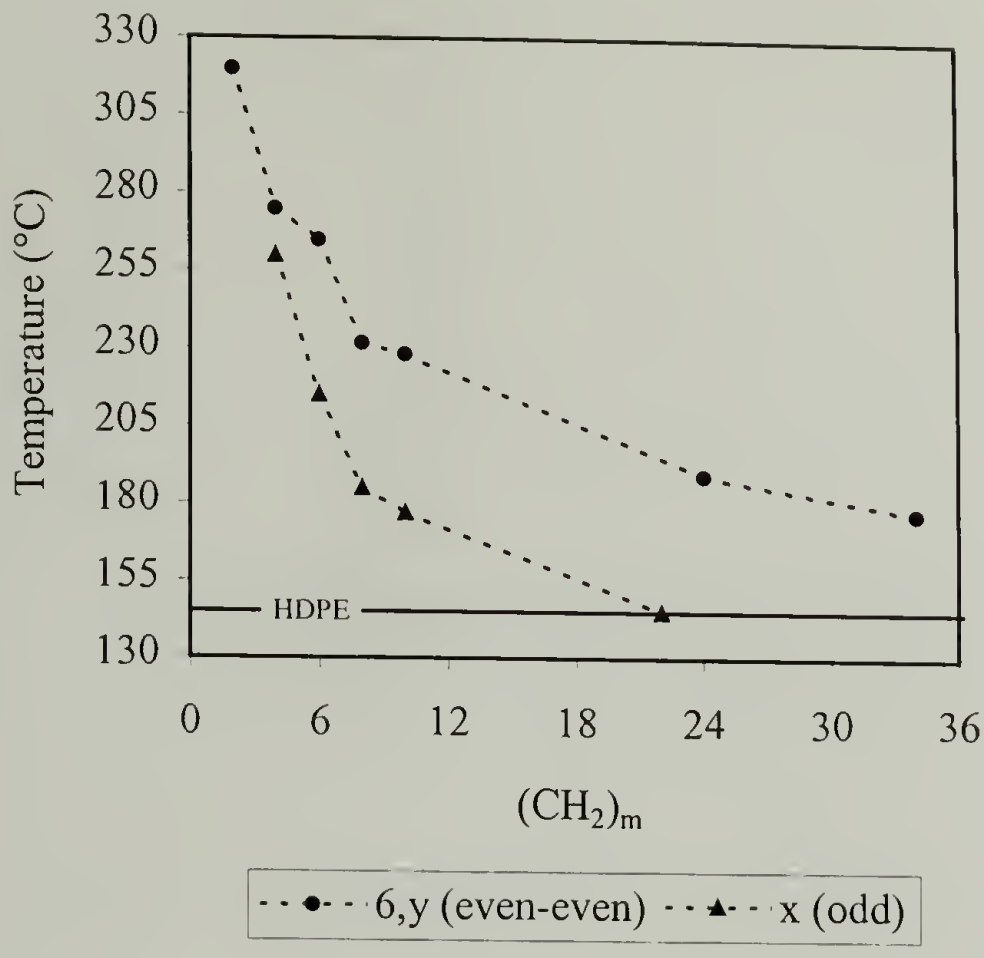

Figure 1.17. T_m of the Even-Even $[NH\text{-}(CH_2)_x\text{-}NH\text{-}C(O)\text{-}(CH_2)_{y\text{-}2}\text{-}C(O)]_n$ and Odd Nylons $[NH\text{-}(CH_2)_{x\text{-}1}\text{-}C(O)]_n$ of Increasing Aliphatic Length (See References 90 and 91).

The presence of amide groups dramatically influences the crystallization behavior of polyamides compared to that of polyethylene (and polyesters). Aliphatic polyamides have much shorter lamellae (typically of the order of 50 to 70 Å)[92-97] then polyethylene. Unlike polyethylene whose lamellae thicken continuously when heated at temperatures above their T_c, polyamide crystals have a lamellar thickness that is a function of the hydrogen-bonding density[98] and can increase only by multiples of their repeat unit (quantum jumps).[2] The crystals tend to be lath-shaped and can aggregate to form sheaves.[55] The crystallization kinetics are also influenced by the presence of the amide groups. The formation of hydrogen-bonds leads to faster crystallization in polyamides

compared to other aliphatic polymers whose crystallization is controlled by van der Waals forces.[2]

1.5.4 Polyurethanes

There are very few literature reports on the crystal structure of purely aliphatic m,n-polyurethanes. Most of the research[99-102] done has focused on the 4,6-polyurethane $[O\text{-}(CH_2)_4\text{-}O\text{-}C(O)\text{-}NH\text{-}(CH_2)_6\text{-}NH\text{-}C(O)]_n$, which was commercialized by Farbenindustrie under the trade name Perlon U.[103] In 1950, Zahn and Kohler[99] noted that the WAXS pattern of the 4,6-polyurethane resembled that of the corresponding polyamide, and that the chain repeat distance of 19.1 Å agreed with the theoretical value of a fully extended, zig-zag chain. A year later, Borchert[100] suggested that the agreement between the X-ray patterns of the 4,6-polyurethane and the corresponding polyamide implied that like polyamides, the 4,6-polyurethane contained hydrogen-bonds between neighboring polymer chains. He proposed a unit cell containing 2 polymer chains with dimensions a = 4.95 Å, b = 19.2 Å, and c = 8.69 Å and angles $\alpha = 90°$, $\beta = 60.2°$, and γ = 170-176°. In 1952, Zahn and Winter[101] proposed a similar crystal structure, but with 4 polymer chains in the unit cell. Their proposed unit cell had dimensions a = 9.55 Å, b = 19.1 Å, and c = 8.40 Å and angles $\alpha = 90°$, β = 63-65°, and $\gamma = 77°$.

Saito and co-workers examined not only the 4,6-polyurethane, but also a series of aliphatic m,n-polyurethanes.[102,104] They assigned a triclinic unit cell containing only 1 polymer chain to the 4,6-polyurethane with dimensions a = 4.98 Å, b = 4.71 Å, and c = 19.4 Å and angles $\alpha = 116°$, $\beta = 105°$, and $\gamma = 109°$. The series of m,n-polyurethanes that they examined included even-even (2,6-, 4,6-, and 6,6-polyurethanes), odd-even (3,6- and

5,6-polyurethanes), and even-odd polymers (4,3- and 6,3-polyurethanes). They reported that the even-even polyurethanes all had triclinic packing similar to the α-phase of polyamides, while the odd-even polyurethanes all had monoclinic packing similar to the γ-phase of polyamides. Saito et al. proposed that in order for all the carbamate esters of the odd-even polyurethanes to be hydrogen-bonded (as indicated by IR studies), the chains were tilted 30° from the lamellar surface normal. The crystal structures assigned to the m,n-polyurethanes by Saito et al. were the same as that assigned to the corresponding aliphatic polyamides.[105,106]

Despite the relatively few literature references describing the crystal structure of aliphatic polyurethanes, it seems reasonable to extrapolate that if the number of carbamate esters is decreased (as in this work), the crystal structure should still be similar to that of the corresponding polyamide. Since aliphatic polyurethanes have properties (such as T_m) intermediate of the analogous polyesters and polyamides (Table 1.2), it is important when examining the thermal and morphological properties of polyurethanes to also keep in mind the corresponding polyesters.[90]

Table 1.2. T_m of Analogous Aliphatic Polyester, Polyurethane, and Polyamide.

Polymer	Repeat Unit	T_m[a] (°C)
Polyester	$[O\text{-}(CH_2)_4\text{-}O\text{-}C(O)\text{-}(CH_2)_8\text{-}C(O)]$	62
Polyurethane	$[O\text{-}(CH_2)_4\text{-}O\text{-}C(O)\text{-}NH\text{-}(CH_2)_6\text{-}NH\text{-}C(O)]$	182
Polyamide	$[(CH_2)_6\text{-}C(O)\text{-}NH\text{-}(CH_2)_6\text{-}NH\text{-}C(O)]$	235

a) See reference 90.

1.6 Summary of Each Chapter

Chapter 2: Synthesis and Characterization of Long-Chain, Aliphatic α,ω-Diols. A review of the synthesis, purity, and global yield of long-chain, aliphatic,

monodisperse α,ω-diols is presented. 1,22-Docosanediol HO-$(CH_2)_{22}$-OH, 1,32-dotriacontanediol HO-$(CH_2)_{32}$-OH, and 1,46-hexatetracontanediol HO-$(CH_2)_{46}$-OH were synthesized from modified literature procedures.[42,107-109] A comparison of the thermal properties of these long-chain, aliphatic diols with α,ω-diols of shorter aliphatic length was made. Characterization of the long-chain, monodisperse α,ω-diols provided evidence of a solid-solid, rotator phase transition.

Chapter 3: Synthesis of m,n-Polyurethanes and Resulting Polyethylene-Like Behavior. The synthesis of a series of long-chain, aliphatic m,n-polyurethanes [O-$(CH_2)_m$-O-C(O)-NH-$(CH_2)_n$-NH-C(O)]$_n$ is discussed. The structure and purity of these polymers were examined with an emphasis on the absence of crosslinks. The physical and thermal properties of these increasingly aliphatic polyurethanes were compared with that of HDPE and polyurethanes of higher hydrogen-bonding density. Characterization revealed that the long aliphatic segments $(CH_2)_m$ diluted the influence of the hydrogen-bonds C=O···H-N in the long-chain m,n-polyurethanes.

Chapter 4: Influence of Hydrogen-Bonding on the Crystallization Behavior of m,n-Polyurethanes. A detailed analysis of the crystallization behavior of the long-chain, aliphatic m,n-polyurethanes is provided. Hydrogen-bonding was shown to be the controlling factor in the crystal structure and crystallization kinetics of these polymers. The crystal structure of the 22,12-polyurethane [O-$(CH_2)_{22}$-O-C(O)-NH-$(CH_2)_{12}$-NH-C(O)]$_n$ was described in detail and compared with the crystallization of HDPE, long-chain polyesters, and polyamides of higher hydrogen-bonding density. Additionally, the synthesis of perdeuterated 1,6-diisocyanatohexane O=C=N-$(CD_2)_6$-N=C=O is discussed.

Chapter 5: Heteroatom-Containing Polyurethanes and Resulting Thermal Properties. An alternate route to synthesizing long-chain, telechelic diols in high yield and purity is presented. Several heteroatom-containing diols HO-$(CH_2)_{11}$-S-$(CH_2)_2$-X-$(CH_2)_2$-S-$(CH_2)_{11}$-OH, where X = CH_2, O, or O-$(CH_2)_2$-O, were prepared by a one-step, free-radical telomerization[110,111] and reacted in the melt with 1,6-diisocyanatohexane O=C=N-$(CH_2)_6$-N=C=O to produce heteroatom-containing m,6-polyurethanes. A comparison of the thermal properties of the heteroatom-containing diols and polyurethanes with the corresponding aliphatic α,ω-diols and polyurethanes was made. Characterization provided evidence that the heteroatoms influenced the melting behavior but not the decomposition behavior nor crystal structure of the m,n-polyurethanes.

Chapter 6: Chemical Engineering of the Crystal Thickness. Attempts to chemically engineer the lamellar thickness are detailed. Characterization of the long-chain α,ω-diols and m,n-polyurethanes provided evidence that the long aliphatic segments $(CH_2)_m$ self-organized, but that intermolecular hydrogen-bonding did not force the polymer chains to fold. Additionally, the synthesis of the branched 1,1-dimethylisocyanatobutane $CH_3CH_2CH_2CH(CH_2\text{-}N=C=O)_2$ is discussed.

1.7 References

(1) Wunderlich, B. *Crystal Structure, Morphology, Defects*; Academic: New York, 1973; Vol. 1.

(2) Wunderlich, B. *Crystal Nucleation, Growth, Annealing*; Academic: New York, 1976; Vol. 2.

(3) Wunderlich, B. *Crystal Melting*; Academic: New York, 1980; Vol. 3.

(4) Mandelkern, L. In *Physical Properties of Polymers*; Mark, J. E., Ed.; American Chemical Society: Washington, D. C., 1984.

(5) Barham, P. J. Crystallization and Morphology of Semicrystalline Polymers. In *Materials Science and Technology: Structure and Properties of Polymers*; Thomas, E. L., Ed.; John Wiley & Sons: New York, 1993; Vol. 12.

(6) Strobl, G. R. *The Physics of Polymers: Concepts for Understanding Their Structure and Behavior*; 2nd ed.; Springer: Berlin, 1997.

(7) Strobl, G. R. *Eur. Phys. J. E* **2000**, *3*, 165.

(8) Lotz, B. *Eur. Phys. J. E* **2000**, *3*, 185.

(9) Muthukumar, M. *Eur. Phys. J. E* **2000**, *3*, 199.

(10) Keller, A. *Philos. Mag.* **1957**, *2*, 1171.

(11) Keller, A. *Rep. Prog. Phys.* **1968**, *31*, 623.

(12) Khoury, F.; Passaglia, E. In *Treatise on Solid State Chemistry*; Hannay, N. B., Ed.; Plenum: New York, 1976; Vol. 3.

(13) Wittmann, J. C.; Lotz, B. *J. Polym. Sci., Part B: Polym. Phys.* **1985**, *23*, 205.

(14) Patil, R.; Reneker, D. H. *Polymer* **1994**, *35*, 1909.

(15) Flory, P. J. *J. Am. Chem. Soc.* **1962**, *84*, 2858.

(16) Lauritzen, J. I.; Hoffman, J. D. *J. Res. Natl. Bur. Stand., Sect. A.* **1960**, *64*, 73.

(17) Lauritzen, J. I.; Hoffman, J. D. *J. Appl. Phys.* **1973**, *44*, 4340.

(18) Point, J. J. *Discuss. Faraday Soc.* **1978**, *68*.

(19) Point, J. J. *Macromolecules* **1979**, *12*, 770.

(20) Hoffman, J. D.; Guttman, C. M.; DiMarzio, E. A. *Discuss. Faraday Soc.* **1979**, *68*, 177.

(21) Point, J. J.; Kovacs, A. J. *Macromolecules* **1980**, *13*, 399.

(22) DiMarzio, E. A.; Guttman, C. M. *J. Appl. Phys.* **1982**, *53*, 6581.

(23) Hoffman, J. D. *Polymer* **1983**, *24*, 3.

(24) Cheng, S. Z. D.; Wunderlich, B. *J. Polym. Sci., Part B: Polym. Phys.* **1986**, *24*, 557.

(25) Cheng, S. Z. D.; Wunderlich, B. *J. Polym. Sci., Part B: Polym. Phys.* **1986**, *24*, 595.

(26) Hoffman, J. D.; Miller, R. L. *Macromolecules* **1989**, *21*, 3038.

(27) Mansfield, M. L. *Polymer* **1988**, *29*, 1755.

(28) Mansfield, M. L. *Polym. Commun.* **1990**, *31*, 283.

(29) Toda, A. *Polymer* **1991**, *32*, 771.

(30) Armistead, K.; Goldbeck-Wood, G.; Keller, A. *Adv. Polym. Sci.* **1992**, *100*, 219.

(31) Ungar, G.; Zeng, K. B. *Chem. Rev.* **2001**, *101*, 4157.

(32) Wagener, K. B.; Valenti, D. J.; Hahn, S. F. *Macromolecules* **1997**, *30*, 6688.

(33) Smith, J. A.; Brzezinska, K. R.; Valenti, D. J.; Wagener, K. B. *Macromolecules* **2000**, *33*, 3781.

(34) Valenti, D. J.; Wagener, K. B. *Macromolecules* **1998**, *31*, 2764.

(35) Smith, D. W., Jr.; Wagener, K. B. *Macromolecules* **1991**, *24*, 6073.

(36) Brzezinska, K. R.; Wagener, K. B. *Macromolecules* **1992**, *25*, 2049.

(37) Wagener, K. B.; Patton, J. T.; Boncella, J. M. *Macromolecules* **1992**, *25*, 3862.

(38) Wagener, K. B.; Patton, J. T. *Macromolecules* **1993**, *26*, 249.

(39) O'Gara, J. E.; Portmess, J. D.; Wagener, K. B. *Macromolecules* **1993**, *26*, 2837.

(40) Smith, D. W., Jr.; Wagener, K. B. *Macromolecules* **1993**, *26*, 3533.

(41) Wagener, K. B.; Tao, D. *Macromolecules* **1994**, *28*, 1281.

(42) Le Fevere de Ten Hove, C. Controlling Solid-State Microstructure of Semi-Crystalline Polymers Through Chemical Design of Chains: A Study of Model Polyesters. Ph.D. Thesis, Université Catholique de Louvain, Louvain-la-Neuve, 2001.

(43) Schall, J. D. Condensation Polymers with Regularly-Spaced, Strongly-Segregating Functionalities. Ph.D. Thesis, University of Massachusetts, Amherst, 2001.

(44) Schneider, J. P.; Kelly, J. W. *Chem. Rev.* **1995**, *95*, 2169.

(45) Loudon, G. M. *Organic Chemistry*; 2nd ed.; Benjamin/Cummings: Menlo Park, 1988.

(46) Chum, S. P.; Knight, G. W.; Ruiz, J. M.; Phillips, P. J. *Macromolecules* **1994**, *27*, 656.

(47) Bunn, C. W.; Alcock, T. C. *Trans. Faraday Soc.* **1945**, *41*, 317.

(48) Bunn, C. W. *Trans. Faraday Soc.* **1939**, *35*, 482.

(49) Seto, T.; Hara, T.; Tanaka, T. *Jpn. J. Appl. Phys.* **1968**, *7*, 31.

(50) Yasuniwa, F.; Enoshito, R.; Takemura, T. *Jpn. J. Appl. Phys.* **1970**, *15*, 142.

(51) Bassett, D. C.; Block, S.; Piermarina, S. *Jpn. J. Appl. Phys.* **1974**, *45*, 4146.

(52) Jones, A. T. *J. Polym. Sci.* **1962**, *62*, 553.

(53) Tashiro, K.; Sasaki, S.; Kobayashi, M. *Macromolecules* **1996**, *29*, 7460.

(54) Israelachvili, J. N. *Intermolecular and Surface Forces*; 2nd ed.; Academic: New York, 1992.

(55) Dreyfuss, P.; Keller, A. *J. Macromol. Sci., Phys.* **1970**, *4*, 811.

(56) Alamo, R. G.; Chan, E. K. M.; Mandelkern, L. *Macromolecules* **1993**, *26*, 5740.

(57) Statton, W. O.; Geil, P. H. *J. Appl. Polym. Sci.* **1960**, *3*, 357.

(58) Flory, P. J.; Vrij, A. *J. Am. Chem. Soc.* **1963**, *85*, 3548.

(59) Nakajima, A.; Hamada, F. *Kolloid Z. Z. Polym.* **1965**, *205*, 55.

(60) Hellmuth; Wunderlich, B. *J. Appl. Phys.* **1965**, *36*, 3039.

(61) Quirk, R. P.; Alsamarraie, M. A. A. Physical Constants of Polyethylene. In *Polymer Handbook*; 3rd ed.; Brandrup, J., Immergut, E. H., Eds.; John Wiley & Sons: New York, 1989.

(62) Odian, G. *Principles of Polymerization*; 3rd ed.; John Wiley & Sons: New York, 1991.

(63) Wunderlich, B.; Poland, D. *J. Polym. Sci., Part A* **1963**, *1*, 357.

(64) Gerum, W.; Hohne, G. W. H.; Wilke, W.; Arnold, M.; Wegner, T. *Macromol. Chem. Phys.* **1995**, *196*, 3797.

(65) Prasad, A. Polyethylene, Low-Density. In *Polymer Data Handbook*; Mark, J. E., Ed.; Oxford University: New York, 1999; p 518.

(66) Prasad, A. Polyethylene, Linear Low-Density. In *Polymer Data Handbook*; Mark, J. E., Ed.; Oxford University: New York, 1999; p 508.

(67) Prasad, A. Polyethylene, Metallocene Linear Low-Density. In *Polymer Data Handbook*; Mark, J. E., Ed.; Oxford University: New York, 1999; p 529.

(68) Fuller, C. S. *Chem. Rev.* **1940**, *26*, 143.

(69) Fuller, C. S.; Frosch, C. J. *J. Am. Chem. Soc.* **1939**, *61*, 2575.

(70) Maglio, G.; Marchetta, C.; Botta, A.; Palumbo, R.; Pracella, M. *Eur. Polym. J.* **1979**, *15*, 695.

(71) Cho, I.; Lee, K. *Macromol. Chem. Phys.* **1997**, *198*, 861.

(72) Williams, D. H.; Westwell, M. S. *Chem. Rev.* **1998**, *27*, 57.

(73) Atkins, E. D. T.; Hill, M.; Hong, S. K.; Keller, A.; Organ, S. *Macromolecules* **1992**, *25*, 917.

(74) Jones, N. A.; Atkins, E. D. T.; Hill, M. J.; Cooper, S. J.; Franco, L. *Macromolecules* **1996**, *29*, 6011.

(75) Jones, N. A.; Atkins, E. D. T.; Hill, M. J.; Cooper, S. J.; Franco, L. *Macromolecules* **1997**, *30*, 3569.

(76) Champetier, G.; Aélion, R. *Bull. Soc. Chim. Fr.* **1948**, 683.

(77) Hill, R.; Walker, E. E. *J. Polym. Sci.* **1948**, *3*, 609.

(78) Trifan, D. S.; Terenzi, J. F. *J. Polym. Sci.* **1958**, *28*, 443.

(79) Navarro, E.; Franco, L.; Subirana, J. A.; Puiggali, J. *Macromolecules* **1996**, *28*, 8742.

(80) Navarro, E.; Aleman, C.; Subirana, J. A.; Puiggali, J. *Macromolecules* **1996**, *29*, 5406.

(81) Puiggali, J.; Aceituno, J. E.; Navarro, E.; Campos, J. L.; Subirana, J. A. *Macromolecules* **1996**, *29*.

(82) Franco, L.; Cooper, S. J.; Atkins, E. D. T.; Hill, M. J.; Jones, N. A. *J. Polym. Sci., Part B: Polym. Phys.* **1998**, *36*, 1153.

(83) Veda, S.; Kimura, T. *Chem. High Polym. (Japan)* **1958**, *15*, 243.

(84) Tsuruda, M.; Arimoto, H.; Ishibashi, M. *Chem. High Polym. (Japan)* **1958**, *15*, 619.

(85) Ziabicki, A. *Kolloid-Z.* **1960**, *167*, 132.

(86) Ziabicki, A.; Kedzierska, A. *J. Appl. Polym. Sci.* **1959**, *2*, 14.

(87) Brill, R. *Z. Phys. Chem. (Munich)* **1943**, *1353*, 61.

(88) Ramesh, C.; Keller, A.; Eltink, S. J. E. A. *Polymer* **1994**, *35*, 2483.

(89) *Nylon Plastics Handbook*; Kohan, M. I., Ed.; Hanser: Munich, 1995.

(90) Miller, R. L. Crystallographic Data and Melting Points for Various Polymers. In *Polymer Handbook*; 4th ed.; Brandrup, J., Immergut, E. H., Grulke, E. A., Eds.; John Wiley & Sons: New York, 1999.

(91) Ehrenstein, M.; Dellsperger, S.; Kocher, C.; Stutzmann, N.; Weder, C.; Smith, P. *Polymer* **2000**, *41*, 3531.

(92) Dreyfuss, P.; Keller, A. *J. Polym. Sci., Part B: Polym. Phys.* **1970**, *8*, 253.

(93) Atkins, E. D. T.; Keller, A.; Sadler, D. M. *J. Polym. Sci., Part A: Polym. Chem.* **1972**, *10*, 863.

(94) Burmester, A. F.; Dreyfuss, P.; Geil, P. H.; Keller, A. *J. Polym. Sci., Polym. Lett. Ed.* **1972**, *10*, 769.

(95) Hinrichsen, G. *Makromol. Chem.* **1973**, *166*, 291.

(96) Dreyfuss, P. *J. Polym. Sci., Polym. Phys. Ed.* **1973**, *11*, 201.

(97) Magill, J. H.; Girolamo, M.; Keller, A. *Polymer* **1981**, *22*, 43.

(98) Subirana, J. A.; Aceituno, J. E. *Macromol. Symp.* **1996**, *102*, 317.

(99) Zahn, H.; Kohler, K. *Kolloid-Z.* **1950**, *118*, 115.

(100) Borchert, W. Z. *Angew. Chem.* **1951**, *63*, 31.

(101) Zahn, H.; Winter, V. *Kolloid-Z.* **1952**, *128*, 142.

(102) Saito, Y.; Nansai, S.; Kinoshita, S. *Polym. J. (Tokyo)* **1972**, *3*, 113.

(103) Frisch, K. C.; Klempner, D. K. Polyurethanes. In *Comprehensive Polymer Science*; Pergamon: Oxford, 1989; Vol. 5, p 413.

(104) Saito, Y.; Hara, K.; Kinoshita, S. *Polym. J. (Tokyo)* **1982**, *14*, 19.

(105) Kinoshita, Y. *Makromol. Chem.* **1959**, *33*, 21.

(106) Vogelsong, D. C. *J. Polym. Sci., Part A* **1963**, *1*, 1055.

(107) Rusanova, E. E.; Sebyakin, Y. L.; Volkova, L. V.; Evstigneeva, R. P. *Zh. Org. Khim. (Engl. Transl.)* **1984**, *20*, 279.

(108) Buysch, H.; Hünig, S. *Angew. Chem.* **1966**, *78*, 145.

(109) Hünig, S.; Buysch, H. *Chem. Ber.* **1967**, *100*, 4017.

(110) Améduri, B.; Berrada, K.; Boutevin, B.; Bowden, R. D. *Polym. Bull. (Berlin)* **1992**, *28*, 389.

(111) Améduri, B.; Berrada, K.; Boutevin, B.; Bowden, R. D. *Polym. Bull. (Berlin)* **1992**, *28*, 497.

CHAPTER 2. SYNTHESIS AND CHARACTERIZATION OF LONG-CHAIN, ALIPHATIC α,ω-DIOLS

2.1 Introduction

For this research project, model long-chain, aliphatic polyurethanes of the general structure $[O\text{-}(CH_2)_m\text{-}O\text{-}C(O)\text{-}NH\text{-}(CH_2)_n\text{-}NH\text{-}C(O)]_n$ were desired. Polyurethanes are typically synthesized from either a polyaddition of diols and diisocyanates or by a polycondensation of bischloroformates and diamines. In order to synthesize these model polymers, long-chain, monodisperse, aliphatic α,ω-monomers (e.g. diols, diisocyanates, bischloroformates, or diamines) were needed.

Previous work in the Penelle group on long-chain, semi-crystalline polyesters by Cedric Le Fevere de Ten Hove[1] and Joel Schall[2] reported on the synthesis of increasingly long-chain, telechelic diols (22, 30, and 44 methylene units long). This research project expanded their work and includes the synthesis of more aliphatic α,ω-diols (22, 32, and 46 methylene units long). These diols were synthesized following literature procedures,[3,4] that were modified and optimized. The 1,22-diol was synthesized by the Wurtz-coupling method developed by Rusanova et al.[3] (and later modified by Le Fevere de Ten Hove). The final step in this procedure was modified and optimized, resulting in a shorter reaction time and higher yield. An alternate synthetic route employing the enamine-coupling method originally developed by Hünig et al.[4] for the synthesis of long-chain α,ω-diacids was modified and used to make the longer 1,32- and 1,46-diols.

It was desired that the aliphatic segment of these model polyurethanes derived from the long-chain diols be long enough to crystallize at room temperature. By

examining the melting temperature of the corresponding *n*-alkanes series[5] (Figure 2.1), it was determined that a monomer length of at least 20 consecutive methylene units should be satisfactory. To give a complete picture, a series of increasingly aliphatic polyurethanes were synthesized from several monodisperse, telechelic diols of length 12 (short-chain), 22 (around the minimum length to be considered long-chain), and 32 and 46 (both long-chain) consecutive methylene units.

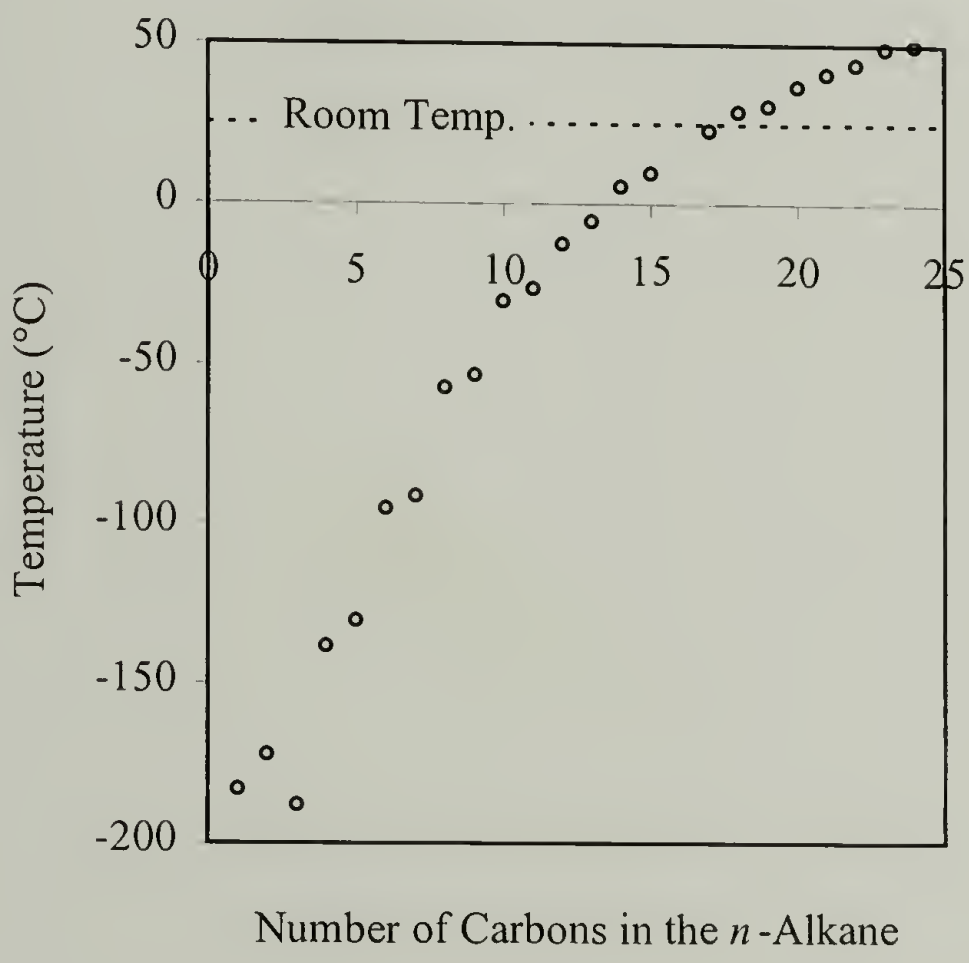

Figure 2.1. Necessary Length of the Aliphatic Segment (See Reference 5).

2.2 Experimental

2.2.1 Characterization

^{1}H- and ^{13}C-nuclear magnetic resonance (NMR) spectra were obtained either in deuterated chloroform ($CDCl_3$), benzene (C_6D_6), or methanol (CD_3OD) from a Bruker 300 MHz NMR spectrometer at room temperature or in deuterated $CDCl_3$ or dimethylsulfoxide (DMSO-d_6) from a Bruker 500 or 600 MHz NMR spectrometer at elevated temperatures. Infrared (IR) spectra were recorded on a Bio-Rad FTS 175C spectrometer using a total of 16 scans. Elemental analysis was carried out by the Microanalytical Laboratory of the University of Massachusetts, Amherst, via the classical Modified Pregl-Dumas reaction using an Exeter Analytical 240A elemental analyzer.

2.2.2 Thermal Analysis

Thermogravimetric analysis (TGA) was performed on 5 to 10 mg samples using a Thermal Analysis Instruments TGA 2950 flushed with nitrogen at a scan rate of 10 $K \cdot min^{-1}$. Decomposition temperatures T_d were taken at 5% weight loss. Melting points and transition temperatures T_t were observed using either a Perkin Elmer Pyris or Thermal Analysis Instruments Universal V2.5H DSC flushed with helium. The 5 to 10 mg samples were heated above their melting points to 200 °C, cooled to room temperature, and then reheated, all at a rate of 10 $K \cdot min^{-1}$. The first heating and cooling run was performed in order to erase the different thermal histories present in the samples. The T_m and T_t were taken as the peak of the melting and transition endotherms,

respectively, during the second heating run. The temperature scale was calibrated using indium and eicosane, and the heat of enthalpy was calibrated using indium.

2.2.3 Monomer Synthesis

2.2.3.1 General Considerations

Reagents used in the synthesis of these diols were obtained commercially, and unless otherwise stated, they were used without further purification. Triethylamine was dried over calcium hydride. Cyclohexane and chloroform were dried using phosphorous pentoxide. Acetone was dried with potassium carbonate. Benzene and tetrahydrofuran (THF) was dried over sodium and benzophenone. The Wurtz coupling reaction was performed using a 20 kHz, 600 Watt Sonics & Materials Inc. VCX ultrasonicator at 30% amplitude.

2.2.3.2 Synthesis of 1,22-Docosanediol Via Wurtz-Coupling

11-Bromo-1-(trimethylsilyloxy)undecane (1). Under an argon atmosphere, 11-bromo-1-undecanol (53.91 g, 0.21 mol) was dissolved in triethylamine (210 mL) at room temperature. Trimethylchlorosilane (25.68 g, 0.24 mol) was added dropwise to the rapidly stirred, light brown solution, and a white solid formed immediately. After 3.5 hours, petroleum ether (200 mL) was added to the mixture. The mixture was then filtered and washed with additional petroleum ether (500 mL). The transparent yellow solution was evaporated yielding 11-bromo-1-(trimethylsilyloxy)undecane (**1**) as a white powder (49.30 g, 94%). ^{1}H-NMR (300 MHz, $CDCl_3$) δ 3.56 (t, J = 6.8 Hz, 2H, CH_2-OTMS),

3.40 (t, J = 6.8 Hz, 2H, CH_2-Br), 1.85 (quintet, J = 6.8 Hz, 2H, CH_2-CH_2-Br), 1.52 (quintet, J = 6.8 Hz, 2H, CH_2-CH_2-OTMS), 1.50-1.20 (m, 14H, CH_2-CH_2-CH_2), 0.11 (s, 9H, OSi-(CH_3)$_3$).

11-Iodo-1-(trimethylsilyloxy)undecane (2). 11-Bromo-1-(trimethylsilyloxy)undecane (**1**) (46.29 g, 0.14 mol), sodium iodide (37.48 g, 0.25 mol), and acetone (205 mL) were mixed together and then refluxed for 2 hours. The resulting yellow solution was evaporated. Petroleum ether was then added, and the mixture was filtered and washed with more petroleum ether (500 mL). Evaporation of the solvent yielded 11-iodo-1-(trimethylsilyloxy)undecane (**2**) (46.08 g, 95%) as a light yellow solution. ^{1}H-NMR (300 MHz, $CDCl_3$) δ 3.57 (t, J = 6.8 Hz, 2H, CH_2-OTMS), 3.19 (t, J = 7.2 Hz, 2H, CH_2-I), 1.82 (quintet, J = 7.2 Hz, 2H, CH_2-CH_2-I), 1.53 (quintet, J = 6.8 Hz, 2H, CH_2-CH_2-OTMS), 1.40-1.25 (m, 14H, CH_2-CH_2-CH_2), 0.11 (s, 9H, OSi-(CH_3)$_3$).

1,22-Docosanediol (3). Finely cut pieces of sodium (1.19 g, 51.76 mmol) were added to cyclohexane (28.5 mL) in an argon-purged, double-jacketed, four-necked glass vessel. In order to both remove any water that might have been present and to clean the surface of the sodium, the mixture was pre-sonicated at 30% amplitude for 30 minutes, during which time the mixture turned a slight gray. During sonication, cold water was circulated through the jacket of the vessel in order to cool the mixture. 11-Iodo-1-(trimethylsilyloxy)undecane (**2**) (10.55 g, 28.48 mmol) was added, and the mixture immediately turned a deep opaque blue. The homogenous mixture was then sonicated for an additional 3.5 hours. After cooling to room temperature, methanol (14 mL) was slowly added to decompose any remaining sodium, and a white solid immediately appeared. The mixture was then carefully treated with deionized water (2.5 mL)

followed by sulfuric acid (1 mol·L^{-1}, 10 mL). The product was filtered and washed with deionized water (70 mL) until the pH was neutral. The resulting white solid was recrystallized from methanol (215 mL) to yield pure 1,22-docosanediol (**3**) (2.89 g, 59%); m.p. 106.8 °C, lit: 106.5-107 °C,[3] 106.3 °C,[1] 106.2 °C,[6] 106-107 °C,[7] 105.7-106.2 °C,[8] 105.7-105.9 °C,[9] 105.6-105.7 °C,[10] 105-106 °C,[11] 105-105.5 °C,[12] 104-105 °C,[13] 102-103 °C.[2] ^{1}H-NMR (300 MHz, $CDCl_3$) δ 3.65 (t, J = 6.6 Hz, 4H, CH_2-OH), 1.58 (m, 4H, CH_2-CH_2-OH), 1.40-1.20 (m, 36H, CH_2-CH_2-CH_2). ^{13}C-NMR (500 MHz, $CDCl_3$, 323 K) δ 63.36 (*C*H_2OH), 33.15 (*C*H_2CH_2OH), 29.92, 29.91, 29.90, 29.86, 29.84, 29.69 (all remaining aliphatic *C*H_2), 26.03 (*C*$H_2CH_2CH_2$OH). IR (KBr): 3304 cm^{-1} (OH stretch), 2918 cm^{-1} (asymmetric CH stretch), 2849 cm^{-1} (symmetric CH stretch), 1474 and 1462 cm^{-1} (CH_2 bend), 731 cm^{-1} (in-phase CH_2 rock), 719 cm^{-1} (out-of-phase CH_2 rock). Anal. Calc. for $C_{22}H_{46}O_2 \cdot (H_2O)_{2.1}$ (344.5): C, 76.68; H, 13.52. Found: C, 76.62: H, 13.83.

2.2.3.3 Synthesis of 1,32-Dotriacontanediol Based on Enamine-Coupling

1-Morpholino-1-cyclododecene (4). Cyclododecanone (30.50 g, 0.17 mol), morpholine (29.05 g, 0.33 mol), benzene (75 mL), and *p*-toluenesulfonic acid (*p*-TSOH, trace amounts) were added to a two-necked flask equipped with a Dean-Stark trap. The mixture was refluxed (approximately 2 to 3 days) until no additional water was collected in the trap. Benzene and any excess morpholine were then evaporated off. Cyclododecanone, a white solid at room temperature, was distilled with the aid of a heat gun in order to keep the cyclododecanone from solidifying in the distillation apparatus. Distillation of the remaining brown liquid resulted in isolating 1-morpholino-1-cyclododecene (**4**) as a clear liquid (33.99 g, 81%). ^{1}H-NMR (300 MHz, $CDCl_3$) δ 4.20

(t, J = 7.7 Hz, 1H, C*H*=CR), 3.42 (t, J = 4.7 Hz, 4H, CH_2-O), 2.40 (t, J = 4.7 Hz, 4H, CH_2-N), 2.00 (m, 4H, CH_2-CH=CR), 1.40-1.20 (m, 20H, CH_2-CH_2-CH_2).

1,4-Bis-(2,14-dioxo-cyclotetradecyl)butane (5). 1-Morpholino-1-cyclododecene (**4**) (4.94 g, 19.64 mmol), chloroform (2.5 mL), and triethylamine (3 mL) were added to an argon-purged, three-necked flask and cooled in an ice/water/salt bath. Suberoyl chloride (1.58 g, 7.50 mmol) in chloroform (2.5 mL) was slowly added dropwise while keeping the temperature of the mixture below 15 °C. After addition of the acid, the yellow mixture was allowed to warm to room temperature and stirred for 4 hours. Chloroform (40 mL) and hydrochloric acid (2.5 mol·L^{-1}, 20 mL) were added, and the mixture was stirred for 24 hours. The two phases were then separated. The aqueous layer was extracted with chloroform (6 x 5 mL aliquots) and the organic phase with deionized water (6 x 5 mL aliquots). The chloroform from the combined organic phases was evaporated. The resulting yellow solid was recrystallized from ethyl acetate (100 mL) yielding 1,4-bis-(2,14-dioxo-cyclotetradecyl)butane (**5**) as a white powder (1.05 g, 28%); m.p. 187.3 °C, lit.: 183-184 °C.[4,14] ^{1}H-NMR (300 MHz, $CDCl_3$) δ 3.57 (t, J = 7.2 Hz, 2H, C*H*-$(C=O)_2$), 2.50-2.30 (m, 8H, CH_2-(C=O)), 1.80-1.50 (m, 12H, CH_2-CHR-(C=O)), 1.40-1.10 (m, 26H, CH_2-CH_2-CH_2). IR (KBr): 2944 cm^{-1} (cyclic, asymmetric CH stretch), 2921 cm^{-1} (acyclic, asymmetric CH stretch), 2862 (cyclic, symmetric CH stretch), 2850 cm^{-1} (acyclic, symmetric CH stretch), 1695 cm^{-1} (CO stretch), 1462 cm^{-1} (CH_2 bend), 732 cm^{-1} (in-phase CH_2 rock), 724 cm^{-1} (out-of-phase CH_2 rock).

13,20-Dioxo-dotriacontanedioic Acid (6). Sodium hydroxide (5.80 g, 0.15 mol) and 1,4-bis-(2,14-dioxo-cyclotetradecyl)butane (**5**) (11.21 g, 22.29 mmol) were each separately refluxed in 2-methoxyethanol (65 and 110 mL, respectively) until they

dissolved. The two red solutions were then combined, and a white solid quickly formed. After refluxing the combined mixture for 1.5 hour, the mixture was filtered and washed first with 2-methoxyethanol and then ethanol. The resulting pink solid was recrystallized from acetic acid (400 mL) to yield 13,20-dioxo-dotriacontanedioic acid (**6**) as a white powder (11.75 g, 99%); m.p. 145.9 °C, lit: 142 °C.[4] ^{1}H-NMR (500 MHz, DMSO-d_6, 373 K) δ 2.37 (t, J = 7.3 Hz, 8H, CH_2-(C=O)), 2.19 (t, J = 7.3 Hz, 4H, CH_2-COOH), 1.54-1.48 (m, 12H, CH_2-CH_2-(C=O)), 1.32-1.25 (m, 32H, CH_2-CH_2-CH_2). IR (KBr): 3046 (OH stretch), 2918 cm^{-1} (asymmetric CH stretch), 2851 cm^{-1} (symmetric CH stretch), 1703 cm^{-1} (CO stretch), 1474 and 1462 cm^{-1} (CH_2 bend), 729 cm^{-1} (in-phase CH_2 rock), 718 cm^{-1} (out-of-phase CH_2 rock).

1,32-Dotriacontanedioic Acid (7). 13,20-Dioxo-dotriacontanedioic acid (**6**) (3.83 g, 71.07 mmol), hydrazine hydrate (85%, 10 mL), and triethanolamine (32 mL) were added to a three-necked flask fitted with a condenser and thermometer. The mixture was heated at 125 °C for 2 hours. Potassium hydroxide (2.15 g, 38.32 mmol) in triethanolamine (11.5 mL) was heated at 160 °C until the potassium hydroxide dissolved. Both mixtures were cooled to around 80 °C, and the potassium hydroxide solution was then carefully added to the dihydrazone solution. The temperature of the solution was increased to 135 °C at which point foaming occurred. The solution was stirred at this temperature for 0.5 hours. The condenser was then removed, and the temperature was increased to 195 °C over 1.5 hours in order to drive off the water. Care is needed when raising the temperature in order to avoid excessive foaming. The reaction was stirred at 195 °C for 6.5 hours. After cooling to room temperature, deionized water (60 mL) was added to the white solid. The temperature was raised to 100 °C and filtered hot. The

sample was then recrystallized from acetic acid (150 mL) yielding 1,32-dotriacontanedioic acid (**7**) as a white solid (3.19 g, 88%); m.p. 129.3 °C, lit.: 128-129 °C,[4] 124-127 °C.[15] ^{1}H-NMR (500 MHz, DMSO-d_6, 373 K) δ 2.20 (t, J = 7.2 Hz, 4H, CH_2-COOH), 1.57 (quintet, J = 6.7 Hz, 4H, CH_2-CH_2-COOH), 1.36-1.26 (m, 52H, CH_2-CH_2-CH_2). IR (KBr): 3028 (OH stretch), 2920 cm^{-1} (asymmetric CH stretch), 2851 cm^{-1} (symmetric CH stretch), 1706 cm^{-1} (CO stretch), 1474 and 1465 cm^{-1} (CH_2 bend), 730 cm^{-1} (in-phase CH_2 rock), 720 cm^{-1} (out-of-phase CH_2 rock).

Dimethyl 1,32-Dotriacontanoate (8). 1,32-Dotriacontanedioic acid (**7**) (6.38 g, 12.49 mmol), methanol (120 mL), and concentrated sulfuric acid (4.5 mL) were combined and refluxed for 16 hours. After cooling, the mixture was filtered and washed with deionized water. The white powder was then recrystallized from methanol (50 mL) yielding dimethyl 1,32-dotriacontanoate (**8**) (6.48 g, 96%); m.p. 90.3 °C, lit.: 87-89 °C,[15] 85.5-87 °C.[16] ^{1}H-NMR (300 MHz, C_6D_6) δ 3.46 (s, 6H, CH_3-O-(C=O)), 2.23 (t, J = 7.3 Hz, 4H, CH_2-(C=O)), 1.68 (quintet, J = 6.4 Hz, 4H, CH_2-CH_2-(C=O)), 1.50-1.30 (m, 52H, CH_2-CH_2-CH_2). IR (KBr): 2918 cm^{-1} (asymmetric CH stretch), 2850 cm^{-1} (symmetric CH stretch), 1743 cm^{-1} (CO stretch), 1475 and 1463 cm^{-1} (CH_2 bend), 730 cm^{-1} (in-phase CH_2 rock), 720 cm^{-1} (out-of-phase CH_2 rock).

1,32-Dotriacontanediol (9). Dimethyl 1,32-dotriacontanoate (**8**) (0.98 g, 1.82 mmol) was added to THF (200 mL) and refluxed. Lithium aluminum hydride (total 0.57 g, 15.02 mmol) was carefully added to the refluxing solution in three portions over the course of one day. The mixture was then refluxed for an additional day. After cooling the gray mixture, deionized water was carefully added until there was no more evolution of hydrogen gas. Concentrated hydrochloric acid was then added to the white mixture

until a pH of 2 was reached. The mixture was filtered, and the white sample was recrystallized from a mixture (1:1 volume ratio) of methanol (50 mL) and chloroform (50 mL) to yield pure 1,32-dotriacontanediol (**9**) (0.57 g, 62%); m.p. 114.9 °C, lit.: 115-117 °C,[16] 98 °C,[17] 94 °C.[18] ^{1}H-NMR (600 MHz, DMSO-d_6, 373 K) δ 3.42 (t, J = 6.5 Hz, 4H, CH_2-OH), 1.45 (quintet, J = 6.5 Hz, 4H, CH_2-CH_2-OH), 1.42-1.26 (m, 56H, CH_2-CH_2-CH_2). ^{13}C-NMR (500 MHz, DMSO-d_6, 373 K) δ 60.36 (*C*H_2OH), 31.96 (*C*H_2CH_2OH), 28.37, 28.30, 28.27, 28.24 (all remaining aliphatic *C*H_2), 24.89 (*C*$H_2CH_2CH_2$OH). IR (KBr): 3318 cm^{-1} (OH stretch), 2918 cm^{-1} (asymmetric CH stretch), 2849 cm^{-1} (symmetric CH stretch), 1472 and 1463 cm^{-1} (CH_2 bend), 732 cm^{-1} (in-phase CH_2 rock), 720 cm^{-1} (out-of-phase CH_2 rock). Anal. Calc. for $C_{32}H_{66}O_2 \cdot (H_2O)_{21.1}$ (490.91): C, 77.33; H, 13.70. Found: C, 77.36: H, 13.69.

2.2.3.4 Synthesis of 1,46-Hexatetracontanediol Based on Multiple Enamine-Couplings

1-Morpholino-1-cyclohexane (10). Cyclohexanone (58.65 g, 0.60 mol), morpholine (61.94 g, 0.71 mol), benzene (150 mL), and *p*-TSOH (trace amounts) were added to a two-necked flask equipped with a Dean-Stark trap. The mixture was refluxed (approximately 1 day) until no additional water was collected in the trap. Benzene and any excess morpholine were then evaporated off. Distillation of the remaining liquid resulted in isolating 1-morpholino-1-cyclohexene (**10**) as a clear liquid (61.69 g, 62%). ^{1}H-NMR (300 MHz, C_6D_6) δ 4.57 (t, J = 3.8 Hz, 1H, C*H*=CR), 3.55 (t, J = 4.7 Hz, 4H, CH_2-O), 2.55 (t, J = 4.7 Hz, 4H, CH_2-N), 2.08 (m, 2H, CH_2-CH=CR), 1.88 (t, J = 5.8 Hz, 2H, CH_2-CR=CH), 1.62-1.45 (m, 4H, CH_2-CH_2-CH_2).

2,2'-Sebacoyldicyclohexanone (11). 1-Morpholino-1-cyclohexene (**10**) (61.69 g, 0.37 mol), chloroform (175 mL), and triethylamine (50 mL) were added to an argon-purged, three-necked flask and heated in an oil bath set at 35 °C. Sebacoyl chloride (35.87 g, 0.15 mol) in chloroform (70 mL) was slowly added dropwise to the mixture. The solution was stirred for an additional 3 hours at 35 °C during which time the solution turned first yellow, then orange, and finally red. Hydrochloric acid (20%, 150 mL) was added, and the mixture was refluxed for 5.5 hours. After cooling to room temperature, the two phases were then separated. The orange, organic phase was extracted with water (6 x 50 mL aliquots). The aqueous phase and washings were combined, and the pH was adjusted from 0 to 6 with a sodium hydroxide solution (25%). The combined aqueous phase was then extracted with chloroform (5 x 30 mL aliquots). The chloroform from the combined organic phase and washings was then evaporated yielding the crude 2,2'-sebacoyldicyclohexanone (**11**) as a viscous, yellow oil (77.54 g, 124%). ^{1}H-NMR (300 MHz, $CDCl_3$) δ 3.65 (t, J = 6.5 Hz, 2H, C*H*-(C=O)$_2$), 2.57-2.22 (m, 8H, CH_2-(C=O)), 1.87-1.51 (m, 12H, CH_2-CHR-(C=O)), 1.46-1.21 (m, 12H, CH_2-CH_2-CH_2).

Disodium Salt of 7,16-Dioxo-docosanedioic Acid (12). Sodium hydroxide (47.94 g, 1.20 mol) was heated in ethanol (560 mL) until all the salt dissolved, and the orange solution was then cooled to room temperature. 2,2'-Sebacoyldicyclohexanone (**11**) (77.54 g, 0.21 mol) in warm ethanol (120 mL) was added, a precipitate quickly formed, and the mixture was refluxed for 1.5 hours. The mixture was then cooled, filtered, and the white solid was washed with ethanol to yield the crude disodium salt of 7,16-dioxo-docosanedioic acid (**12**) (79.16 g, 84%).

1,22-Docosanedioic Acid (13). The crude disodium salt of 7,16-dioxo-docosanedioic acid (**12**) (201.91 g, 0.46 mol) in triethanolamine (420 mL) was added to a three-necked flask fitted with a condenser and thermometer. The orange mixture was heated at 180 °C until the salt dissolved. The solution was cooled to 130 °C, and hydrazine hydrate (250 mL) was then added. The mixture was refluxed at 130 °C for 4 hours. Potassium hydroxide (69.56 g, 1.24 mol) in triethanolamine (170 mL) was heated at 160 °C until the salt dissolved. Both mixtures were cooled to below 100 °C, and the potassium hydroxide solution was then carefully added to the dihydrazone solution. The temperature was increased to 140 °C at which point foaming occurred. The condenser was then removed, and the temperature was increased to 195 °C over 2 hours in order to drive off the water. Care is needed when raising the temperature in order to avoid excessive foaming. The reaction was stirred at 195 °C for 6 hours. After cooling below 100 °C, deionized water (1.5 L) was added to the white solid. The mixture was then acidified to a pH of 2 using hydrochloric acid (600 mL), cooled, and filtered. The sample was recrystallized from 2-methoxyethanol (750 mL) and then 2-butanone (750 mL) yielding 1,22-docosanedioic acid (**13**) as a white solid (19.21 g, 11%). ^{1}H-NMR (300 MHz, CD_3OD) δ 2.27 (t, J = 7.4 Hz, 4H, CH_2-COOH), 1.59 (m, 4H, CH_2-CH_2-COOH), 1.37-1.24 (m, 32H, CH_2-CH_2-CH_2).

1,22-Docosanediacid Chloride (14). 1,22-Docosanedioic acid (**13**) (29.61 g, 0.08 mol), thionyl chloride (28.56 g, 0.24 mol), and benzene (160 mL) were heated to 50 °C in an argon-purged flask for 3.5 hours. The solution was then cooled, and benzene as well as any excess thionyl chloride were evaporated off yielding crude 1,22-docosanediacid chloride (**14**) as a viscous, brown oil. Due to the instability of the

compound to water, the diacid chloride was used immediately in the next step without further purification or characterization.

1,18-Bis-(2,14-dioxo-cyclotetradecyl)octadecane (15). 1-Morpholino-1-cyclododecene (**4**) (49.40 g, 0.20 mol), chloroform (20 mL), and triethylamine (34 mL) were added to an argon-purged, three-necked flask and cooled in an ice/water/salt bath. 1,22-Docosanediacid chloride (**14**) in chloroform (240 mL) was slowly added dropwise, while keeping the temperature of the mixture below 15 °C. After addition of the acid, the brown mixture was allowed to warm to room temperature and was then stirred for 16 hours. Chloroform (600 mL) and hydrochloric acid (2.5 $mol \cdot L^{-1}$, 600 mL) were added, and the mixture was stirred for 24 hours. The two phases were then separated. The aqueous layer was extracted with chloroform (6 x 50 mL aliquots) and the organic phase with deionized water (6 x 50 mL aliquots). The chloroform from the combined organic phases was evaporated. The resulting solid was recrystallized from ethyl acetate (1.5 L) yielding 1,18-bis-(2,14-dioxo-cyclotetradecyl)octadecane (**15**) as a tan powder (33.28 g, 60% from the diacid). ^{1}H-NMR (300 MHz, $CDCl_3$) δ 3.60 (t, J = 7.25 Hz, 2H, C*H*-$(C=O)_2$), 2.58-2.33 (m, 8H, CH_2-(C=O)), 1.90-1.55 (m, 12H, CH_2-CHR-(C=O)), 1.48-1.00 (m, 60H, CH_2-CH_2-CH_2).

Disodium Salt of 13,34-Dioxo-hexatetracontanedioic Acid (16). Sodium hydroxide (10.33 g, 0.26 mol) and 1,18-bis-(2,14-dioxo-cyclotetradecyl)octadecane (**15**) (30.17 g, 0.04 mol) were each separately refluxed in 2-methoxyethanol (180 and 300 mL, respectively) until they dissolved. After cooling slightly, the two solutions (yellow and orange, respectively) were combined, and a white solid quickly formed. After refluxing the combined mixture for 1.5 hours, the mixture was filtered and washed first with 2-

methoxyethanol and then ethanol to yield the crude disodium salt of 13,34-dioxo-hexatetracontanedioic acid (**16**) (30.38 g, 90%).

1,46-Hexatetracontanedioic Acid (17). The crude disodium salt of 13,34-dioxo-hexatetracontanedioic acid (**16**) (9.99 g, 0.01 mol) in triethanolamine (67 mL) was added to a three-necked flask fitted with a condenser and thermometer. The mixture was heated at 170 °C until the salt dissolved. The solution was cooled to 130 °C, and hydrazine hydrate (85%, 20 mL) was added. The mixture was then refluxed at 170 °C for 16 additional hours. Potassium hydroxide (3.78 g, 0.07 mol) in triethanolamine (66 mL) was heated at 160 °C until the salt dissolved. Both mixtures were cooled to below 100 °C, and the potassium hydroxide solution was then carefully added to the dihydrazone solution. The temperature was increased to 160 °C at which point foaming occurred. The condenser was then removed, and the temperature was increased to 210 °C over 2 hours in order to drive off the water. Care is needed when raising the temperature in order to avoid excessive foaming. The reaction was stirred at 210 °C for 7 hours. After cooling to room temperature, deionized water (150 mL) was added to the orange solid. The temperature was raised to 100 °C, and the mixture was filtered hot. The sample was recrystallized from acetic acid (600 mL) and then from dioxane (600 mL) yielding 1,46-hexatetracontanedioic acid (**17**) as a white solid (5.14 g, 57%). ^{1}H-NMR (600 MHz, DMSO-d_6, 373 K) δ 2.50 (t, J = 7.4 Hz, 4H, CH_2-COOH), 1.48 (quintet, J = 7.3 Hz, 4H, CH_2-CH$_2$-COOH), 1.66-1.30 (m, 80H, CH$_2$-CH_2-CH$_2$).

Dimethyl 1,46-Hexatetracontanoate (18). 1,46-Hexatetracontanedioic acid (**17**) (5.14 g, 7.27 mmol), methanol (120 mL), and concentrated sulfuric acid (4.5 mL) were combined and refluxed for 16 hours. After cooling, the mixture was filtered and washed

with deionized water. The white powder was then recrystallized from methanol (50 mL) yielding dimethyl 1,46-hexatetracontanoate (**18**) (4.98 g, 93%). ^{1}H-NMR (300 MHz, C_6D_6) δ 3.37 (s, 6H, C*H*$_3$-O-(C=O)), 2.13 (t, *J* = 7.5 Hz, 4H, C*H*$_2$-(C=O)), 1.52 (m, 4H, C*H*$_2$-CH$_2$-(C=O)), 1.44-1.18 (m, 80H, CH$_2$-C*H*$_2$-CH$_2$).

1,46-Hexatetracontanediol (19). Dimethyl 1,46-hexatetracontanoate (**18**) (4.98 g, 6.78 mmol) was added to THF (400 mL) and refluxed. Lithium aluminum hydride (total 3.05 g, 0.04 mol) was carefully added to the refluxing solution in three portions over the course of one day. The mixture was then refluxed for an additional day. After cooling the gray mixture, deionized water was carefully added until there was no more evolution of hydrogen gas. Concentrated hydrochloric acid was then added to the white mixture until a pH of 2 was reached. The mixture was filtered, and the white sample was recrystallized from a mixture (1:1 volume ratio) of methanol (100 mL) and chloroform (100 mL) to yield pure 1,46-hexatetracontanediol (**19**) (1.21 g, 26%); m.p. 117.0 °C. ^{1}H-NMR (600 MHz, DMSO-d$_6$, 373 K) δ 3.42 (t, *J* = 6.3 Hz, 4H, C*H*$_2$-OH), 1.45 (m, 4H, C*H*$_2$-CH$_2$-OH), 1.41-1.37 (m, 84H, CH$_2$-C*H*$_2$-CH$_2$). IR (KBr): 3357 cm^{-1} (OH stretch), 2918 cm^{-1} (asymmetric CH stretch), 2851 cm^{-1} (symmetric CH stretch), 1475 and 1465 cm^{-1} (CH$_2$ bend), 730 cm^{-1} (in-phase CH$_2$ rock), 719 cm^{-1} (out-of-phase CH$_2$ rock). Anal. Calc. for $C_{46}H_{94}O_2 \cdot (H_2O)_{2.0}$ (680.16): C, 81.23; H, 13.95. Found: C, 81.22: H, 14.12.

2.3 Results and Discussion

2.3.1 Monomer Synthesis

2.3.1.1 Overview of Synthetic Methods

Long-chain (20 or more consecutive methylene units), aliphatic α,ω-diols can be extracted and isolated from natural products such as wood, cork, and waxes.[19] However, the purity of these diols is often low, and removal of the contaminants (typically other α,ω-diols or -diacids of similar length) is difficult. These long-chain diols can also be obtained by the reduction of the corresponding commercial α,ω-diacids. For example, 1,22-docosanediol can be synthesized from the reduction of 1,22-docosanedioic acid (available from Aldrich).[6,20] However, the purity of these α,ω-diacids is low (e.g. 1,22-docosanedioic acid is available in 85% purity), and the risk of producing α,ω-diols contaminated with their homologues (i.e. 1,20- and 1,24-diols) is high. Since the polyurethanes under examination in this project were model polymers, the monomers they were synthesized from had to be monodisperse. For this reason, the long-chain α,ω-diols were synthesized using organic procedures.

There are numerous methods to synthesize short-chain (less than 20 consecutive methylene units), monodisperse α,ω-diols in high purity and high yield. Patwardhan[21] compiled an excellent review of these general methods along with the specific conditions for the synthesis of the diols ranging from 5 to 19 consecutive methylene units long. However, these methods are typically limited in the length of the diol that can be

synthesized. The synthesis of long-chain, monodisperse α,ω-diols often requires multiple steps, and the products produced are often in low purity or low yield.

There are several literature procedures, most of which involve some sort of coupling of shorter mono- or di-functionalized compounds, for the synthesis of monodisperse, aliphatic, long-chain α,ω-diols. Drake and co-workers[8] employed the Kolbe reaction in 1941 to synthesize the 1,22-docosanediol. Different variations of this electrolysis-coupling reaction have been employed to make other long-chain α,ω-diols by Saotome et al.[22] (1,20-diol), Kimura et al.[12] (1,20- and 1,22-diols), Signer and Sprecher[23] (1,22-diol), Popovitz-Biro et al.[24] (1,22-diol), Murray and Schoenfeld[10] (1,24-diol), Musgrave et al.[25] (1,26-diol), and Adams and Bonnett[26] (1,30-diol). In 1961, Lukes and co-workers[27] and Slezak and co-workers[13] independently used a Grignard-coupling reaction to synthesize the 1,21- and 1,22-, 1,24-, and 1,26-diols, respectively. Similar methods were employed by Schall[2] (1,30-diol), Cho and Lee[28] (1,30-diol), and Schill and Merkel[29] (1,34-, 1,35-, and 1,38-diols). Two years later, Duhamel[7] made the 1,22- and 1,24-diols via a Wurtz-coupling procedure. Rusanova and co-workers[3] (1,22- and 1,44-diols) also employed a Wurtz-coupling reaction whose procedure was later modified by Le Fevere de Ten Hove.[1] An enamine-coupling reaction originally proposed by Hünig and Buysch[4] to make long-chain α,ω-diacids was used by White and co-workers[30] in 1971 to synthesize the 1,22-, 1,34-, and 1,46-diols. This enamine-coupling reaction has also been employed by Schill et al.[31] (1,24-diol), Ogawa and Nakamura[6] (1,24-diol), Furukawa et al.[18] (1,32-diol), and Moss et al.[17] (1,32-diol). In recent years, long-chain α,ω-diols were synthesized by Ogawa and Nakamura[6] (1,21- and 1,23-diols) and Grechishnikova and co-workers[16] (1,32-diol) through a ketene-dimerization method and a

Wittig reaction, respectively. These methods allow for a variety of long-chain, monodisperse α,ω-diols (containing up to 46 consecutive methylene units) to be synthesized, although their yields are often lower than that for the short-chain α,ω-diols.

2.3.1.2 Synthesis of the Long-Chain Diols Used in This Study

1,22-Docosanediol (**3**) HO-$(CH_2)_{22}$-OH is a natural product found in potato tuber skin,[32] stem bark and wood,[33] cork,[7] apple wax,[34] and carnauba wax.[10] However, as mentioned in the preceding section, the isolated diol is not monodisperse. Therefore, 1,22-diol was instead synthesized in a global yield of 53% by the Wurtz-coupling procedure (Scheme 2.1) originally developed by Rusanova et al.[3] and modified by Le Fevere de Ten Hove.[1] Using this method, commercially available 11-bromo-1-undecanol Br-$(CH_2)_{11}$-OH was converted to the hydroxyl-protected trimethylsilyl ether (**1**) Br-$(CH_2)_{11}$-$OSiMe_3$ (94% yield). The bromine was replaced with the more reactive iodine via the Finkelstein reaction, forming the protected iodo-alcohol (**2**) I-$(CH_2)_{11}$-$OSiMe_3$ (95% yield). Two equivalents of the protected iodo-alcohol were then coupled using a sonically activated Wurtz-coupling reaction. The sample was then deprotected and purified via recrystallization to yield 1,22-docosanediol (**3**) (59% yield).

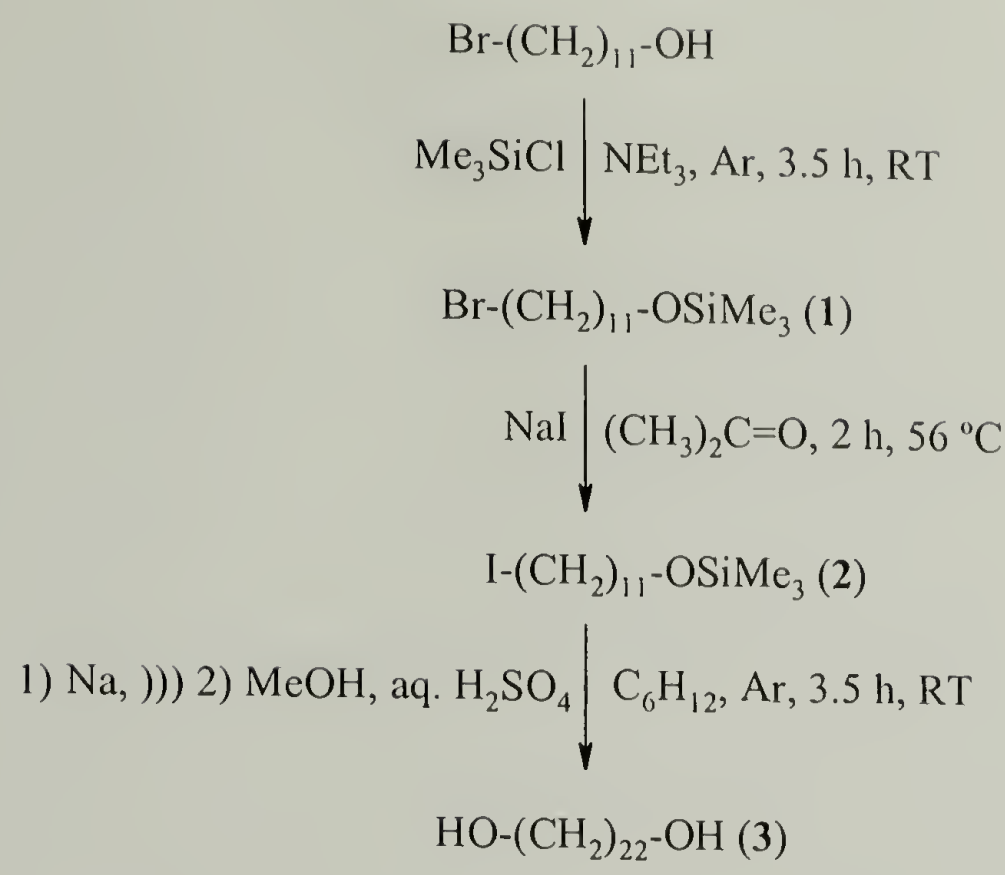

Scheme 2.1. Synthesis of 1,22-Docosanediol (**3**).

The final step (Wurtz-coupling in the presence of metallic sodium) of the 1,22-docosanediol synthesis had a significant side reaction (Scheme 2.2). This side reaction came from the abstraction of a hydrogen atom from a protected iodo-alcohol (which formed an additional side product, the 10-undecen-1-ol $HO\text{-}(CH_2)_9\text{-}CH{=}CH_2$), from the solvent, or from any water that was present to form 1-undecanol $HO\text{-}(CH_2)_{10}\text{-}CH_3$. In addition, the coupling reaction usually did not go to completion, resulting in some remaining protected iodo-alcohol. All of these side products were observed before purification of the diol using ^{1}H-NMR (Figure 2.2).

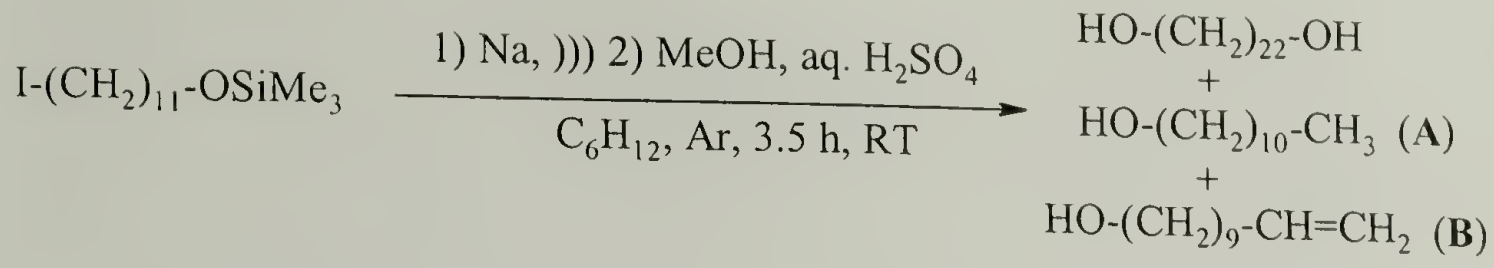

Scheme 2.2. Formation of the Side Products (A = 1-Undecanol and B = 10-Undecen-1-ol) During the Synthesis of 1,22-Docosanediol.

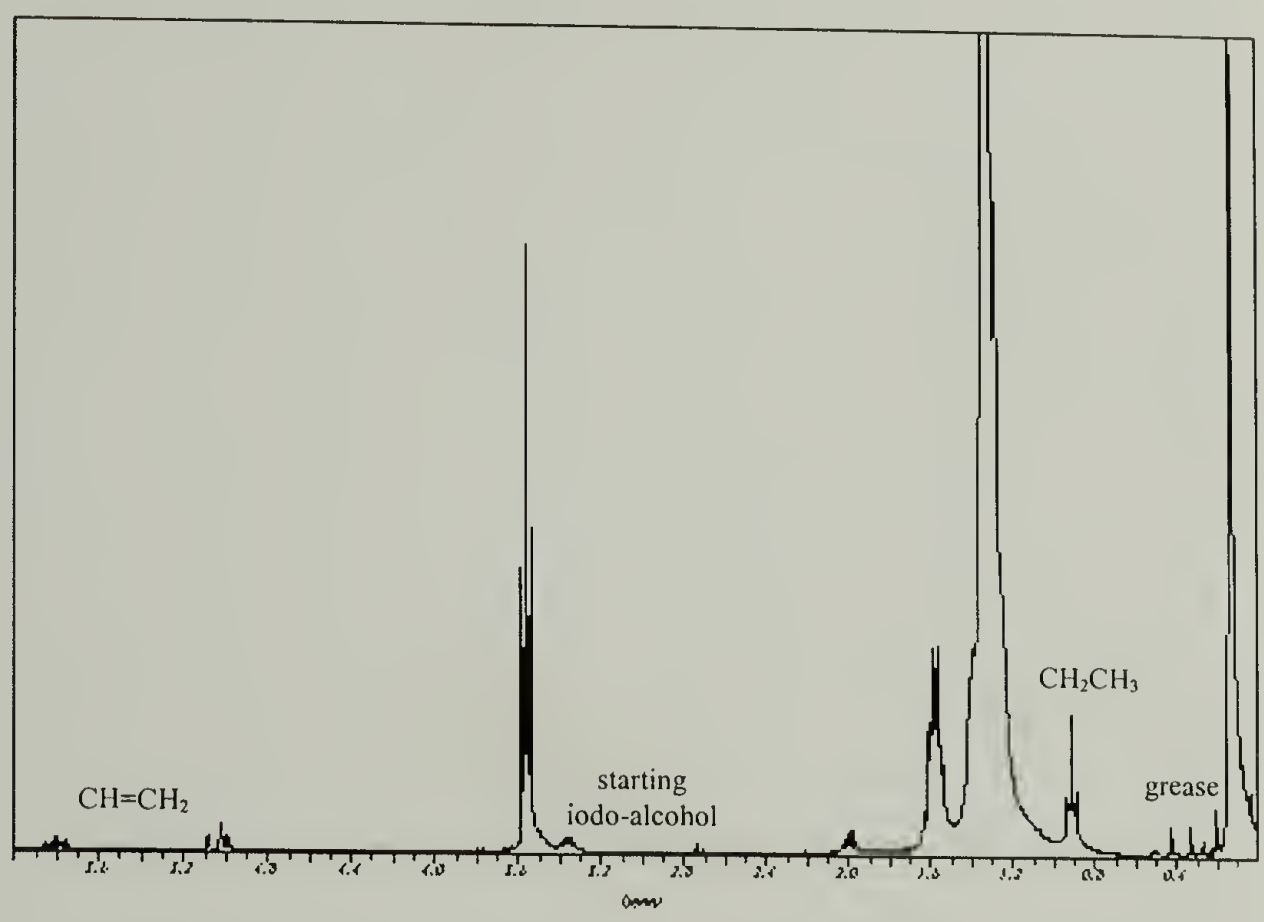

Figure 2.2. NMR Spectrum of 1,22-Docosanediol Before Recrystallization Showing the Presence of Side Products (A = 1-Undecanol and B = 10-Undecen-1-ol).

The exact mechanism of the Wurtz-coupling reaction is under considerable debate.[35] Two reaction mechanisms have been proposed.[36] In the first mechanism (S_N2 substitution), sodium alkyl is formed and then condenses with a molecule of alkylhalide to form the carbon-carbon bond. In the second mechanism (free-radical), an alkyl free-radical is formed, and two radicals then combine to form the hydrocarbon. The results (amount and type of side products) obtained in this study are more consistent with a free-

radical mechanism. In a free-radical mechanism, the free-radical is destroyed by either combination with another free-radical (forming 1,22-docosanediol) or by disproportionation with another molecule (forming 1-undecanol and 10-undecen-1-ol). The higher proportion of combination versus disproportionation is consistent with that observed for the free-radical polymerization of ethylene (extent of disproportionation is no greater than 10% at most).[37,38]

In order to both limit the side reaction as well as optimize the use of the sonication equipment, the literature procedure developed by Rusanova et al.[3] and the modified synthetic method by Le Fevere de Ten Hove[1] were again modified and optimized (Table 2.1). The modifications reported by Le Fevere de Ten Hove involved using benzene rather than ether as the solvent and applying sonication. The result was an increase in the yield, although the overall reaction took longer. In this work, several variables including solvent, temperature, sonication, and sodium concentration were examined.

Table 2.1. Optimization of the Wurtz-Coupling Reaction.

Solvent	Iodo-alcohol (mol)	Na (mol)	Heat/ Cool	Pre-sonicate[c] (h)	Pulse (s)	Time (h)	Yield (%)
Ether[a]	0.04	0.09	Heat	No[d]	No	10	42
Benzene[b]	0.2	0.35	Heat	0.5	No	18	58
Benzene	0.03	0.05	Heat	No	No	6	21
Benzene	0.03	0.05	Cool	No	No	3	48
Cyclohexane	0.03	0.05	Cool	No	No	4	38
Cyclohexane	0.03	0.05	Cool	No	2.5	5.5	35
Cyclohexane	0.03	0.05	Cool	0.5	No	3.5	55
Cyclohexane	0.03	0.03	Cool	0.5	No	4	36
Cyclohexane	0.03	0.05	Cool	0.5	No	3.5	59

a and b) See references 3 and 1, respectively.
c) 20 kHz, 600 Watt Sonics & Materials Inc. VCS ultrasonicator at 30% amplitude.
d) No sonication was used in this method.

Unlike the original procedure, the Wurtz-coupling procedure in this study was always performed with the aid of sonication. Han and Boudjouk[39] and shortly thereafter Lash and Berry[40] showed that sonic waves activate the coupling of alkyl and aryl chlorosilanes or organic halides in the presence of lithium. Since then sonication has proven useful in many organometallic reactions.[41-44] The enhanced reactivity by sonication of organometallic reactions has been attributed to several factors. Most widely accepted is the belief that cavitation cleans the surface of the metal by removing any passivating coatings (e.g. oxides) that may be present.[43] However, the increased reactivity has also been accredited to the breaking of the metal particles into smaller pieces and thus increasing the overall surface area[43] as well as to the tribochemical effect caused by the ejection of electrons from the metal surface.[45]

The sonicator (20 kHz, 600 Watt Sonics & Materials Inc. VCX ultrasonicator at 30% amplitude) used in this study differed from that employed by Le Fevere de Ten Hove (20 kHz, 350 Watt Sonifier ultrasonicator Model B-30 at no more than 30% amplitude). Keeping the other variables the same, the different sonication equipment resulted in a shorter reaction time but lower yield. Pulsing (turning the sonicator on and off at 2.5 second intervals) did not influence the yield and increased the reaction time. Although pre-sonication (sonication of the solvent and sodium mixture before addition of the iodo-alcohol) did not affect the reaction time, it did significantly increase the yield. This increase in yield could be attributed to better preparation of the metal surface or to the elimination of any water present, which would decrease the amount of side product produced and allow for an increase in the yield of the desired product.

Sonochemical reactions tend to have a temperature dependence.[42] Increased temperatures to produce more cavities, which in turn increases the effectiveness of the sonication. However, as the temperature is further increased, the vapor pressure is also increased. This creates a cushioning effect on the collapse of the bubbles created by sonication and lowers the sonication effectiveness. As a result, sonochemical reactions typically display an inverse-Arrhenius behavior and accelerate at lower temperatures.[44] For this reason, the Wurtz-coupling reaction was performed in a double-jacketed vessel, and cold water was circulated through the jacket. In the absence of this cooling mechanism, sonication caused the solvent to boil. Controlling the reaction temperature resulted in both a shorter reaction time and higher yield.

It is well accepted that the solvent used can greatly alter the effectiveness of sonication.[43] The vapor pressure, viscosity, and chemical reactivity of the solvent can all play a factor. However, the influence of the solvent could also be due to its ability to act as a chain transfer agent if the Wurtz-coupling reaction proceeds through a free-radical mechanism. For any of the above reasons, replacing benzene with cyclohexane as the solvent resulted in a shorter reaction time but lower yield.

The Wurtz-coupling reaction is typically performed under a large excess of sodium.[46] Decreasing the amount of sodium resulted in both a longer reaction time and lower yield.

The final, optimized procedure consisted of sonication, no pulsing, pre-sonication, cooling, cyclohexane as the solvent, and an excess of sodium. Compared to literature procedures, the reaction took less time (3.5 hours rather than 10 to 18 hours by Rusanova and Le Fevere de Ten Hove, respectively) and resulted in a slight increase in the yield of

the pure 1,22-diol (59% versus 48 to 58% by Rusanova and Le Fevere de Ten Hove, respectively).[1,3] A slightly higher yield should be achievable by using benzene rather than cyclohexanc as the solvent.

Following monobromination of the 1,22-diol, the Wurtz-coupling procedure could be repeated to make 1,44-tetratetraeontaneddiol HO-$(CH_2)_{44}$-OH. However, this procedure was found by Le Fevere de Ten Hove[1] to take a considerably longer time, and purification was much more difficult than was thc case for the synthesis of the 1,22-diol. Part of the purification problem was that the monobromination step led to the formation of three chemieally similar eompounds (starting diol, monobrominated alcohol, and the dibromo-eompound), and therefore, purification of the monobrominated product by means of medium-pressure liquid chromatography was neeessary. Additionally, in the final step of the proecdure, thc side produet 1-docosanol (and possibly 21-doeosen-1-ol) had a solubility behavior similar to the desired product, the 1,44-diol. As a result, in order to remove the by-produet and obtain the pure diol, several recrystallizations and extraetions were performed.

As a result of the increased reaction times and the greater difficulty in purifying thc produet, the Wurtz-coupling procedure was not used to synthesize longer α,ω-diols. Schall[2] attempted to make diols longer than 20 conseeutive methylene units using a eopper-eatalyzed, Grignard-eoupling of 2 equivalents of a protected bromo-alcohol Br-$(CH_2)_{11}$-OTHP with a diGrignard reagent BrMg-$(CH_2)_8$-MgBr. However, thc 1,30-triaeontancdiol HO-$(CH_2)_{30}$-OH he synthesized also had a relatively low yield (38%), and its low T_m of 75 to 78 °C (lit: 112-116 °C,[47] 112.8-113 °C,[9] 111-112 °C[28]) implied that even after recrystallization the diol was not pure (probably bromine- and methyl-

terminated impurities). Therefore, it was determined that another synthetic method would be necessary to obtain long-chain, monodisperse α,ω-diols. It was decided to try the enamine-coupling route developed by Hünig et al.[4] to make long-chain, telechelic diacids (32 and 46 methylene units long) that could then be reduced to the corresponding diols.

1,32-Dotriacontanediol (**9**) HO-$(CH_2)_{32}$-OH, like the 1,22-diol, is a natural product found in carnauba wax.[48] In this study, the diol was synthesized in a global yield of 12% from the reduction of the analogous diacid obtained from a [2 + 2] chain-extending, cycloaddition procedure (Scheme 2.3). Enamine (**4**) was synthesized (81% yield) by the acid-catalyzed condensation of commercially available morpholine and cyclododecanone. The enamine was actually commercially available, however it was cheaper to synthesize it then to purchase it. A [2 + 2] cycloaddition of the enamine and suberoyl chloride Cl-C(O)-$(CH_2)_6$-C(O)-Cl produced the cyclic tetraketone (**5**) (28% yield), which was ring-opened under basic conditions to the dioxo-dioic acid (**6**) HO_2C-$(CH_2)_{11}$-C(O)-$(CH_2)_6$-C(O)-$(CH_2)_{11}$-CO_2H (99% yield) and then reduced via the Wolff-Kishner reaction to form the diacid (**7**) HO_2C-$(CH_2)_{30}$-CO_2H (88% yield). In order to increase its solubility in THF, the diacid was converted to the diester (**8**) CH_3CO_2-$(CH_2)_{30}$-CO_2CH_3 (96% yield) via an acid-catalyzed esterification. The diester was then reduced using lithium aluminum hydride to yield 1,32-dotriacontanediol (**9**) (62% yield).

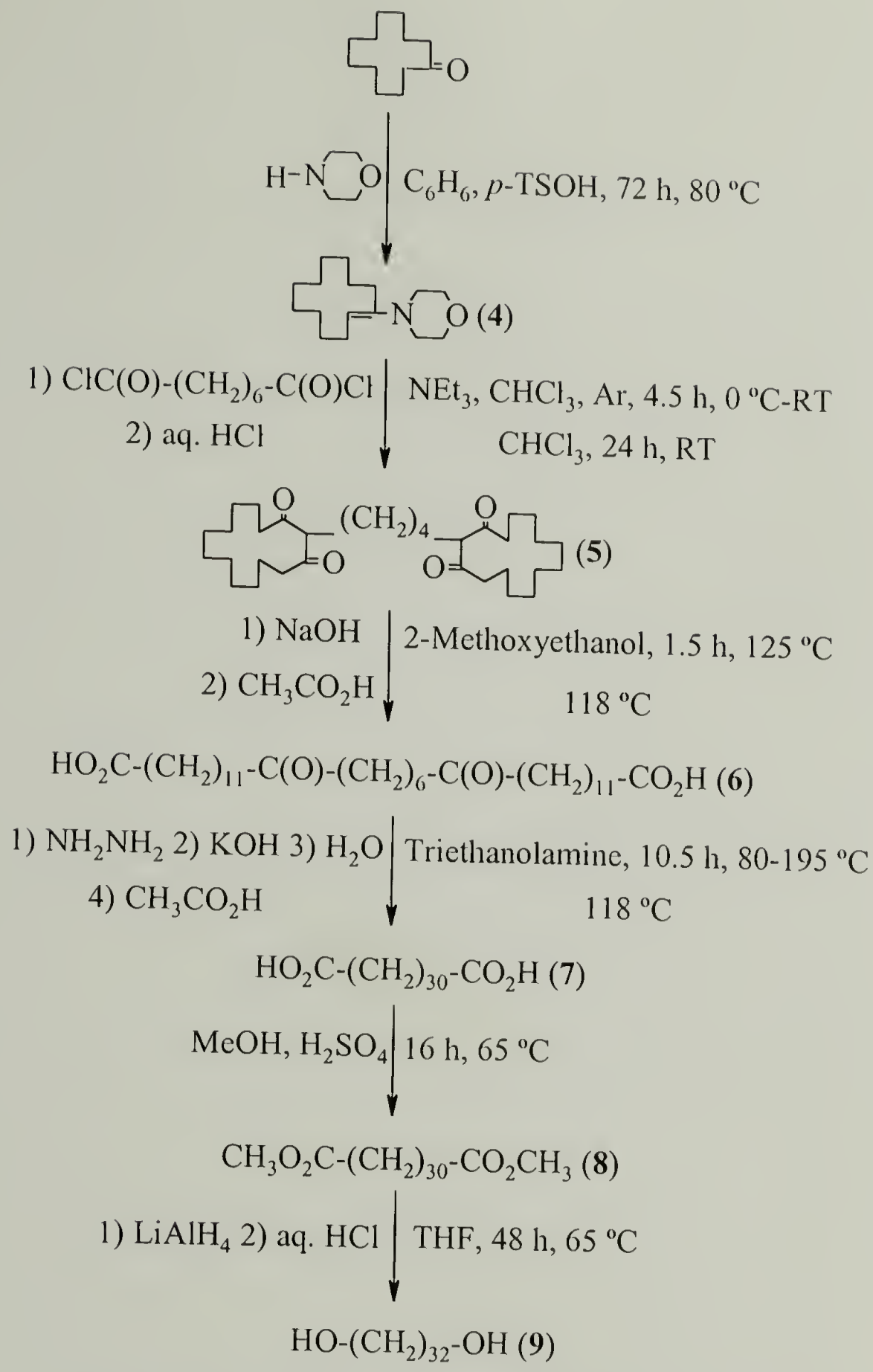

Scheme 2.3. Synthesis of 1,32-Dotriacontanediol (**9**).

The low overall yield (12%) was due to the poor yield (28%) achieved during the enamine-coupling step. There were a variety of side reactions (Scheme 2.4) that occurred during the [2 + 2] cycloaddition as a result of the sensitivity to water of both the enamine

and the diacid chloride. The byproducts of their reaction with water, cyclododecanone and 1-chlorosuberic acid, respectively, resulted in smaller tetraketones and diketo-acids, which were observed prior to purification by using ^{1}H-NMR (Figure 2.3).

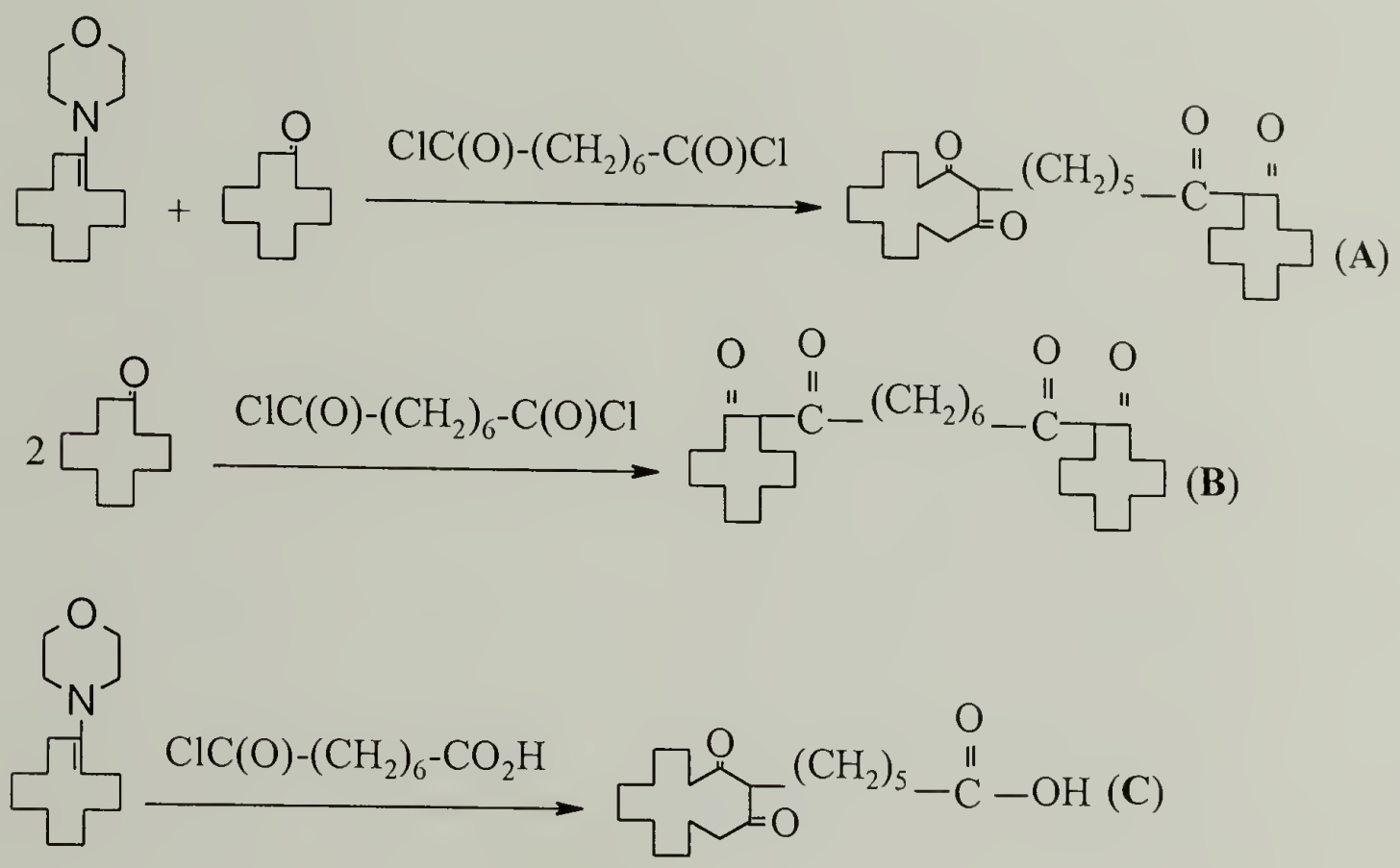

Scheme 2.4. Formation of Side Products (A = 6-(2,14-Dioxo-cyclotetradecyl)-1-hexanoylcylododecanone, B = 2,2'-Suberoyldicylododecanone, and C = 6-(2,14-Dioxo-cyclotetradecyl)-1-hexanoic acid) During the Enamine-Coupling Step.

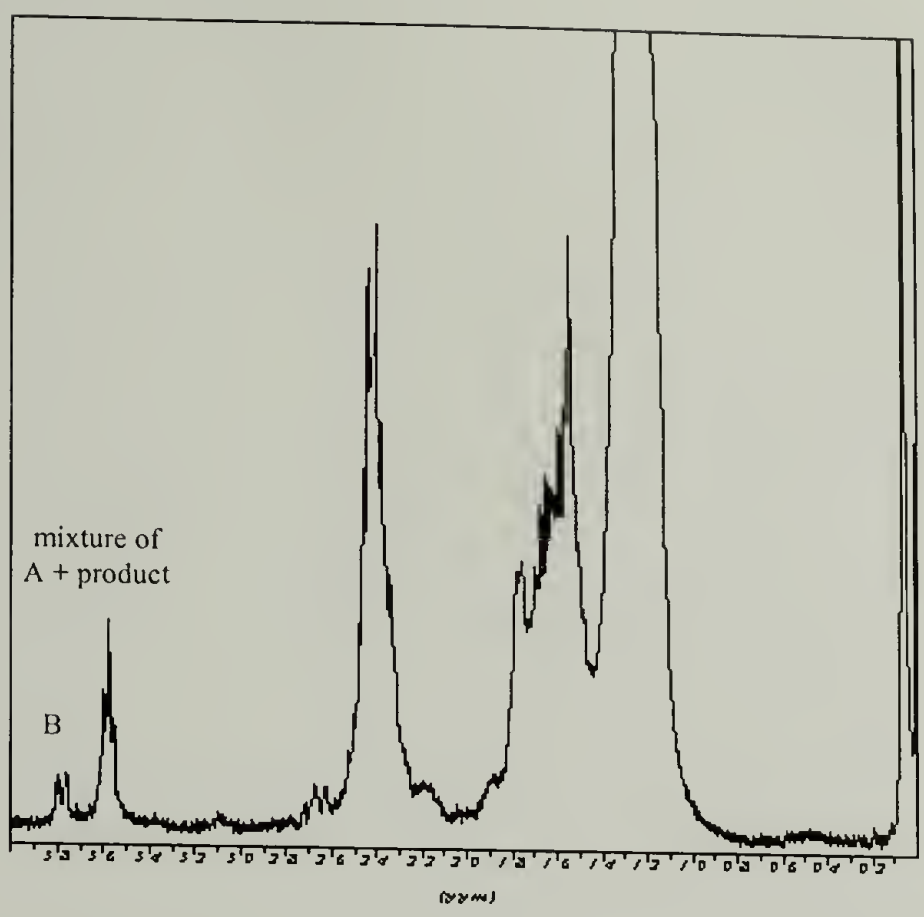

Figure 2.3. NMR Spectrum of 1,4-Bis-(2,14-dioxo-cyclotetradecyl)butane Before Recrystallization Showing the Presence of Side Products (A = 6-(2,14-Dioxo-cyclotetradecyl)-1-hexanoylcylododecanone and B = 2,2'-Suberoyldicylododecanone).

Instead of reducing the diacid synthesized using the enamine-coupling procedure to the diol, the diacid can instead be converted to the diacid chloride. This diacid chloride can then be used as the starting material for another [2 + 2] chain-extending cycloaddition. This consecutive enamine-coupling procedure was used to synthesize the long-chain 1,46-diol and could in theory be used to make even longer α,ω-diols. The synthetic procedure for the 1,46-diol was very similar to the method used for the synthesis of the 1,32-diol with some minor changes in the reaction times, temperature, and solvents. As with the 1,32-diol synthesis, the enamine-coupling steps resulted in very low yield resulting in a global yield for the 1,46-diol of just 1%.

First, 1,22-docosanediacid chloride (**14**) Cl-C(O)-$(CH_2)_{20}$-C(O)-Cl was synthesized by reacting thionyl chloride to the corresponding diacid synthesized by the

enamine-coupling procedure (Scheme 2.5) The enamine (**10**) was synthesized (62% yield) by the acid-catalyzed condensation of commercially available morpholine and cyclohexanone. Like the enamine synthesized in the 1,32-diol reaction, this enamine was commercially available, but it was again cheaper to synthesize it. A [2 + 2] cycloaddition of the enamine and sebacoyl chloride Cl-C(O)-$(CH_2)_8$-C(O)-Cl produced the tetraketone (**11**) (124% yield), which was ring-opened under basic conditions to the disodium salt of the dioxo-dioic acid (**12**) NaO_2C-$(CH_2)_5$-C(O)-$(CH_2)_8$-C(O)-$(CH_2)_5$-CO_2Na (84% yield). Unlike the dioic acid used in the 1,32-diol synthesis, this compound was not converted to the dioxo-dioic acid. Instead the crude salt was directly reduced to the diacid (**13**) HO_2C-$(CH_2)_{20}$-CO_2H (11% yield) using a Wolff-Kishner reaction. The diacid was then converted to 1,22-docosanediacid chloride (**14**) using thionyl chloride.

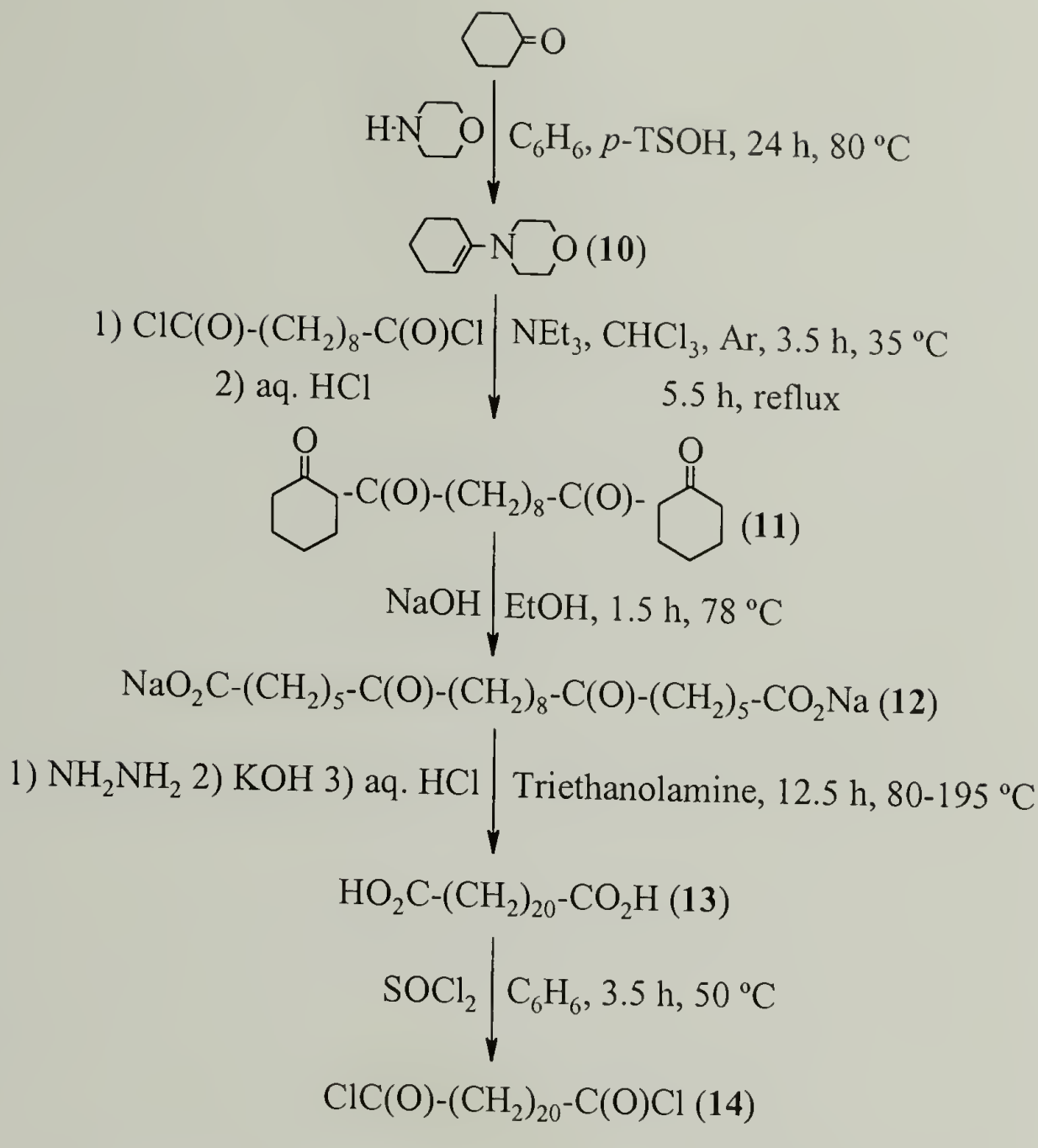

Scheme 2.5. Synthesis of 1,22-Docosanediacid Chloride (**14**).

1,46-Hexatetracontanediol (**19**) HO-$(CH_2)_{46}$-OH was then synthesized using the 1,22-docosanediacid chloride as the starting diacid chloride in the [2 + 2] chain-extending cycloaddition (Scheme 2.6). The enamine (**4**) previously used in the 1,32-diol synthesis was again employed, and a [2 + 2] cycloaddition of 2 equivalents of the enamine with the diacid chloride produced the cyclic tetraketone (**15**) (60% yield). The cyclic tetraketone was ring-opened under basic conditions to the disodium salt of the dioxo-dioic acid (**16**) NaO_2C-$(CH_2)_{11}$-C(O)-$(CH_2)_{20}$-C(O)-$(CH_2)_{11}$-CO_2Na (90% yield), which was again used directed as the salt, and reduced via a Wolff-Kishner reaction to the diacid (**17**) HO_2C-

$(CH_2)_{44}$-CO_2H (57% yield). The diacid was converted to the diester (**18**) CH_3CO_2-$(CH_2)_{44}$-CO_2CH_3 (93% yield) via an acid-catalyzed esterification and then reduced using lithium aluminum hydride to yield 1,46-hexatetracontanediol (**19**) (26% yield).

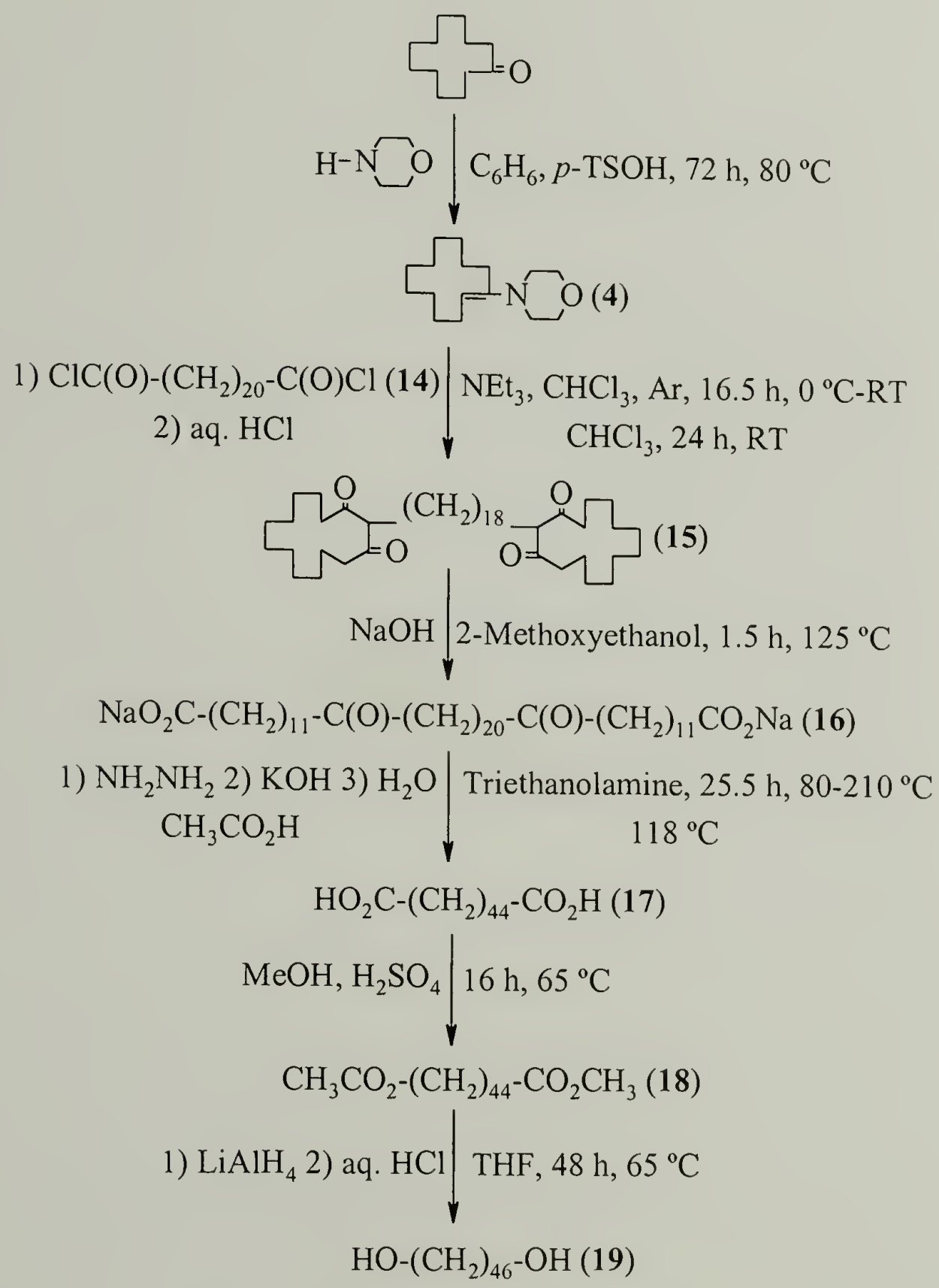

Scheme 2.6. Synthesis of 1,46-Hexatetracontanediol (**19**).

2.3.2 Characterization

2.3.2.1 Monomer Purity

The efficiency of the multi-step, synthetic reactions was monitored using several different characterization methods including NMR, IR, elemental analysis, and DSC. The ^{1}H- and ^{13}C-NMR spectra of the 1,22-, 1,32-, and 1,46-diols (no ^{13}C-NMR spectra was taken for the 1,46-diol due to solubility limitations) were all fully compatible with the expected structures.

^{1}H-NMR was particularly useful in following the course of the synthesis and purification of the 1,22-docosanediol. The methyl groups of the protecting groups as well as the methylene group alpha to the changing functional groups (OH, OTMS, Br, I, and then OTMS and OH again) were readily observable using ^{1}H-NMR. The side products (1-undecanol, 10-undecen-1-ol, and remaining unreacted protected iodo-alcohol) in the Wurtz-coupling reaction were also readily observable in the NMR spectrum of the 1,22-diol before purification and were absent in the spectrum of the purified diol.

The synthesis and purification of the 1,32- and 1,46-diols were also followed using ^{1}H-NMR, however IR often proved a more useful tool for examining the extent of contamination of these diols with other products. Before purification, the diols were often contaminated with compounds (mono- and di-functionalized ketones, acids, and esters) containing unreduced carbonyl groups. Due to the low percentage of methylene group alpha to these functionalities, these impurities often did not appear in the ^{1}H-NMR spectra of the diols. However, the carbonyl group is very active in the IR, and trace

amounts of the impurities were detectable before purification of the long-chain diols by using IR.

The IR spectra of the all the diols showed the Davydov splittings typically seen for orthorhombically packed *n*-parrafins.[49] Although the exact crystal structure of these diols was not examined in detail, it was not surprising to observe splitting in the CH_2 bending (1460 and 1470 cm^{-1}) and rocking (720 and 730 cm^{-1}) modes when a comparison with other long-chain *n*-alkanes and α,ω-diols is taken into consideration. Odd *n*-alkanes $H\text{-}(CH_2)_n\text{-}H$ have been shown to possess orthorhombic packing, while even *n*-alkanes have been reported as having either triclinic ($n < 26$) or monoclinic ($n \geq 26$) packing.[50] The series of α,ω-diols ranging from 13 to 24 consecutive methylene units have been reported to have either orthorhombic (odd n) or monoclinic (even n) packing.[6] In particular, both the 1,22- and 1,44-diols have been reported to adopt an orthorhombic sub-cell.[1] It seems reasonable to believe that the long-chain, telechelic diols in this study (22, 32, and 46 consecutive methylene units) adapted an orthorhombic sub-cell, and therefore exhibited Davydov splitting in the IR.

Elemental analysis results for the 1,22- and 1,46-diols indicated that these diols contained about two moles of water for every mole of diol. The results for the 1,32-diol suggested a more hydroscopic nature that currently can not be explained.

The agreement with literature values for the melting points of the 1,22-diol also indicated that the diol was fully purified. The experimental T_m of the 1,32-diol agrees with the value reported by Grechishnikova and co-workers,[16] but is 20 °C higher than the other two reported values.[17,18] However, as will be shown in the next section, these lower values are incorrectly assigned in the literature as melting points and actually correspond

to a solid-solid phase transition. There is no reported literature melting point for the 1,46-diol, however the melting point reported here fits nicely with extrapolated values (Figure 2.4).

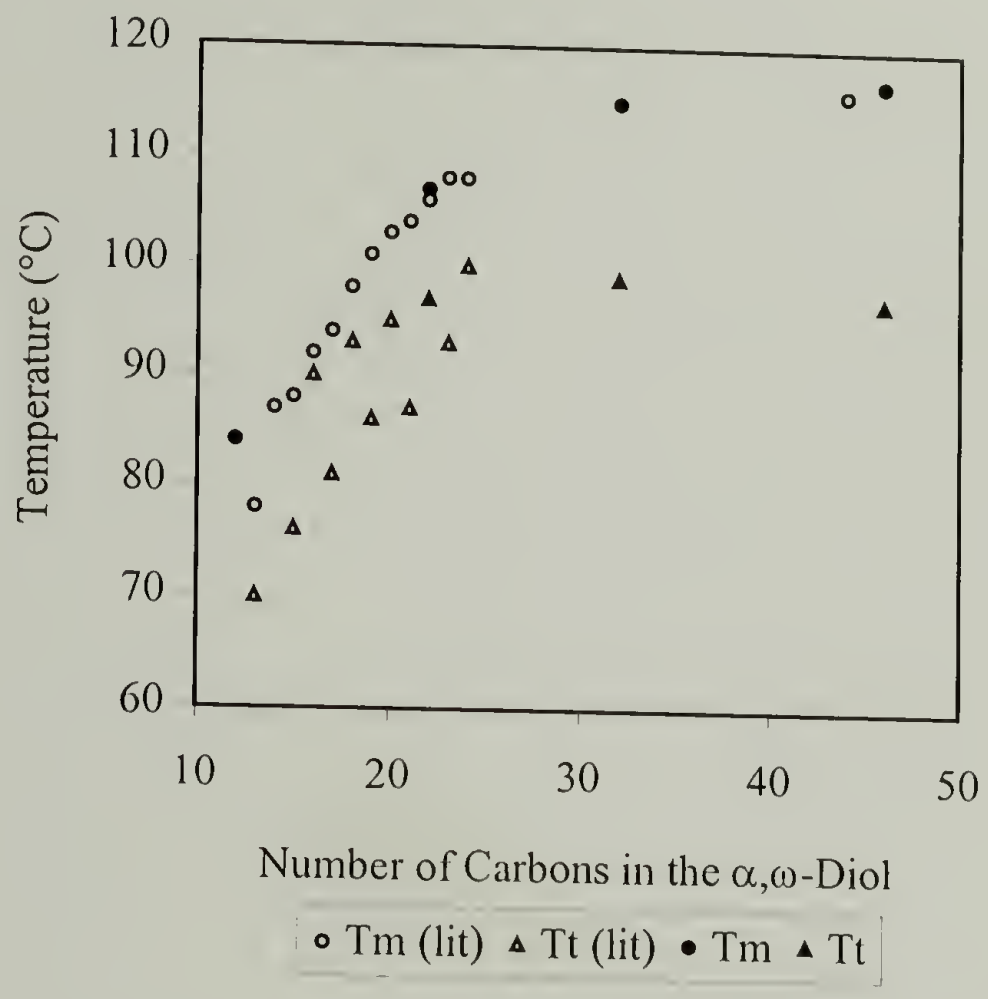

Figure 2.4. Comparison of the Melting and Transition Temperatures of the α,ω-Diols. • and o Represent Data from this Work and Literature (See References 1 and 6), Respectively; o and Δ Represent Melting and Transition Temperatures, Respectively.

It would have been desirable to further check the purity of these long-chain diols using liquid chromatography. However, due to the aliphatic nature of both the diols and the expected impurities, they gave very weak signals when using common ultraviolet-visible (UV-vis) or fluorescence detectors. The weak signal was also accredited to the low solubility of the diols in traditional high-pressure liquid chromatography (HPLC)

solvents. However, the combined NMR, IR, elemental analysis, and DSC results suggests that these long-chain, telechelic diols have a high purity appropriate for the step-growth polymerization targeted in this study. The purity of these diols was confirmed by their excellent reactivity during polymerization under conditions that are known to be critical of high purity.

2.3.2.2 Thermal Properties

The thermal properties of the long-chain α,ω-diols investigated in this study, along with those reported in the literature,[1,6] are shown in Table 2.2. These diols exhibited increasing T_d (Figure 2.5) and T_m (Figure 2.4) values with increasing chain length. The longer diols (1,32- and 1,46-diols) appeared to decompose at a slower rate than the other diols (1,12- and 1,46-diols) and at 500 °C were not fully decomposed. However, it is possible that the shorter diols (1,12- and 1,22-diols) are not actually decomposing, but rather are evaporating (b.p. of 1,12-diol is 189 °C at 12 torr, ~ 250 °C at 760 torr).[51]

Table 2.2. Thermal Properties of the α,ω-Diols.

α,ω-Diols	Decomposition Temp.[c] (°C)	Melting Temp.[d] (°C)	Transition Temp. (°C)	Enthalpy ($J \cdot g^{-1}$)
1,13[a]		78	70	217
1,14[a]		87	None	269
1,15[a]		88	76	241
1,16[a]		92	90	248
1,17[a]		94	81	242
1,18[a]		98	93	251
1,19[a]		101	86	243
1,20[a]		103	95	245
1,21[a]		104	87	247
1,22[a]		106	97	254
1,23[a]		108	93	250
1,24[a]		108	100	254
1,44[b]		116	None	273
1,12	182	84	None	264
1,22	235	107	97	268
1,32	292	115	99	240
1,46	299	117	97	136

a and b) See references 6 and 1, respectively.

c) Decomposition temperatures were taken at 5% weight loss using a scan rate of 10 $K \cdot min^{-1}$.

d) Melting temperatures were taken as the peak of the melting endotherm during the second heating run using a scan rate of 10 $K \cdot min^{-1}$.

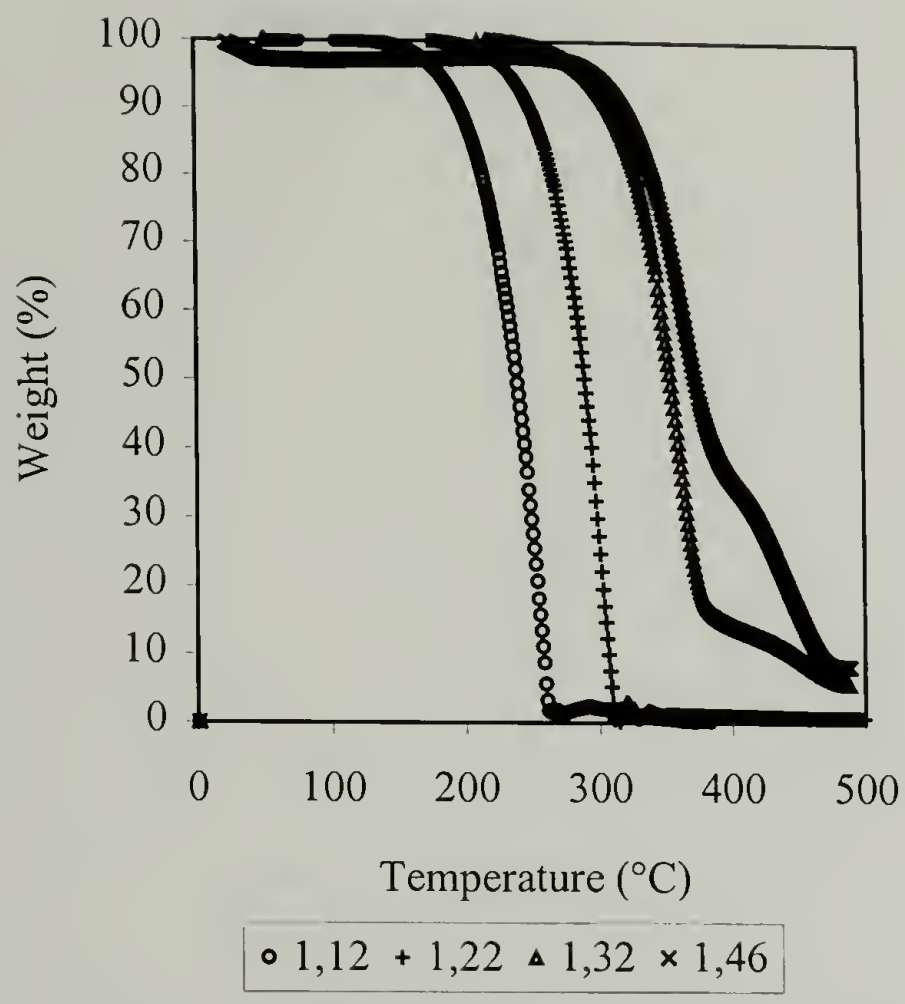

Figure 2.5. TGA Thermograms of the α,ω-Diols.

All of the diols showed two peaks in the DSC upon both heating and cooling (Figure 2.6). This behavior has been reported in the literature[1,6,52] for several long-chain, aliphatic α,ω-diols. It is believed that the lower temperature peak is a solid-solid phase transition, while the higher temperature peak is the melting or solid-liquid transition. Ogawa and Nakamura[6] previously reported the existence of two thermal transitions for the 1,13- to 1,24-diols, with the exception of the 1,14-diol. These transitions can be followed using DSC, polarized optical microscopy, and WAXS. A closer examination of the 1,16-hexadecanediol by Kobayashi and Nakamura[52] proved that the higher temperature solid was a rotator phase that adapted a smectic G liquid crystalline structure. Le Fevere de Ten Hove[1] observed two exotherms upon cooling the 1,44-tetratetracontanediol from the melt, but he observed only one broad melting peak upon

heating the diol. This current study confirmed the existence[1,6] of this transition for the 1,22-diol. It is the first time that this phase transition has been reported for the 1,32- and 1,46-diols. These results are similar to those seen for *n*-alkanes. *n*-Alkanes with $n = 9$ to 19 (odd n only) as well as $n = 20$ to 43 (even and odd n) have been shown to exhibit high-temperature phase transitions.[50]

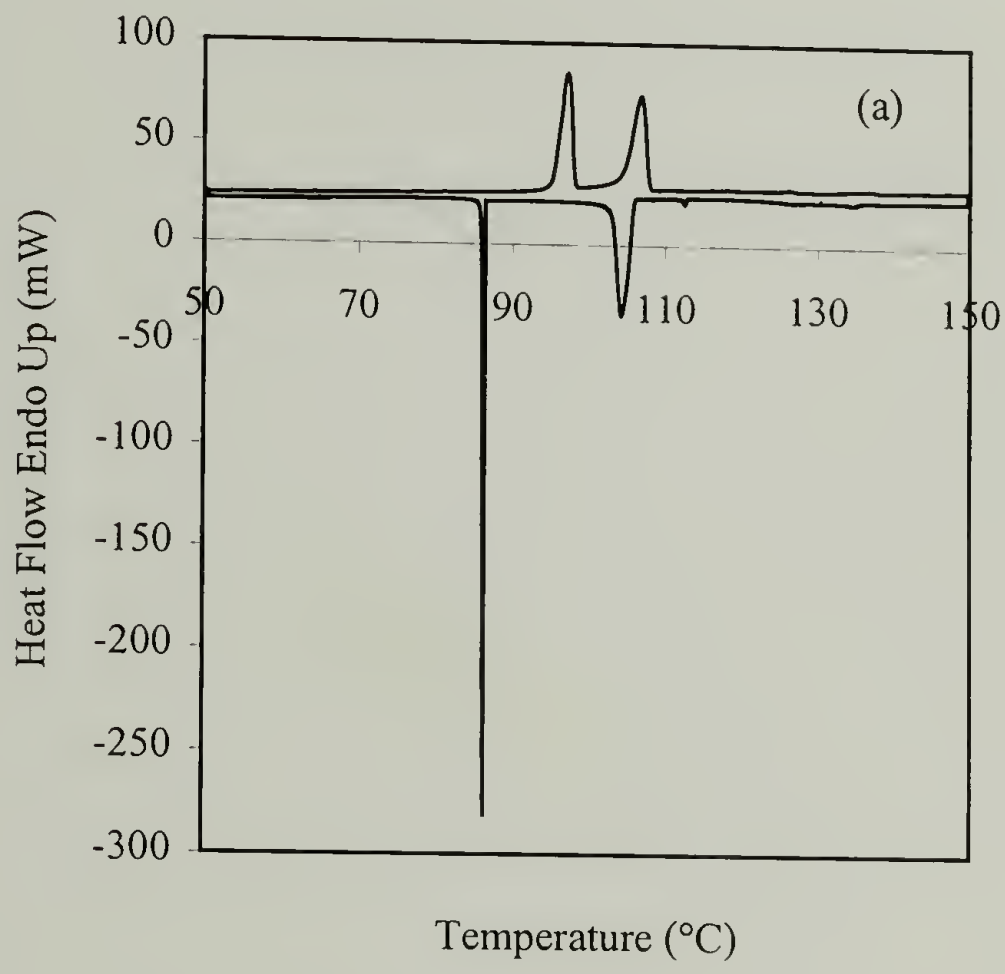

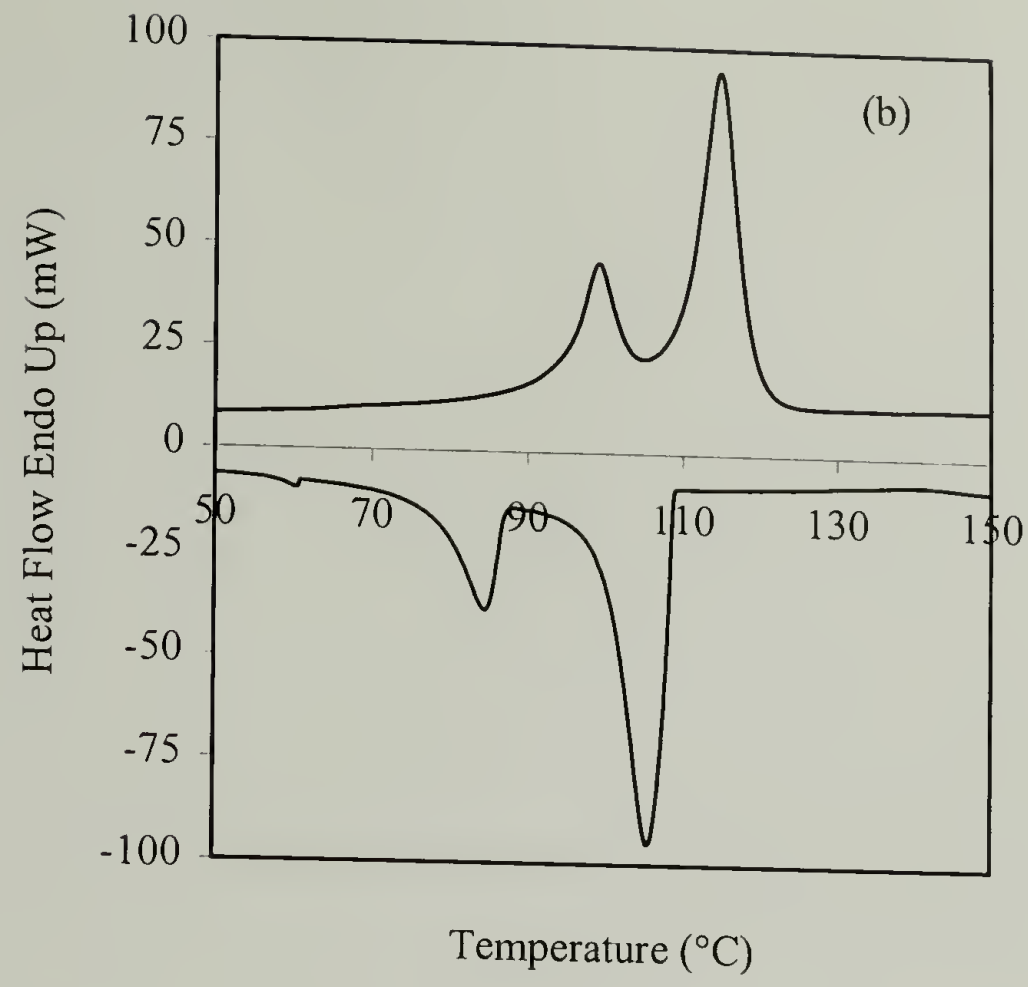

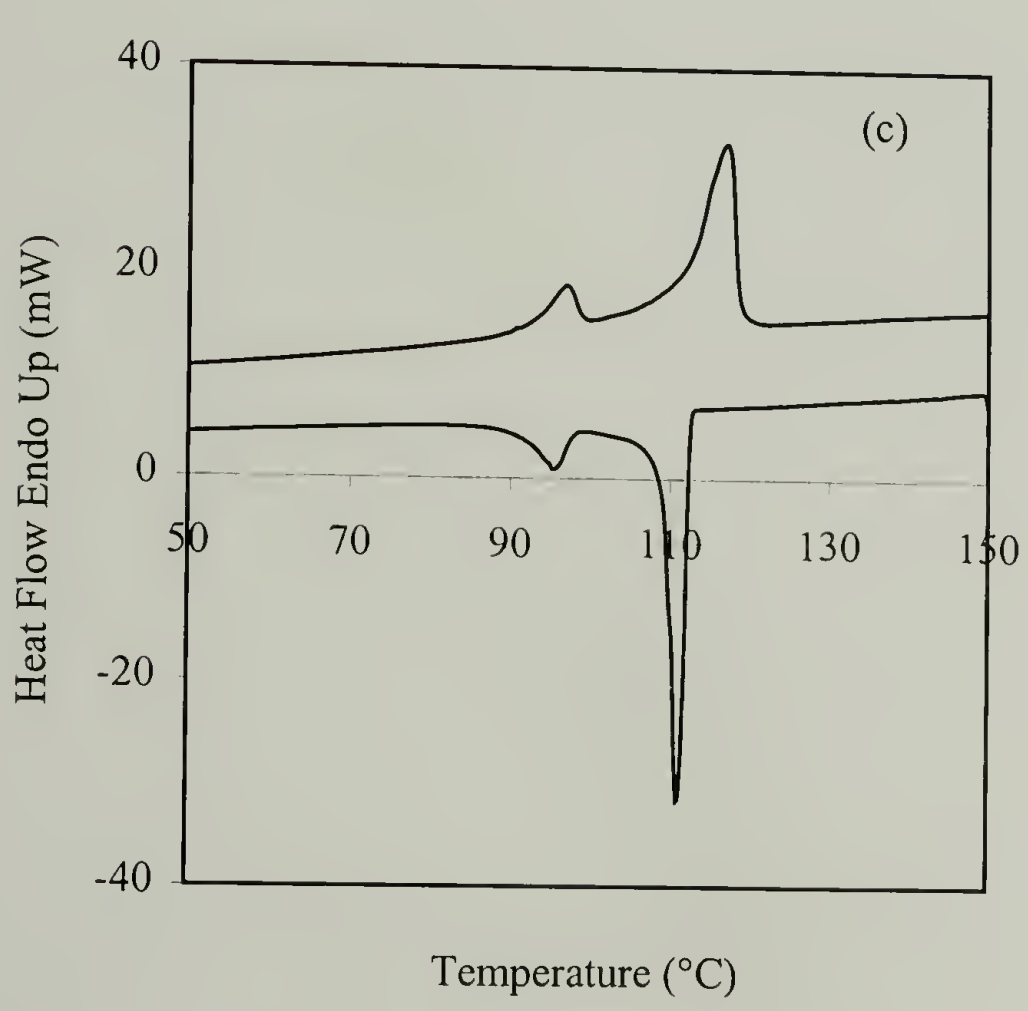

Figure 2.6. DSC Thermograms (Scan Rate of 10 K·min^{-1}) of the α,ω-Diols: (a) 1,22-Diol, (b) 1,32-Diol, and (c) 1,46-Diol.

2.4 Conclusions and Perspectives

Several long-chain, monodisperse α,ω-diols were synthesized in high purity. 1,22-Docosanediol was synthesized in a global yield of 53% using a Wurtz-coupling procedure. An enamine-coupling method was used to synthesize 1,32-dotriacontanediol and 1,46-hexatetracontanediol in global yields of 12% and 1%, respectively. The feasibility of expanding this work to synthesize even longer aliphatic, telechelic diols is doubtful unless the yield of the [2 + 2] cycloaddition step can be increased. However, there remain other synthetic possibilities to synthesize even longer diols. In particular, Brooke and co-workers[53] have succeeded in synthesizing 1,50-pentacontanedioic acid and 1,194-tetranonacontahectanedioic acid by a multi-step procedure based on several Wittig-couplings. Assuming these diacids are soluble in the appropriate solvents, they could be reduced to the corresponding diols. In Chapter 5, an affordable synthetic method to achieve long-chain, telechelic diols in both high yield and purity will be discussed.

Although the yields were low for the long-chain, telechelic diols synthesized by the enamine-coupling method, they did have advantages over the other two methods previously employed in the Penelle group. Purification of the desired diol was much easier in this method then in the multiple Wurtz-coupling method used to synthesize the 1,44-diol by Cedric Le Fevere de Ten Hove.[1] In the Wurtz-coupling reaction, the two main products, the desired 1,44-diol and the side product 1-docosanol, had a similar solubility behavior and similar ^{1}H-NMR spectra making purification both time consuming and difficult to prove. In the enamine-coupling method, the main side products all contained carbonyl groups that were easily detected in even trace amounts by

IR. The global yield for the 1,30-diol synthesized by Joel Schall[2] had similarly low yield, but the melting point of the product was much lower then both the reported literature values and extrapolated values indicating that the diol was impure. On the other hand, the diols synthesized by the enamine-coupling method had NMR, IR, elemental analysis, and DSC results that indicated a very high purity.

Both the T_d and T_m of these long-chain α,ω-diols increased with increasing alkane length. The 1,22-, 1,32-, and 1,46-diols all exhibited a solid-solid phase transition upon either heating or cooling. This is the first time that this behavior has been reported for both the 1,32- and 1,46-diols.

2.5 References

(1) Le Fevere de Ten Hove, C. Controlling Solid-State Microstructure of Semi-Crystalline Polymers Through Chemical Design of Chains: A Study of Model Polyesters. Ph.D. Thesis, Université Catholique de Louvain, Louvain-la-Neuve, 2001.

(2) Schall, J. D. Condensation Polymers with Regularly-Spaced, Strongly-Segregating Functionalities. Ph.D. Thesis, University of Massachusetts, Amherst, 2001.

(3) Rusanova, E. E.; Sebyakin, Y. L.; Volkova, L. V.; Evstigneeva, R. P. *Zh. Org. Khim. (Engl. Transl.)* **1984**, *20*, 279.

(4) Hünig, S.; Buysch, H. *Chem. Ber.* **1967**, *100*, 4017.

(5) Loudon, G. M. *Organic Chemistry*; 2nd ed.; Benjamin/Cummings: Menlo Park, 1988.

(6) Ogawa, Y.; Nakamura, N. *Bull. Chem. Soc. Jpn.* **1999**, *72*, 943.

(7) Duhamel, L. *Ann. Chim. (Paris)* **1963**, *8*, 315.

(8) Drake, N. L.; Carhart, H. W.; Mozingo, R. *J. Am. Chem. Soc.* **1941**, *63*, 617.

(9) Murray, K. E.; Schoenfeld, R. *Aust. J. Chem.* **1955**, *8*, 437.

(10) Murray, K. E.; Schoenfeld, R. *Aust. J. Chem.* **1955**, *8*, 432.

(11) Kirrmann, A.; Duhamel, L. *Hebd. Seances Acad. Sci.* **1962**, *254*, 1303.

(12) Kimura, K.; Takahashi, M.; Tanaka, A. *Chem. Pharm. Bull.* **1960**, *8*, 1059.

(13) Slezak, F. B.; Stallings, J. P.; Wagner, D. H.; Wotiz, J. H. *J. Org. Chem.* **1961**, *26*, 3137.

(14) Buysch, H.; Hünig, S. *Angew. Chem.* **1966**, *78*, 145.

(15) Buchta, E.; Huhn, C. *Liebigs Ann. Chem.* **1966**, *695*, 42.

(16) Grechishnikova, I. V.; Johansson, L. B.-Å.; Molotkovsky, J. G. *Chem. Phys. Lipids* **1996**, *81*, 87.

(17) Moss, R. A.; Fujita, T.; Okumura, Y. *Langmuir* **1991**, *7*, 2415.

(18) Furukawa, A.; Shoji, H.; Nakaya, T.; Imoto, M. *Makromol. Chem.* **1987**, *188*, 265.

(19) *Dictionary of Natural Products*; 1st ed.; Buckingham, J., Ed.; Chapman & Hall: London, 1994.

(20) Bierer, D. E.; Gerber, R. E.; Jolad, S. D.; Ubillas, R. P.; Randle, J.; Nauka, E.; Latour, J.; Dener, J. M.; Fort, D. M.; Kuo, J. E.; Inman, W. D.; Dubenko, L. G.; Ayala, F.; Ozioko, A.; Obialor, C.; Elisabetsky, E.; Carlson, T.; Truong, T.; C., B. R. *J. Org. Chem.* **1995**, *60*, 7022.

(21) Patwardhan, S. A. *Org. Prep. Proced. Int.* **1994**, *26*, 645.

(22) Saotome, K.; Komoto, H.; Yamazaki, T. *Bull. Chem. Soc. Jpn.* **1966**, *39*, 480.

(23) Signer, R.; Sprecher, P. *Helv. Chim. Acta* **1947**, *30*, 1001.

(24) Popovitz-Biro, R.; Majewski, J.; Margulis, L.; Cohen, S.; Leiserowitz, L.; Lahav, M. *J. Phys. Chem.* **1994**, *98*, 4970.

(25) Musgrave, O. C.; Stark, J.; Spring, F. S. *J. Chem. Soc.* **1952**, 4393.

(26) Adams, K. R.; Bonnett, R. *Phytochemistry* **1971**, *10*, 1885.

(27) Lukes, R.; Havlickova, L.; Dudek, V. *Collect. Czech. Chem. Commun.* **1961**, *26*, 1719.

(28) Cho, I.; Lee, K. *Macromol. Chem. Phys.* **1997**, *198*, 861.

(29) Schill, G.; Merkel, C. *Chem. Ber.* **1978**, *111*, 1446.

(30) White, E. V.; Tsuboyama, S.; McCloskey, J. A. *J. Am. Chem. Soc.* **1971**, *92*, 6340.

(31) Schill, G.; Bechmann, W.; Vetter, W. *Chem. Ber.* **1980**, *113*, 941.

(32) Kolattukudy, P. E.; Agrawal, V. P. *Lipids* **1974**, *9*, 682.

(33) Austin, P. W.; Seshadri, T. R.; Sood, M. S. *Indian J. Chem.* **1969**, *7*, 43.

(34) Mazliak, P. *Phytochemistry* **1962**, *1*, 79.

(35) Beletskaya, I. P.; Artamkina, G. A.; Reutov, O. A. *Russ. Chem. Rev. (Engl. Transl.)* **1976**, *45*, 330.

(36) Lewis, H. F.; Tryon, M. *J. Chem. Educ.*, *7*, 2712.

(37) Bamford, C. H.; Eastmond, G. C.; Whittles, D. *Polymer* **1969**, *10*, 771.

(38) Bamford, C. H.; Dyson, R. W.; Eastmond, G. C. *Polymer* **1969**, *10*, 885.

(39) Han, B. H.; Boudjouk, P. *Tetrahedron Lett.* **1981**, *22*, 2757.

(40) Lash, T. D.; Berry, D. *J. Chem. Educ.* **1985**, *62*, 85.

(41) Einhorn, C.; Einhorn, J.; Luche, J. *Synthesis* **1989**, *11*, 787.

(42) Pestman, J. M.; Engberts, J. B. F. N.; de Jong, F. *Recl. Trav. Chim. Pays-Bas* **1994**, *113*, 533.

(43) Mason, T. J.; Luche, J. L. Ultrasound as a New Tool for Synthetic Chemists. In *Chemistry Under Extreme or Non-Classical Conditions*; van Eldik, R., Hubbard, C. D., Eds.; John Wiley & Sons: New York, 1997.

(44) Price, G. J. Applications of High Intensity Ultrasound in Polymer Chemistry. In *Chemistry Under Extreme or Non-Classical Conditions*; van Eldik, R., Hubbard, C. D., Eds.; John Wiley & Sons: New York, 1997.

(45) Boldyrev, V. V. *J. Chim. Phys.* **1986**, *83*, 821.

(46) Morton, A. A.; Davidson, J. B.; Best, R. J. *J. Am. Chem. Soc.* **1942**, *64*, 2239.

(47) Thakkar, S. M.; Deshmukh, V. K.; Saoji, A. N.; Duragkar, N. J. *J. Indian Chem. Soc.* **1986**, *63*, 619.

(48) Downing, D. T.; Kranz, Z. H.; Murray, K. E. *Aust. J. Chem.* **1961**, *14*, 619.

(49) Lee, K.-S.; Wagner, G.; Hsu, S. L. *Polymer* **1987**, *28*, 889.

(50) Broadhurst, M. G. *J. Res. Natl. Bur. Stand., Sect. A.* **1962**, *66*, 241.

(51) Chuit, P. *Helv. Chim. Acta* **1926**, *12*, 264.

(52) Kobayashi, H.; Nakamura, N. *Cryst. Res. Technol.* **1995**, *30*, 495.

(53) Brooke, G. M.; Burnett, S.; Mohammed, S.; Proctor, D.; Whiting, M. C. *J. Chem. Soc. Perkin Trans. 1* **1996**, 1635.

CHAPTER 3. SYNTHESIS OF m,n-POLYURETHANES AND RESULTING POLYETHYLENE-LIKE BEHAVIOR

3.1 Introduction

In recent years, there has been renewed interest in the synthesis and characterization of very long-chain, aliphatic, regularly functionalized polymers synthesized by step-growth polymerizations. In particular, Cho and Lee[1] examined the biodegradability of a 30,30-polyester and Ehrenstein et al.[2] studied the blend-compatibilization behavior of 6,24- and 6,34-polyamides. Cho and Lee reported that the long-chain 30,30-polyester had a T_m value and thermal stability comparable to LDPE, and mechanical properties (e.g. tensile strength and modulus) that were higher than that of LDPE. Ehrenstein and co-workers claimed that the long-chain 6,24- and 6,34-polyamides had both a T_m value and Young's modulus intermediate between that of polyamides of higher hydrogen-bonding density and polyethylene. However, neither of these studies examined structure-property relationships with a particular emphasis on the influence of the long-chain segments on the crystallization of these polymers. Additionally, there is no corresponding study on very long-chain, aliphatic polyurethanes. Saotome and Komoto[3] did examine the influence of increasing aliphatic length on the T_m of a series of m,6- and m,10-polyurethanes and reported that the T_m decreased with increasing aliphatic length. They synthesized the previously longest, purely aliphatic polyurethane, the 16,10.

In order to better understand the relationship between chemical architecture and crystalline microstructure, recent research in the Penelle group has focused on the

synthesis and examination of polyethylene-like polyesters.[4-6] In this study, a series of increasingly aliphatic, semi-crystalline polyurethanes were synthesized, and urethane units (carbamate esters) O-C(O)-NH capable of undergoing hydrogen-bonding were introduced in a well-controlled manner onto a poly(m)ethylene chain $(CH_2)_m$ or $(CH_2-CH_2)_m$. These model, long-chain polyurethanes had the general structure $[O-(CH_2)_m-O-C(O)-NH-(CH_2)_n-NH-C(O)]_n$.

By systematically increasing the length of the aliphatic α,ω-diols $HO-(CH_2)_m-OH$ used as monomers, the hydrogen-bonding density of the polyurethanes was diluted. In theory, the polymers should become more polyethylene-like. Consider a spectrum of polymers (Figure 3.1) with polyolefins where the crystal structure is controlled by van der Waals forces, such as polyethylene, on one side and polymers whose crystal structure is controlled by hydrogen-bonding, such as polyurethanes and polyamides, on the other side. A major goal of this research project was to answer the question of where these increasingly aliphatic, long-chain polymers were on this spectrum. In particular, it was desired to determine what the minimum length of the aliphatic segment needed to be for this transition from polyurethane-like to polyethylene-like to occur. To examine this transition, the physical, chemical, thermal, and mechanical properties of these polymers must be examined. By relating these properties to the crystallization behavior and structure of the polymers, a better understanding of structure-property relationships should be gained.

Aliphatic: HDPE LLDPE	← -[O-$(CH_2)_m$-O-C(O)-NH-$(CH_2)_n$-NH-C(O)]$_X$- →	Hydrogen-Bonded: Polyamides Polyurethanes

Figure 3.1. Spectrum Ranging from Aliphatic to Hydrogen-Bonded Polymers.

3.2 Experimental

3.2.1 Characterization

^{1}H- and ^{13}C-NMR spectra of the polymers were obtained in either deuterated DMSO-d_6 or *N,N*-dimethylformamide (DMF-d_7) from a Bruker 500 MHz NMR at elevated temperatures. IR spectra were recorded on a Bio-Rad FTS 175C spectrometer using a total of 16 scans.

3.2.2 Molecular Weight Analysis

Absolute molecular weights and distributions were determined by high temperature, triple detector gel permeation chromatography (GPC). A Polymer Laboratory PL-GPC 220 ultra high temperature chromatograph with a Hewlett-Packard 1100 series isocratic pump and PL gel 20 μm mixed-A columns was employed. The system was equipped with a Polymer Labs differential refractive index detector, Viscotek viscometer, and Wyatt Technology heated miniDAWN light scattering detector that used a wavelength of 690 nm. Instrument constants were determined using a 200,000 molecular weight polystyrene standard. Wyatt Technology's ASTRA software (version 4.70) was used to work up the data. All of the GPC experiments were performed using 1,2,4-trichlorobenzene as the mobile phase at 135 °C. In order to determine the dn/dc

values, the columns from the high-temperature GPC were removed, and the refractive index was measured at varying polymer concentrations.

3.2.1 Sample Preparation

Melt-crystallized samples were prepared by heating the polymers to 200 °C and then allowing the polymers to cool to room temperature at a rate of 10 $K \cdot min^{-1}$.

3.2.4 Thermal Analysis

TGA was performed on 5 to 10 mg samples using a Thermal Analysis Instruments TGA 2950 flushed with nitrogen at a scan rate of 10 $K \cdot min^{-1}$. The T_d was taken at 5% weight loss. Melting points were observed using either a Perkin Elmer Pyris or Thermal Analysis Instruments Universal V2.5H DSC flushed with helium. The 5 to 10 mg samples were heated above their melting points to 200 °C, cooled to room temperature, and then reheated, all at a rate of 10 $K \cdot min^{-1}$. The first heating and cooling run was performed in order to erase the different thermal histories present in the samples. The melting points were taken as the peak of the melting endotherm during the second heating run. The temperature scale was calibrated using indium and eicosane, and the heat of enthalpy was calibrated using indium.

3.2.5 X-ray Scattering

SAXS patterns were obtained at room temperature using Ni-filtered Cu Kα radiation of wavelength 1.542 Å from a Rigaku rotating anode operating at 40 kV and 200 mA. A point-collimated 300 μm diameter beam was used, and the X-ray diffraction

patterns were recorded using an evacuated Siemens GADDS 2-dimensional area detector. SAXS experiments were also performed on the Advanced Polymers Beamline (X27C) at the National Synchrotron Light Source, Brookhaven National Laboratory, Upton, New York. The camera length was calibrated using an Ag-B_0 (d = 63.02 Å) standard. The X-ray beam had a 3 mm^2 area and a wavelength of 1.307 Å. Custom software was used to subtract the background, circularly average the data, and convert the data to a logarithmic intensity scale.

3.2.6 Electron Microscopy

In order to differentiate the crystalline and amorphous regions of the polymers, the prepared polymer samples were stained using a 2% solution of ruthenium (III) chloride hydrate in sodium hypochlorite. The ruthenium oxide-stained samples were then microtomed at room temperature into 40 nm slices using a Leica ULTRACUT UCT Universal Ultramicrotome. The microtomed samples were deposited onto copper grids and dried in a vacuum oven at room temperature. Transmission electron microscope (TEM) images were recorded at room temperature using a JEOL 100 CX TEM operating at 100 kV. The magnification was calibrated using a crossed lined grating replica with 2160 lines per mm.

3.2.7 Polymer Synthesis

3.2.7.1 General Considerations

All of the diisocyanates were commercially available and distilled immediately before use. 1,12-Dodecanediol HO-$(CH_2)_{12}$-OH was also commercially available. The synthesis of the 1,22-, 1,32-, and 1,46-diols was discussed in Chapter 2. All of the α,ω-diols (commercial and synthesized) were dried in a vacuum oven prior to polymerization in order to remove any absorbed water.

3.2.7.2 Synthesis of m,n-Polyurethanes by Melt Polyaddition

The diols (0.5 g) were heated above their melting temperature in argon-purged glass vessels. Stoichiometric amounts of diisocyanates were syringed into the reaction vessels, and the mixtures were vigorously stirred for up to 1 hour or until they solidified. After cooling to room temperature, DMF (10 mL) was added, and the mixtures were heated until the polymers dissolved. The hot solutions were then poured dropwise into rapidly stirred methanol (100 mL). The resulting cloudy white mixtures were filtered and dried in a vacuum oven yielding m,n-polyurethanes (**20**) [O-$(CH_2)_m$-O-C(O)-NH-$(CH_2)_n$-NH-C(O)]$_n$ as white solids. ^{1}H-NMR (500 MHz, DMSO-d_6, 393-413 K) δ 6.37-6.27 (bs, 2H, N*H*), 3.96 (t, J = 6.5 Hz, 4H, CH_2-O-C(O)), 3.16-3.00 (m, 4H, CH_2-NH-C(O)), 1.57 (quintet, J = 6.3 Hz, 4H, CH_2-CH_2-O-C(O)), 1.45 (m, 4H, CH_2-CH_2-NH-C(O)), 1.30 (m, remaining H, CH_2-CH_2-CH_2). ^{1}H-NMR (500 MHz, DMF-d_7, 393-413 K) δ 6.22-5.72 (bs, 2H, N*H*), 4.04-4.01 (t, J = 6.5 Hz, 4H, CH_2-O-C(O)), 3.14-3.10 (m, 4H, CH_2-NH-C(O)), 1.64-1.59 (quintet, J = 6.3 Hz, 4H, CH_2-CH_2-O-C(O)), 1.57-1.54 (m, 4H, CH_2-

CH_2-NH-C(O)), 1.36-1.33 (m, remaining H, CH_2-C*H*$_2$-CH_2). ^{13}C-NMR (500 MHz, DMSO-d_6, 393-413 K) δ 155.88-155.84 (O-*C*(O)-NH), 63.25-63.18 (*C*H_2-O-C(O)-NH), 29.00-24.88 (remaining *C*H_2). ^{13}C-NMR (500 MHz, DMF-d_7, 393-413 K) δ 162.49-162.44 (O-*C*(O)-NH), 69.82-69.72 (*C*H_2-O-C(O)-NH), 46.73-46.41 (*C*H_2-NH-C(O)-O), 34.33-31.46 (remaining *C*H_2). IR (KBr): 3333-3310 cm^{-1} (NH stretch), 2922-2918 cm^{-1} (asymmetric CH stretch), 2852-2849 cm^{-1} (symmetric CH stretch), 1696-1682 cm^{-1} (amide I), 1540-1537 cm^{-1} (amide II), 1475-1468 cm^{-1} (CH_2 bend).

3.3 Results and Discussion

3.3.1 Polymer Synthesis

3.3.1.1 Overview of Polyurethane Synthesis

Polyurethanes [O-R-O-C(O)-NH-R'-NH-C(O)]$_n$ were first synthesized by Bayer and co-workers for I. G. Farbenindustrie in 1937.[7] Bayer et al. synthesized both polyurethanes and polyureas in an attempt to produce fibers that were competitive with Carothers's recently synthesized nylon 6,6 without impinging on the patent held by E. I. DuPont de Nemours and Company.[8] The polyurethanes were synthesized via a polyaddition of diol HO-R-OH and diisocyanate O=C=N-R'-N=C=O. The initial aliphatic m,n-polyurethanes produced had the general structure [O-(CH_2)$_m$-O-C(O)-NH-(CH_2)$_n$-NH-C(O)]$_n$, where m and n represent the number of carbons originating from the diol and diisocyanate, respectively.

The monomers employed may be aliphatic, aromatic, cycloaliphatic, branched, or halogenated, as well as di- or polyfunctional. The polyaddition of diol and diisocyanate occurs with no formation of byproducts. This simplifies the purification of these polymers. Solvents, such as dioxane, chlorobenzene, toluene, and higher boiling paraffins, are often employed in solution polymerizations.[9] However, most polyurethanes have poor solubility, and they are therefore often synthesized directly from the melt. For both solution and melt polyadditions, high reaction temperatures are necessary. Dibutyltin dilaurate (DBTDL) or Lewis bases, such as tertiary amines, are often used to catalyze the isocyanate-alcohol reaction. However, care must be taken as some basic catalysts can promote trimerization[10] as well as the formation of crosslinks.[11]

In 1945, an alternative procedure for synthesizing polyurethanes at room temperature was reported by Wittbecker et al.[12,13] In this polymerization, the polyurethanes were synthesized by either an interfacial polycondensation or a solution polymerization via the reaction of bischloroformates Cl-C(O)-O-R-O-C(O)-Cl and diamines H_2N-R'-NH_2. Since hydrochloric acid is produced, an acid acceptor is necessary. Many other methods for synthesizing polyurethanes have been developed,[14-17] but they have found limited use in industry.

3.3.1.2 Synthesis of the m,n-Polyurethanes Used in This Study

The m,n-polyurethanes (**20**) were all synthesized by a step-growth polyaddition in the melt (Scheme 3.1). Equimolar amounts of diol (Chapter 2) and diisocyanate were used. Since the emphasis of this research was not to make commercial polyurethanes where reactivity rates and molecular weights would be the critical criteria, but rather to

synthesize model polymers whose purity and structure could be ensured, catalysts were not used. The use of catalysts would have required their removal from the resulting polymers, which can be a difficult process. Additionally, as mentioned in the previous section, catalysts can result in undesired side products that would have required their removal as well. Isolated polymerization yields of 50 to 100% based on gravimetric results were obtained. Table 3.1 summarizes the polymerization conditions. The following m,n-polyurethanes (in order of increasing aliphatic length) were produced: 12,4, 12,6, 12,8, 12,12, 22,4, 22,6, 22,8, 22,12, 32,4, 32,6, 32,8, 32,12 and 46,6. Except for the 12,6-polyurethane, which had earlier been synthesized by Saotome and Komoto[3] in 1967 by a solution polyaddition in 60% yield, none of the other polyurethanes discussed in this chapter had been previously synthesized.

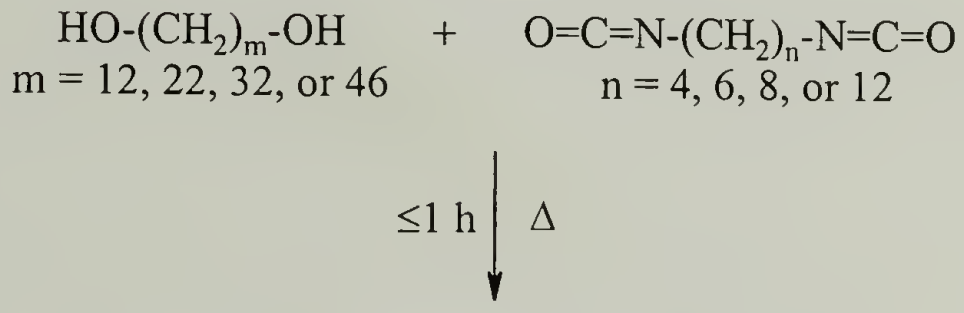

Scheme 3.1. Synthesis of m,n-Polyurethanes (**20**).

Table 3.1. Polymerization Conditions and Resulting Molecular Weights of the m,n-Polyurethanes.

m,n-Polymer	Polym. Temp. (°C)	Yield (%)	NMR Solvent	$M_w \cdot 10^{-3}$	PDI	dn/dc ($mL \cdot g^{-1}$)
12,4	100	83	DMSO	4.7	1.6	-0.047
12,6	100	98	DMSO	3.2	2.0	-0.053
12,8	100	90	DMSO	11.4	1.9	-0.031
12,12	100	77	DMSO	19.5	2.2	-0.043
22,4	120	90	DMF	37.5	2.0	-0.039
22,6	120	97	DMSO	7.1	2.0	-0.058
22,8	120	81	DMF	13.8	2.0	-0.071
22,12	120	98	DMF	16.7	2.2	-0.063
32,4	130	59	DMF	20.3	2.1	-0.057
32,6	130	100	DMF	80.6	2.2	-0.069
32,8	130	78	DMF	63.8	2.2	-0.069
32,12	130	54	DMF	25.3	2.2	-0.039
46,6	130	100	DMF	12.5	1.4	-0.055

In the synthesis of aliphatic polyurethanes from diols and diisocyanates, there are several side reactions[11] that can occur and for this research project had to be avoided (Scheme 3.2). The one that was of most concern in this study was the formation of crosslinks. The lone pair on the nitrogen of the carbamate ester can attack an isocyanato group to form an allophanate crosslink. To minimize the amount of allophanates formed, the polymerization temperature had to be well controlled. If water was present, it can react with an isocyanato group to form carbon dioxide and an amino group. The amine can then react with an isocyanato group to form an urea group. As with the carbamate ester, the lone pair of the nitrogen of the urea can also attack an isocyanato group to form a crosslink called a biuret. All three of these reactions can be avoided by eliminating the presence of any water during polymerization. Depending on the starting diisocyanate, dimerization to the carbodiimide or trimerization to the cyclic was also possible. These side reactions could usually be avoided by the choice of catalyst.

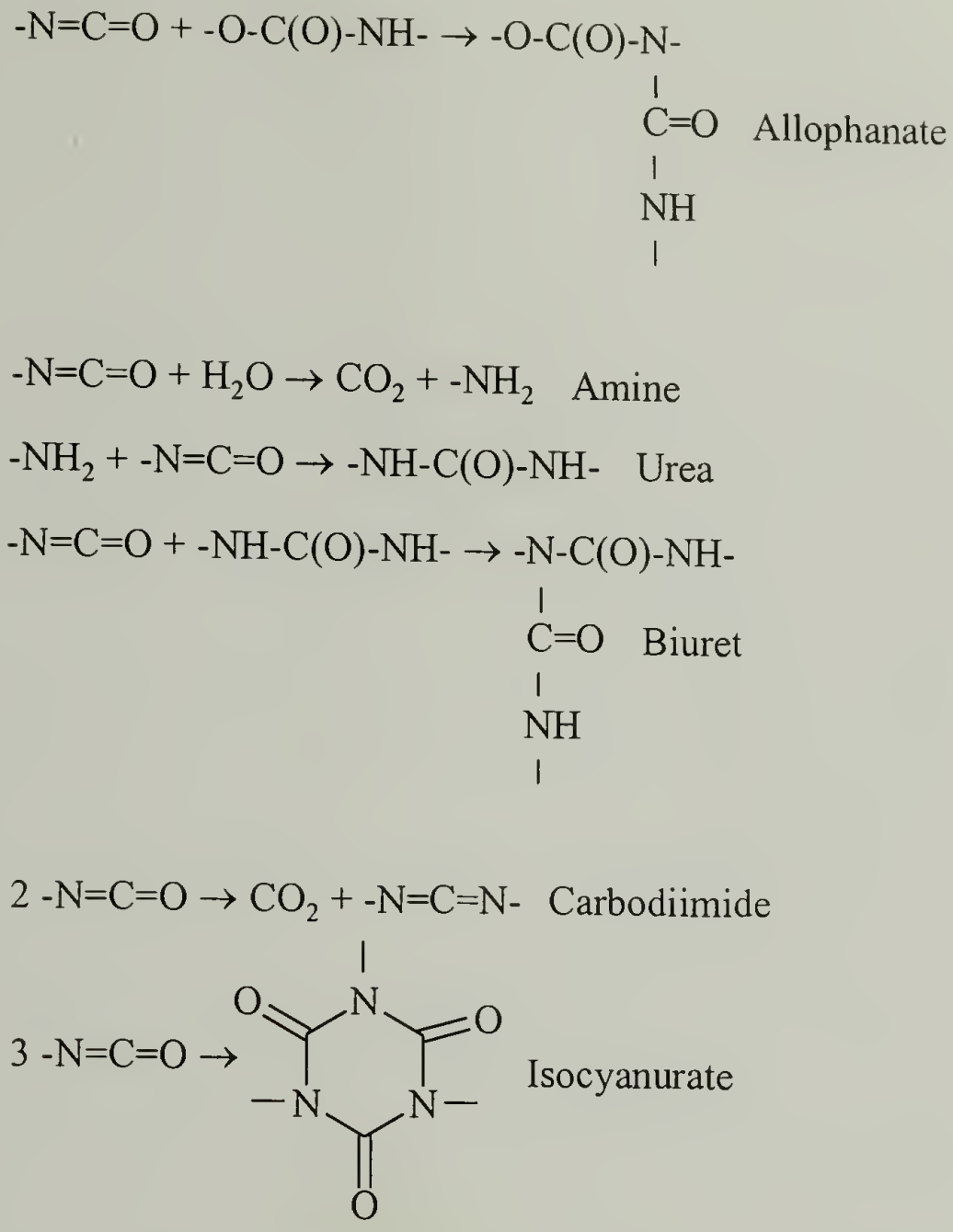

Scheme 3.2. Possible Side Reactions that Can Occur During Polymerization.

3.3.2 Characterization

3.3.2.1 Structure and Purity

Preliminary experiments proved the importance of the polymerization conditions (e.g. temperature and presence of water). The reaction temperature had to be high enough to melt the diol, but too high a temperature resulted in known side reactions such as crosslinking via the formation of allophanates. These crosslinks could be detected by GPC via the much higher than expected PDI. A PDI of 2 is expected for a normal step-

growth polymerization.[18] Additionally, the hydroscopic diols had to be fully dried. Failure to do so resulted in the formation of known side products including amines, ureas, and crosslinks via the formation of biurets. These side products could be detected using IR.

The purity of all the polymers was carefully examined using IR, NMR, and GPC. These characterization methods indicated the absence of all known side products including crosslinks. Some macrocyclics were expected since the polyurethanes were synthesized by a step-growth polymerization,[19] but neither their presence nor concentration could be confirmed. IR and high temperature ^{1}H- and ^{13}C-NMR spectra were fully compatible with the expected structures. Very low amounts of the methylene group alpha to hydroxyl and isocyanato end-groups were occasionally detected via ^{1}H-NMR and IR, respectively. The presence of these end-groups and their detection was expected based on the molecular weights of the polymers as determined by GPC. The ^{13}C-NMR spectra of the m,n-polyurethanes in DMSO-d_6 did not show a peak for the carbon of the methylene group alpha to the nitrogen of the carbamate ester. Presumably, the septet peak of the solvent at 39.7 ppm overlapped this peak. The peak was seen at 46.73 to 46.41 ppm when DMF-d_7 was used as the solvent. The absolute weight-average molecular weights M_w of the polymers ranged from 3,000 to 80,000 (Table 3.1). For all of the m,n-polyurethanes, the PDI was approximately 2 as expected.

3.3.2.2 Solubility

None of the crude m,n-polyurethanes dissolved in any common organic solvents at room temperature in an attempted range of concentration (1 to 5 $g \cdot L^{-1}$). A number of

solvents typically used for dissolving polyamides and polyurethanes[20] were tried at elevated temperatures with varying success. *o*-Dichlorobenzene, a solvent typically used to dissolve high-density polyethylene,[20] was also tried. The results are summarized in Table 3.2.

Table 3.2. Temperature[a] at which the m,n-Polyurethanes (1 to 5 $g \cdot L^{-1}$) Dissolved.

m,n-Polymer	*o*-Dichloro-benzene	*m*-Cresol	DMF	DMSO	Formic Acid	Sulfuric Acid
12,4	130	50	105	100	80	70
12,6	130	80	105	110	110	70
12,8	120	55	110	115	I	70
12,12	110	55	110	120	I	75
22,4	125	65	115	I	I	D
22,6	105	55	120	120	120	D
22,8	105	60	115	I	I	D
22,12	100	65	115	I	I	D
32,4	100	85	125	I	I	D
32,6	100	85	125	I	I	D
32,8	95	70	120	I	I	D
32,12	90	70	120	I	I	D
46,6	95	90	130	I	I	D

a) Reported in °C; D and I represent degradation and insolubility (at temperatures up to the polymer's melting point) of the sample, respectively.

All of the polymers dissolved in *m*-cresol, DMF, and *o*-dichlorobenzene at elevated temperatures. The temperatures needed to dissolve the samples in *m*-cresol were considerably lower than for the other solvents. However upon cooling, the polymers did not reprecipitate from the *m*-cresol, whereas they did reprecipitate from the other solvents. Therefore, *m*-cresol could not be used as a solvent for growing single crystals. The solubility of the m,n-polyurethanes in *o*-dichlorobenzene increased with increasing alkane length as the polymers became more polyethylene-like. On the other hand, the solubility of the polymers decreased with increasing alkane length in more typical

polyurethane solvents such as *m*-cresol and DMF. DMSO and formic acid, solvents typically used to dissolve polyamides and polyurethanes, were both able to dissolve all of the 12,n-polyurethanes as well as the 22,6-polyurethane. However, they were unable to dissolve the more aliphatic polyurethanes. Sulfuric acid was able to dissolve the 12,n-polyurethanes at only slightly elevated temperature, but degraded the rest of the m,n-polyurethanes.

3.3.2.3 Thermal Analysis

The thermal properties of the m,n-polyurethanes, along with those of polyurethanes of higher hydrogen-bonding density[21] and both HDPE[22] and LLDPE,[23] are summarized in Table 3.3. T_d values of ~ 300 °C were observed for all the polyurethanes. This value is between the 220 °C or higher T_d typically seen for polyurethanes of higher hydrogen-bonding density[10] and the 370 °C T_d seen for HDPE. The TGA thermograms of the m,6-polyurethanes are shown in Figure 3.2 and illustrate the decomposition behavior of all the m,n-polyurethanes. The m,n-polyurethanes synthesized from the longer α,ω-diols (1,32- and 1,46-diols) had just a slightly slower decomposition rate than the other polymers, and like the diols they were synthesized from they have a bump in their decomposition curves at higher temperatures (400 to 500 °C). Polyurethanes typically decompose through an unzipping mechanism to form either diisocyanates and diols or diamine, carbon dioxide, and olefins.[10] The TGA results could be attributed to the decomposition of the polyurethanes at temperatures around 300 °C to the diisocyanate (which would evaporate) and the diol (which in the case of the 1,12- and 1,22-diols would also evaporate, while the 1,32- and 1,46-diols would actually decompose).

Table 3.3. Thermal Properties of the m,n-Polyurethanes.

m,n-Polymer	Decomposition Temperature[d] (°C)	Melting Temperature[e] (°C)	Enthalpy ($J \cdot g^{-1}$)
2,6[a]		166	39
4,6[a]		182	70
6,6[a]		171	70
8,6[a]		162	60
10,6[a]		161	56
12,4	292	167[f]	
12,6	303	160[f]	
12,8	303	150	110
12,12	307	141	89
22,4	286	158	71
22,6	292	146	89
22,8	301	144	90
22,12	306	137	93
32,4	295	150	123
32,6	291	143	112
32,8	316	139	104
32,12	309	135	117
46,6	278	135[f]	
HDPE[b]	370	145[g] or 133 to 138[h]	295
LLDPE[c]		121 to 125	98 to 155

a, b, and c) See references 21, 22, and 23, respectively.

d) Decomposition temperatures were taken at 5% weight loss using a scan rate of 10 $K \cdot min^{-1}$.

e) Melting temperatures were taken as the peak of the melting endotherm during the second heating run using a scan rate of 10 $K \cdot min^{-1}$.

f) These polymers had more than one endotherm (see Figure 3.4); the melting points given were from the second endotherm, and enthalpy values were not calculated.

g and h) Theoretical and experimental values, respectively.

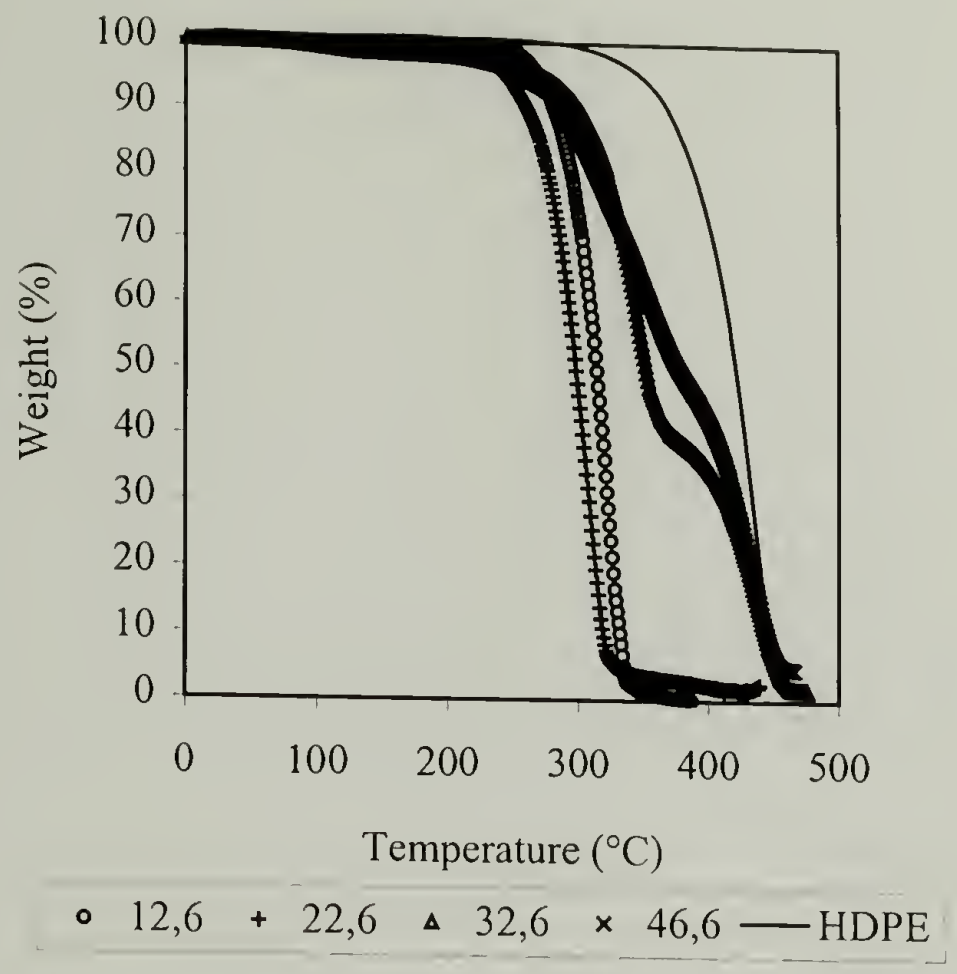

Figure 3.2. TGA Thermograms of the m,6-Polyurethanes.

As expected, the polymers exhibited decreasing melting points with increasing m or n (i.e. decreasing hydrogen-bonding density). As demonstrated by the m,6-polyurethanes in Figure 3.3, increasing the length of the alkane segments resulted in decreased melting points. With long enough alkane segments, the melting points of the m,n-polyurethanes approached that of HDPE (133 to 138 °C).[22]

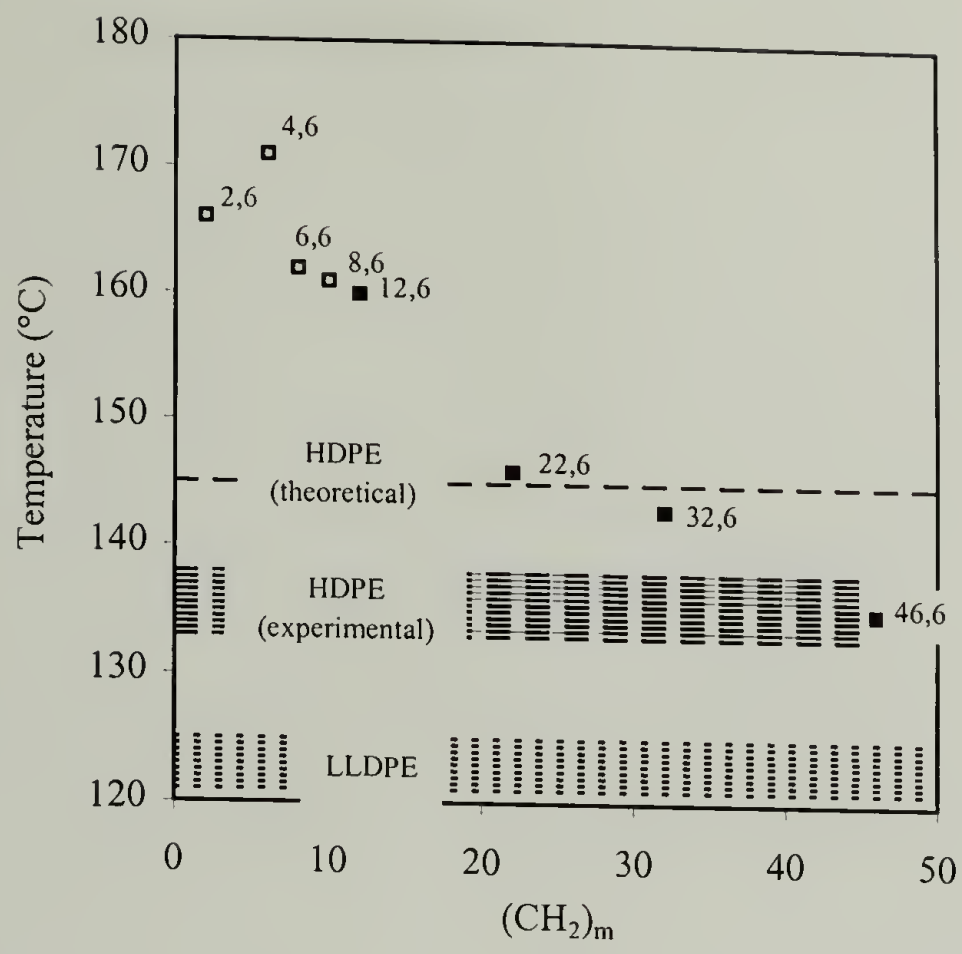

Figure 3.3. Comparison of the Melting Points of the m,6-Polyurethanes. ε and ω Represent Data from this Paper and Literature (See Reference 21), Respectively.

The melting and recrystallization behavior of the 12,4-, 12,6, and 46,6-polyurethanes differed from that of the other m,n-polyurethanes. These 3 polymers, which had a lower M_w than the other polymers (Table 3.1), exhibited a melting endotherm, followed immediately by an exothermic peak, and then another endotherm (Figure 3.4) upon heating. Upon cooling, all the polyurethanes exhibited only one exothermic peak. Melting of the folded chain, followed by crystallization to the fully extended chain, and then melting of the extended chain[24] could explain the melting behavior of these 3 polyurethanes. The other m,n-polyurethanes with their higher M_w exhibited only one melting endotherm corresponding to the melting of the chain-folded

polymers. Presumably, if the 12,4-, 12,6-, and 46,6-polyurethanes were of higher M_w, the 2 melting endotherms would not be observed.

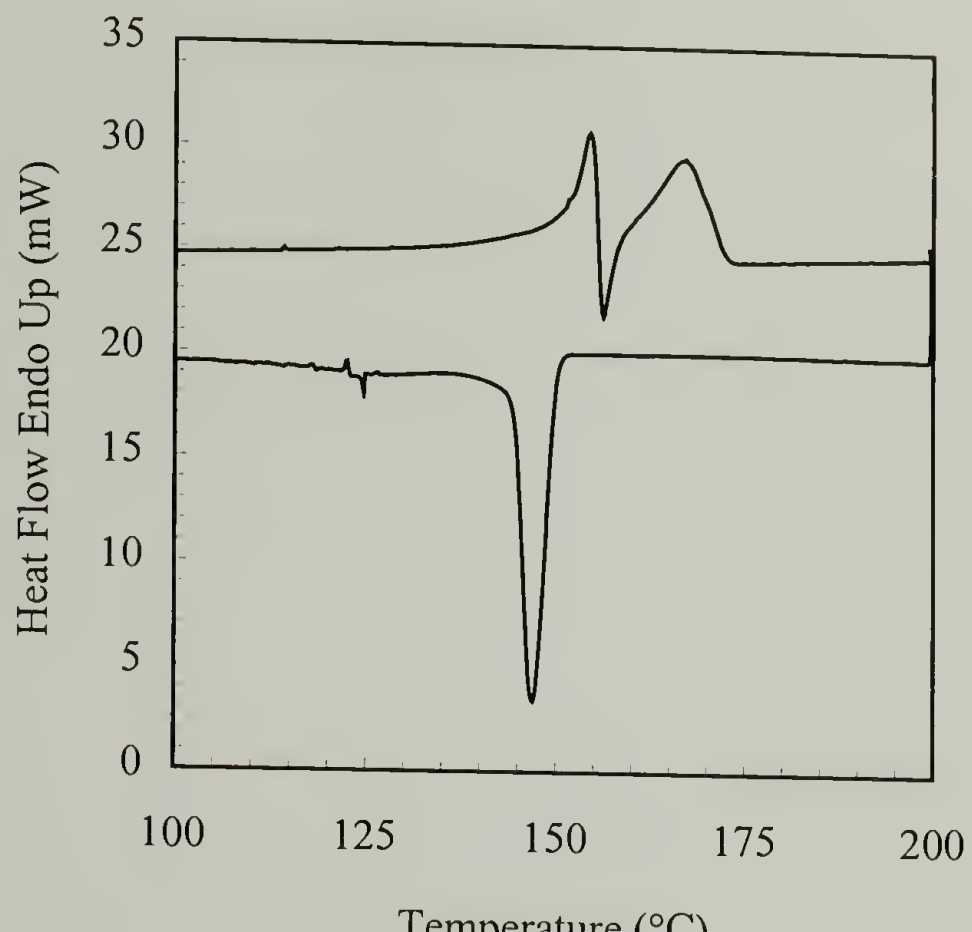

Figure 3.4. DSC Thermogram of the Low Molecular Weight 12,4-Polyurethane.

The measured heat of fusion of the m,n-polyurethanes increased with increasing m or n (i.e. decreasing hydrogen-bonding density). As with the melting temperature, the enthalpy appeared to be approaching that of HDPE (295 $J \cdot g^{-1}$).[22] This last parameter, and the possible correlation with the structure of the polymer, has to be considered with prudence since there are other factors (e.g. differences in the percent crystallinity of the polymers) that could cause this increase.

3.3.2.4 Lamellar Stacking Periodicity

The lamellar stacking periodicity (LSP, defined as the total length of the amorphous and crystalline regions) of the melt-crystallized polyurethanes were determined using SAXS (Table 3.4). Aliphatic polyurethanes and polyamides of high hydrogen-bonding density typically have LSPs in the range of 50 to 70 Å.[25-30] However, the m,n-polyurethanes in this study with their longer aliphatic segments showed LSPs more typical of polyethylene (110 to 140 Å).[31] The SAXS results for the 46,6-polyurethane is shown in Figure 3.5 and is representative of the behavior seen for all of the m,n-polyurethanes. The lower scattering vector q corresponded to the reciprocal of the LSP, while the higher value q was the consequence of the higher electron density of the systematically spaced carbamate esters (reciprocal of the d_{001}). It is important to note that the LSP values derived from the SAXS results do not take into account any tilting of the crystalline chains. However, the tilt angle can be derived from Equation 3.1, where the theoretical repeat length is calculated assuming an all *trans* conformation with 109° bond angles and bond lengths of: C-C = 1.54 Å, C-N = 1.47 Å, and C-O = 1.43 Å.[32]

$$\text{tilt angle} = \cos^{-1}(\text{observed } d_{001}/\text{theoretical repeat length}) \qquad \text{(Eq. 3.1)}$$

The d_{001} values for the 12,n-polyurethanes were below the detection of the instrumentation. For the 22,n-, 32,n-, and 46,6-polymers the tilt angle ranged from 36 to 46°, approximately that of nylons (e.g. 42° for nylon 6,6).[33]

Table 3.4. LSP and Tilt Angle of the m,n-Polyurethanes.

m,n-Polymer	Observed LSP (Å)	Observed d_{001} (Å)	Theoretical Repeat Distance (Å)	Tilt Angle (°)
12,4	104			
12,6	108			
12,8	119			
12,12	134			
22,4	149	28.4	39.5	44
22,6	102	30.3	42.0	44
22,8	136	30.7	45.5	46
22,12	139	39.1	49.5	38
32,4	182	42.3	52.0	36
32,6	137	42.9	54.5	38
32,8	130	44.5	57.0	39
32,12	131	45.8	62.0	42
46,6	130	55.1	72.0	40

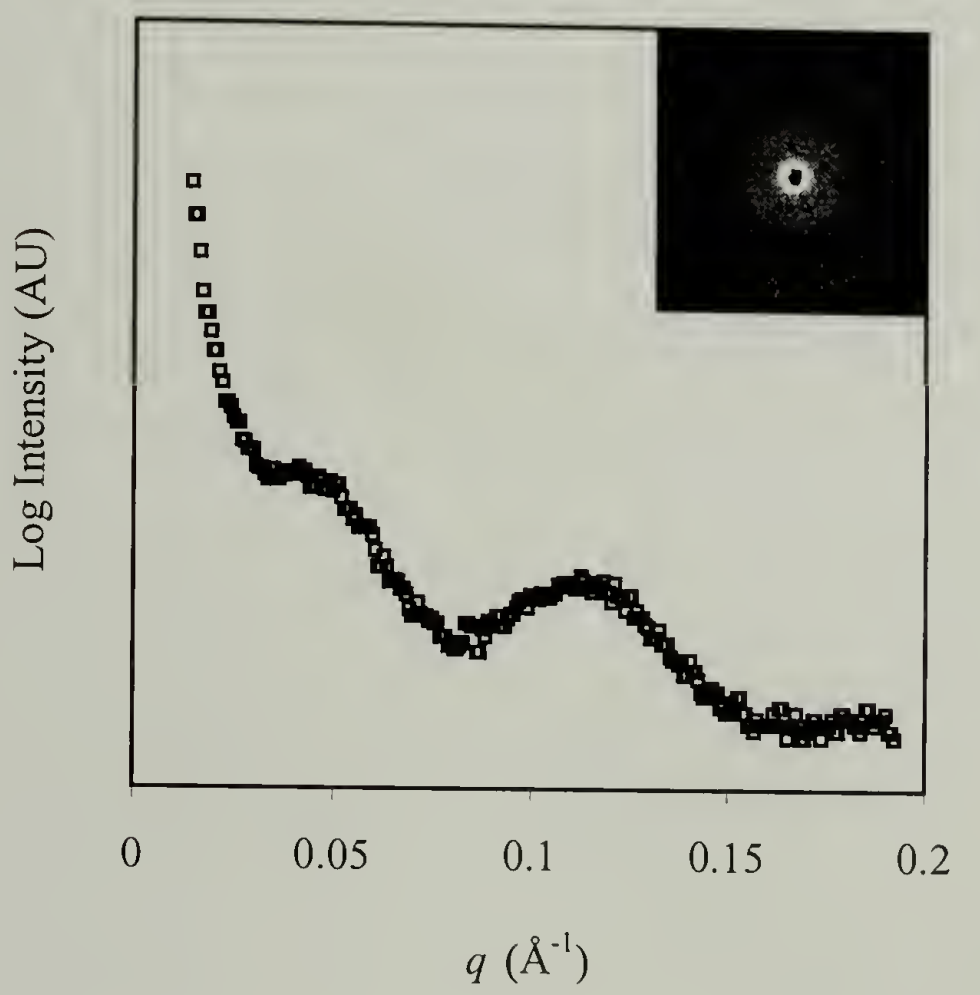

Figure 3.5. SAXS Results for the Melt-Crystallized 46,6-Polyurethane.

The LSP values of the 22,n-polyurethanes were also examined using TEM imaging. Ruthenium oxide was used to stain the melt-crystallized polymers. The stain preferentially complexed with the amorphous regions (thus making them darker in the TEM) and allowed for the visualization of the lamellar morphology. The experimental LSP values determined using TEM were consistent with that found using SAXS. Figure 3.6 shows the lamellar morphology of the stained 22,12-polyurethane, which is representative of that observed for all the polymers. Since the estimated chain length of the polyurethanes were an order of magnitude greater than the measured LSP values, chain-folding was expected in these lamellar crystals.

Figure 3.6. TEM Image of the Melt-Crystallized 22,12-Polyurethane Lamellae (Amorphous Regions are Black and Crystalline Regions are White) Stained with RuO_4.

3.4 Conclusions

A series of novel m,n-polyurethanes were synthesized by melt, step polyadditions of equimolar amounts of aliphatic, long-chain α,ω-diols and short-chain α,ω-diisocyanates. By progressively increasing the length of the diol, the hydrogen-bonding density of the polyurethanes was systematically diluted. The resulting polyurethanes ranged from the shortest, the 12,4, to the longest, the 46,6. Most of these polyurethanes had much lower hydrogen-bonding densities than the previously longest, purely aliphatic polyurethane, the 16,10.[3] With the exception of the 12,6-polyurethane none of the other polyurethanes had been previously synthesized.

Characterization of the m,n-polyurethanes showed that the polymers had M_w and PDI values typical of step-growth polymers. The formation of common side products including crosslinks was avoided by controlling the reaction temperature, eliminating the presence of water, and by not employing any catalysts. The purity of the m,n-polyurethanes was checked using IR, NMR, and GPC.

These increasingly aliphatic m,n-polyurethanes contained long aliphatic segments $(CH_2)_m$ characteristic of polyethylene as well as carbamate esters O-(CO)-NH capable of undergoing hydrogen-bonding and characteristic of polyamides and polyurethanes. As the physical and thermal properties (i.e. solubility, melting temperature, enthalpy, and lamellar stacking periodicity) of these long-chain polyurethanes were examined, a behavior typical of polyethylene became apparent. It would appear that the long aliphatic segments diluted the influence of the hydrogen-bonds on the polymers. It is still of interest to know where on the spectrum ranging from aliphatic to hydrogen-bonded polymers, the mechanical properties (i.e. yield stress, strain, and percent elongation) of

these polyethylene-like polyurethanes lie. However, examination of the mechanical properties requires grams of polymer. Due to the multiple steps and overall low yield in the synthesis of the long-chain α,ω-diols, currently only half gram quantities of the m,n-polyurethanes have been synthesized. A more detailed discussion on the crystal structure and crystallization behavior of these polymers will be discussed in the next chapter.

3.5 References

(1) Cho, I.; Lee, K. *Macromol. Chem. Phys.* **1997**, *198*, 861.

(2) Ehrenstein, M.; Dellsperger, S.; Kocher, C.; Stutzmann, N.; Weder, C.; Smith, P. *Polymer* **2000**, *41*, 3531.

(3) Saotome, K.; Komoto, H. *J. Polym. Sci., Part A: Polym. Chem.* **1967**, *5*, 119.

(4) Le Fevere de Ten Hove, C. Controlling Solid-State Microstructure of Semi-Crystalline Polymers Through Chemical Design of Chains: A Study of Model Polyesters. Ph.D. Thesis, Université Catholique de Louvain, Louvain-la-Neuve, 2001.

(5) Schall, J. D. Condensation Polymers with Regularly-Spaced, Strongly-Segregating Functionalities. Ph.D. Thesis, University of Massachusetts, Amherst, 2001.

(6) Menges, G. University of Massachusetts, Amherst. Unpublished work, 2002.

(7) Bayer, O.; Rinke, H.; Siefken, W.; Orthner, L.; Schild, H. German Patent DE 728,981, 1942.

(8) Bayer, O. *Angew. Chem.* **1947**, *59 A*, 275.

(9) Rinke, H.; Schlid, H.; Siefken, W. U.S. Patent 2,511,544, 1950.

(10) Polyurethanes. In *Polymer Synthesis*; 2 ed.; Sandler, S. T., Karo, W., Eds.; Academic: San Diego, 1994; Vol. 1, p 232.

(11) Parodi, F. Isocyanate-Derived Polymers. In *Comprehensive Polymer Science*; Allen, G., Bevington, J. C., Eds.; Pergamon: Oxford, 1989; Vol. 5, p 387.

(12) Wittbecker, E. L.; Katz, M. *J. Polym. Sci.* **1959**, *20*, 367.

(13) Wittbecker, E. L.; Morgan, P. W. *J. Polym. Sci.* **1959**, *40*, 289.

(14) Culbertson, B. M.; Sedor, E. A.; Slagel, R. C. *Macromolecules* **1968**, *1*, 254.

(15) Miyaki, Y.; Ozaki, S.; Hirata, Y. *J. Polym. Sci., Part A: Polym. Chem.* **1969**, *7*, 899.

(16) Burk Jr., E. H.; Carlos, D. D. U.S. Patent 3,423,449, 1969.

(17) Dieter Jr., J. A.; Kutts, H. W.; Wolgenuth, L. B. U.S. Patent 3,531,425, 1970.

(18) Odian, G. *Principles of Polymerization*; 3rd ed.; John Wiley & Sons: New York, 1991.

(19) Allcock, H. A.; Lampe, F. W. *Contemporary Polymer Chemistry*; 2nd ed.; Prentice Hall: New Jersey, 1990.

(20) Bloch, D. R. Solvents and Non Solvents for Polymers. In *Polymer Handbook*; 4th ed.; Brandrup, J., Immergut, E. H., Grulke, E. A., Eds.; John Wiley & Sons: New York, 1999.

(21) MacKnight, W. J.; Yang, M.; Kajiyama, T. *Polym. Prepr. (Am. Chem. Soc. Div. Polym. Chem.)* **1968**, *9*, 860.

(22) Mandelkern, L.; Alamo, R. G. Polyethylene, Linear High-Density. In *Polymer Data Handbook*; Mark, J. E., Ed.; Oxford University: New York, 1999; p 493.

(23) Prasad, A. Polyethylene, Linear Low-Density. In *Polymer Data Handbook*; Mark, J. E., Ed.; Oxford University: New York, 1999; p 508.

(24) Barham, P. J. Crystallization and Morphology of Semicrystalline Polymers. In *Materials Science and Technology: Structure and Properties of Polymers*; Thomas, E. L., Ed.; John Wiley & Sons: New York, 1993; Vol. 12.

(25) Dreyfuss, P.; Keller, A. *J. Polym. Sci., Part B: Polym. Phys.* **1970**, *8*, 253.

(26) Atkins, E. D. T.; Keller, A.; Sadler, D. M. *J. Polym. Sci., Part A: Polym. Chem.* **1972**, *10*, 863.

(27) Burmester, A. F.; Dreyfuss, P.; Geil, P. H.; Keller, A. *J. Polym. Sci., Polym. Lett. Ed.* **1972**, *10*, 769.

(28) Hinrichsen, G. *Makromol. Chem.* **1973**, *166*, 291.

(29) Dreyfuss, P. *J. Polym. Sci., Polym. Phys. Ed.* **1973**, *11*, 201.

(30) Magill, J. H.; Girolamo, M.; Keller, A. *Polymer* **1981**, *22*, 43.

(31) Dreyfuss, P.; Keller, A. *J. Macromol. Sci., Phys.* **1970**, *4*, 811.

(32) Allen, F. H.; Kennard, O.; Watsun, D. G.; Brammer, L.; Orpen, A. G.; Taylor, R. *J. Chem. Soc. Perkin Trans. 2* **1987**, S1.

(33) Atkins, E. D. T.; Hill, M.; Hong, S. K.; Keller, A.; Organ, S. *Macromolecules* **1992**, *25*, 917.

CHAPTER 4. INFLUENCE OF HYDROGEN-BONDING ON THE CRYSTALLIZATION BEHAVIOR OF THE m,n-POLYURETHANES

4.1 Introduction

The introduction of hydrogen-bonding groups (e.g. amide C(O)-NH or urethane O-C(O)-NH groups) on an otherwise purely aliphatic polymer dramatically influences the way the macromolecule crystallizes (e.g. crystal structure, morphology, crystallization kinetics, and resulting thermal properties).[1] Typical aliphatic m,n-polyurethanes of high hydrogen-bonding density have been reported to have a similar crystal structure as the corresponding aliphatic polyamides.[2-6] Aliphatic polyamides have either monoclinic (characterized by WAXS reflections at *d*-spacings of 4.4 Å (d_{200}) and 3.7 Å (d_{020} and d_{220})) or triclinic packing (characterized by WAXS reflections at *d*-spacings of 4.4 Å (d_{100}) and 3.7 Å (d_{010} and d_{110})) depending on whether the polymer is type AB or AABB, whether the aliphatic segments are even or odd, and on the length of the aliphatic segment.[7] Depending on the crystallization conditions, a varying amount of pseudohexagonal packing (characterized by a WAXS reflection at a *d*-spacing of 4.2 Å (d_{200})) has also been proposed.[8] Triclinic polyamides contain all *trans* chains that are oriented parallel to each other in order to maximize the contribution of the hydrogen-bonds C=O···H-N between neighboring stems to the overall stability of the crystal structure (Figure 4.1a). In contrast, linear polyethylene also has an all *trans* conformation, but with no hydrogen-bonding groups in the aliphatic backbone crystallizes by packing into an orthorhombic unit cell (characterized by WAXS

reflections at *d*-spacings of 4.1 Å (d_{110}) and 3.7 Å (d_{200})) in order to maximize the van der Waals forces between the polymer chains (Figure 4.1b).[9]

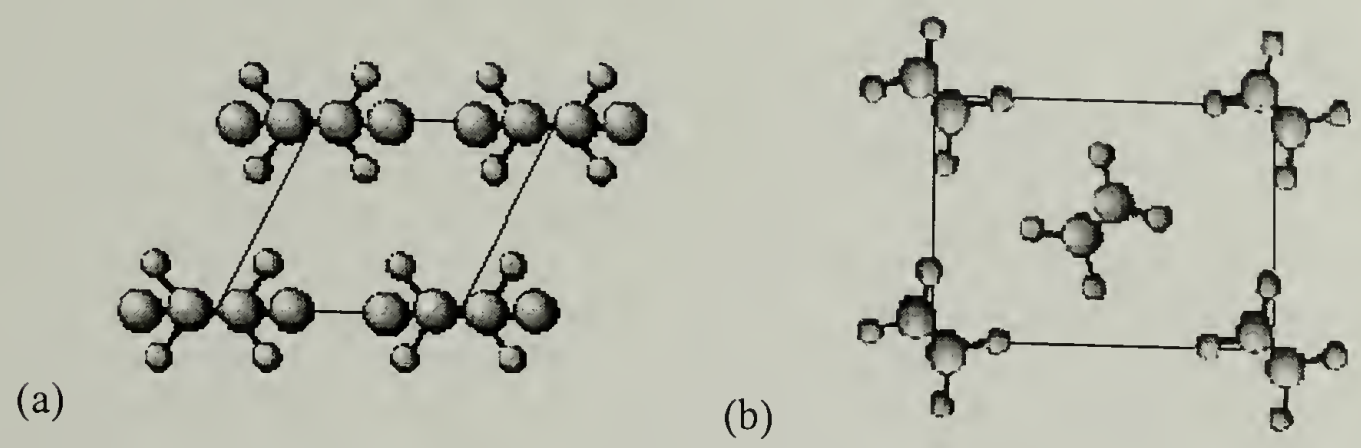

Figure 4.1. Crystal Structure: (a) Typical of Polyamides and Polyurethanes (Triclinic Packing) and (b) Typical of Polyethylene (Orthorhombic Packing).

By increasing the length of the aliphatic segments of the m,n-polyurethanes [O-$(CH_2)_m$-O-C(O)-NH-$(CH_2)_n$-NH-C(O)]$_n$, the influence of the carbamate esters O-C(O)-NH was progressively diluted. As discussed in the previous chapter, the physical and thermal properties (e.g. solubility, melting temperature, enthalpy, and lamellar stacking periodicity) of the increasingly aliphatic polyurethanes resembled that of linear HDPE. It could reasonably be expected that above a certain methylene/carbamate ester ratio, the crystallization behavior (e.g. crystal structure, morphology, annealing behavior, and kinetics) of these aliphatic polyurethanes would approach that of linear HDPE.

A main goal of this research study was to determine the onset of this transition from a polyurethane- or polyamide-like behavior to a polyethylene-like behavior and to investigate the details of the crystallization process at and close to that transition region. This was accomplished by examining the crystal structure (with the aid of Dr. E. D. T. Atkins and his student Pawel Skorski from the University of Bristol), annealing behavior,

and crystallization kinetics (in collaboration with Amy Heintz under the supervision of Dr. S. L. Hsu) of the m,n-polyurethanes. A better understanding of the balance between methylene-methylene van der Waals interactions and hydrogen-bonding in semi-crystalline polymer structures is expected to be extremely useful in the design of self-assembling polymers and aid in the engineering and fine-tuning of the crystallinity of these systems.

4.2 Experimental

4.2.1 Characterization

^{1}H-NMR spectra were obtained in $CDCl_3$, DMSO-d_6, or C_6D_6 from a Bruker 300 MHz NMR at room temperature.

4.2.2 Sample Preparation

The synthesis of the m,n-polyurethanes $[O\text{-}(CH_2)_m\text{-}O\text{-}C(O)\text{-}NH\text{-}(CH_2)_n\text{-}NH\text{-}C(O)]_n$ was discussed in Chapter 3. Melt-crystallized samples were prepared by heating the polymers to 200 °C and then allowing the polymers to cool to room temperature at a rate of 10 $K \cdot min^{-1}$. Solution-grown crystals of the 22,12-polyurethane were prepared by dissolving the polymer in DMF at 120 °C (temperature maintained in an oil bath) to make a 0.01% (w/v) solution. The temperature was rapidly cooled to room temperature and then slowly reheated to the temperature (115 °C) where the polymer dissolved. The temperature was gradually lowered over a period of 1 h to 105 °C, and the polymer was isothermally crystallized for 20 h before being allowed to cool to room temperature.

Oriented crystal mats suitable for X-ray diffraction were prepared by draining the crystal suspension through a 0.22 μm filter.

4.2.3 Thermal Analysis

Melting points were observed using a Perkin Elmer Pyris DSC flushed with helium. The 5 to 10 mg samples were heated above their melting points to 200 °C, cooled to room temperature, and then reheated, all at a rate of 10 $K \cdot min^{-1}$. The first heating and cooling run was performed in order to erase the different thermal histories present in the samples. The melting points were taken as the peak of the melting endotherm during the second heating run. The temperature scale was calibrated using indium and eicosane, and the heat of enthalpy was calibrated using indium.

4.2.4 Spectroscopy

Fourier transform (FT) IR spectra were recorded on a Bio-Rad FTS 175C spectrometer at room temperature and on a Perkin Elmer Spectrum 2000 system with a wide band MCT detector at elevated temperatures. A home-built heating cell attached to an Omega proportioning temperature controller with an accuracy of 2 °C was employed to control the temperature of the IR cell. The temperature was calibrated to the melting point of benzoic acid. A total of 16 scans were performed, and spectral resolution was 4 cm^{-1}. Analysis of the data was performed using Spectrum 2000 software, and literature procedures[10] were used to deconvolute the amide I region of the spectra. Pellets were prepared by grinding a small amount of the m,n-polyurethane with KBr and then pressing the mixture into pellets. Films were prepared by dissolving the polymer in hot *o*-

dichlorobenzene and then casting the sample onto KBr plates. The resulting polymer films were approximately 5 to 10 μm thick.

A Bruker FRA 106 spectrometer equipped with a Nd:Yag laser (1.064 μm) was used to record the FT Raman spectra. A total of 256 scans were performed, and spectral resolution was 4 cm^{-1}. The laser power was 150 mW, and the excitation/collection geometry was 180°. The polyurethanes were examined in the bulk without any special crystallization treatment.

4.2.5 X-ray Scattering

X-ray scattering patterns, in the medium- to wide-angle range, were obtained at room temperature using Ni-filtered Cu Kα radiation of wavelength 1.542 Å from a Siemens sealed tube X-ray generator operating at 40 kV and 30 mA. A point-collimated beam was used, and the X-ray scattering patterns were recorded using a flat image plate in an evacuated Statton camera. Calcite (d_b = 3.035 Å) was dusted onto selected samples for calibration purposes. WAXS experiments were also performed on the Advanced Polymers Beamline (X27C) at the National Synchrotron Light Source, Brookhaven National Laboratory, Upton, New York. The camera length was calibrated using calcite. The X-ray beam had a 3 mm^2 area and a wavelength of 1.307 Å. Custom software was used to subtract the background, circularly average the data, and convert the data to a logarithmic intensity scale.

X-ray scattering patterns, in the small-angle range, were obtained at room temperature using Ni-filtered Cu Kα radiation of wavelength 1.542 Å from a Rigaku rotating anode operating at 40 kV and 200 mA. A point-collimated 300 μm diameter

beam was used, and the X-ray scattering patterns were recorded using an evacuated Siemens GADDS 2-dimensional area detector.

4.2.6 Electron Microscopy

Carbon-coated TEM grids were dipped into the crystal suspension, and the solvent was allowed to evaporate in a vacuum oven at room temperature. Some samples were shadowed with Pd-Pt to enhance the contrast of the TEM images, while other samples were shadowed with gold (d_{111} = 2.35 Å) to calibrate the electron diffraction patterns. The magnification was calibrated using a crossed lined grated replica with 2160 lines per mm. The TEM images and electron diffraction patterns were recorded at room temperature using a JEOL 100 CX microscope operating at 100 kV.

4.2.7 Model Building

The software package Cerius2, version 3.8 (MSI) was used in the structural modeling and diffraction simulations. The software packages Insight II and Discover 3 (MSI), employing the CVFF force field, were used in the molecular dynamic (MD) simulations. Periodic boundary conditions, with bonds across the boundaries in the chain direction, were used in these dynamic simulations. The Ewald summation method was used in the calculation of non-bonded interactions. The simulations were performed at room temperature, under constant pressure, and temperature assembly conditions (NPT) and consisted of 50,000 MD steps in time steps of 1 fs.

4.2.8 Monomer Synthesis

4.2.8.1 General Considerations

Reagents used in the synthesis of the diisocyanate were obtained commercially, and unless otherwise stated, they were used without further purification. Formic acid was dried over phthalic anhydride. Benzene and THF were dried over sodium and benzophenone. Dichloromethane was dried using phosphorous pentoxide.

4.2.8.2 Synthesis of 1,6-Diisocyanatohexane from the Diamine Using Formic Acid and Bromine

Hexamethylene Diformamide (21). Hexamethylenediamine (2.94 g, 0.03 mol) was added to formic acid (3.66 g, 0.07 mol), and the mixture was refluxed for 15 minutes in a Kugelrohr distillation apparatus. A vacuum was then applied, and the temperature was slowly increased to 130 °C over a time period of 4 hours. The temperature was then increased to 180 °C and held there for 30 minutes. After cooling, the product was recrystallized twice from isoamyl alcohol (50 mL) yielding hexamethylene diformamide (**21**) as a white solid (3.06 g, 71%); m.p. 106.2 °C, lit.: 106-108 °C,[11] 106-107 °C.[12]

1,6-Diisocyanatohexane (22). Hexamethylene diformamide (**21**) (1.00 g, 5.88 mmol), 1,4-diazabicyclo[2.2.2]octane (DBO, 1.30 g, 0.01 mol), and benzene (17 mL) were added to a three-necked flask and heated to 70 °C. Bromine (3.65 g, 0.02 mol) was slowly added dropwise. The yellow solution was then refluxed for 3 hours. After cooling, the sample was a red solid. The red solid (1,4-diazabicyclo[2.2.2]octane

dihydrobromide) was filtered, but no liquid (desired product 1,6-diisocyanatohexane (**22**) and benzene) was present.

4.2.8.3 Synthesis of 1,6-Diisocyanatohexane from the Diamine via Phosgenation with Triphosgene

1,6-Diisocyanatohexane (22). Hexamethylenediamine (0.45 g, 3.88 mmol), 1,8-bis(dimethylamino)-naphthalene (Proton-Sponge™, 3.32 g, 0.02 mol), and dichloromethane (10 mL) were added to an argon-purged, three-necked flask and cooled in an ice bath. The argon outlet was bubbled through a solution of sodium hydroxide (25%). Over a period of 5 minutes, bis(trichloromethyl)carbonate (trisphogene, 1.38 g, 4.66 mmol) in dichloromethane (10 mL) was slowly added dropwise. The ice bath was removed, and the mixture was stirred for 10 minutes. During this time, the mixture turned yellow and finally brown. The solution was evaporated leaving a bright yellow solid. The solid was dissolved in dichloromethane (20 mL) and hydrochloric acid was added (1 $mol \cdot L^{-1}$, 10 mL). The organic phase was separated and washed with hydrochloric acid (1 $mol \cdot L^{-1}$, 3 x 10 mL aliquots) and then with sodium hydroxide (1 $mol \cdot L^{-1}$, 10 mL). The organic phase was again separated and then dried with magnesium sulfate. Evaporation of the dichloromethane left a white solid. 1,6-Diisocyanatohexane (**22**) was not, however, synthesized. The white solid was determined to be the starting material, hexamethylenediamine. ^{1}H-NMR (300 MHz, C_6D_6) δ 2.57 (t, J = 6.6 Hz, 4H, CH_2-NH_2), 0.92 (t, J = 6.3 Hz, 4H, CH_2-CH_2-NH_2), 0.74 (quintet, J = 3.6 Hz, 4H, CH_2-CH_2-CH_2).

4.2.8.4 Synthesis of 1,6-Diisocyanatohexane from the Diacid Using Proton-Sponge™ and DPPA

1,6-Diisocyanatohexane (22). Suberic acid (2.43 g, 0.01 mol) and THF (17.5 mL) were added to a nitrogen-purged flask. Proton-Sponge™ (5.99 g, 0.03 mol) was added, and the mixture was stirred at room temperature for 15 minutes. During this time the reagents all dissolved, and the solution turned pink. Diphenyl phosphoryl azide (DPPA, 7.66 g, 0.03 mol) was slowly added dropwise, and the solution turned yellow. The mixture was then refluxed for 6 hours. The solution was cooled to -5 °C in order to precipitate out the ammonium phosphate salt. The white solid was filtered, but no liquid (desired product 1,6-diisocyanatohexane (**22**) and THF) was present.

4.2.8.5 Synthesis of 1,6-Diisocyanatohexane from the Diacid via a Curtius Rearrangement

Diethyl Suberate (23). Suberic acid (6.95 g, 0.04 mol), ethanol (150 mL), and concentrated sulfuric acid (5 mL) were combined and refluxed for 16 hours. After cooling the mixture, benzene (300 mL) and deionized water (600 mL) were added. The two phases were then separated. The aqueous layer was extracted with benzene (6 x 50 mL aliquots) and then ether (6 x 50 mL aliquots). The combined organic phases were evaporated yielding diethyl suberate (**23**) as a clear liquid (8.13 g, 89%). ^{1}H-NMR (300 MHz, $CDCl_3$) δ 4.10 (q, J = 7.1 Hz, 4H, CH_2-O-C(O)), 2.27 (t, J = 7.5 Hz, 4H, CH_2-C(O)-O), 1.98 (quintet, J = 7.2 Hz, 4H, CH_2-CH$_2$-C(O)-O), 1.45 (quintet, J = 3.7 Hz, 4H, CH$_2$-CH_2-CH$_2$), 1.20 (t, J = 7.1 Hz, 6H, CH_3-CH$_2$-O-C(O)).

Suberic Dihydrazide (24). Diethyl suberate (**23**) (8.13 g, 0.04 mol), hydrazine monohydrate (6 mL), ethanol (95%, 70 mL), and deionized water (10 mL) were combined and refluxed for 72 hours. Upon cooling, suberic dihydrazide (**24**) crystallized as a white solid (5.26 g, 73%). ^{1}H-NMR (300 MHz, DMSO-d_6) δ 8.90 (bs, 2H, N*H*-C(O)), 4.14 (bs, 4H, N*H*$_2$-NH-C(O)), 1.98 (t, J = 7.3 Hz, 4H, C*H*$_2$-C(O)-NH), 1.45 (m, 4H, C*H*$_2$-CH$_2$-C(O)), 1.20 (m, 4H, CH$_2$-C*H*$_2$-CH$_2$).

Suberic Diazide (25). Ice (22.4 g, 1.24 mol), carbon tetrachloride (3.7 mL), and concentrated hydrochloric acid (2.6 mL) were cooled in an ice/water/salt bath, and suberic dihydrazide (**24**) was then added. Sodium nitrite (1.81 g, 0.03 mol) in ice-cold, deionized water (3.7 mL) was slowly added dropwise while keeping the temperature of the mixture below 8 °C. After stirring the mixture for an additional 30 minutes, the two phases were separated. The aqueous layer was then extracted with benzene (6 x 5 mL aliquots). The combined organic phases were dried with calcium chloride yielding crude suberic diazide (**25**). Due to the instability and explosive nature of the compound, the diazide was used immediately in the next step without further purification. Raman: 2135 cm^{-1} (N_3 stretch), 1718 cm^{-1} (CO stretch).

1,6-Diisocyanatohexane (22). Suberic diazide (**25**) was filtered and refluxed in a nitrogen-purged flask for five hours. The benzene was then evaporated at 140 °C under vacuum pressure. 1,6-Diisocyanatohexane (**22**) was not, however, synthesized. Instead, due to contamination of water, 1,6-hexamethylenediamine was made. ^{1}H-NMR (300 MHz, C_6D_6) δ 2.59 (bs, 4H, C*H*$_2$-NH$_2$), 0.97 (bs, 4H, C*H*$_2$-CH$_2$-NH$_2$), 0.79 (m, 4H, CH$_2$-C*H*$_2$-CH$_2$).

4.3 Results and Discussion

4.3.1 Crystal Structure of the Increasingly Aliphatic m,n-Polyurethanes

The WAXS patterns of this family of m,n-polyurethanes (regardless of the length of the aliphatic segments) were all similar with the exception of the melt-crystallized 12,12-polyurethane (Figure 4.2a), which for reasons currently under examination had only 2 observable diffraction peaks, and the 46,6-polyurethane (Figure 4.2b), which had the same *d*-spacings as the other polyurethanes but different intensities. The diffraction patterns obtained from powdered mats or taken with the incident X-ray beam orthogonal to the mat surface exhibited the same diffraction features and measured *d*-spacings (Figure 4.2c), thus the lamellae obtained by crystallizing from the melt and isothermally from solution were the same. There was no preferred orientation, and the Bragg diffraction signals therefore appeared as rings.

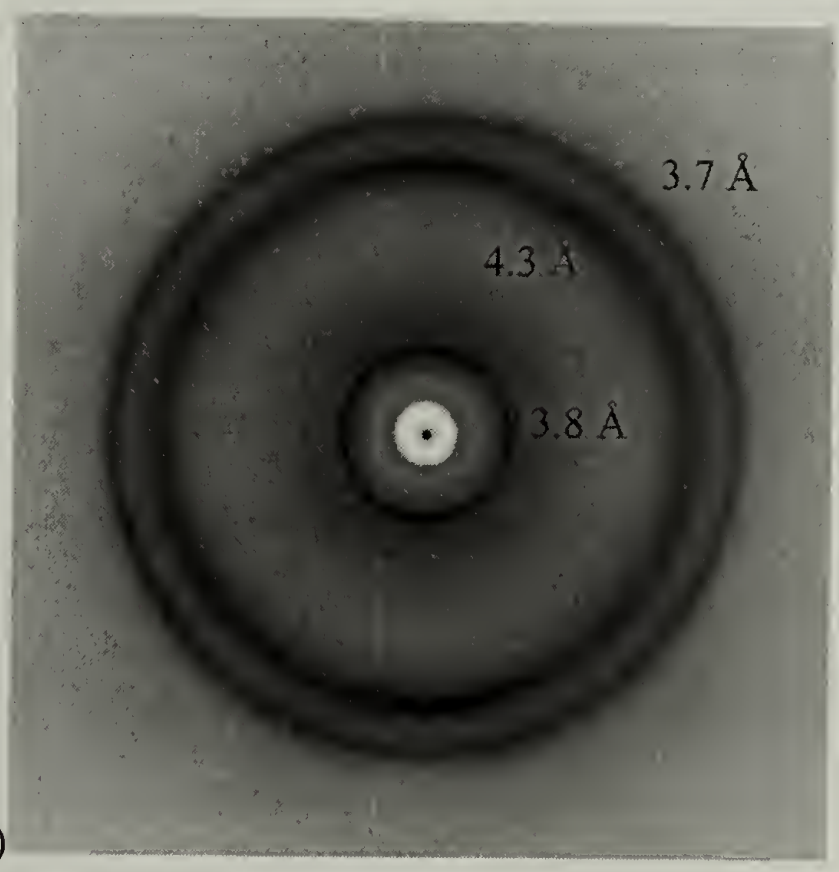

(a)

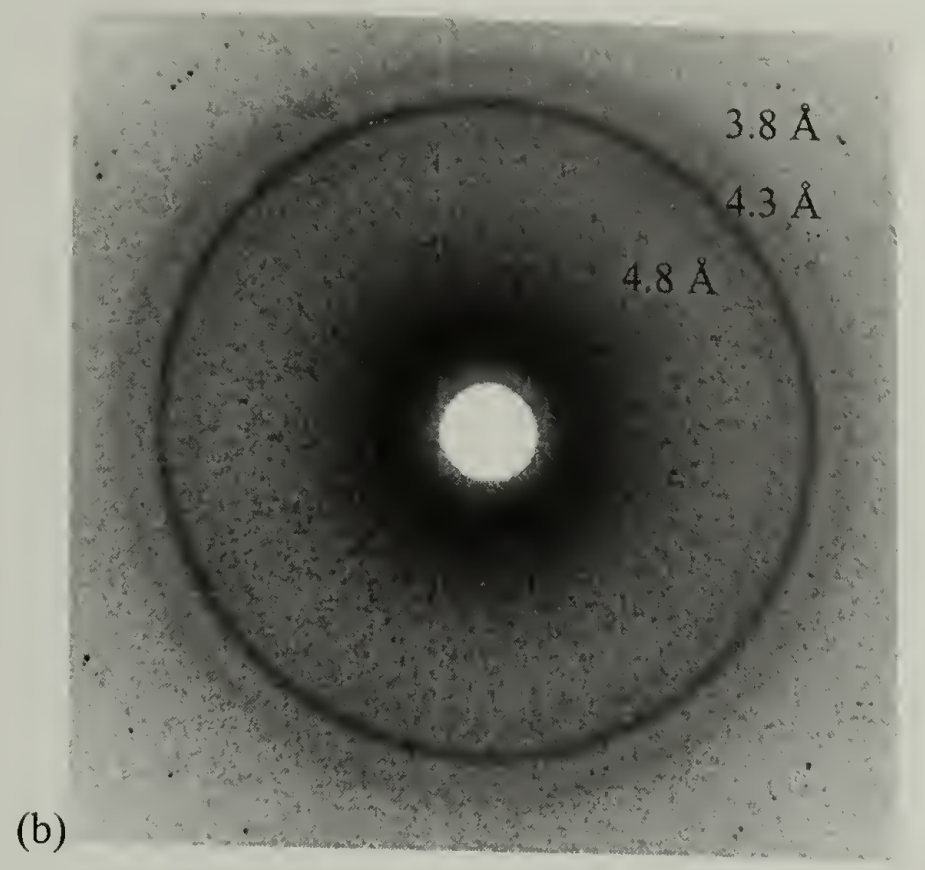

(b)

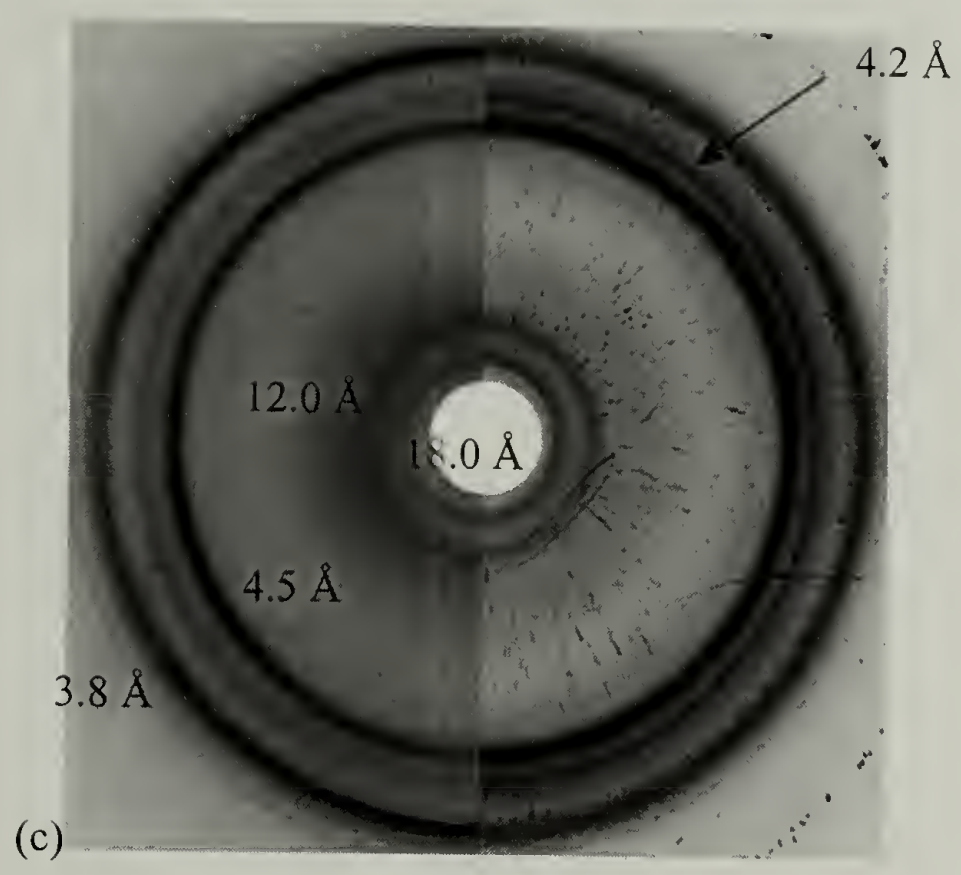

(c)

Figure 4.2. WAXS Pattern of the: (a) Melt-Crystallized 12,12-Polyurethane, (b) Melt-Crystallized 46,6-Polyurethane, and (c) (Left) Solution-Grown and (Right) Melt-Crystallized 22,12-Polyurethane.

The m,n-polyurethanes exhibited strong intensities at *d*-spacings of 4.7 to 4.5 Å and 3.8 to 3.7 Å (Table 4.1). A weaker diffraction peak at a *d*-spacing of 4.2 to 4.1 Å was sometimes observed; the relative intensity of which was a function of the

crystallization conditions. The longest polyurethane, the 46,6, had the opposite diffraction pattern with very weak diffraction rings at *d*-spacings of 4.8 Å and 3.8 Å and a very strong diffraction ring at a *d*-spacing of 4.3 Å. The *d*-spacings of the 2 prominent diffraction peaks appear to be related to the characteristic 4.4 Å interchain/intrasheet distance (d_{100}) and the 3.7 Å intersheet distance (d_{010}) typically seen for even-even, aliphatic, triclinic polyamides. Figure 4.3 shows the proposed triclinic packing of these m,n-polyurethanes. The diffraction ring at 4.1 to 4.2 Å was consistent with a pseudohexagonal packing similar to that seen for some polyamides.[8]

Table 4.1. WAXS Results for the m,n-Polyurethanes.

m,n-Polymer	d_{100} (Å)	d_{200} (Å)	d_{010} (Å)	1st Order d_{001} (Å)	2nd Order d_{001} (Å)	3rd Order d_{001} (Å)	Theoretical Repeat Distance (Å)	Tilt Angle (°)
12,4	4.6	4.1	3.8	20.4			27	41
12,6	4.7	4.1	3.7	21.0	10.5	7.0	29.5	45
12,8	4.5	4.1	3.7	24.4	12.2		32	40
12,12	4.3		3.7		13.8		37	42
22,4	4.6	4.1	3.8			11.3	39.5	31
22,6	4.6	4.1	3.7			11.0	42	38
22,8	4.6	4.1	3.7		17.3	11.5	44.5	39
22,12	4.5	4.2	3.8	36.0	18.0	12.0	49.5	43
32,4	4.5	4.1	3.7					
32,6	4.5	4.1	3.7					
32,8	4.5	4.1	3.7					
32,12	4.5	4.1	3.7					
46,6	4.8	4.3	3.8					

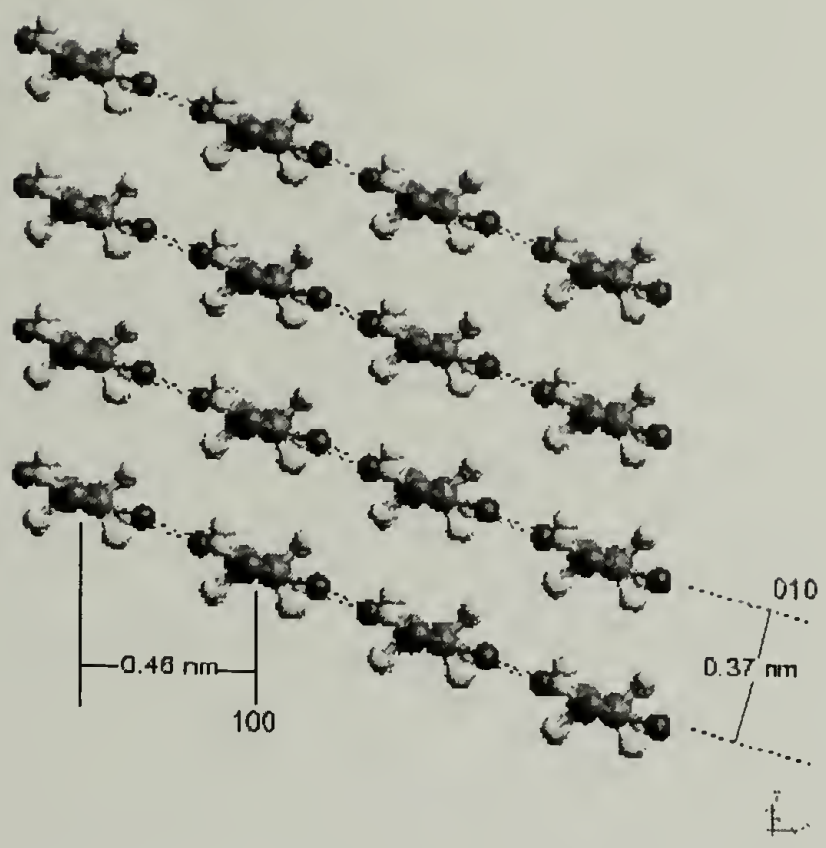

Figure 4.3. Proposed Triclinic Crystal Structure of the m,n-Polyurethanes Viewed Down the Chain Axis.

Some of the polymers also displayed diffraction peaks, with varying intensities within the polyurethane family, at larger *d*-spacings of 7.0 to 36.0 Å (Figure 2a and c). Figure 4.4 is the diffraction pattern (medium-angle X-ray scattering, MAXS) of the 22,12-polyurethane recorded at a larger specimen to detector distance and shows that these spacings were in fact orders of the fundamental structural repeat (d_{001}). Observation of up to the 3rd order of the d_{001}-spacing for the 12,6- and 22,12-polyurethanes indicated excellent packing of these crystals. Using these d_{001}-spacings, the angle of the chain tilt with respect to the lamellar surface was estimated (Equation 4.1).

$$\text{tilt angle} = \cos^{-1}(\text{observed } d_{001}/\text{theoretical repeat length}) \qquad \text{(Eq. 4.1)}$$

At this level of analysis, an all *trans* conformation was assumed for the chains. Clearly, perturbations from an all *trans* conformation would increase the tilt angle slightly. The tilt angles (Table 4.1) calculated from the WAXS data ranged from 31 to 45° and was consistent with that obtained from the SAXS data, which ranged from 36 to 46° (see Section 3.3.2.4). Both the WAXS and SAXS had some degree of error associated with the derived tilt angle due to the weak intensity and broad peak, respectively of the d_{001} reflections.

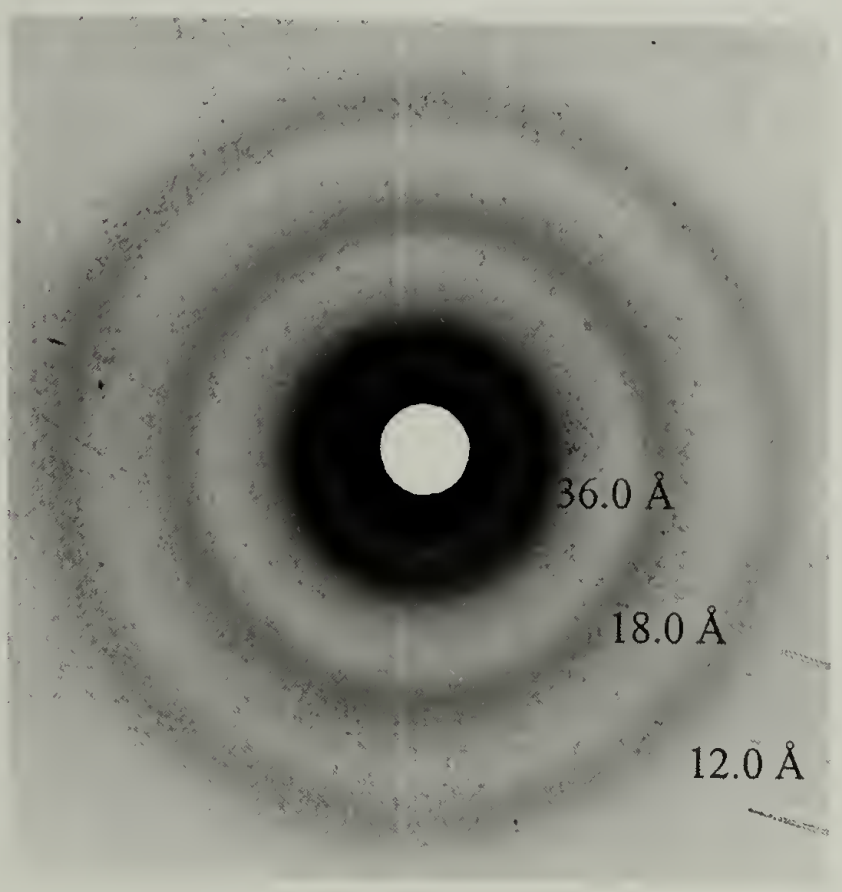

Figure 4.4. MAXS Pattern of the Melt-Crystallized 22,12-Polyurethane.

Attempts to get oriented samples proved unsuccessful for all but the 22,12-polyurethane. These attempts included pulling and stretching fibers, trying to orient thin polymer films made from the melt, and making single crystal mats from a variety of solvents. This was probably the result of the low percent crystallinity of the polyurethanes (see Section 4.3.3). In the case of the solution-grown 22,12-polyurethane,

sedimented mats were obtained that exhibited partial orientation as can be seen in the X-ray diffraction pattern (Figure 4.5). It was judged that this data was of sufficient quality to warrant a more detailed analysis (e.g. unit cell parameters and chain conformation and packing) of the crystallization structure of the 22,12-polyurethane; these results will be discussed in Section 4.3.2.

Figure 4.5. WAXS Pattern of the Oriented, Solution-Grown, Sedimented Mat of the 22,12-Polyurethane with the Incident X-ray Beam Directed Parallel to the Mat Surface

In order to obtain the [001] zone electron diffraction from an individual, solution-grown lamellae (Figure 4.6a), the sample had to be tilted by a large angle in a specific direction. This selected area electron diffraction procedure was technically demanding (as a result of beam damage, the electron diffraction pattern only lasts for seconds), but as shown in Figure 4.6a completely possible. This [001] zone electron diffraction pattern was useful since it recorded the a^*b^*-reciprocal net and allowed for the direct

measurement of γ* (115°). Twining, typical of chain-folded crystals of aliphatic polyamides,[13,14] also occurred. Additionally, the electron diffraction pattern showed that the composition plane was (010) and was parallel to the long axis of the crystalline lamellae. TEM imaging at 20,000 times magnification (Figure 4.6b) revealed that these solution-grown polymers formed extended aggregates of overlaying, lath-like lamellae similar to those formed by polyamides under similar experimental conditions.[2]

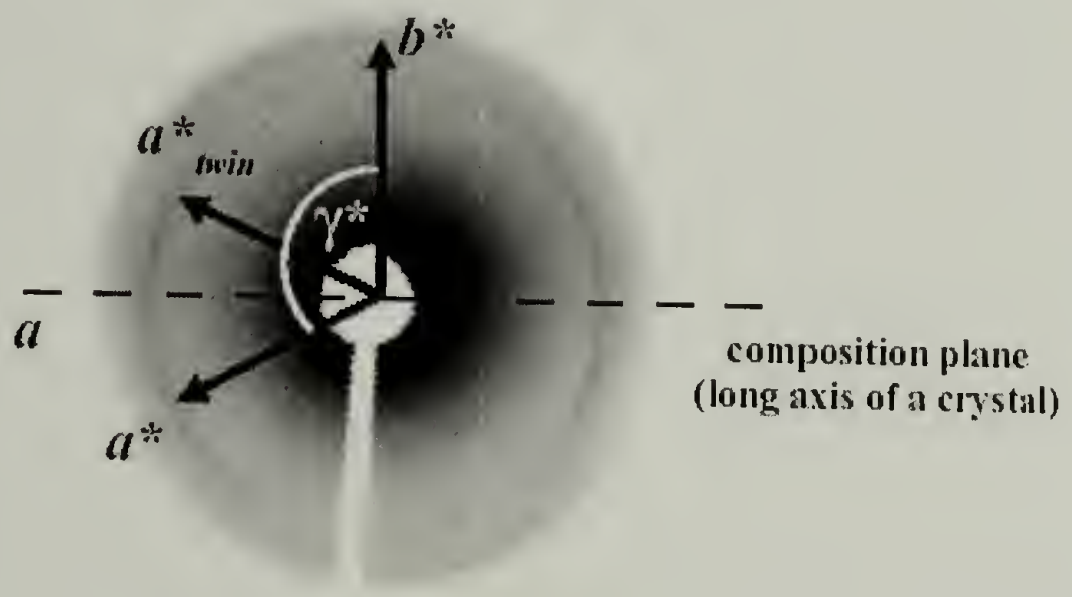

(a)

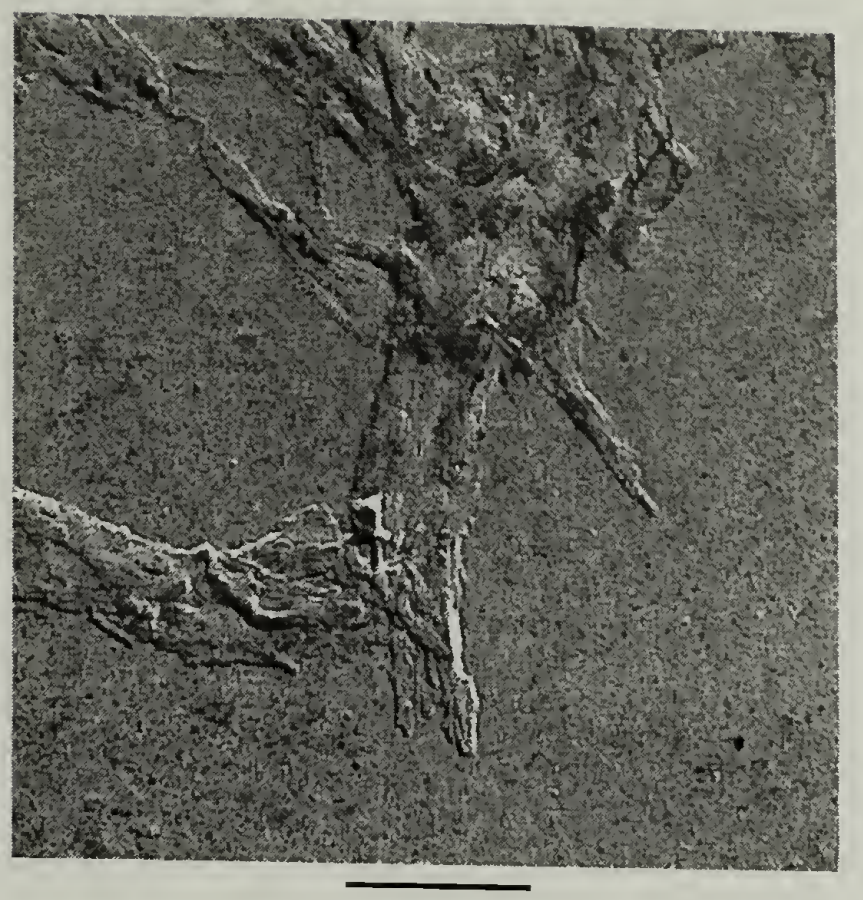

(b)

Figure 4.6. Solution-Grown 22,12-Polyurethane: (a) Electron Diffraction at 45° Tilt (Gold-Coated for Calibration Purposes) and (b) TEM Image (Coated with Pd-Pt to Increase the Contrast).

Further confirmation that the m,n-polyurethanes, regardless of their low hydrogen-bonding density, did not have an orthorhombic crystal structure similar to polyethylene came from the IR and Raman spectra. The m,n-polyurethanes (Figure 4.7a) did not display the Davydov splittings at 720 to 730 cm^{-1} (CH_2 rock) and 1460 to 1470 cm^{-1} (CH_2 bend) that is typically seen for orthorhombically packed polyethylene (Figure 4.7b), polyesters, and long-chain *n*-paraffins.[15,16] The splitting (or doublet) occurs due to chain vibrations which results in an overall dipole moment parallel to either the a or b axis.[15] The Raman spectra of orthorhombic *n*-paraffins and polyethylene (Figure 4.7c) and monoclinic *n*-paraffins exhibit bands (CH_2 bend) at 1418, 1441, and 1463 cm^{-1} and 1418, 1441, and 1462 cm^{-1}, respectively.[17] However, the Raman spectra of the m,n-

polyurethanes did not exhibit the band at 1418 cm^{-1} (Figure 4.7d). Instead, their Raman spectra were similar to that of triclinic and hexagonal *n*-paraffins with bands at 1445, 1463, and 1484 cm^{-1} and 1438 and 1458 cm^{-1}, respectively.[17] Combined, the diffraction and spectroscopic studies implied that the long-chain polyurethanes had triclinic packing as well as a varying degree of pseudohexagonal packing.

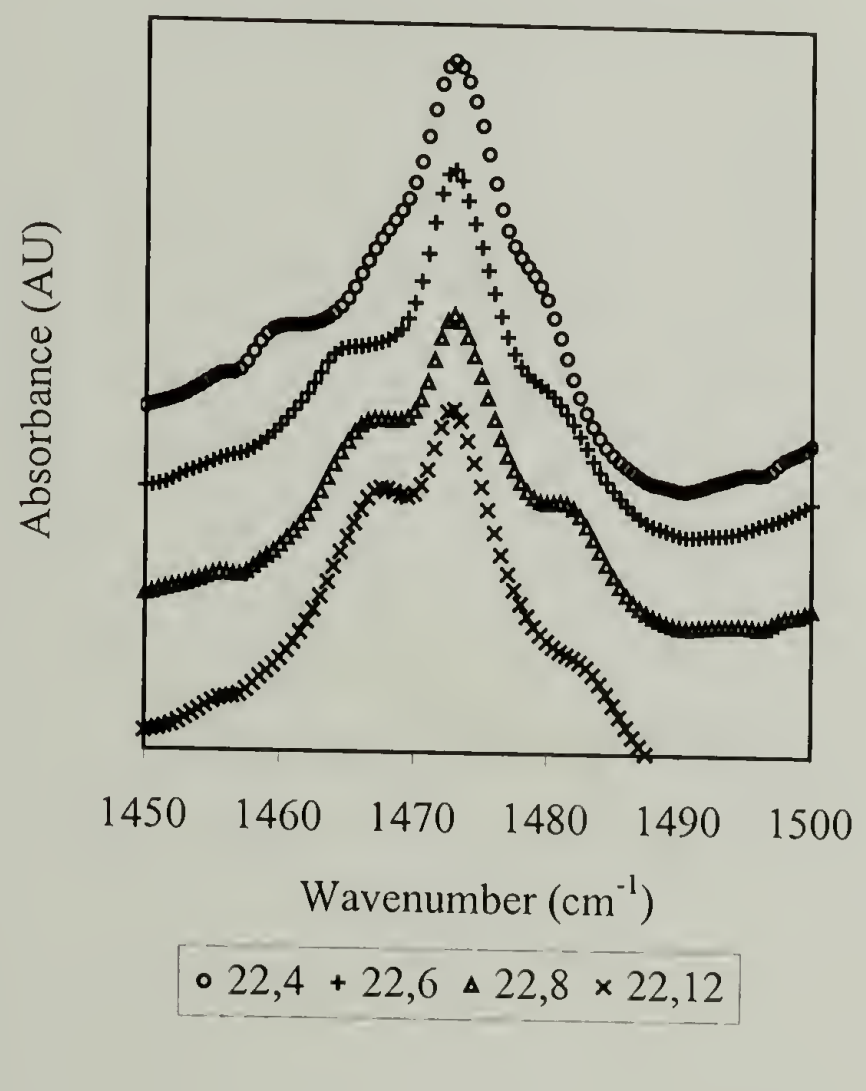

(a)

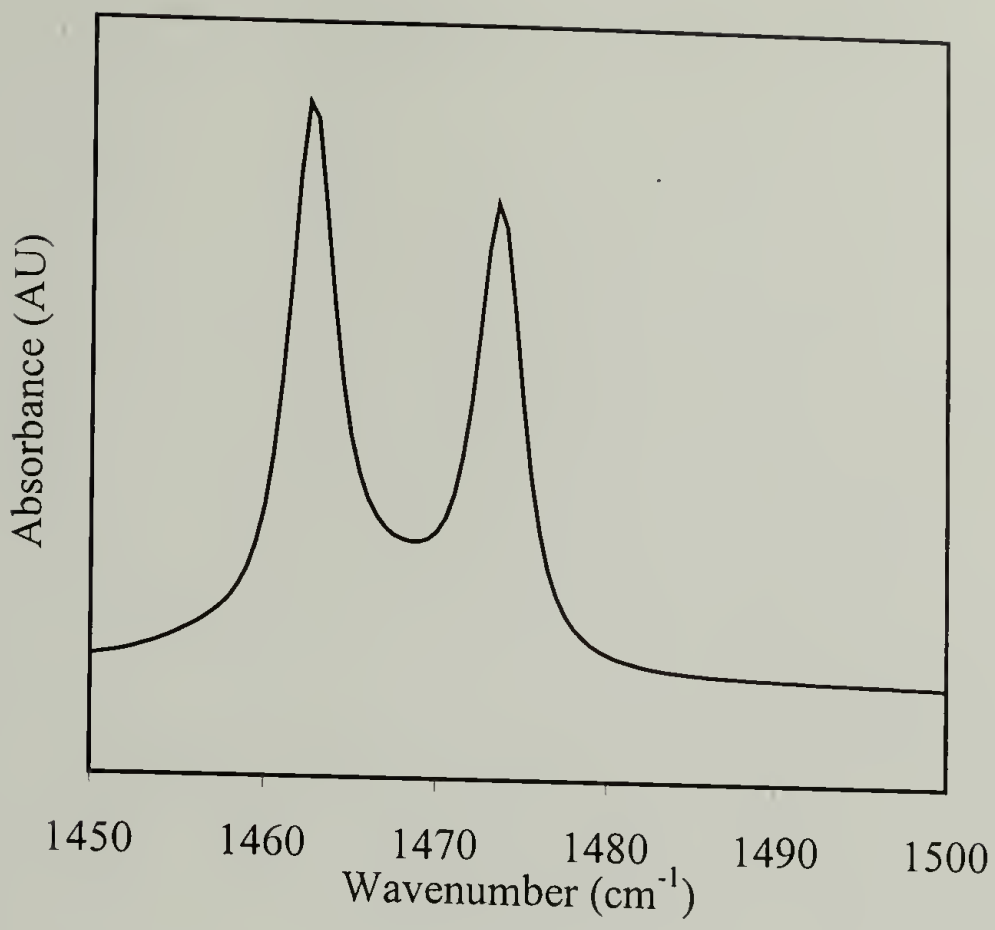
Absorbance (AU)
1450
1460
1470
1480
1490
1500
Wavenumber (cm-1)

(b)

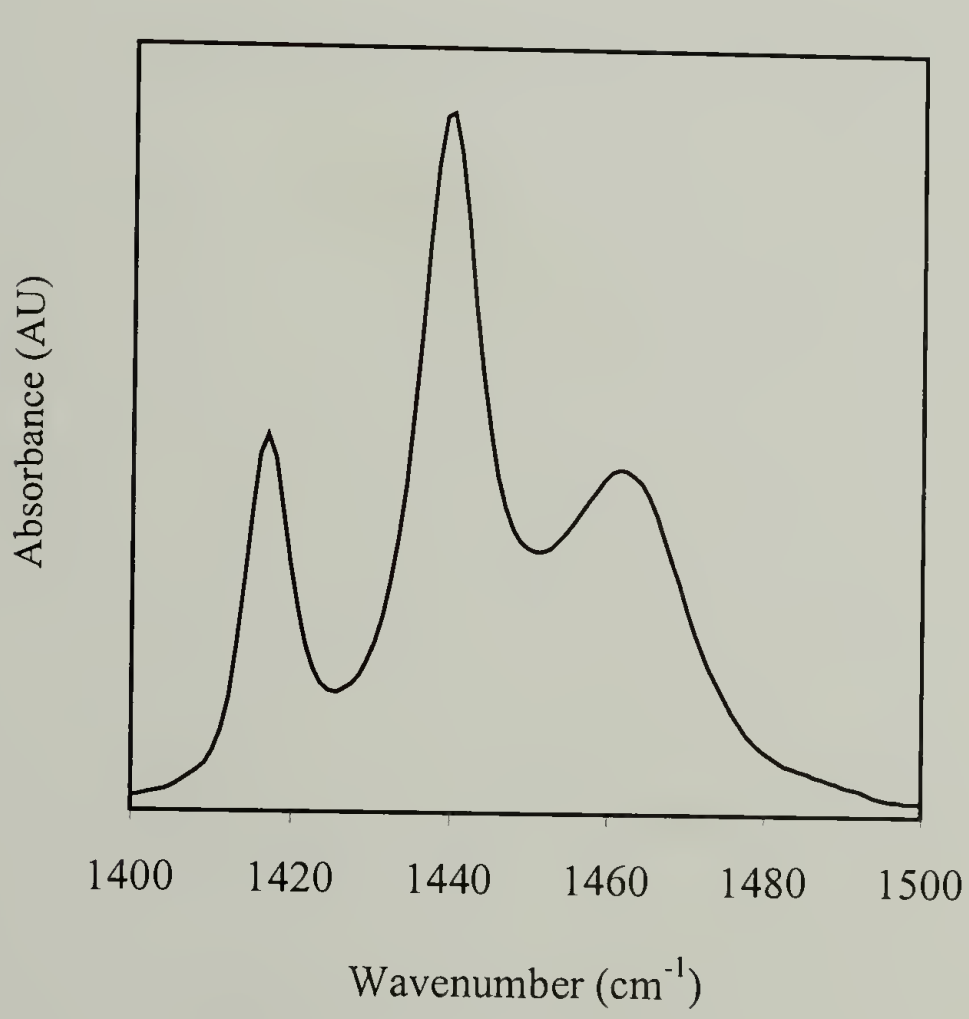
Absorbance (AU)
1400
1420
1440
1460
1480
1500
Wavenumber (cm-1)

(c)

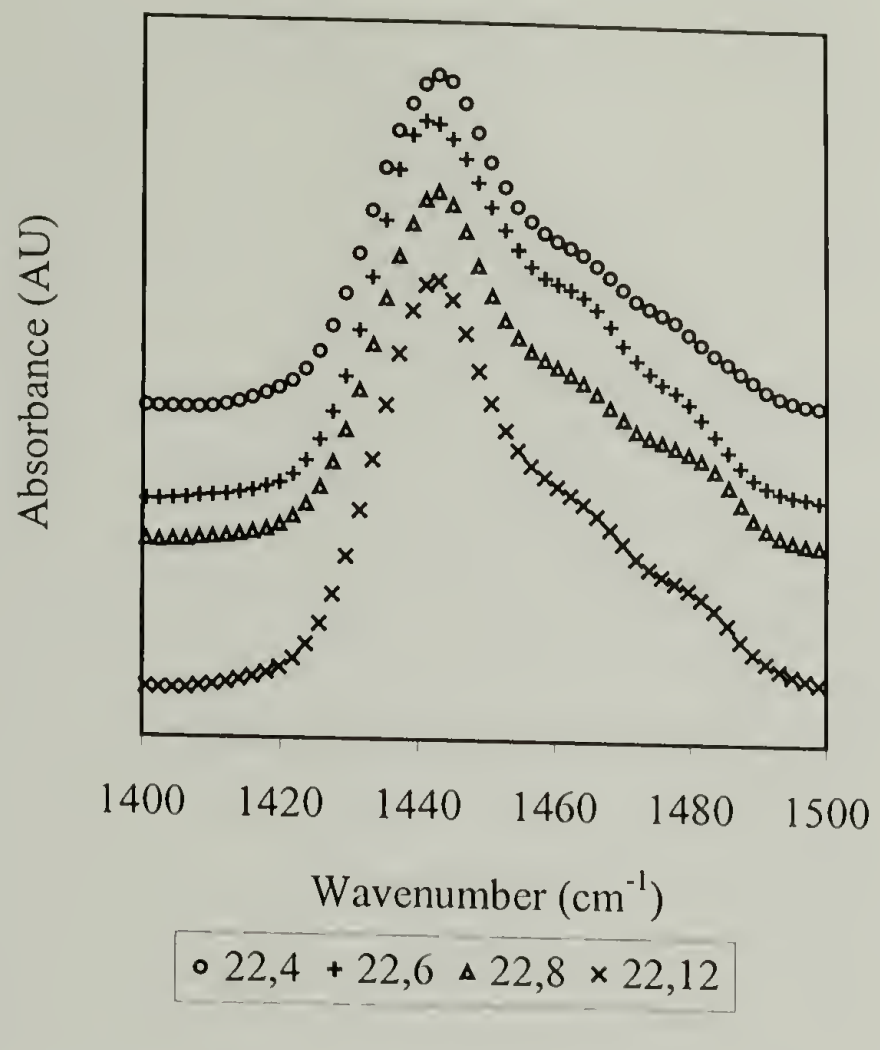

(d)

Figure 4.7. CH_2 Bending Region: (a) IR Spectra of 22,n-Polyurethanes, (b) IR Spectrum of HDPE, (c) Raman Spectrum of HDPE, and (d) Raman Spectra of 22,n-Polyurethanes.

4.3.2. Structure of the 22,12-Polyurethane in Chain-Folded Lamellar Crystals

The 22,12-polyurethane gave the best combined data set from X-ray and selected area, electron diffraction as well as from TEM imaging. Additionally, the 22,12-polyurethane was representative of the overall structural features and generalized crystallization behavior of this family of even-even, aliphatic polyurethanes. Therefore, this polymer was focused on, and the structure of the lamellar crystals is now described in more detail. Due to the quality of the oriented crystal lamellae obtained, the diffraction data alone was not sufficient to support a detailed structural determination comparable to that of nylon 6,6 fibers.[8] In an attempt to obtain a better understanding of the molecular

interactions involved in the crystallization of the 22,12-polyurethane and to ensure that stereochemically feasible structures for the polymer could be generated to match the basic and limited diffraction data, 2 types of crystal structure models (based on 2 different modeling strategies) were explored.

In the first strategy (Model A), the analysis was aided by using the basic structural scaffolding of triclinic, single-chain nylon 6,6. Based on the lamellar structures of the even-even polyamides, values for γ^* (115°), d_{100} (4.5 Å), and d_{010} (3.8 Å) were obtained from the selected area, electron diffraction pattern (Figure 4.6a). Assuming a planar zig-zag conformation (chain length = 1.54 Å and angle = 109.5° resulted in a rough estimate of the *c*-axis identity period of ~ 50.3 Å), the angle $c \wedge c^*$ (44°) was determined from the X-ray diffraction pattern (Figure 4.5). If the polymer chains hydrogen-bonded together in a cooperative manner similar to the p-sheets (p = progressive shearing) of nylon 6,6, then β (77°) and *c* (50.3 Å) could be estimated. Based on these assumptions, the 22,12-polyurethane was assigned a triclinic unit cell with dimensions $a = 5.1$ Å, $b = 5.8$ Å, and $c = 50.3$ Å and angles $\alpha = 46°$, $\beta = 77°$, and $\gamma = 117°$. These values were compared to that of nylon 6,6 in Table 4.2 and were within a 7% maximum difference, except of course for the distinctly different *c*-values.

Table 4.2. Comparison of the Real and Reciprocal Unit Cell Parameters.

Unit Cell Parameter	Model A	Model B	Nylon 6,6[a]
a	5.1 Å	4.9 Å	4.9 Å
b	5.8 Å	5.9 Å	5.4 Å
c	50.3 Å	48.5 Å	17.2 Å
α	46°	54°	48.5°
β	77°	87°	77°
γ	63°	59°	63.5°
*a**	2.20 $Å^{-1}$	2.53 $Å^{-1}$	2.29 $Å^{-1}$
*b**	2.70 $Å^{-1}$	2.64 $Å^{-1}$	2.71 $Å^{-1}$
*c**	0.28 $Å^{-1}$	0.27 $Å^{-1}$	0.78 $Å^{-1}$
α*	133°	131°	130°
β*	82°	69°	84°
γ*	115°	127°	114°
a^*a**	28°	37°	27°
b^*b**	49°	50°	47°
c^*c**	44°	41°	42°

a) See reference 13.

Figure 4.8 shows the structure (Model A) of the 22,12-polyurethane based on this unit cell. The polymer chains associated into chain-folded, fully saturated, hydrogen-bonded, nylon-like p-sheets (Figure 4.8a). The hydrogen-bonded sheets then stacked via van der Waals forces and progressively sheared in the *ac*-planes in the *a*-direction (Figure 4.8b). The sheets also had substantial progressive *ac*-plane shear in the *c*-direction (Figure 4.8c). This triclinic packing model of the 22,12-polyurethane was conceptually similar to that of the chain-folded, lamellar crystals of nylon 6,6.[13] The WAXS pattern for this structure (generated using the Cerius X-ray diffraction procedure and incorporating the appropriate correction factors) is shown in Figure 4.9 and could be directly compared (Table 4.3) with the experimental pattern of the solution-grown, sedimented mat of the 22,12-polyurethane (Figure 4.5). In this method, the incorporation of the ester groups adjacent to the amide groups in the backbone appeared to have little effect on the crystalline structure.

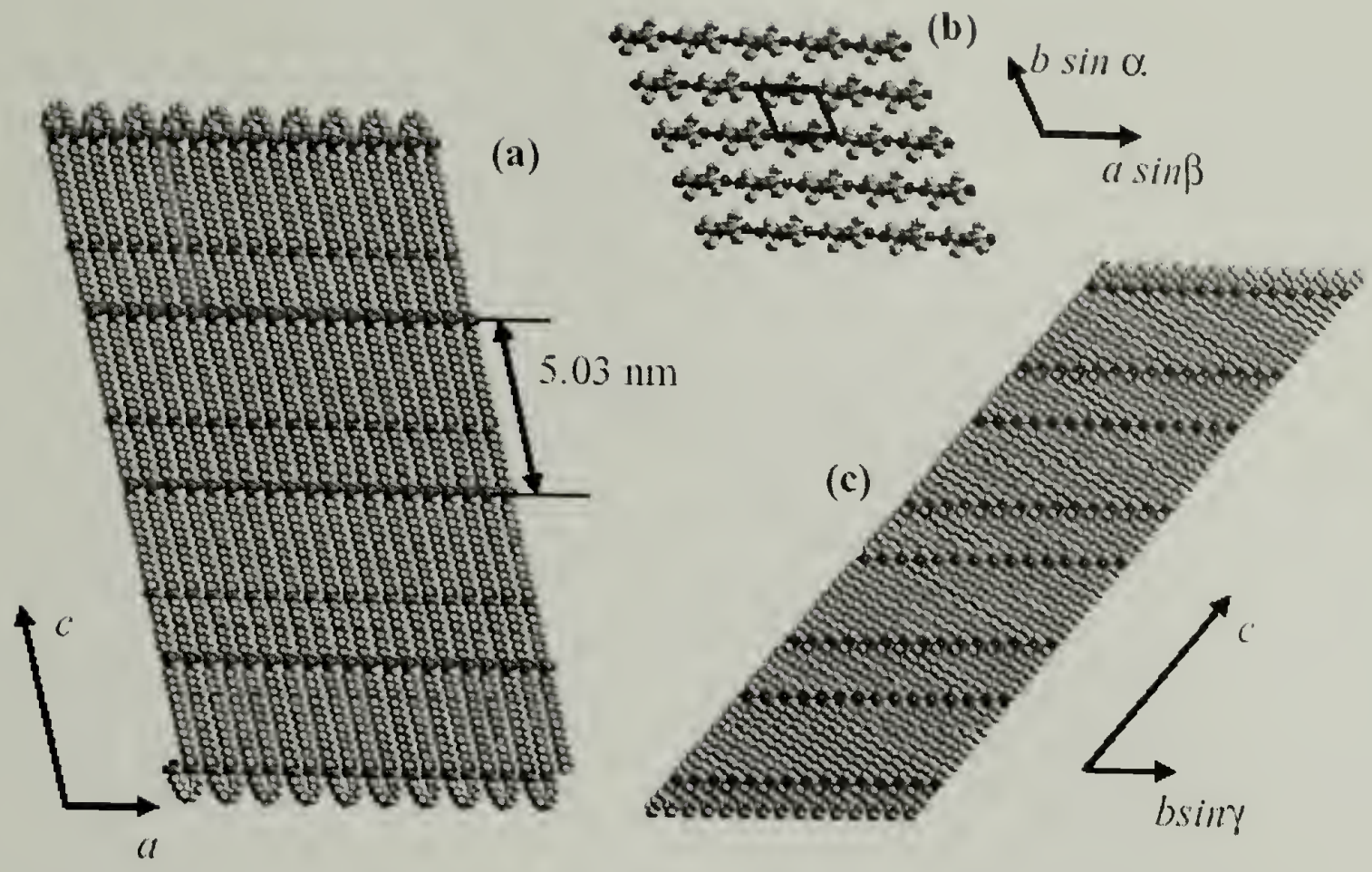

Figure 4.8. Structural Model A of 22,12-Polyurethane Based on Triclinic Nylon 6,6: (a) View of the Hydrogen-Bonded p-Sheets (Orthogonal to *ac*-Plane), (b) View Parallel to the Chain Axis of the Straight-Stem Portion of the Crystal (Hydrogen-Bonds are Shown in Dashes in the Horizontal Direction and the Box Represents the Projection of the Unit Cell) and (c) View Orthogonal to the *a*-Axis of the Progressively Sheared Hydrogen-Bonded Sheets.

Figure 4.9. Computer Generated, Simulated WAXS Pattern of the 22,12-Polyurethane Derived from Model A.

Table 4.3. Comparison of Observed and Calculated *d*-Spacings and Estimated Relative Intensities of the 22,12-Polyurethane Isothermally Crystallized from DMF.

		Model A		Model B	
d_{obs} (Å)	$Intensity_{obs}$ [a]	d_{cal} (Å)	*hkl*	d_{cal} (Å)	*hkl*
4.53 ± 0.02	vs	4.50	1 0 0	4.57	1 1 2
				4.47	1 1 1
4.22 ± 0.02	m	4.28	$1\,0\,\bar{4}$	4.18	$1\,0\,\bar{2}$
				4.23	$1\,0\,\bar{3}$
3.76 ± 0.02	s	3.79	0 1 0	3.78	0 1 0
36.0 ± 0.2	vs	36.0	0 0 1	36.3	0 0 1
18.0 ± 0.1	s	18.0	0 0 2	18.1	0 0 2
12.0 ± 0.05	m	12.0	0 0 3	12.1	0 0 3

a) vs = very strong, s = strong, and m = medium.

In an attempt to ascertain possible variations and limitations on the overall theme, the 22,12-polyurethane structure was also examined using a different approach. In this second strategy (Model B), MD simulations were used to find an optimal chain conformation, the preferred mode of chain packing, and the unit cell. The starting model

consisted of the 22,12-polyurethane chains (in an all *trans* conformation) situated at the corners of a tetragonal lattice with sides $a = b = 7$ Å and $c = 50.3$ Å. The interchain (a and b) distances were purposely in excess of the final values in the fully crystalline state. In order to minimize the effect of the periodic boundary conditions imposed, calculations were performed in a super-cell that consisted of 36 polymer chains with each chain composed of 2 chemical repeats in length (i.e. a super-cell of 6 x 6 x 2 unit cells). The starting setting angle was chosen to be distinctly different from that found in nylon 6,6. The system was then subjected to MD simulation procedures, and in the process the system density and chain conformation were allowed to change in order to minimize the overall potential energy of the system. No constraints were placed on the 22,12-polyurethane chain conformation or unit cell parameters. The resulting crystal structure (Table 4.2) was a result of the intra- and interchain interactions and their interplay. The crystalline structural features were determined by factors such as hydrogen-bonding, influence of the ester and amide groups on the chain conformation, and van der Waals interactions between the relatively long aliphatic segments.

Figure 4.10 shows the structure (Model B) of the 22,12-polyurethane based on the results of the MD simulations (Table 4.2). The polymer chains formed hydrogen-bonded sheets (*ac*-plane) with noticeable self-correcting or recuperative kinks in the localized region of the carbamate ester groups in the backbone (Figure 4.10a). These chain kinks emanated from 10° torsional rotations from the all *trans* conformation about the terminal bonds of the carbamate ester groups. In contrast, the aliphatic segments remained in the all *trans* conformation. The sheets then stacked with a progressive shear in the a- and c-directions parallel to the *ac*-planes (Figure 4.10b) similar to that seen in Model A. Since

the slip in the *c*-direction was small (3.5 Å) , the aliphatic segments of juxtapositioned sheets remained parallel (i.e. there was no crossing of the chain directions that would lead to poorer intersheet packing). This is illustrated in Figure 4.10a, where a second sheet is shown lying on top of the underlying first sheet. The WAXS pattern for this structure (generated using the Cerius X-ray diffraction procedure and incorporating the appropriate correction factors) is shown in Figure 4.11 and showed good agreement (Table 4.3) with the experimental pattern of the solution-grown, sedimented mat of the 22,12-polyurethane (Figure 4.5). The incorporation of kinks in the otherwise all *trans* backbone proposed in this method was similar to the bond rotations reported in aliphatic polyesters.[18]

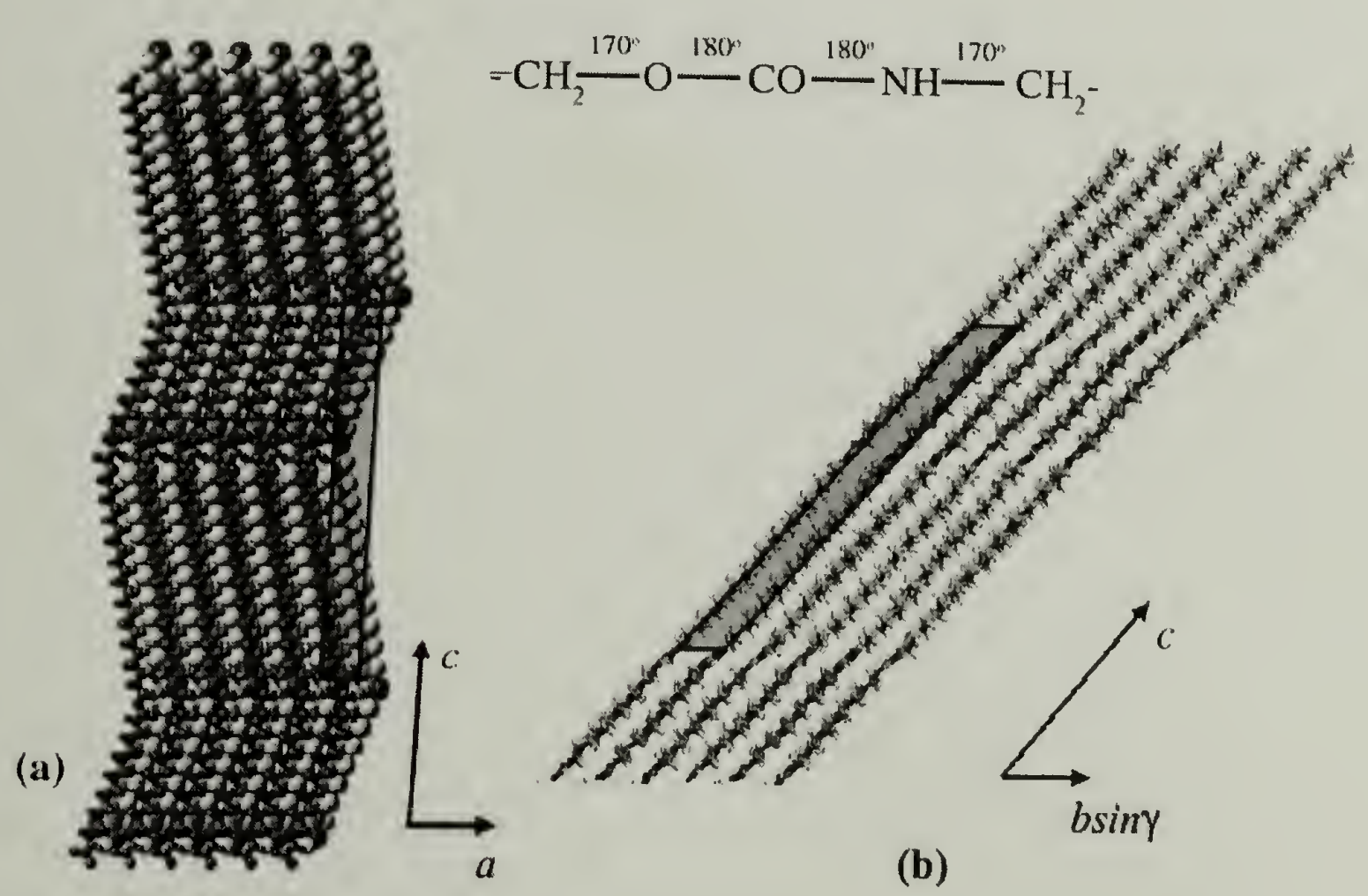

Figure 4.10. Structural Model B of 22,12-Polyurethane Based on MD Simulations. The Projections of the Unit Cell are Represented by the Boxes: (a) A Pair of Overlaid Sheets Viewed Orthogonal to the *ac*-Plane and (b) View Parallel to the *a*-Axis.

Figure 4.11. Computer Generated, Simulated WAXS Pattern of the 22,12-Polyurethane Derived from Model B.

Examination of the real and reciprocal unit cell parameters (Table 4.2) of Model B revealed that there were 2 noticeable differences in comparison to Model A. The first was that, naturally, the value of *c* was reduced by 3.6% as a consequence of the recuperative, intrasheet kinking. More significant, the value of γ^* was increase to 127° (an increase of 10.4%) and at first sight appeared to contradict the measure value of 115°. However, it should be noted that in Model B, the selected area, electron diffraction pattern (Figure 4.6a) was the [-201] zone, and therefore did not directly measure γ^*. The Model B data in Table 4.3 illustrates this point. The strong arcs in the X-ray and electron diffraction were not all *hk*0 diffraction signals (e.g. the strong 4.5 Å arc was a combination of the 112 and 111 diffraction). It should be remembered that the *c*-value was large (~ 50 Å), and therefore the reciprocal planes with $l = 1$ or 2 contributed. Indeed in Model B, the [-201] zone axis contained the strong interchain diffraction

signals. The 3 strong diffraction signals found in the calculated X-ray pattern (Figure 4.11) favorably matched the experimental spacings of 4.5 Å, 4.2 Å, and 3.8 Å.

Based on the limited diffraction data available from the 22,12-polyurethane lamellar crystals, a serious delineation between the 2 models was not possible, and the models were merely meant to indicate the tolerances involved in the structural analysis. Nonetheless, each model did have its own merits and weaknesses. Both models suggested that the basic structure was of chain-folded, hydrogen bonded sheets in which the dipoles were aligned and there existed some intersheet shearing (Figures 4.8a and 4.10a). The sheets stacked with progressive shear (Figures 4.8b and 4.10b) to give a single-chain, triclinic structure. Thus, the general direction of the chains (*c*-axis) was substantially tilted (44° for Model A and 41° for Model B) to the crystalline lamellar normals. The resulting architecture was similar to that reported for the even-even nylons.

Table 4.2 provides a comparison of the 22,12-polyurethane models to that of nylon 6,6. It is important to note that the 22,12-polyurethane *c*-repeat was about 3 times that of nylon 6,6, and therefore the 00*l* reciprocal planes were more closely spaced. Additionally, the limited crystal thickness of the polyurethane (~ 140 Å) lengthened the reciprocal lattice points in the *c**-direction. Together with the partial disorientation, this led to strong diffraction signals with *h* and *k* of 0 or 1 and a small, but nonzero, *l*. For instance, a diffraction signal appeared at 4.3 Å (Figure 4.9) from the $d_{10}\overline{4}$ and at 4.2 Å (Figure 4.11) from the combined $d_{10}\overline{2}$ and $d_{10}\overline{3}$ for Models A and B, respectively. The later case (Model B) had a better match with the experimental diffraction signal at 4.2 Å (Figure 4.5).

4.3.3 Annealing Behavior

Annealing studies also indicated that the hydrogen-bonds still influenced the crystallization of the long-chain m,n-polyurethanes. The 22,n-polyurethanes were annealed at 10 °C below their melting points for 1 to 15 hours and then quenched to room temperature. Rather than observing higher melting points during the subsequent heating runs as a result of lamellar thickening, the polymers exhibited the same melting points as before as well as a smaller endotherm at lower temperatures (Figure 4.12). Upon cooling the annealed polymers, only one exothermic peak was exhibited. The absence of chain thickening upon annealing suggested that unlike polyethylene, these long-chain, aliphatic polyurethanes could only increase their lamellar thickness in distinct steps. This behavior was similar to polyamides, whose lamellae can only thicken by multiples of their repeat unit.[19]

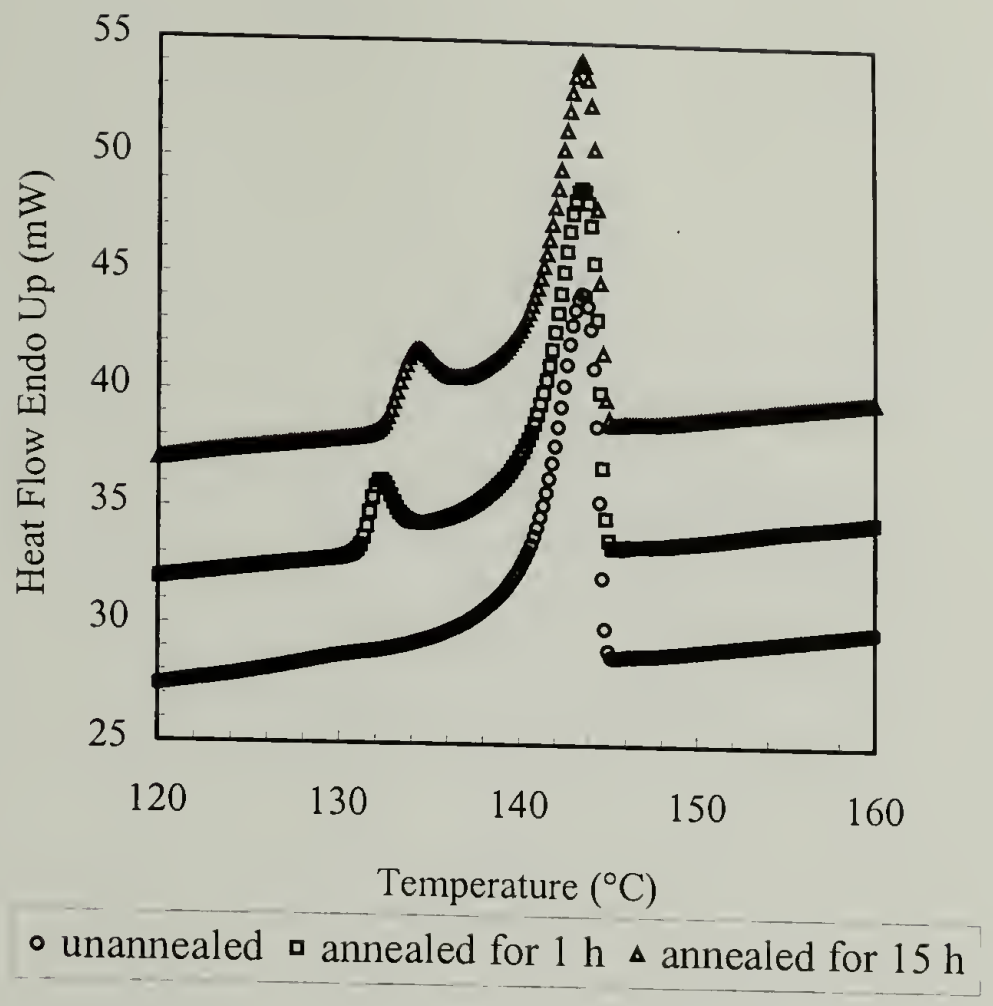

Figure 4.12. Appearance of a Second, Smaller Endotherm Upon Annealing the 22,8-Polyurethane.

The melting point of the smaller endotherms occurred at temperatures very close to the annealing temperature (Table 4.4). With increased annealing time, the peaks of the smaller endotherm shifted to higher temperatures. These endotherms were most likely the result of some secondary crystallization resulting in the perfection of the crystalline regions and will be discussed further in Section 4.3.3.

Table 4.4. Melting Points of Annealed and Unannealed 22,n-Polyurethanes.

22,n-Polymer	Unannealed	Annealed for 1 h	Annealed for 15 h
22,4	158 °C	148 and 158 °C	
22,6	146 °C	137 and 146 °C	
22,8	144 °C	132 and 144 °C	134 and 144 °C
22,12	137 °C	126 and 137 °C	129 and 137 °C

4.3.4 High Temperature Studies

In order to determine when and how much hydrogen-bonding occured during crystallization, the amide I region of the m,n-polyurethanes was examined using high-temperature IR spectroscopy. The amide I region is typically sensitive to free carbonyl groups (1732 cm^{-1}) and disordered (1718 to 1709 cm^{-1}) and ordered (1685 cm^{-1}) hydrogen-bonded carbonyl groups.[10] Analysis of the amide I region of the m,n-polyurethanes indicated the presence of another carbonyl group at 1692 cm^{-1}. However, at most, this component contributed only 5% to the overall intensity of this region. It is extremely possible that this component was the result of the portion of polyurethanes that underwent pseudohexagonal packing.

The amide I region of the IR spectra showed the presence of hydrogen-bonding in the melt (Figure 4.13a) and the ordering of these bonds upon crystallization (Figure 4.13b). In the melt, approximately 75% of the carbamate esters were hydrogen-bonded, and after crystallization, 90% were hydrogen-bonded (Figure 4.14). The presence of hydrogen-bonds in the melt might help explain why the T_m of the increasingly aliphatic m,n-polyurethanes approached the melting point of polyethylene (Chapter 3). Since the polymers could still contain hydrogen-bonds in the melt, only enough heat to break up the crystalline aliphatic segments of the polymers was needed in order for the m,n-polyurethanes to melt. The increasing solubility of these polyurethanes in solvents like *o*-dichlorobenzene used for HDPE and decreasing solubility in solvents like *m*-cresol and DMF typically used for polyamides (Chapter 3) might also be the result of a similar presence of hydrogen-bonding in solution.

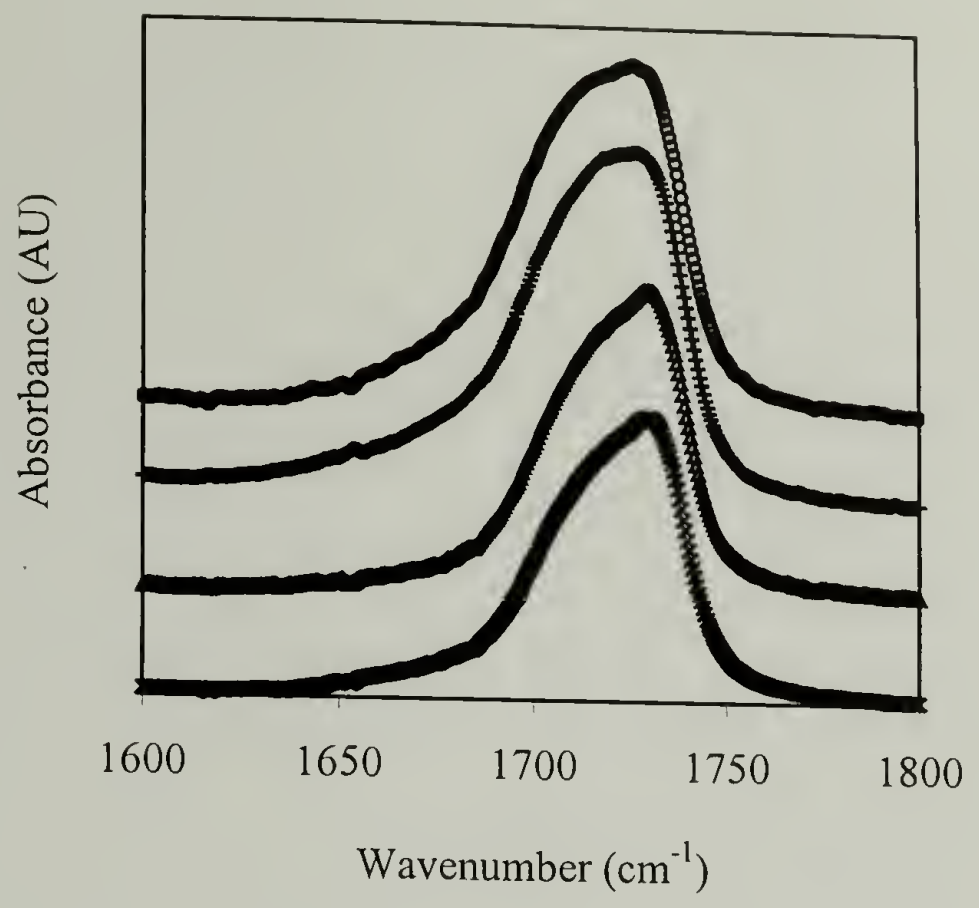

(a)

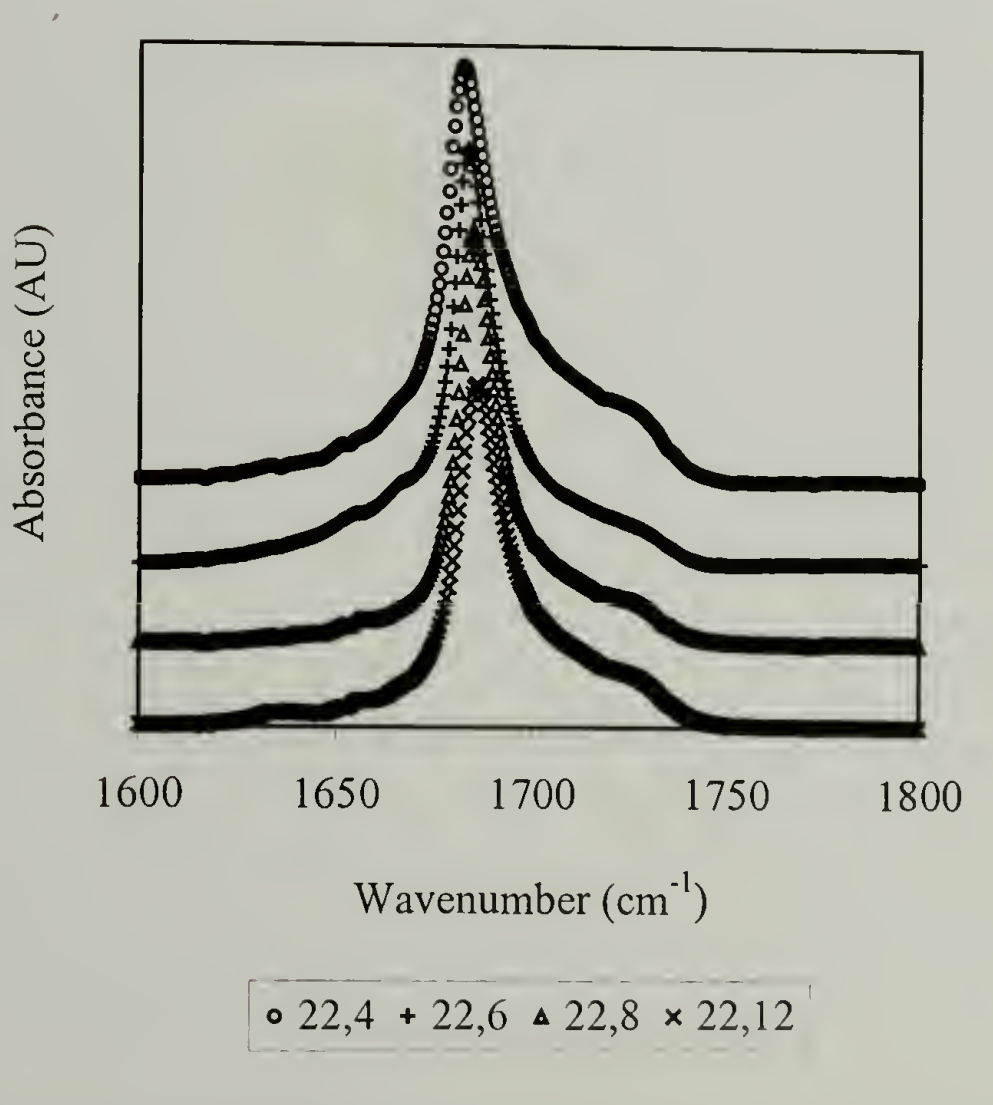

(b)

Figure 4.13. IR Spectra (Amide I Region) of the 22,n-Polyurethanes: (a) in the Melt and (b) After Crystallization.

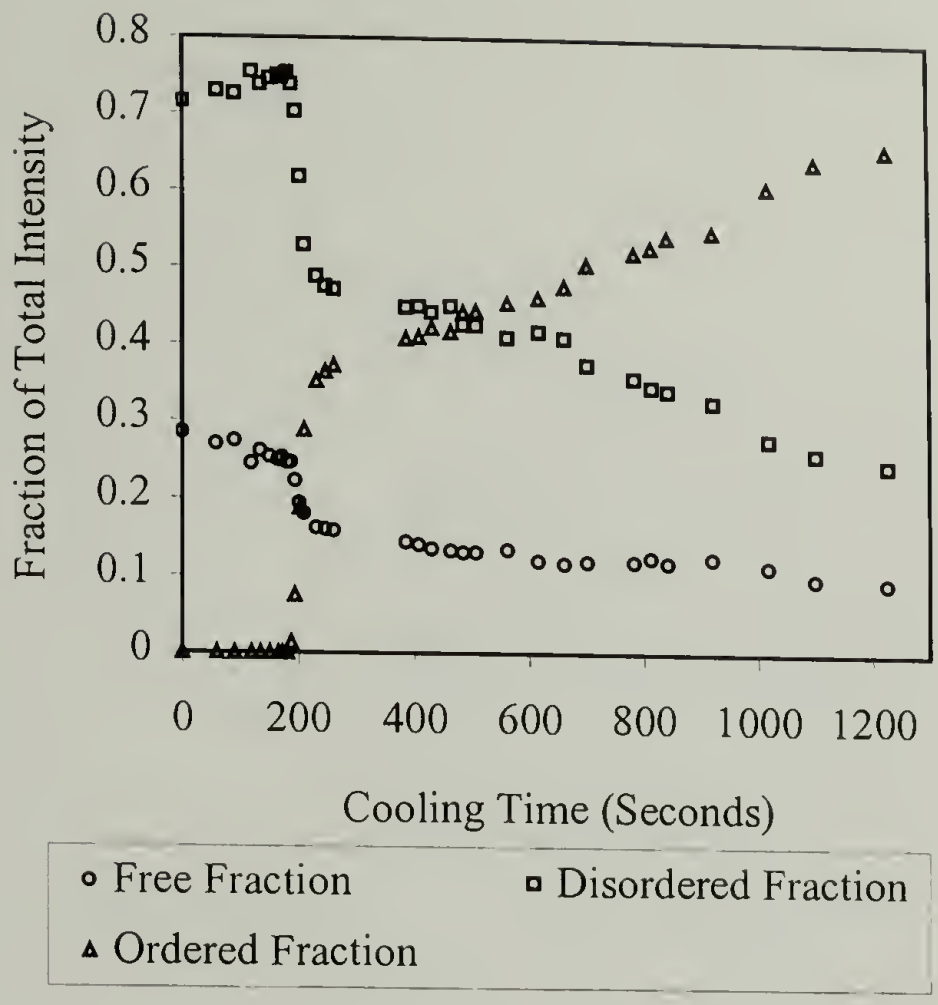

Figure 4.14. Evolution of Ordered Hydrogen-Bonding During the Crystallization of the 22,8-Polyurethane (Cooling Rate of 5 $K \cdot min^{-1}$).

Further examination of the amide I region during the crystallization of the m,n-polyurethanes showed two stages (Figure 4.14). Initially, crystallization was marked by a sharp increase in the ordered carbonyl groups and a corresponding decrease in the free and disordered carbonyl groups. In the second stage, the rate of crystallization then slowed and the ordering of the carbonyl groups continued. This second stage was defined as secondary crystallization and was the same ordering that was seen using DSC after annealing the polymers (see Section 4.3.3). Secondary crystallization typically occurs due either to crystallization of the amorphous region[20-22] (doubtful for these polymers since no lamellar thickening was observed in the DSC) or to the perfection of

the existing crystal[23,24] (e.g. conversion of some pseudohexagonal packing to triclinic packing).

It is difficult to estimate the degree of crystallinity of these polymers using most common methods.[9] Methods using the enthalpy of melt determined by DSC require a 100% crystalline sample, while density or WAXS methods require a completely amorphous sample. TEM imaging of the ruthenium oxide-stained samples (Figure 3.6) indicated a relatively low percent crystallinity for the samples. However, this method was not quantitative since the stain needed enough time to complex with the amorphous regions, but too much time and the stain penetrated the crystalline regions as well. The sharp IR band at 1685 cm^{-1} (ordered, hydrogen-bonded carbonyl groups) could however, be used to estimate the percent crystallinity. Assuming that this band correlated to the volume fraction of the crystalline regions in the polymer, a degree of crystallinity of approximately 25% was obtained. This value is typical of that seen for purely aliphatic, neat polyamides of higher hydrogen-bonding density.[25] The percent crystallinity could also be estimated from the sharp CH_2 wagging band (ordered chain stems) at 1308 cm^{-1}, and a higher value of 40% was obtained. That the percent crystallinity values for the same polymer as determined by IR are different shows just how difficult it is to obtain a truly quantitative value.

The amide I region also provided information on the strength of the hydrogen-bonds. Under the assumption that the carbamate esters underwent hydrogen-bonding to form dimers N-H···O=C, the equilibrium constant K_{eq} was determined from the fraction of free carbamate esters (Equation 4.2).[26]

$$K_{eq} = (1\text{-}[C{=}O])\cdot(2\cdot[C{=}O]^2)^{-1} \qquad \text{(Eq. 4.2)}$$

From the slope of the van't Hoff plot of ln K_{eq} versus inverse temperature (Equation 4.3, where R = gas constant), the strength of the hydrogen-bonds of the 22,8-polyurethane in the melt was experimentally determined to be -7.20 kJ·mol^{-1} per urethane.

$$\Delta G^0 = -RT\cdot\ln K_{eq} = \Delta H - T\Delta S \qquad \text{(Eq. 4.3)}$$

Like the amide I region, the NH stretching region of the IR is sensitive to free NH groups (3456 cm^{-1}) and disordered (3370 cm^{-1}) and ordered (3322 cm^{-1}) NH groups.[27] However, unlike the carbonyl groups, the absorbance coefficient of the NH stretching groups is sensitive to the strength of the hydrogen-bonds. Therefore, this region could not be used to quantitatively determine the percent of carbamate esters that were hydrogen-bonded.[28] The strength of the hydrogen-bonds in the melt could be experimentally determined and was found to range from -7.03 to -6.40 kJ·mol^{-1} per urethane for the 22,8-polyurethane (dependent on the temperature) from the frequency difference $\Delta\nu$ between the free and hydrogen-bonded NH groups (Equation 4.4).[29]

$$-\Delta H = (59.3\cdot\Delta\nu)\cdot(\Delta\nu + 674)^{-1} \qquad \text{(Eq. 4.4)}$$

This value was in relative agreement with the hydrogen-bonding strength in the melt determined from the amide I region. This same equation was used to determine the

strength of the hydrogen-bonds after crystallization, and a value of -22.93 $kJ \cdot mol^{-1}$ per repeat for the 22,8-polyurethane was found.

4.3.5 Monomer Synthesis

4.3.5.1 Overview of Synthetic Methods

Mono- and difunctional isocyanates O=C=N-R and O=C=N-R-N=C=O, respectively, can be synthesized in the laboratory by a multitude of methods. Several reviews[30-33] exist comparing and contrasting these different methods. However, in industry only the phosgenation of primary amines is used.[32] In this synthetic method, developed in 1884 by Hentschel,[34] phosgene reacts with aliphatic and aromatic mono- and difunctional amines H_2N-R and H_2N-R-NH_2, respectively, producing chloroformamides Cl-C(O)-NH-R or Cl-C(O)-NH-R-NH-C(O)-Cl (depending on the functionality of the starting amine), which then releases HCl to form the isocyanate.

In order to help differentiate in the IR the consecutive methylene units derived from the diol and diisocyanate, the perdeuterated 1,6-diisocyanatohexane O=C=N-$(CD_2)_6$-N=C=O was desired. Although no reported method exists for the synthesis of perdeuterated 1,6-diisocyanatohexane, there are numerous articles on the synthesis of the purely aliphatic 1,6-diisocyanatohexane O=C=N-$(CH_2)_6$-N=C=O. Phosgenation of hexamethylenediamine dihydrochloride H_2N-$(CH_2)_6$-$NH_2 \cdot 2HCl$ was first reported in 1940,[35] however the product was always a mixture of mono- and difunctional isocyanatohexane.[36-39] Two years later, Bayer[40] at Farbenindustrie reported on the phosgenation of hexamethylenediamine H_2N-$(CH_2)_6$-NH_2 to synthesize 1,6-

diisocyanatohexane. Modifications of this original procedure have been reported,[41-46] including the use of the supposedly safer diphosgene Cl-C(O)-$OCCl_3$.[47] 1,6-Diisocyanatohexane can also be synthesized from the corresponding diacyl azide N_3-C(O)-$(CH_2)_6$-C(O)-N_3 through a Curtius rearrangement. The diacyl azide is typically prepared either by reacting the corresponding acid chloride Cl-C(O)-$(CH_2)_6$-C(O)-Cl with sodium azide NaN_3 or by converting the corresponding diethyl ester $CH_3CH_2O_2C$-$(CH_2)_6$-$CO_2CH_2CH_3$ to the dihydrazide NH_2NH-C(O)-$(CH_2)_6$-C(O)-$NHNH_2$ and then to the diacyl azide.[48] Curtius[49] first reported on this rearrangement to the isocyanate in 1890, and the reaction was first employed to synthesize 1,6-diisocyanatohexane in 1922 by Schmidt.[50]

4.3.5.2 Attempted Synthesis of 1,6-Diisocyanatohexane

Although the perdeuterated 1,6-diisocyanatohexane is not commercially available, it should be possible to synthesize it from the corresponding, commercially available, perdeuterated diamine or diacid. Concerns about the safety of phosgene resulted in the search of literature methods not requiring its use. Attempts were first made to reproduce several literature methods to synthesize the purely aliphatic 1,6-diisocyanatohexane. Currently, none of the methods have resulted in the synthesis of the pure diisocyanate.

The first method attempted was based on a procedure reported by Lesiak and Seyda[12] for the synthesis of 1,6-diisocyanatohexane in two steps with an overall yield of 56% (Scheme 4.1). Hexamethylene diformamide (**21**) H-C(O)-NH-$(CH_2)_6$-NH-C(O)-H was synthesized in 71% yield by the dehydration of the corresponding diamine with 2 equivalents of formic acid. 1,6-Diisocyanatohexane (**22**) should then have been

synthesized by the dehydrohalogenation of the diformamide with 2 equivalents of bromine in the presence of the tertiary amine DBO. However, for reasons not currently understood, only a solid, red product was formed (1,6-diisocyanatohexane at room temperature is a liquid).

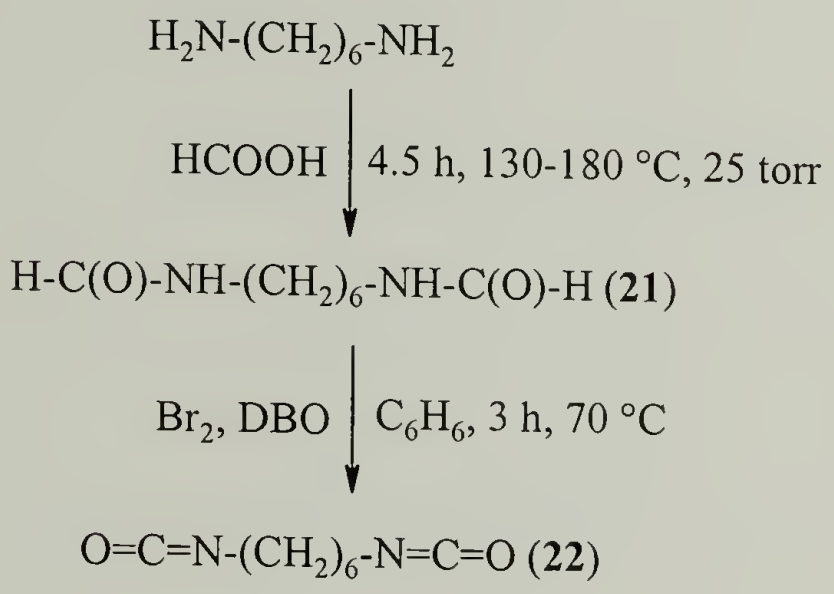

Scheme 4.1. Synthesis of 1,6-Diisocyanatohexane (**22**) from Hexamethylenediamine Using Formic Acid and Bromine.

The next attempt was a modification of the phosgenation procedure described by Sigurdsson et al.,[47] who synthesized 1,6-diisocyanatohexane in 73% yield (Scheme 4.2). In the original procedure, the authors reported that trichloromethyl chloroformate (diphosgene) converted aliphatic amines to isocyanates only in the presence of a non-nucleophilic base. The procedure was modified by using triphosgene rather than diphosgene. Diphosgene and triphosgene behave as 2 and 3 moles of phosgene, respectively.[51] Unlike the toxic phosgene, which is a gas at room temperature, diphosgene and triphosgene, are a liquid and a solid, respectively, at room temperature. For this reason, these alternatives to phosgene have been reported as safer chemicals for laboratory work. However, since these compounds do form phosgene in the presence of

trace amounts of water or upon heating, the safety of their use is under debate.[51-54] In theory, 1,6-diisocyanatohexane (**22**) should have been synthesized by the phosgenation of the corresponding diamine with triphosgene in the presence of the non-nucleophilic base Proton-Sponge™. However based on the ^{1}H-NMR results, the final product was determined to be hexamethylenediamine (if present, the methylene group alpha to the isocyanato group would show up as a triplet at 3.3 ppm). This synthetic failure was probably the result of either wet starting material (the diamine is very hygroscopic) or the use of triphosgene rather than diphosgene. The reaction time (15 minutes) was very quick and might not have been sufficiently long enough for the triphosgene to decompose into phosgene.

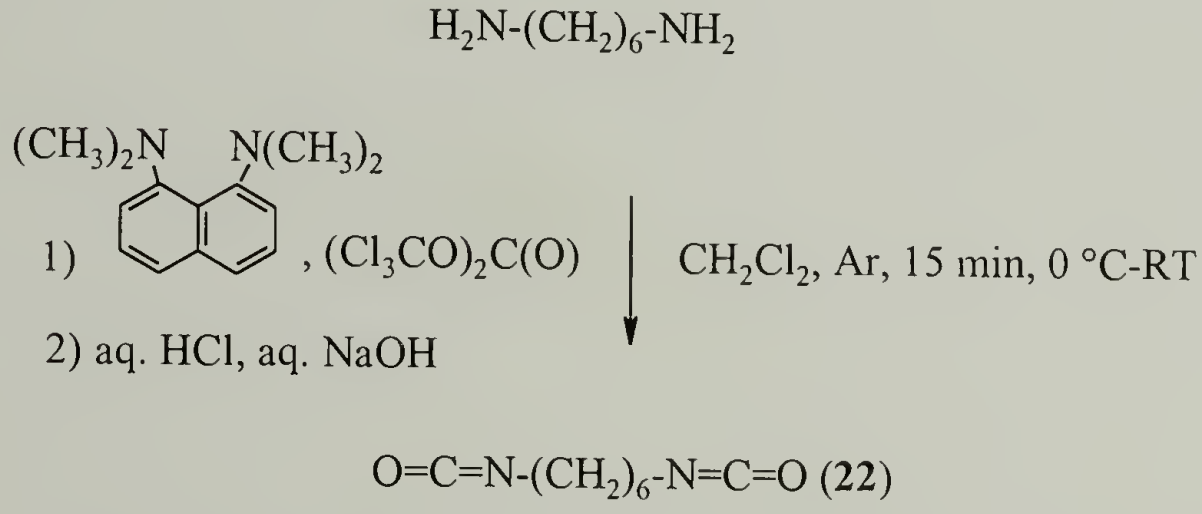

Scheme 4.2. Synthesis of 1,6-Diisocyanatohexane (**22**) from Hexamethylenediamine via Phosgenation with Triphosgene.

The synthesis of mono- and difunctional isocyanates in yields ranging from 40 to 80% by a one-step Curtius-type rearrangement of the corresponding acid was reported by Gilman and Otonari[55] (Scheme 4.3). The addition of the non-nucleophilic base Proton-Sponge™ and tertiary amine DPPA should have converted suberic acid HO_2C-$(CH_2)_6$-CO_2H to 1,6-diisocyanatohexane (**22**). However, for reasons not currently understood,

only a solid, white product was formed (1,6-diisocyanatohexane at room temperature is a liquid).

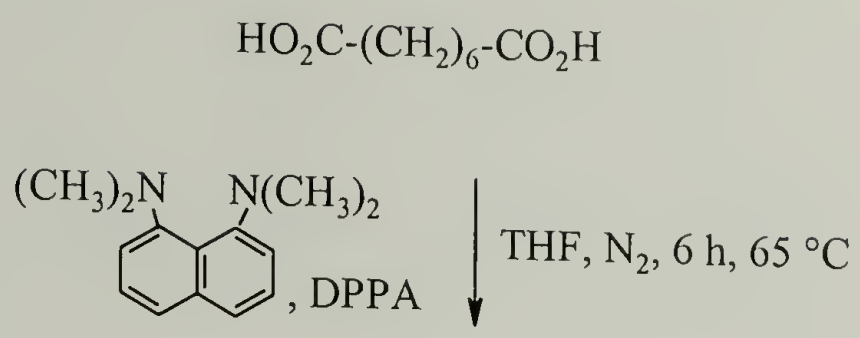

Scheme 4.3. Synthesis of 1,6-Diisocyanatohexane (**22**) from Suberic Acid Using Proton-Sponge™ and DPPA.

The final method attempted was based on the multi-step Curtius rearrangement of the corresponding diacid reported by King[56] for the synthesis of 1,3-diisocyanatopropane in 62% yield (Scheme 4.4). Suberic acid was esterified under acidic conditions to the diethylester (**23**) $CH_3CH_2O_2C$-$(CH_2)_6$-$CO_2CH_2CH_3$, which was then converted to the dihydrazide (**24**) NH_2NH-C(O)-$(CH_2)_6$-C(O)-$NHNH_2$ via aminolysis. The dihydrazide was diazotized with nitrous acid to form the diazide (**25**) N_3-C(O)-$(CH_2)_6$-C(O)-N_3. The global yield of the first 2 steps was 65%. Due to the sensitivity of the diazide to water and its explosive nature, the yield of the third step was not calculated. However, the presence of the azide functionality (N_3) was confirmed using Raman spectroscopy. In the absence of water, the diazide should have formed 1,6-diisocyanatohexane (**22**) and nitrogen gas when heated. However, the corresponding diamine was instead produced. The most probable reason for this was the presence of even a trace amount of moisture.

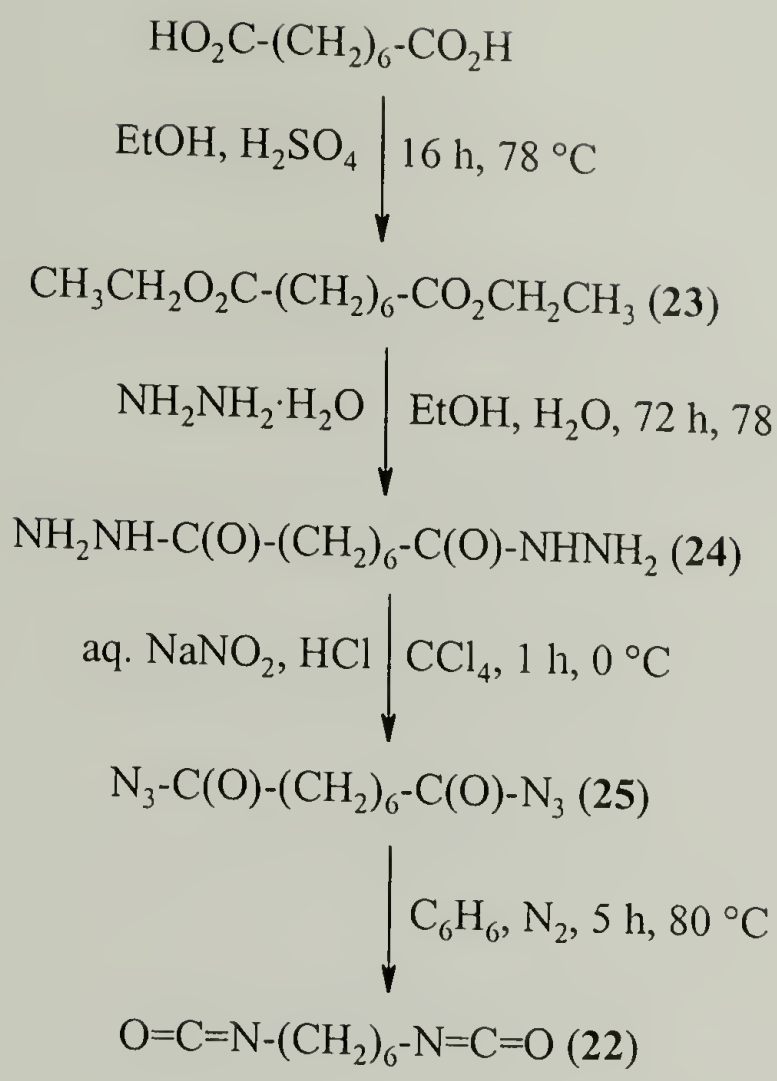

Scheme 4.4. Synthesis of 1,6-Diisocyanatohexane (**22**) from Suberic Acid via a Curtius Rearrangement.

4.4 Conclusions

As reported in the previous chapter, the long-chain m,n-polyurethanes exhibited physical and thermal characteristics typical of polyethylene. However, although respectively long aliphatic segments were incorporated with a consequential reduction in the frequency of carbamate esters along the backbone, interamide hydrogen-bonding remained the dominant feature in the crystallization process and the room temperature crystalline structure. Diffraction and spectroscopic results suggested that the m,n-polyurethanes contained both triclinic and pseudohexagonal packing. Based on the diffraction results, 2 different crystal structure models were proposed. The first model (based on nylon 6,6) had unit cell dimensions a = 5.1 Å, b = 5.8 Å, and c = 50.3 Å and

angles $\alpha = 46°$, $\beta = 77°$, and $\gamma = 63°$ for the 22,12-polyurethane. In the other model (based on MD simulations), the 22,12-polyurethane had unit cell dimensions $a = 4.9$ Å, $b = 5.9$ Å, and $c = 48.5$ Å and angles $\alpha = 54°$, $\beta = 87°$, and $\gamma = 59°$. Electron imaging of the solution-grown polyurethanes showed lath-shaped crystals similar to that observed for polyamides crystallized under similar conditions. The m,n-polyurethanes did not display an increase in melting temperature in the DSC after annealing, implying that no lamellar thickening took place. Secondary crystallization could be observed by both DSC and high temperature IR, and it is believed that this crystallization involved the perfection of the crystals via transformation of pseudohexagonal packing to triclinic packing. In short, the crystallization behavior was more akin to the even-even, aliphatic polyamides[8,13,14] than either polyethylene[57] or the corresponding aliphatic polyesters.[18]

The high temperature IR studies were helpful in following the actual crystallization behavior of the m,n-polyurethanes. Examination of the amide I region showed that 75% of the carbamate esters were hydrogen-bonded in the melt and 90% of them were hydrogen-bonded after crystallization. The high amount of hydrogen-bonding in the melt helps to explain much of the physical and thermal behavior reported in Chapter 2. Both the IR and TEM results indicated a low percent crystallinity, typical of neat, aliphatic polyamides. The hydrogen-bonding strength of 23 $kJ \cdot mol^{-1}$ per repeat was typical of the energy gained from hydrogen-bonding (10 to 40 $kJ \cdot mol^{-1}$).

In the IR studies, it was difficult to distinguish between the aliphatic segments derived from the diol and diisocyanate. C-D bonds have a lower frequency than C-H bonds in the IR, and therefore it was desired to synthesize some model polyurethanes from a perdeuterated diisocyanate. Attempts of synthesizing the 1,6-diisocyanatohexane

have thus far been unsuccessful. These methods have included phosgenation of the corresponding diamine and a Curtius-rearrangement of the corresponding diacid. The multi-step Curtius-rearrangement is well documented in the literature, and elimination of even trace amounts of moisture in the final step should produce the desired diisocyanate.

4.5 References

(1) Wunderlich, B. *Crystal Structure, Morphology, Defects*; Academic: New York, 1973; Vol. 1.

(2) Dreyfuss, P.; Keller, A. *J. Macromol. Sci., Phys.* **1970**, *4*, 811.

(3) Saito, Y.; Nansai, S.; Kinoshita, S. *Polym. J. (Tokyo)* **1972**, *3*, 113.

(4) Blackwell, J.; Gardner, K. H. *Polymer* **1979**, *20*, 13.

(5) Blackwell, J.; Ross, M. *J. Polym. Sci., Polym. Lett. Ed.* **1979**, *17*, 447.

(6) Saito, Y.; Hara, K.; Kinoshita, S. *Polym. J. (Tokyo)* **1982**, *14*, 19.

(7) Born, L.; Crone, J.; Hespe, H.; Müller, E. H.; Wolf, K. H. *J. Polym. Sci., Part B: Polym. Phys.* **1984**, *22*, 63.

(8) Bunn, C. W.; Garner, E. V. *Proc. Roy. Soc. (London), Part A* **1947**, *189*, 39.

(9) Young, R. J.; Lovell, P. A. *Introduction to Polymers*; 2nd ed.; Chapman & Hall: London, 1991.

(10) Coleman, M. M.; Lee, K. H.; Shrovanek, D. J.; Painter, P. C. *Macromolecules* **1986**, *19*, 2149.

(11) Allen, J.; Drewitt, J. G. *Chem. Abstr.* **1948**, *42*, 4603h.

(12) Lesiak, T.; Seyda, K. *J. Prakt. Chem.* **1979**, *321*, 161.

(13) Atkins, E. D. T.; Keller, A.; Sadler, D. M. *J. Polym. Sci., Part A: Polym. Chem.* **1972**, *10*, 863.

(14) Jones, N. A.; Atkins, E. D. T.; Hill, M. J. *J. Polym. Sci., Polym. Phys. Ed.* **2000**, *38*, 1209.

(15) Bower, D. I.; Maddams, W. F. *The Vibrational Spectroscopy of Polymers*; Cambridge University: Cambridge, 1989.

(16) Lee, K.-S.; Wagner, G.; Hsu, S. L. *Polymer* **1987**, *28*, 889.

(17) Boerio, F. J.; Koenig, J. L. *J. Chem. Phys.* **1970**, *52*, 3425.

(18) Le Fevere de Ten Hove, C. Controlling Solid-State Microstructure of Semi-Crystalline Polymers Through Chemical Design of Chains: A Study of Model Polyesters. Ph.D. Thesis, Université Catholique de Louvain, Louvain-la-Neuve, 2001.

(19) Wunderlich, B. *Crystal Nucleation, Growth, Annealing*; Academic: New York, 1976; Vol. 2.

(20) Hoffman, J. D.; Weeks, J. J. *J. Chem. Phys.* **1965**, *42*, 4301.

(21) Wunderlich, B.; Mellilo, J. *Macromol. Chem.* **1968**, *118*, 250.

(22) Schultz, J. M.; Scott, R. D. *J. Polym. Sci., Part A: Polym. Chem.* **1969**, *7*, 659.

(23) Fischer, E. W.; Fakirov, S. *J. Mater. Sci.* **1976**, *11*, 1041.

(24) Fakirov, S.; Fischer, E. W.; Hoffmann, R.; Schmidt, G. F. *Polymer* **1977**, *18*, 1121.

(25) *Nylon Plastics Handbook*; Kohan, M. I., Eds.; Hanser: Munich, 1995.

(26) Coleman, M. M.; Graf, J. F.; Painter, P. C. *Specific Interactions and the Miscibility of Polymer Blends*; Technomic: Lancaster, 1991.

(27) Skrovanek, D. J.; Painter, P. C.; Coleman, M. M. *Macromolecules* **1986**, *19*, 699.

(28) Tsubomura, H. *J. Chem. Phys.* **1956**, *24*, 927.

(29) Stolov, A. A.; Borisover, M. D.; Solomonov, B. N. *J. Phys. Org. Chem.* **1996**, *9*, 241.

(30) Smith, P. A. S. The Curtius Reaction. In *Organic Reactions*; Adams, R., Ed.; John Wiley & Sons: New York, 1942; Vol. 3.

(31) Ozaki, S. *Chem. Rev.* **1972**, *72*, 457.

(32) Twitchett, H. J. *Chem. Soc. Rev.* **1974**, *3*, 209.

(33) Smith, M. B.; March, J. *March's Advanced Organic Chemistry: Reactions, Mechanism, and Structure*; 5th ed.; John Wiley & Sons: New York, 2001.

(34) Hentschel, W. *Ber.* **1884**, *17*, 1284.

(35) DuPont de Nemours & Co. U.S. Patent 2,374,340, 1940.

(36) Imp. Chem. Ind. U.S. Patent 2,379,948, 1943.

(37) Bayer, O. *Angew. Chem.* **1947**, *59 A*, 275.

(38) Siefken, W. *Liebigs Ann. Chem.* **1949**, *562*, 122.

(39) Farlow *Org. Synth.* **1951**, *31*, 63.

(40) I. G. Farbenindustrie. German Patent DE 870,097, 1942.

(41) I. G. Farbenindustrie. German Patent DE 844,896, 1944.

(42) BASF. German Patent DE 801,993, 1948.

(43) Goodrich Co. U.S. Patent 2,642,449, 1953.

(44) Mashio, F.; Nomachi, T. *Kogyo Kagaku Zasshi* **1953**, *56*, 289.

(45) I. G. Farbenindustrie. German Patent DE 947,471, 1956.

(46) Gen. Aniline & Film Corp. U.S. Patent 2,847,440, 1956.

(47) Sigurdsson, S. T.; Seeger, B.; Kutzke, U.; Eckstein, F. *J. Org. Chem.* **1996**, *61*, 3883.

(48) Loudon, G. M. *Organic Chemistry*; 2nd ed.; Benjamin/Cummings: Menlo Park, 1988.

(49) Curtius *Ber.* **1890**, *23*, 3023.

(50) Schmidt, F. *Chem. Ber.* **1922**, *55*, 1584.

(51) Damle, S. B. *Chem. Eng. News* **1993**, 4.

(52) Mayer, A.; Magne, H.; Plantefol, L. *Compt. Rend.* **1921**, *172*, 136.

(53) Hollingsworth, M. D. *Chem. Eng. News* **1992**, *70*, 4.

(54) Cotarca, L. *Org. Proc. Research and Devel.* **1999**, *3*, 377.

(55) Gilman, J. W.; Otonari, Y. A. *Synth. Commun.* **1993**, *23*, 335.

(56) King, C. *J. Am. Chem. Soc.* **1964**, *86*, 437.

(57) Bunn, C. W. *Trans. Faraday Soc.* **1939**, *35*, 482.

CHAPTER 5. HETEROATOM-CONTAINING POLYURETHANES AND RESULTING THERMAL PROPERTIES

5.1 Introduction

There has recently been a renewed interest in step-growth polymers based on very long-chain monomers such as α,ω-diols and -dicarboxylic acids. Various types of polymers, including polyesters,[1-3] polyamides,[4] and polyurethanes[5] have been synthesized, and their morphological features, thermal properties, and (bio)degradability investigated. The introduction of long, aliphatic chains $(CH_2)_m$ to the segmented polymer induces a polyethylene-like character and can be systematically extended by increasing the length of the monomer. Model systems can be obtained that provide crucial information on how "defects" influence the crystallization of commercial, semi-crystalline polymers such as polyolefins. The introduction of weak links (such as ester groups O-C(O)) in the backbone is also expected to make these polyethylene-like polymers more easily biodegradable.[1,2]

Although very interesting fundamental results have been obtained based on such model systems, commercial use of these or similar segmented polymers is prevented by the prohibitive costs (a result of the multiple steps, difficulty in purification, and overall low yield) associated with the synthesis of long-chain monomers as discussed in Chapter 2. To overcome this problem, long-chain diols (29 to 32 atoms in the backbone) containing heteroatoms (sulfur and oxygen) were employed. These highly pure, monodisperse diols were prepared (in collaboration with Grégoire Cardoen under the supervision of Dr. Bernard Boutevin and Dr. Bruno Améduri from Ecole Nationale

Supérieure de Chimie de Montpellier) by a one-step procedure with yields ranging from 80 to 95%. The heteroatom-containing diols were combined in the melt with commercially available 1,6-diisocyanatohexane to make m,6-polyurethanes of the general structure $[O\text{-}(CH_2)_{11}\text{-}S\text{-}(CH_2)_2\text{-}X\text{-}(CH_2)_2\text{-}S\text{-}(CH_2)_{11}\text{-}O\text{-}C(O)\text{-}NH\text{-}(CH_2)_6\text{-}NH\text{-}C(O)]_n$, where m represents the total number of atoms (carbon + sulfur + oxygen) originating from the heteroatom-containing diols and X = CH_2, O, or $O\text{-}(CH_2)_2\text{-}O$ depending on the diol used.

A main goal of this study was to determine the effect that these heteroatoms had on the thermal properties (e.g. T_d, T_m, and enthalpy) and crystallization behavior of these polyurethanes. As discussed in Chapter 1, non-aliphatic, strongly interacting functional groups can have a dramatic influence on the T_m of aliphatic polymers. Ester groups lower the melting point, whereas hydrogen-bonding groups (e.g. urea, amide, and urethane groups) raise the melting point (Figure 5.1).[6] Hill and Walker[6] examined the effect of heteroatoms on the T_m of otherwise aliphatic polyamides. They concluded that the oxide group dramatically lowered the melting point, while the sulfide group had little effect. Additionally, as discussed in Chapter 4, the introduction of strongly interacting functional groups on an otherwise aliphatic backbone can alter the crystal structure and crystallization kinetics of the polymer. Depending on the influence of the heteroatoms, these more economical diols could be used commercially in the synthesis of long-chain polymers such as biodegradable polyesters,[1] polyamide-polyolefin blend compatibilizers,[4] and polyesters of chemically controlled lamellar thickness.[7]

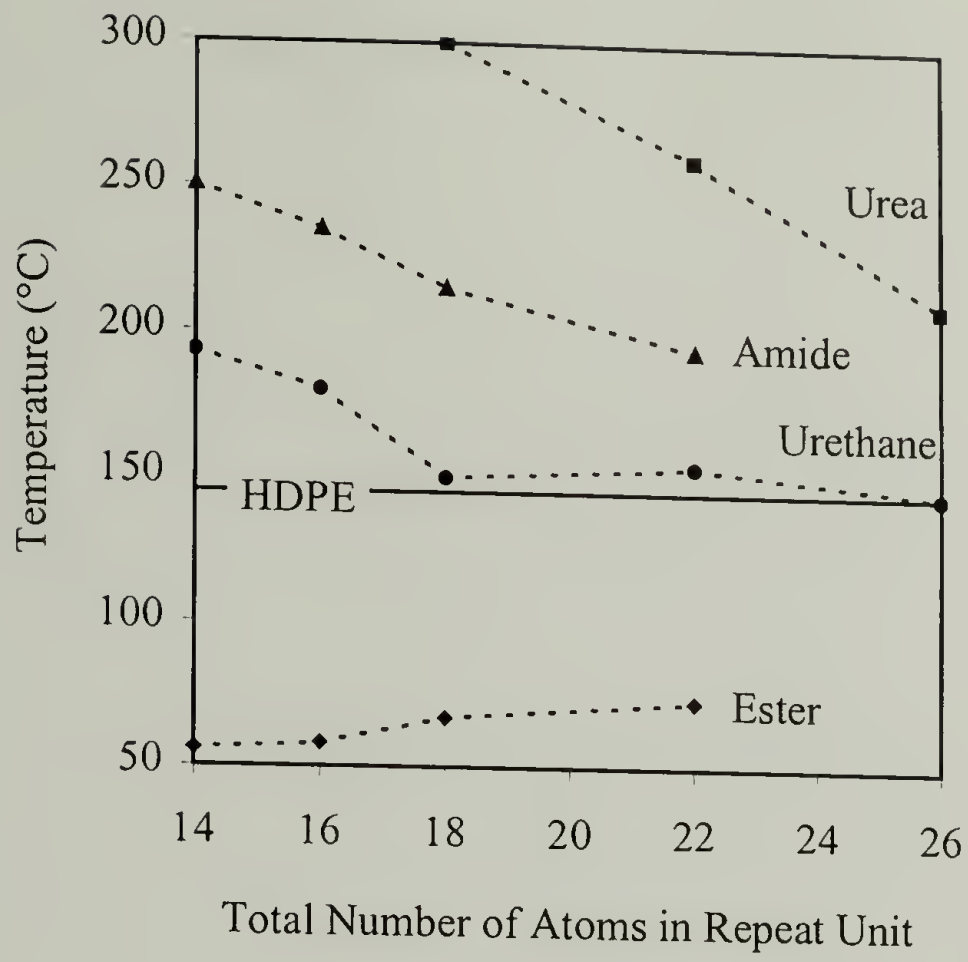

Figure 5.1. Influence of Strongly Interacting Functional Groups on the T_m of Otherwise Aliphatic m,n-Polymers.

5.2 Experimental

5.2.1 Characterization

^{1}H- and ^{13}C-NMR spectra of the monomers were obtained in deuterated $CDCl_3$ from either a Bruker 200 or 300 MHz NMR spectrometer at room temperature. The NMR spectra of the polymers were obtained in deuterated DMF from either a Bruker 500 or 600 MHz spectrometer at elevated temperatures. Elemental analysis was carried out by the Microanalytical Laboratory of the University of Massachusetts, Amherst. Carbon and hydrogen were detected via the classical Modified Pregl-Dumas reaction, while

sulfur was detected by titrating the sulfate product produced during combustion with barium ion. Both methods used an Exeter Analytical 240A elemental analyzer.

5.2.2 Molecular Weight Analysis

GPC chromatograms of the heteroatom-containing monomers were taken at room temperature in THF. A Waters 510 HPLC pump, Waters differential refractometer R401, and Polymer Laboratory gel 5 μm mixed-D columns were employed. The absolute molecular weights and distributions of the polymers were determined using high temperature, triple detector GPC. A Polymer Laboratory PL-GPC 220 ultra high temperature chromatograph with a Hewlett-Packard 1100 series isocratic pump and Polymer Laboratory gel 20 μm mixed-A columns was employed. The system was equipped with a Polymer Laboratory differential refractive index detector, Viscotek viscometer, and Wyatt Technology heated miniDAWN light scattering detector that used a wavelength of 690 nm. Instrument constants were determined using a 200,000 molecular weight polystyrene standard. Wyatt Technology's ASTRA software (version 4.70) was used to treat the data. The high temperature experiments were performed using 1,2,4-trichlorbenzene as the mobile phase at 135 °C. In order to determine the dn/dc values, the columns from the high-temperature GPC were removed, and the refractive index was measured at varying polymer concentrations.

5.2.3 Sample Preparation

Melt-crystallized samples were prepared by heating the polymers to 200 °C and then allowing the polymers to cool to room temperature at a rate of 10 $K \cdot min^{-1}$.

5.2.4 Thermal Analysis

TGA was performed on the monomers and polymers (5 to 10 mg) using a TA Instruments TGA 2950 flushed with nitrogen at a scan rate of 10 $K \cdot min^{-1}$. The T_d was taken at 5% weight loss. Melting points were observed using a Perkin Elmer Pyris DSC flushed with helium. The samples (5 to 10 mg) were heated above their melting points, cooled to room temperature, and then reheated, all at a rate of 10 $K \cdot min^{-1}$. The first heating and cooling run was performed in order to erase the different thermal histories present in the samples. The melting points were taken as the peak of the melting endotherm during the second heating run. The temperature scale was calibrated using indium and eicosane, and the heat of enthalpy was calibrated using indium.

5.2.5 Spectroscopy

IR spectra were recorded on a Bio-Rad 175C spectrometer. A total of 16 scans were performed, and spectral resolution was 4 cm^{-1}. A Bruker FRA 106 spectrometer equipped with a Nd:Yag laser (1.064 μm) was used to record the Raman spectra. A total of 256 scans were performed, and spectral resolution was 4 cm^{-1}. The laser power was 150 mW, and the excitation/collection geometry was 180°. The polyurethanes were examined in the bulk without any special crystallization treatment.

5.2.6 X-ray Scattering

WAXS patterns were obtained at room temperature using Ni-filtered Cu Kα radiation of wavelength 1.542 Å from a Siemens sealed tube X-ray generator operating at 40 kV and 30 mA. A point-collimated beam was used, and the X-ray diffraction patterns

were recorded using a flat image plate in an evacuated Statton camera. Calcite (d_b = 3.035 Å) was dusted onto selected samples for calibration purposes.

5.2.7 Monomer Synthesis

5.2.7.1 General Considerations

The synthesis of 12,18-dithianonacosanediol (**26**) was described previously.[8,9] Reagents used during the synthesis of the heteroatom-containing diols were all commercially available, and they were used without further purification.

5.2.7.2 Synthesis of Heteroatom-Containing Diols via Free-Radical Telomerization

12,18-Dithia-15-oxanonacosanediol (27). 2,2-Oxydiethanethiol (6.27 g, 0.05 mol), 10-undecene-1-ol (18.45 g, 0.11 mol), and acetonitrile (50 mL) were mixed under an argon atmosphere. The mixture was heated to 75 °C, and *t*-butyl peroxypivalate (0.46 g, 1.98 mmol) in acetonitrile (10 mL) was added dropwise to the mixture. After refluxing the solution for 5 hours, the precipitated product was recrystallized from acetonitrile to yield 12,18-dithia-15-oxanonacosanediol (**27**) as a white powder (19.33 g, 82%); m.p. 75.6 °C, lit: 78 °C.[9] ^{1}H-NMR (300 MHz, $CDCl_3$) δ = 3.63 (quintet, J = 6.9 Hz, 8H, CH_2-O), 2.70 (t, J = 6.9 Hz, 4H, S-CH_2-CH_2-O), 2.55 (t, J = 7.4 Hz, 4H, S-CH_2-CH_2-CH_2), 1.62-1.51 (m, 8H, CH_2-CH_2-O and CH_2-CH_2-S), 1.38-1.27 (m, 28H, CH_2-CH_2-CH_2). ^{13}C-NMR (200 MHz, $CDCl_3$) δ 70.75 (O-*C*H_2-CH_2-S), 63.05 (*C*H_2-OH), 32.80 (*C*H_2-S), 32.67 (S-*C*H_2-CH_2-O), 31.54 (*C*H_2-CH_2-OH), 29.79-25.72 (all remaining aliphatic *C*H_2). IR (KBr): 3300 cm^{-1} (OH stretch), 2920 cm^{-1} (asymmetric CH stretch), 2851 cm^{-1}

(symmetric CH stretch), 1487 and 1463 cm^{-1} (CH_2 bend), 1131 cm^{-1} (C-O-C asymmetric stretch), 732 cm^{-1} (in-phase CH_2 rock), 719 cm^{-1} (out-of-phase CH_2 rock). Anal. Calc. for $C_{26}H_{54}O_3S_2$ (479.0): C, 65.22; H, 11.37; S, 13.39. Found: C, 65.27; H, 11.19; S, 13.48.

12,21-Dithia-15,18-dioxadotriacontanediol (28). The above procedure was followed using 3,6-dioxa-1,8-octanediol (7.84 g, 0.04 mol) and 10-undecene-1-ol (16.11 g, 0.10 mol) to yield 12,21-dithia-15,18-dioxadotriacontanediol (**27**) as a white powder (19.33 g, 86%); m.p. 70.3 °C. ^{1}H-NMR (300 MHz, $CDCl_3$) δ = 3.63 (t, J = 7.0 Hz, 12H, CH_2-O), 2.71 (t, J = 7.1 Hz, 4H, S-CH_2-CH_2-O), 2.54 (t, J = 7.4 Hz, 4H, S-CH_2-CH_2-CH_2), 1.63-1.52 (m, 8H, CH_2-CH_2-O and CH_2-CH_2-S), 1.38-1.27 (m, 28H, CH_2-CH_2-CH_2). ^{13}C-NMR (200 MHz, $CDCl_3$) δ 71.02 (O-*C*H_2-CH_2-S), 70.25 (O-*C*H_2-CH_2-O), 62.83 (*C*H_2-OH), 32.74 (S-*C*H_2-CH_2-O and *C*H_2-S), 31.36 (*C*H_2-CH_2-OH), 29.76-25.71 (all remaining aliphatic *C*H_2). IR (KBr): 3300 cm^{-1} (OH stretch), 2920 cm^{-1} (asymmetric CH stretch), 2851 cm^{-1} (symmetric CH stretch), 1487 and 1463 cm^{-1} (CH_2 bend), 1103 (C-O-C asymmetric stretch), 731 cm^{-1} (in-phase CH_2 rock), 720 cm^{-1} (out-of-phase CH_2 rock). Anal. Calc. for $C_{28}H_{58}O_4S_2$ (523.1): C, 64.32; H, 11.18; S, 12.26. Found: C, 64.28; H, 11.52; S, 12.25.

5.2.8 Polymer Synthesis

5.2.8.1 General Considerations

1,6-Diisocyanatohexane (98%) was purchased from Aldrich and distilled immediately before use. All of the heteroatom-containing diols were dried in a vacuum oven prior to polymerization in order to remove any absorbed water.

5.2.8.2 Synthesis of Heteroatom-Containing m,n-Polyurethanes by Melt-Polyaddition

The heteroatom-containing diols (0.5 g) were heated just slightly above their melting temperature in argon-purged glass vessels. Stoichiometric amounts of 1,6-diisocyanatohexane were syringed into the reaction vessels, and the mixtures were vigorously stirred for up to 1 hour or until they solidified. After cooling to room temperature, DMF (10 mL) was added, and the mixtures were heated until the polymers dissolved. The hot solutions were then poured dropwise into rapidly stirred methanol (100 mL). The resulting cloudy white mixtures were filtered and dried in a vacuum oven yielding heteroatom-containing m,n-polyurethanes (**29**) $[O\text{-}(CH_2)_{11}\text{-}S\text{-}(CH_2)_2\text{-}X\text{-}(CH_2)_2\text{-}S\text{-}(CH_2)_{11}\text{-}O\text{-}C(O)\text{-}NH\text{-}(CH_2)_6\text{-}NH\text{-}C(O)]_n$, where X = CH_2, O, or $O\text{-}(CH_2)_2\text{-}O$, as white solids. ^{1}H-NMR (500 or 600 MHz, DMF-d_7, 413K) δ = 6.35-6.22 (bs, 2H, N*H*), 4.02-4.01 (t, J = 6.6 Hz, 4H, CH_2-O-C(O)), 3.66-3.65 (t, J = 6.6 Hz, 4-8H, CH_2-O), 3.12-3.10 (quintet, J = 6.6 Hz, 4H, CH_2-NH-C(O)), 2.71 (t, J = 6.6 Hz, 4H, S-CH_2-CH_2-O), 2.61-2.55 (t, J = 7.1 Hz, 4-8H, S-CH_2-CH_2-CH_2), 1.61 (quintet, J = 6.3 Hz, 4H, CH_2-CH_2-O-C(O)), 1.54-1.52 (m, 4H, CH_2-CH_2-NH-C(O)), 1.43-1.42 (quintet, J = 6.7 Hz, 4-8 Hz, CH_2-CH_2-CH_2-S), 1.34 (m, remaining H, CH_2-CH_2-CH_2). ^{13}C-NMR (500 or 600 MHz,

DMF-d_7, 413K) δ 162.47-162.43 (O-*C*(O)-NH), 76.80-76.50 (O-*C*H_2-CH_2-S), 75.92 (O-*C*H_2-CH_2-O), 69.77-69.64 (*C*H_2-O-C(O)-NH), 46.63-36.49 (*C*H_2-NH-C(O)-O), 38.00-37.72 (*C*H_2-S), 37.37 (S-*C*H_2-CH_2-O), 34.28-31.46 (all remaining aliphatic *C*H_2). IR (KBr): 3322 cm^{-1} (NH stretch), 2919 cm^{-1} (asymmetric CH stretch), 2850 cm^{-1} (symmetric CH stretch), 1685 cm^{-1} (amide I), 1539 cm^{-1} (amide II), 1468 cm^{-1} (CH_2 bend).

5.3 Results and Discussion

5.3.1 Monomer Synthesis

5.3.1.1 Overview of Synthetic Methods

There has been a great deal of work in the past regarding the synthesis of monodisperse, telechelic diols. Recently, Osakada et al.[5] described the synthesis of 13-oxapentacosanediol HO-$(CH_2)_{12}$-O-$(CH_2)_{12}$-OH and 13,26-dioxaoctatriacontanediol HO-$(CH_2)_{12}$-O-$(CH_2)_{12}$-O-$(CH_2)_{12}$-OH. These long-chain, oxygen-containing, telechelic diols were synthesized by the NaH promoted coupling of a protected bromo-alcohol with a mono-protected diol or a non-protected diol, respectively. Améduri and co-workers[8] provided an excellent review on telomerization to make α,ω-functionalized monomers. The early work was plagued by problems including low yield and the formation of the monoadduct. However, several researchers[10-12] found that monodisperse, telechelic diols could be synthesized in reasonable yields by the telomerization of functional monomers with dithiols in the presence of either an acidic or basic catalyst. In the early 1990s,

Améduri and his research group reported on the synthesis of aliphatic[8,9,13-15] and aromatic[16,17] α,ω-diols based on the anti-Markovnikov, free-radical addition of thiol end-groups onto double bonds.[18-20] Upon comparing different free-radical initiators, Améduri reported that *t*-butyl peroxipyvalate produced pure, monodisperse, telechelic diols in yields of 96%.[8]

5.3.1.2 Synthesis of the Heteroatom-Containing Diols Used in This Study

Telechelic, monodisperse, heteroatom-containing diols HO-$(CH_2)_{11}$-S-$(CH_2)_2$-X-$(CH_2)_2$-S-$(CH_2)_{11}$-OH, where X = CH_2, O, or O-$(CH_2)_2$-O, were produced by a radical telomerization of an excess of 10-undecene-1-ol with commercially available α,ω-dithiols in the presence of *t*-butyl peroxypivalate (Scheme 5.1). This one-step procedure produced the pure heteroatom-containing, telechelic diols in high yield (> 80%). 12,18-Dithianonacosanediol (**26**) HO-$(CH_2)_{11}$-S-$(CH_2)_5$-S-$(CH_2)_{11}$-OH, 12,18-dithia-15-oxanonacosanediol (**27**) HO-$(CH_2)_{11}$-S-$(CH_2)_2$-O-$(CH_2)_2$-S-$(CH_2)_{11}$-OH, and 12,21-dithia-15,18-dioxadotriacontanediol (**28**) HO-$(CH_2)_{11}$-S-$(CH_2)_2$-O-$(CH_2)_2$-O-$(CH_2)_2$-S-$(CH_2)_{11}$-OH were all synthesized. The heteroatom-containing diols had lengths of 29 to 32 atoms and contained 2 sulfide groups each and from 0 to 2 oxide groups. The diols were named after the number of methylene groups as well as heteroatoms in their backbone, and in parenthesis is the number and type of heteroatoms. The heteroatom-containing diols are referred to as the 1,29(2S)-, 1,29(2S+O)-, and 1,32(2S+2O)-diols, respectively.

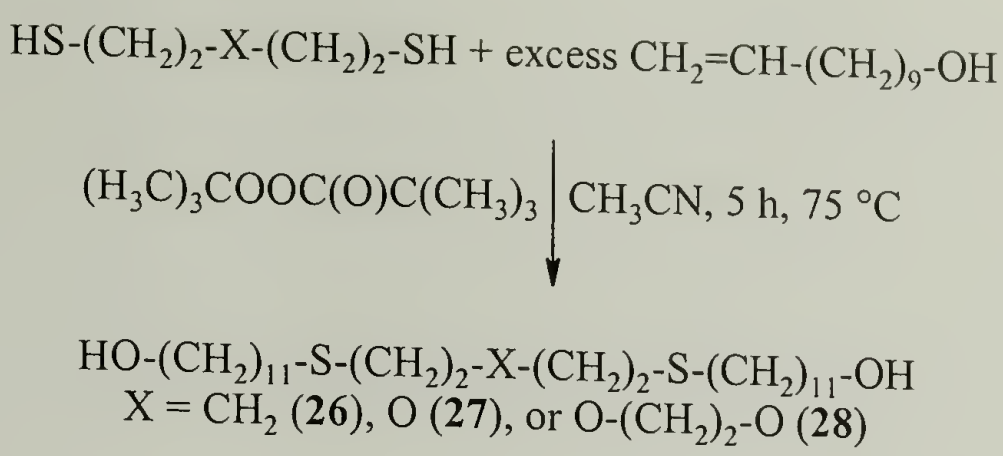

Scheme 5.1. Synthesis of the Heteroatom-Containing, Telechelic Diols (**26-28**).

5.3.2 Monomer Characterization

5.3.2.1 Monomer Purity

Results from ^{1}H- and ^{13}C-NMR, IR, and elemental analysis for all the heteroatom-containing diols were fully compatible with the expected structures. After recrystallization of the diols, the starting material, 10-undecene-1-ol, was not detected by ^{1}H-NMR nor IR. However, the DSC thermogram (Figure 5.2) of the 1,29(2S+O)-diol showed a small, broad peak before the melting endotherm, which was absent for the other two heteroatom-containing diols. This peak was reproducible and probably the result of either an impurity or some sort of crystal reorganization. If this peak arose from an impurity (Scheme 5.2), the impurity was not observable in the NMR implying a low presence and was most likely either the monoadduct HO-$(CH_2)_{11}$-S-$(CH_2)_2$-O-$(CH_2)_2$-SH (although the odor typical of thiols was not present) or the disulfide HO-$(CH_2)_{11}$-S-$(CH_2)_2$-O-$(CH_2)_2$-S-S-$(CH_2)_2$-O-$(CH_2)_2$-S-$(CH_2)_{11}$-OH (produced from the coupling of the corresponding ω-hydroxyl alkyl thiyl free radicals).

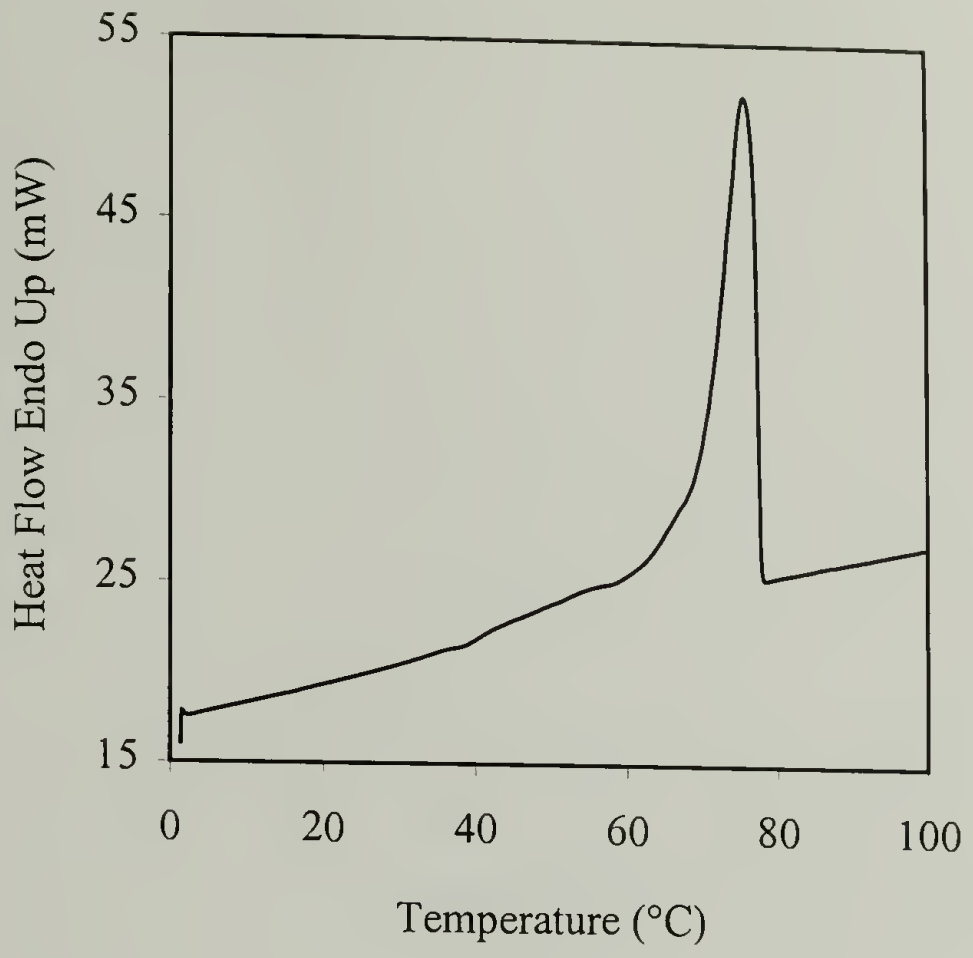

(a)

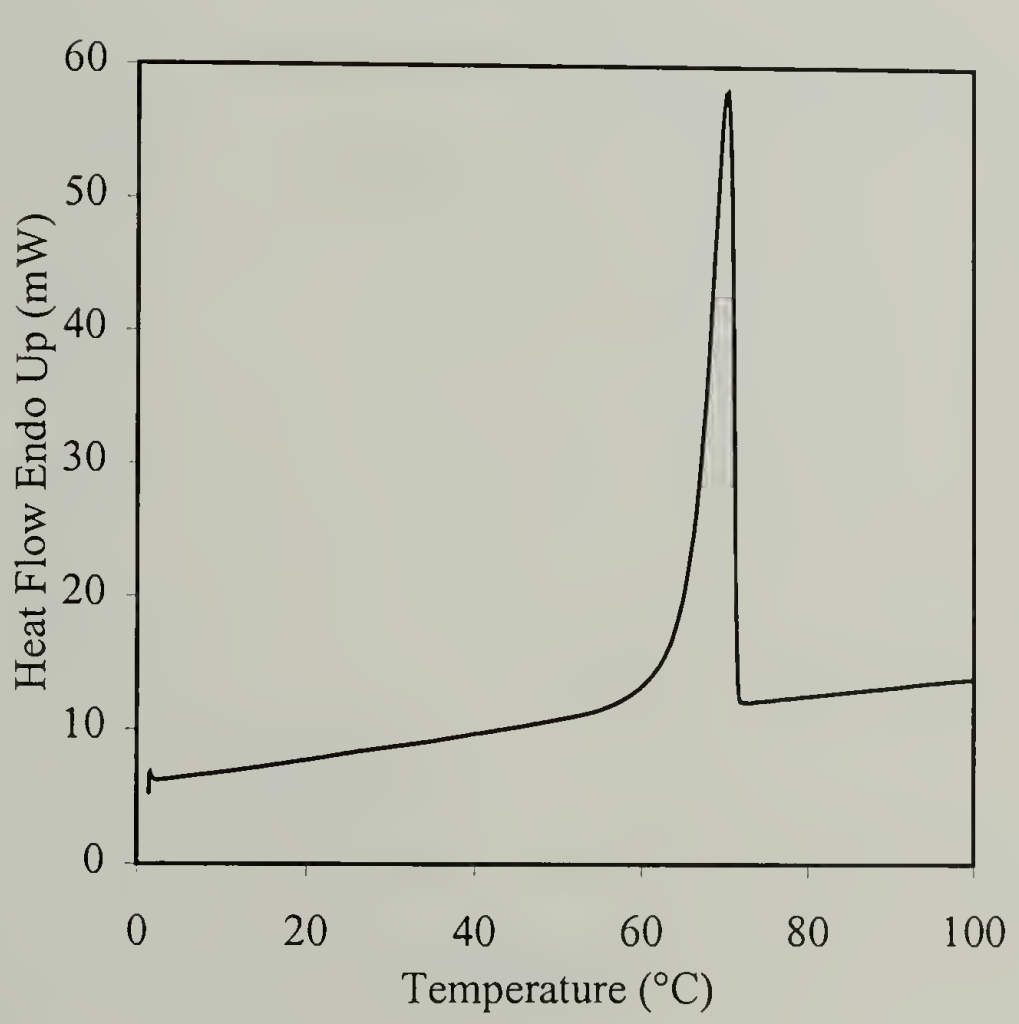

(b)

Figure 5.2. DSC Thermograms of the Heteroatom-Containing α,ω-Diols: (a) 1,29(2S+O)-Diol and (b) 1,32(2S+2O)-Diol.

A) $HS\text{-}(CH_2)_2\text{-}O\text{-}(CH_2)_2\text{-}SH + CH_2{=}CH\text{-}(CH_2)_9\text{-}OH$

$\longrightarrow$ $HO\text{-}(CH_2)_{11}\text{-}S\text{-}(CH_2)_2\text{-}O\text{-}(CH_2)_2\text{-}SH$

B) $2\ HO\text{-}(CH_2)_{11}\text{-}S\text{-}(CH_2)_2\text{-}O\text{-}(CH_2)_2\text{-}S\cdot$ $\longrightarrow$

$HO\text{-}(CH_2)_{11}\text{-}S\text{-}(CH_2)_2\text{-}O\text{-}(CH_2)_2\text{-}S\text{-}S\text{-}(CH_2)_2\text{-}O\text{-}(CH_2)_2\text{-}S\text{-}(CH_2)_{11}\text{-}OH$

Scheme 5.2. Possible Side Reactions that Can Occur During the Synthesis of 12,18-Dithia-15-oxanonacosanediol.

If the monoadduct was present, there should have been a peak present in the GPC chromatogram corresponding to approximately half the molecular weight of the main diol peak. The GPC chromatograms (Figure 5.3) of the 1,29(2S+O)- and 1,32(2S+2O)-diols were examined, and neither showed any evidence of a monoadduct side product. The corresponding disulfide would have a similar enough molecular weight to the desired diol that it might be difficult to distinguish this side product by GPC. However, if present, the sulfur-sulfur single bond should give a strong Raman peak between 400 and 500 cm^{-1},[21] although the S-S stretch has also been reported in the 500 to 550 cm^{-1} range.[22,23] The Raman spectrum of the 1,29(2S+O)-diol showed signals at 438 and 473 cm^{-1}(Figure 5.4), which corresponded to the signals traditionally assigned to the sulfur-sulfur single bond. These signals were not observed for the other 2 heteroatom-containing diols. It is possible, that the 1,29(2S+O)-diol contained a small amount of impurity caused by the presence of the disulfide.

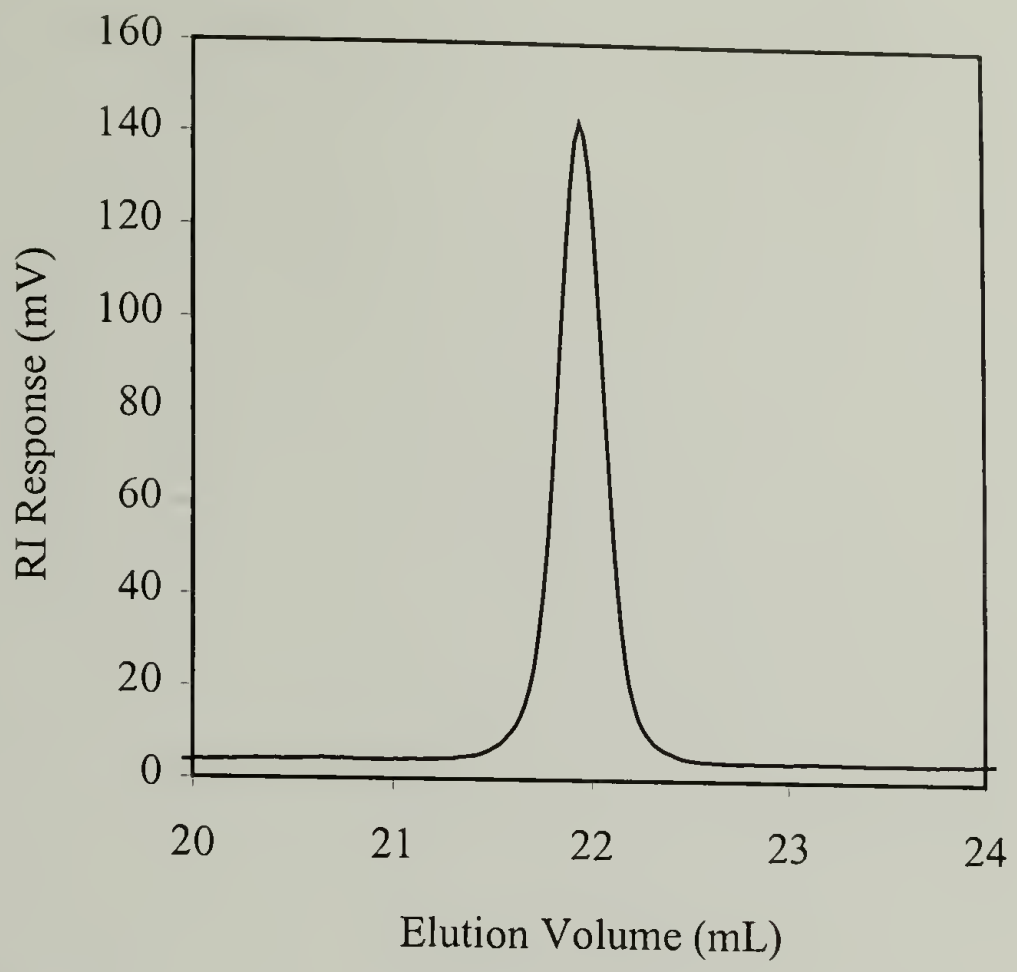

(a)

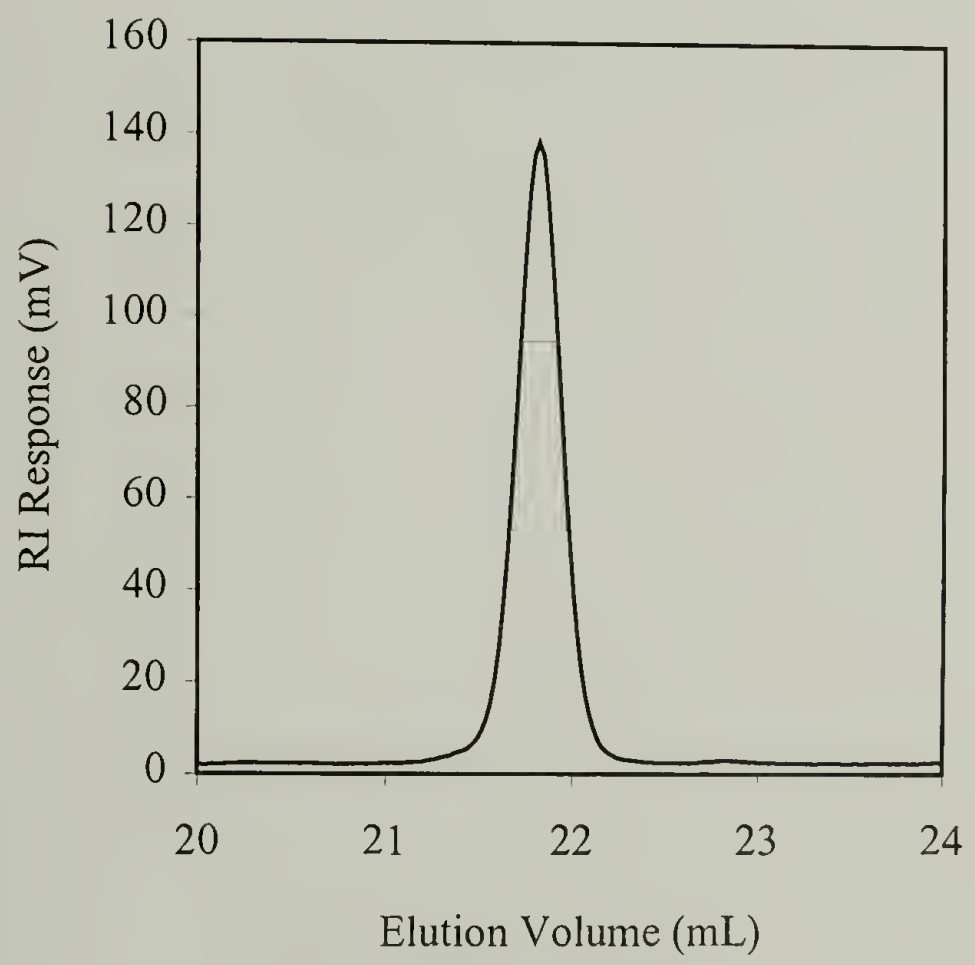

(b)

Figure 5.3. GPC Chromatograms of the Heteroatom-Containing α,ω-Diols: (a) 1,29(2S+O)-Diol and (b) 1,32(2S+2O)-Diol.

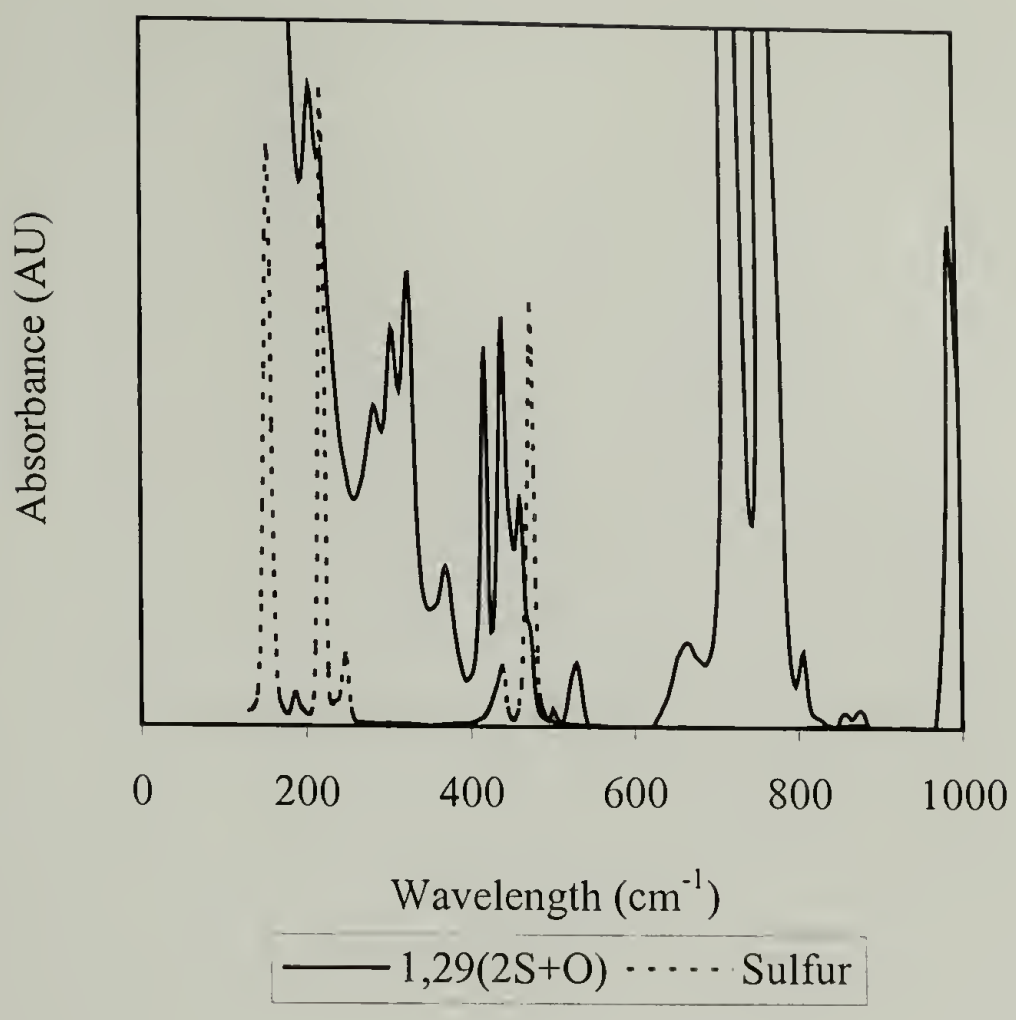

(a)

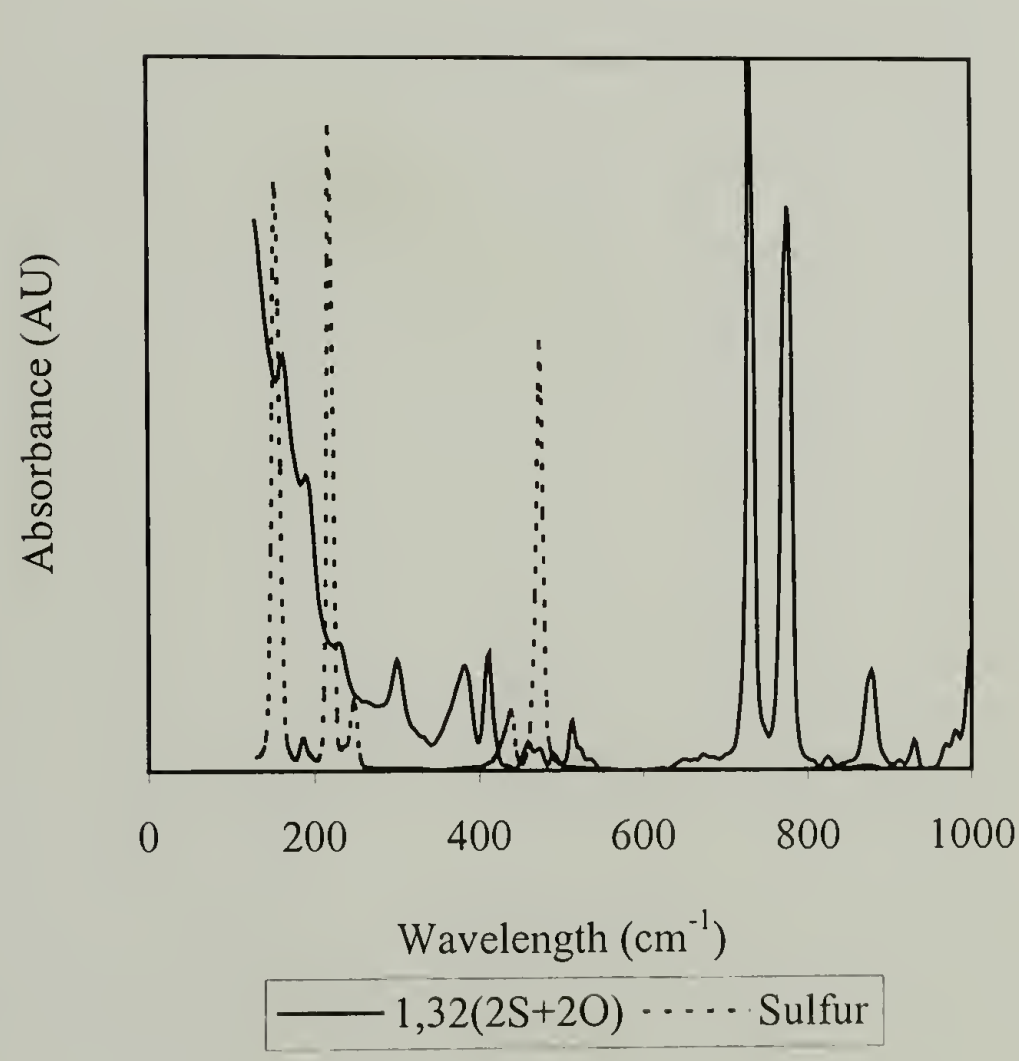

(b)

Figure 5.4. Raman Spectra of Sulfur and the Heteroatom-Containing, Telechelic Diols: (a) 1,29(2S+O)-Diol and (b) 1,32(2S+2O)-Diol.

5.3.2.2 Thermal Properties

The thermal properties of the heteroatom-containing α,ω-diols, along with the purely aliphatic diols of similar length (Chapter 2), are shown in Table 5.1. As the number of heteroatoms (sulfur or oxygen) in the diol increased, the T_m decreased (Figure 5.5). These heteroatom-containing diols had much lower T_m and enthalpy values than the analogous purely aliphatic diols.[7,24] It has been suggested that ether links activate the rotation of neighboring methylene groups resulting in an increase in flexibility, which could cause a lowering of the T_m.[25] Additionally, unlike the corresponding aliphatic diols, the heteroatom-containing, telechelic diols did not exhibit a solid-solid rotator phase transition upon heating.[7,26] Again, this behavior could be explained by the flexibility provided to the diol by the heteroatoms.

Table 5.1. Thermal Properties of the Long-Chain α,ω-Diols.

α,ω-Diol	Melting Temp. (°C)[b]	Transition Temp. (°C)[b]	Enthalpy ($J \cdot g^{-1}$)	Decomposition Temp. (°C)[c]
1,32[a]	115	99	240	292
1,29(2S)	87	None	190	269
1,29(2S+O)	76	None	137	259
1,32(2S+2O)	70	None	175	286

a) See Chapter 2.

b) Melting and transition temperatures were taken as the peak of the melting and transition endotherms during the second heating run using a scan rate of 10 $K \cdot min^{-1}$.

c) Decomposition temperatures were taken at 5% weight loss using a scan rate of 10 $K \cdot min^{-1}$.

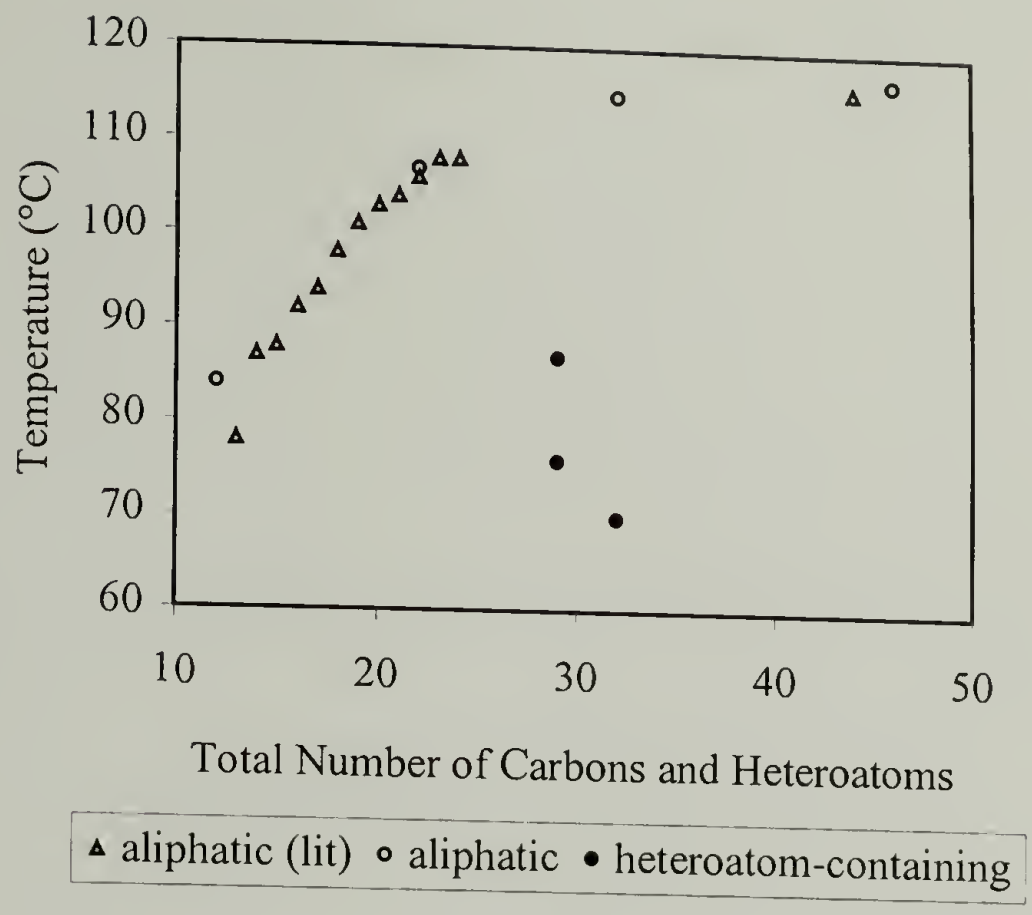

Figure 5.5. Comparison of the T_m of the α,ω-Diols. • and o Represent Data from This Work, and Δ Represents Data from Literature (See References 7 and 24).

Contrary to the melting behavior, the T_d of the heteroatom-containing diols was within the same range as the purely aliphatic diols (Figure 5.6). These monodisperse, telechelic diols have a higher thermal stability than similar commercially available, polydisperse diols (e.g. polytetrahydrofuran).[9] As with the aliphatic diols, the TGA behavior is probably not the result of decomposition, but rather vaporization.

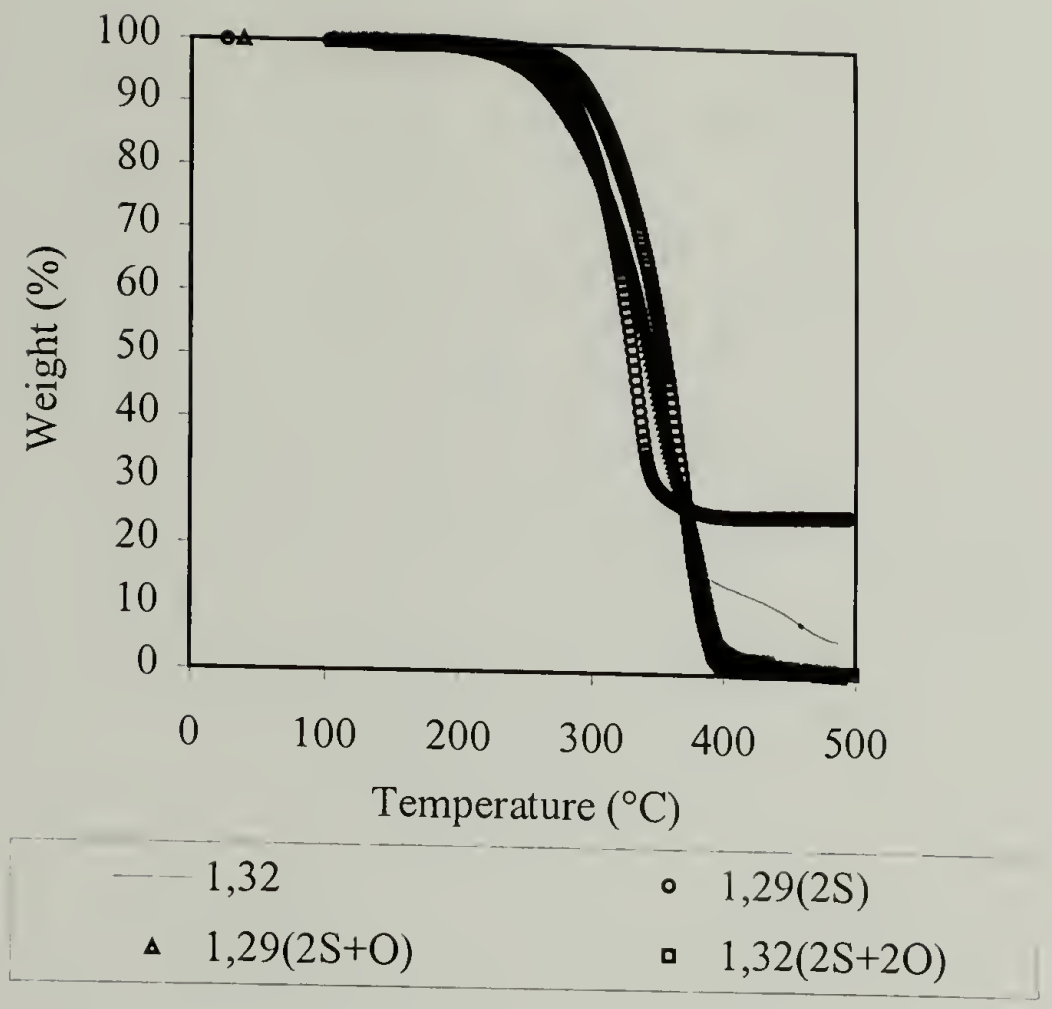

Figure 5.6. TGA Thermograms of the α,ω-Diols.

5.3.3 Polymer Synthesis

The heteroatom-containing m,n-polyurethanes (**29**) were all synthesized by a step-growth polyaddition in the melt (Scheme 5.3). Equimolar amounts of the heteroatom-containing diol and 1,6-diisocyanatohexane were used. As with the aliphatic m,n-polyurethanes discussed in Chapter 3, catalysts were not used in the polymerization in order to avoid any undesired side reactions (e.g. trimerization and the formation of crosslinks)[27,28] as well as to avoid the need to remove their residue from the resulting polymers. Isolated polymerization yields of 50 to 96% based on gravimetric results were obtained. Table 5.2 summarizes the polymerization conditions. The following heteroatom-containing m,n-polyurethanes (in order of increasing aliphatic length) were

produced: 29(2S),6, 29(2S+O),6, and 32(2S+2O),6. None of these polyurethanes had been previously synthesized.

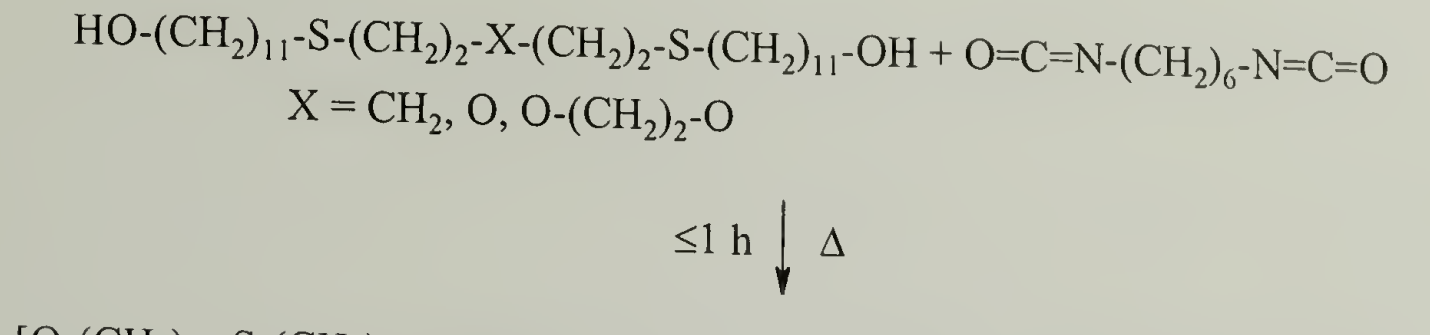

Scheme 5.3. Synthesis of Heteroatom-Containing m,n-Polyurethanes (**29**).

Table 5.2. Polymerization Conditions and Resulting Molecular Weights of the Heteroatom-Containing m,n-Polyurethanes.

m,n-Polymer	Polym. Temp.(°C)	Yield (%)	$M_w \cdot 10^{-3}$	PDI	dn/dc ($mL \cdot g^{-1}$)
29(2S),6	90	96	5.9	1.8	-0.037
29(2S+O),6	80	63	-[a]	-[a]	-0.056
32(2S+2O),6	75	50	56.2	2.3	-0.046

a) Molecular weight and PDI could not be determined due to baseline noise (as a result of a similar refractive index of the polymer solution to the solvent).

5.3.4 Polymer Characterization

5.3.4.1 Structure and Purity

As with the synthesis of the aliphatic m,n-polyurethanes (Chapter 3), careful control of the polymerization temperature was needed, and all water had to be removed before polymerization. The purity of all the polymers was carefully examined using IR, NMR, and GPC. These characterization methods indicated the absence of all known side products (e.g. allophanates, amines, ureas, and biurets). Some macrocyclics were

expected since the polyurethanes were synthesized by a step-growth polymerization,[29] but neither their presence nor concentration could be confirmed. IR and high temperature ^{1}H- and ^{13}C-NMR spectra were fully compatible with the expected structures. Very low amounts of the methylene groups alpha to the hydroxyl end-groups were occasionally detected via ^{1}H-NMR. The presence of end-groups and their detection was expected based on the molecular weights of the polymers as determined by GPC. The absolute weight-average molecular weights of the polymers ranged from 6,000 to 60,000 (Table 5.2), and the PDI values were approximately 2 as expected in a step-growth polymerization.[30]

5.3.4.2 Thermal Analysis

The thermal properties of the heteroatom-containing m,n-polyurethanes, along with the purely aliphatic polyurethanes of similar length and both HDPE[31] and LLDE,[32] are summarized in Table 5.3. T_d values of approximately 300 °C were observed for all of the heteroatom-containing polyurethanes. As with the heteroatom-containing diols, the introduction of sulfur and oxygen did not affect the T_d (Figure 5.7). These values were similar to the 220 °C or higher T_d typically seen for aliphatic polyurethanes of higher hydrogen-bonding densities. The TGA thermogram for the 29(2S),6-polyurethane is shown in Figure 5.8 and was representative of the decomposition behavior of all of the heteroatom-containing polyurethanes.

Table 5.3. Thermal Properties of the Heteroatom-Containing m,n-Polyurethanes.

m,n-Polymer	Decomposition Temperature[d] (°C)	Melting Temperature[e] (°C)	Enthalpy ($J \cdot g^{-1}$)
22,6[a]	292	146	89
32,6[a]	291	143	112
46,6[a]	278	135[f]	
29(2S),6	293	123	105
29(2S+O),6	301	115[f]	
32(2S+2O),6	295	100	60
HDPE[b]	370	145	295
LLDPE[c]		121 to 125	98 to 155

a) See Chapter 3.

b and c) See references 31 and 32, respectively

d) Decomposition temperatures were taken at 5% weight loss using a scan rate of 10 $K \cdot min^{-1}$.

e) Melting temperatures were taken as the peak of the melting endotherm during the second heating run using a scan rate of 10 $K \cdot min^{-1}$.

f) These polymers had more than one endotherm (see Figure 5.10); the melting points given were from the second endotherm, and enthalpy values were not calculated.

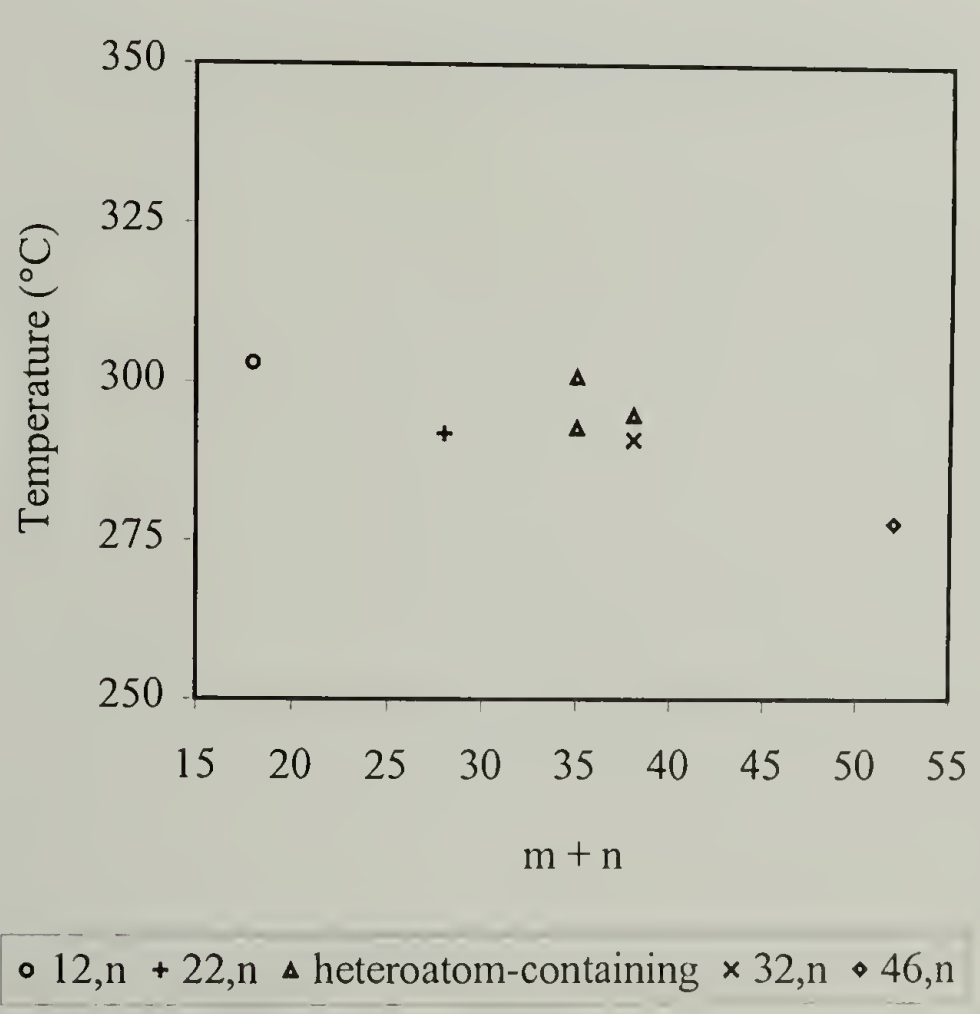

Figure 5.7. Comparison of the T_d of the Aliphatic and Heteroatom-Containing m,6-Polyurethanes.

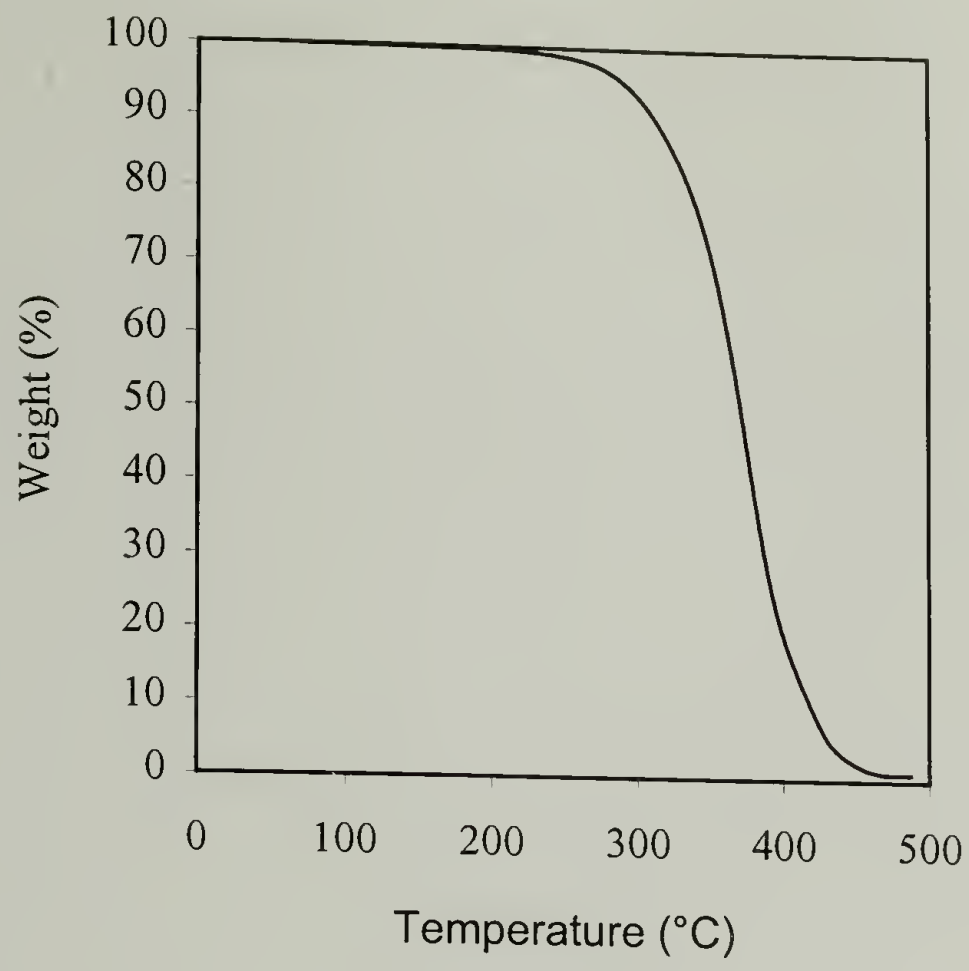

Figure 5.8. TGA Thermogram of 29(2S),6-Polyurethane.

As with the diols they were synthesized from, the heteroatom-containing polyurethanes exhibited much lower T_m and enthalpy values then the purely aliphatic m,6-polyurethanes[33] (Figure 5.9). Unlike the results presented by Hill and Walker,[6] the sulfide group as well as the oxide group appeared to cause a decrease in the melting temperature. As with the corresponding heteroatom-containing diols, the lower T_m can be explained by the resulting increased flexibility of the chain. However, in the case of the 29(2S),6- and 29(2S+O),6-polyurethanes, the decrease in T_m might also be contributed to the fact that these polyurethanes are odd-even and not even-even like the other m,n-polyurethanes (odd-even parity effect).

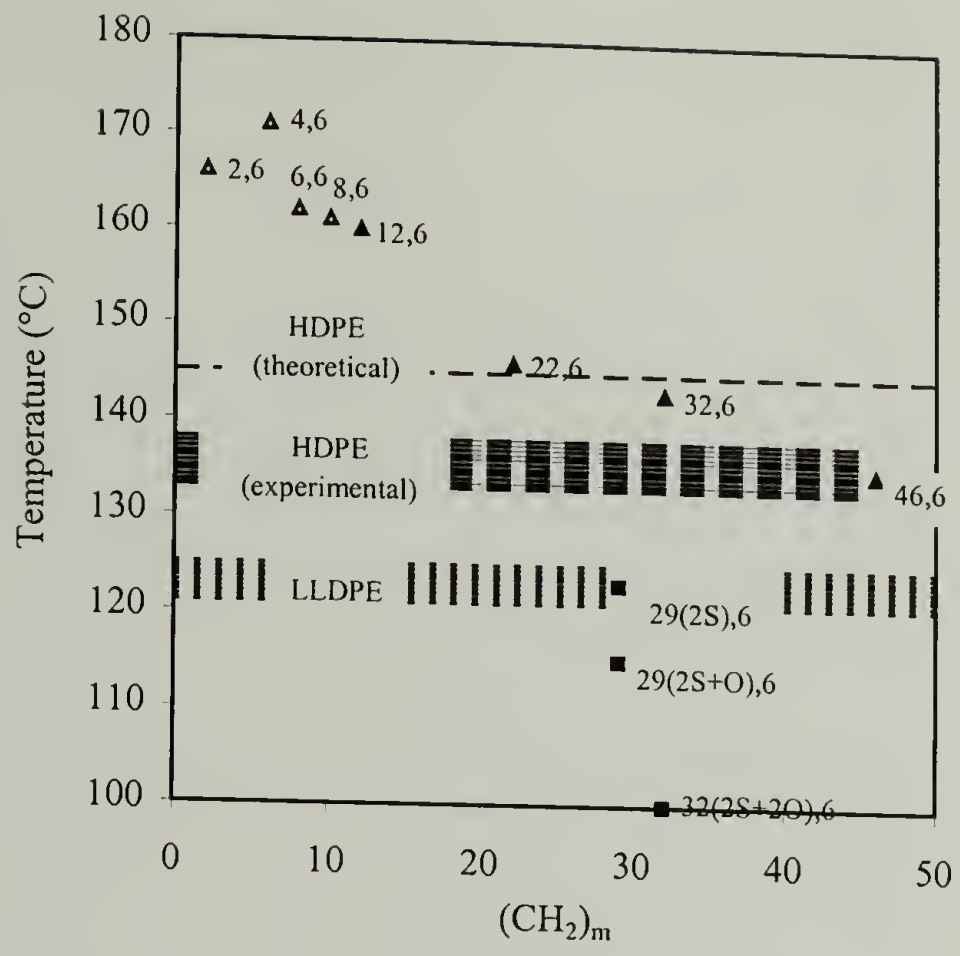

Figure 5.9. Comparison of the T_m of the m,6-Polyurethanes. ☐ and ☐ Represent Data from the Aliphatic Polyurethanes from this Study and Literature (See Reference 32), Respectively, and ε Represents Data from the Heteroatom-Containing Polyurethanes.

T_m values lower than that of polyethylene are typical for polyethers (with the exception of polyoxymethylene).[34] Whereas, due to the strength of their hydrogen-bonds, polyurethanes of high hydrogen-bonding densities typically have a T_m that is higher than that of polyethylene. It would appear that in the competition between the flexibility resulting from the heteroatoms and the hydrogen-bonding strength of the carbamate ester linkages, the heteroatoms have a greater influence on the T_m. However, this was not too surprising since ~ 75% of the carbamate esters were hydrogen-bonded in the melt (see Section 4.3.4). Thus, the hydrogen-bonds did not need to be disrupted in order for these long-chain, heteroatom-containing m,n-polyurethanes to melt.

The 29(2S+O),6-polyurethane exhibited a melting endotherm, followed immediately by an exothermic peak, and then another endotherm (Figure 5.10) upon heating. Upon cooling, the polymer exhibited only one exothermic peak. Melting of the folded chains, followed by crystallization to the fully extended chain, and then melting of the extended chains could explain this behavior. This melting behavior was also observed for the low molecular weight 12,4-, 12,6-, and 46,6-polyurethanes (Chapter 2). The other heteroatom-containing m,n-polyurethanes with their higher molecular weights (Table 5.2) exhibited only one melting endotherm corresponding to the melting of the chain-folded polymers. The low molecular weight of the 29(2S+O),6-polyurethane was probably a result of the impurity in the diol (Section 5.3.2.1).

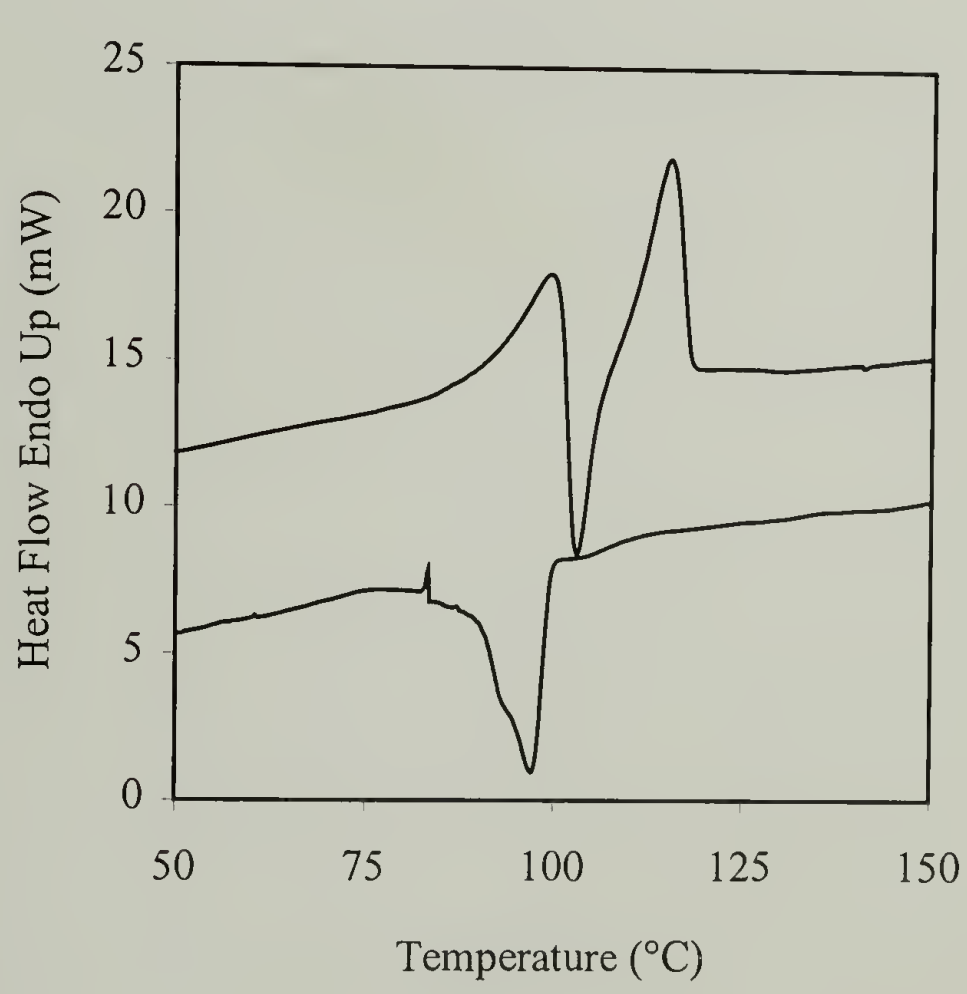

Figure 5.10. DSC Thermogram of the 29(2S+O),6-Polyurethane.

5.3.4.3 Crystal Structure

The WAXS patterns of the melt-crystallized, aliphatic and heteroatom-containing m,6-polyurethanes are summarized in Table 5.4. The polymers all displayed a strong intensity at *d*-spacings of 4.6 and 3.7 Å and a variable intensity at a *d*-spacing of 4.2 Å (Figure 5.11). This diffraction pattern was identical to the patterns observed for the corresponding aliphatic m,n-polyurethanes (see Section 4.3.1). This implied that although the heteroatoms influenced the melting temperature of the polyurethanes, the hydrogen-bonds still controlled the crystallization behavior. It also implied that the decrease in T_m was not the result of a change in crystal structure/packing.

Table 5.4. WAXS Results for the Long-Chain m,n-Polyurethanes.

m,n-Polymer	WAXS Pattern (Å)
purely aliphatic[a]	4.7 to 4.5, 4.2 to 4.1, 3.8 to 3.7
29(2S),6	4.6, 4.2, 3.7
29(2S+O),6	4.6, 4.2, 3.7
32(2S+2O),6	4.6, 4.2, 3.7

a) See Chapter 4.

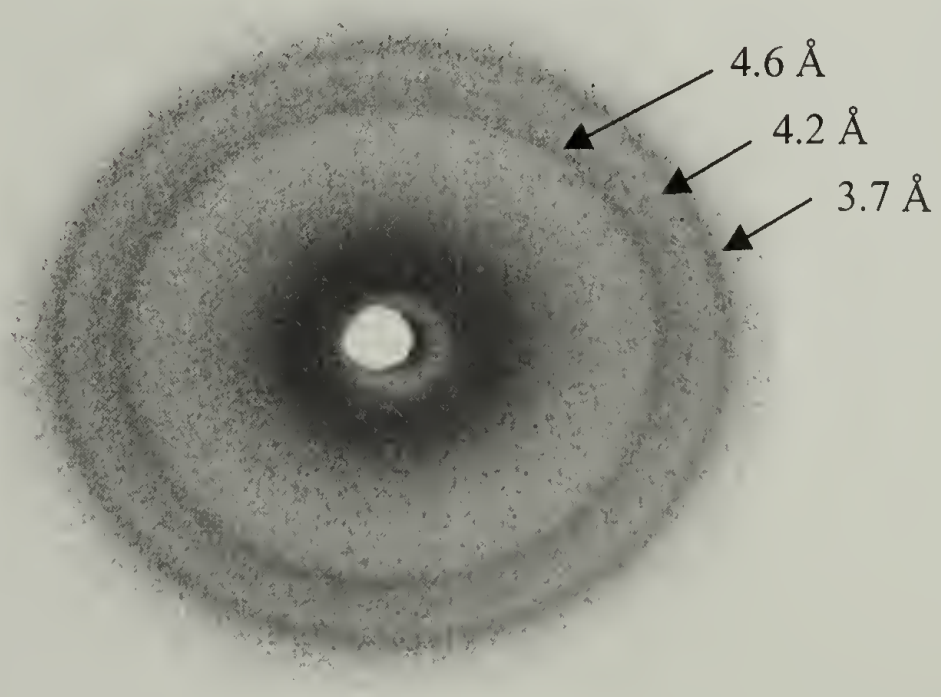

Figure 5.11. WAXS Pattern of the Melt-Crystallized 29(2S),6-Polyurethane.

5.4 Conclusions

Several long-chain, heteroatom-containing α,ω-diols were synthesized in both high yield and purity by a one-step, free-radical telomerization of an excess of 10-undecene-1-ol with commercially available α,ω-dithiols. By altering the α,ω-dithiols used, the number and type of heteroatom could be altered. Examination of the thermal properties of the heteroatom-containing, telechelic diols showed that when compared to the corresponding aliphatic, long-chain diols, the heteroatoms induced a decrease in the T_m and enthalpy of the diols, but not in the T_d. These monodisperse diols had better thermal properties than the polydisperse, macromonomers currently used in industry.

These long-chain, heteroatom-containing diols were used to synthesize a series of m,6-polyurethanes by step polyadditions in the melt of equimolar ratios of the telechelic diols and 1,6-diisocyanatohexane. By systematically increasing the amount and type of heteroatoms, the influence of the heteroatoms on the thermal properties of the m,6-polyurethanes was examined. The resulting polyurethanes each contained 2 sulfur atoms per repeat and from 0 to 2 oxygen atoms per repeat. None of these heteroatom-containing polyurethanes had been previously synthesized.

Characterization of the heteroatom-containing polyurethanes showed that the polymers had molecular weights and PDI values typical of step-growth polymers. The long-chain, heteroatom-containing m,6-polyurethanes had both lower T_m and enthalpy values than the corresponding aliphatic, long-chain polyurethanes. In the case of the odd-even 29(2S),6- and 29(2S+O),6-polyurethanes, this thermal behavior could be the result of the heteroatoms. However, it could also be due to the fact that they were being compared to even-even polyurethanes. In the case of the even-even 32(2S+2O),6-

polyurethane, this thermal behavior was clearly the result of the heteroatoms. Unlike the melting properties, the T_d and crystal structure of all of the heteroatom-containing polyurethanes remained unaltered by the addition of the heteroatoms.

5.5 References

(1) Cho, I.; Lee, K. *Macromol. Chem. Phys.* **1997**, *198*, 861.

(2) Le Fevere de Ten Hove, C.; Jonas, A.; Penelle, J. *Polym. Prepr. (Am. Chem. Soc. Div. Polym. Chem.)* **1998**, *39*, 156.

(3) Penelle, J.; Le Fevere de Ten Hove, C.; Schall, J.; Jonas, A.; Hu, W.; Schmidt-Rohr, K.; Waddon, A. J. *Polym. Prepr. (Am. Chem. Soc. Div. Polym. Chem.)* **1999**, *40*, 617.

(4) Ehrenstein, M.; Dellsperger, S.; Kocher, C.; Stutzmann, N.; Weder, C.; Smith, P. *Polymer* **2000**, *41*, 3531.

(5) Osakada, K.; Takenaka, Y.; Yamaguchi, I.; Yamamoto, T. *Bull. Chem. Soc. Jpn.* **1998**, *71*, 1477.

(6) Hill, R.; Walker, E. E. *J. Polym. Sci.* **1948**, *3*, 609.

(7) Le Fevere de Ten Hove, C. Controlling Solid-State Microstructure of Semi-Crystalline Polymers Through Chemical Design of Chains: A Study of Model Polyesters. Ph.D. Thesis, Université Catholique de Louvain, Louvain-la-Neuve, 2001.

(8) Améduri, B.; Berrada, K.; Boutevin, B.; Bowden, R. D. *Polym. Bull. (Berlin)* **1992**, *28*, 389.

(9) Améduri, B.; Berrada, K.; Boutevin, B.; Bowden, R. D. *Polym. Bull. (Berlin)* **1992**, *28*, 497.

(10) Singh, H.; Hutt, J. W.; Williams, M. E. Eur. Pat. Appl. 81,305,695.9, 1981.

(11) Boutevin, B.; Elidrissi, A.; Parisi, J. P. *Makromol. Chem.* **1990**, *191*, 445.

(12) Nuyken, O.; Völker, T. *Makromol. Chem.* **1990**, *191*, 2465.

(13) Améduri, B.; Berrada, K.; Boutevin, B.; Bowden, R. D. *Phosphorus, Sulfur Silicon Relat. Elem.* **1993**, *74*, 477.

(14) Améduri, B.; Berrada, K.; Boutevin, B.; Melas, M.; Bowden, R. D. *Makromol. Chem.* **1993**, *194*, 3001.

(15) Améduri, B.; Berrada, K.; Boutevin, B.; Bowden, R. D. *Phosphorus, Sulfur Silicon Relat. Elem.* **1993**, *83*, 39.

(16) Améduri, B.; Khamlichi, M.; Robin, J. J.; Elidrissi, A.; Ramdani, A. *Phosphorus, Sulfur Silicon Relat. Elem.* **1993**, *82*, 109.

(17) Améduri, B.; Boutevin, B.; Khamlichi, M.; Robin, J. J.; Elidrissi, A.; Ramdani, A. *Macromol. Chem. Phys.* **1994**, *195*, 3425.

(18) Cahours; Hoffman *Ann.* **1857**, *102*, 291.

(19) Posner, T. *Ber. Dtsch. Chem. Ges.* **1905**, *38*, 646.

(20) Nuyken, O.; Hofinger, M. *Polym. Bull. (Berlin)* **1981**, *4*, 343.

(21) Silverstein, R. M.; Webster, F. X. *Spectrometric Identification of Organic Compounds*; 6th ed.; John Wiley & Sons: New York, 1998.

(22) Sugeta, H.; Go, A.; Miyazawa, T. *Chem. Lett.* **1972**, 83.

(23) Okabayashi, H.; Izawa, K.; Yamamoto, T.; Masuda, H.; Nishio, E.; O'Conner, C. J. *Colloid Polym. Sci.* **2002**, *280*, 135.

(24) Ogawa, Y.; Nakamura, N. *Bull. Chem. Soc. Jpn.* **1999**, *72*, 943.

(25) Guth, E.; James, H. M.; Mark, H. *Advances in Colloid Science*; Interscience: New York, 1946; Vol. II.

(26) Kobayashi, H.; Nakamura, N. *Cryst. Res. Technol.* **1995**, *30*, 495.

(27) Polyurethanes. In *Polymer Synthesis*; 2 ed.; Sandler, S. T., Karo, W., Eds.; Academic: San Diego, 1994; Vol. 1, p 232.

(28) Parodi, F. Isocyanate-Derived Polymers. In *Comprehensive Polymer Science*; Allen, G., Bevington, J. C., Eds.; Pergamon: Oxford, 1989; Vol. 5, p 387.

(29) Allcock, H. A.; Lampe, F. W. *Contemporary Polymer Chemistry*; 2nd ed.; Prentice Hall: New Jersey, 1990.

(30) Odian, G. *Principles of Polymerization*; 3rd ed.; John Wiley & Sons: New York, 1991.

(31) Mandelkern, L.; Alamo, R. G. Polyethylene, Linear High-Density. In *Polymer Data Handbook*; Mark, J. E., Ed.; Oxford University: New York, 1999; p 493.

(32) Prasad, A. Polyethylene, Linear Low-Density. In *Polymer Data Handbook*; Mark, J. E., Ed.; Oxford University: New York, 1999; p 508.

(33) MacKnight, W. J.; Yang, M.; Kajiyama, T. *Polym. Prepr. (Am. Chem. Soc. Div. Polym. Chem.)* **1968**, *9*, 860.

(34) Wunderlich, B. *Crystal Melting*; Academic: New York, 1980; Vol. 3.

CHAPTER 6. CHEMICAL ENGINEERING OF THE CRYSTAL THICKNESS

6.1 Introduction

Chemical engineering of the lamellar thickness of the long-chain, aliphatic m,n-polyurethanes was desired in order to produce polyethylene-like crystals containing hydrogen-bonds at the crystal surface (Figure 6.1). The thickness of these crystals would then depend on the length of the α,ω-diols used in the polymerization and would be independent of the crystallization conditions (e.g. temperature, time, and solvent). This chemical engineering of the crystal thickness is a unique alternative to conventional post-polymerization methods (e.g. annealing and stretching) used to increase the lamellar thickness. In contrast to the post-polymerization methods, the chemical engineering method proposed here would produce an exact and uniform lamellar thickness. This thickness could then be tunable by altering the length of the α,ω-diols employed in the polymerization.

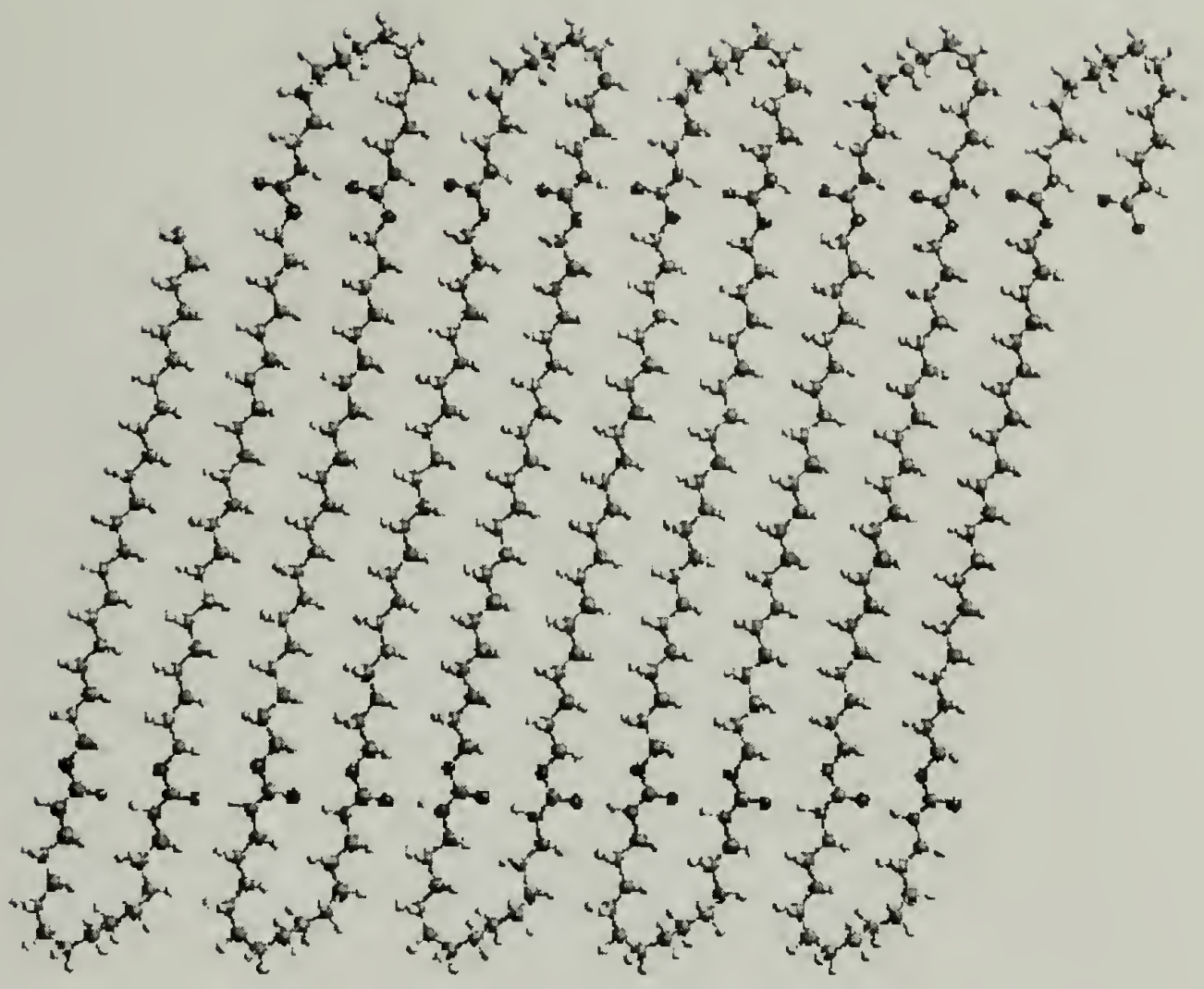

Figure 6.1. Desired Chain-Folding of the 22,12-Polyurethane.

To achieve these crystals, the carbamate esters have to be intramolecularly hydrogen-bonded, and the aliphatic segment from the diol has to be long enough to crystallize (see Section 2.1). Initial work has focused on taking advantage of the periodicity of the hydrogen-bonds alongside the backbone of the long-chain m,n-polyurethanes. If in the melt or solution, intramolecular hydrogen-bonding dominated, the hydrogen-bonds would form cyclics of 5 + n atoms, where n represents the number of methylene units originating from the diisocyanate. These cyclics should help pre-organize the folding of the m,n-polyurethanes before the polymers crystallized, resulting in chemical control of the lamellar thickness. The organization of the aliphatic stems of the diols (with the aid of Dr. D. Padowitz from Amherst College) and the resulting m,n-

polyurethanes (in collaboration with Amy Heintz under the supervision of Dr. S. L. Hsu) were examined to evaluate how successful the attempts at controlled chain-folding really were.

6.2 Experimental

6.2.1 Characterization

^{1}H-NMR spectra were obtained in either deuterated DMSO-d_6 or $CDCl_3$ from a Bruker 300 MHz NMR spectrometer at room temperature. Melting points were observed using a Perkin Elmer Pyris DSC flushed with helium. The 5 to 10 mg samples were heated above their melting point, cooled to room temperature, and then reheated, all at a rate of 10 K·min^{-1}. The first heating and cooling run was performed in order to erase the different thermal histories present in the samples. The melting points were taken as the peak of the melting endotherm during the second heating run. The temperature was calibrated using indium and eicosane.

6.2.2 Sample Preparation

The synthesis of the long-chain, aliphatic m,n-polyurethanes [O-$(CH_2)_m$-O-C(O)-NH-$(CH_2)_n$-NH-C(O)]$_n$ was discussed in Chapter 3. Melt-crystallized samples were prepared by heating the polymers to 200 °C and then allowing the polymers to cool to room temperature at a rate of 10 K·min^{-1}.

6.2.3 Spectroscopy

A Bruker FRA 106 spectrometer equipped with a Nd:Yag laser (1.064 μm) was used to record the FT Raman spectra. A total of 256 scans were performed, and spectral resolution was 4 cm^{-1}. The laser power was 150 mW, and the excitation/collection geometry was 180°.

6.2.4 Microscopy

A Digital Instruments Nanoscope E scanning tunneling microscope (STM) was used to image the individual atoms of the long-chain α,ω-diols. Mechanically cut Pt-10% Ir tips were employed. Typical tunneling conditions were +1.0 V and 500 pA current. Images were planefit but not filtered and were current (constant height) mode. The graphite substrates were ZYH grade supplied by Advanced Ceramics Corporation.

In order to differentiate the amorphous and crystalline regions of the polymers, the prepared polymer samples were stained using a 2% solution of ruthenium (III) chloride hydrate in sodium hypochlorite. The ruthenium oxide-stained samples were then microtomed at room temperature into 40 nm slices using a Leica ULTRACUT UCT Universal Ultramicrotome. The microtomed samples were deposited onto copper grids and dried in a vacuum oven at room temperature. The TEM images were recorded at room temperature using a JEOL 100 CX TEM operating at 100 kV. The magnification was calibrated using a crossed lined grating replica with 2160 lines per mm.

6.2.5 X-ray Scattering

X-ray scattering patterns, in the low-angle range, were obtained at room temperature using Ni-filtered Cu Kα radiation of wavelength 1.542 Å from a Rigaku rotating anode operating at 40 kV and 200 mA. A point-collimated 300 μm diameter beam was used, and the X-ray scattering patterns were recorded using an evacuated GADDS 2-dimensional area detector. SAXS experiments were also performed on the Advanced Polymers Beamline (X27C) at the National Synchrotron Light Source, Brookhaven National Laboratory, Upton, New York. The camera length was calibrated using an Ag-B_0 standard (d = 63.02 Å). The X-ray beam had a 3 mm^2 area and a wavelength of 1.307 Å. Custom software was used to subtract the background, circularly average the data, and convert the data to a logarithmic intensity scale.

6.2.6 Monomer Synthesis

6.2.6.1 General Considerations

Reagents used in the synthesis of the diisocyanate were obtained commercially, and unless otherwise stated, they were used without further purification. Butyraldehyde was distilled immediately before use.

6.2.6.2 Synthesis of 3-*n*-Propylglutaric Acid by Condensation Followed by Hydrolysis

α,α'-Dicyano-β-propylglutaramide (30). Cyanoacetamide (25.22 g, 0.30 mol) was stirred in deionized water (180 mL) for 3 hours during which time the cyanoacetamide completely dissolved. Butyraldehyde (10.80 g, 0.15 mol) and an

aqueous solution of potassium hydroxide (50%, 0.3 mL) were then added. A white precipitate formed almost immediately. After 3 more hours of stirring, the sample was filtered. The white solid was ground with dilute hydrochloric acid (3%, 100 mL) and then washed with deionized water. Recrystallization from a mixture (1:1 volume ratio) of ethanol (200 mL) and benzene (200 mL) yielded α,α'-dicyano-β-propylglutaramide (**30**) as a white solid (27.83 g, 75%); m.p. 162.0 °C, lit.: 136 °C.[1] ^{1}H-NMR (300 MHz, DMSO-d_6) δ 7.89 and 7.65 (s, 4H, NH_2), 3.90 (d, J = 6.7, 2H, N=C-CHR-C(O)), 2.77 (m, 1H, CHR$_3$), 1.36 (m, 4H, CH_3-CH_2-CH_2-CH), 0.84 (m, 3H, CH_3-CH_2).

3-*n*-Propylglutaric Acid (31). α,α'-Dicyano-β-propylglutaramide (**30**) (5.06 g, 0.02 mol), concentrated hydrochloric acid (14 mL), and deionized water (20 mL) were mixed together and then refluxed for 12 hours. After cooling, diethyl ether (20 mL) was added, and the organic phase was extracted. Evaporation of the diethyl ether yielded 3-*n*-propylglutaric acid (**31**) as a white solid (3.48 g, 92%); m.p. 48.0 °C, lit.: 52-54 °C,[2] 52 °C,[1] 52 °C,[3] 50 °C.[4] ^{1}H-NMR (300 MHz, DMSO-d_6) δ 2.20 (bs, 4H, CH_2-CO_2H), 1.25 (m, 5H, CH_3-CH_2-CH_2-CH-R$_2$), 0.84 (t, J = 6.6 Hz, 3H, CH_3-CH_2).

6.2.6.3 Synthesis of 1,1-Dimethylisocyanatobutane via a Curtius Rearrangement

3-*n*-Propylglutaric Acid Dimethyl Ester (32). 3-*n*-Propylglutaric acid (6.96 g, 0.04 mol), ethanol (150 mL), and concentrated sulfuric acid (5 mL) were combined and then refluxed for 16 hours. After cooling the mixture, benzene (300 mL) and deionized water (600 mL) were added. The two phases were then separated. The aqueous layer was extracted with benzene (6 x 50 mL aliquots) and then ether (6 x 50 mL aliquots). The combined organic phases were evaporated yielding 3-*n*-propylglutaric acid dimethyl

ester (**32**) as a clear liquid (8.29 g, 90%). ^{1}H-NMR (300 MHz, $CDCl_3$) δ 4.11 (q, J = Hz, 4H, CH_2-O_2C), 2.32 (bs, 4H, CH_2-CO_2), 1.35-1.21 (m, 11H, CH_2-CH_2-CH and CH_3-CH_2-CO_2), 0.88 (m, 3H, CH_3-CH_2-CH_2).

3-*n*-Propylglutaric Dihydrazide (33). 3-*n*-Propylglutaric acid dimethyl ester (**32**) (8.29 g, 0.04 mol), hydrazine monohydrate (6 mL), ethanol (95%, 70 mL), and deionized water (10 mL) were combined and then refluxed for 72 hours. Unlike the suberic diazide (see Section 4.3.5.2), the resulting product did not crystallize upon cooling. The solvent was evaporated leaving a yellowish-orange solid. ^{1}H-NMR analysis indicated that there were trace amounts of both starting material and the desired product 3-*n*-propylglutaric dihydrazide (**33**). However, the majority of the product did not dissolve in any common, organic solvent and was believed to be some type of cyclic side product.

6.3 Results and Discussion

6.3.1 Chain-Folding

6.3.1.1 Overview of Controlled Chain-Folding

In the early 1970s, it was first reported that hydrogen-bonding constricts the lamellar thickness of polyamides to multiples of the repeat unit.[5-7] Since then, several research groups have attempted to control the lamellar thickness of other polymers with varying degrees of success. Bioengineering has proven a successful technique for controlling the lamellar thickness of several polypeptides.[8-10] Other interactions, besides

hydrogen-bonding, have also been proposed as ways to force chain-folds. Hessel and Ringsdorf[11] used mesogeneous interactions in polymers containing hydrophilic pyridinum head groups connected to stiff aromatic cores by hydrophobic spacers. Lokey and Iverson[12] made "aedamers" or pleated polymers whose chain-folding was dictated by the *a*romatic *e*lectron *d*onor/*a*cceptor interactions. Steric hindrance was employed by Lindsay et al.[13] to make accordion-like polymers where the flexible groups containing long side branches were forced into the amorphous regions and the rigid chromophores formed the crystalline regions. Going one step further, Magagnini and co-workers[14] used even longer side branches that were able to themselves crystallize to try to force comb-like polyesters to fold. Meta-substituted aromatic rings were employed by both Weissbuch et al.[15] and Schmidt et al.[16] to form chain-folds.

6.3.1.2 Attempt at Chain-Folding Using Intramolecular Hydrogen-Bonding

Typically, long-chain, aliphatic sequences of 20 or more methylene groups can form self-assembled monolayers (SAMs).[17] The aliphatic and heteroatom-containing α,ω-diols used in the synthesis of the long-chain m,n-polyurethanes in this study contained long (CH_2) segments that should under the right conditions be able to self-organize into layered structures. STM images (Figure 6.2) of the heteroatom-containing 1,29(2S)-diol HO-$(CH_2)_{11}$-S-$(CH_2)_5$-S-$(CH_2)_{11}$-OH clearly showed that the aliphatic chains align parallel to each other. In these images, the sulfur atoms are lighter than the methylene groups, while the oxygen atoms are darker than the methylene groups.[18,19] The organization of the aliphatic segments is the first step in creating polymers with a chemically engineered lamellar thickness.

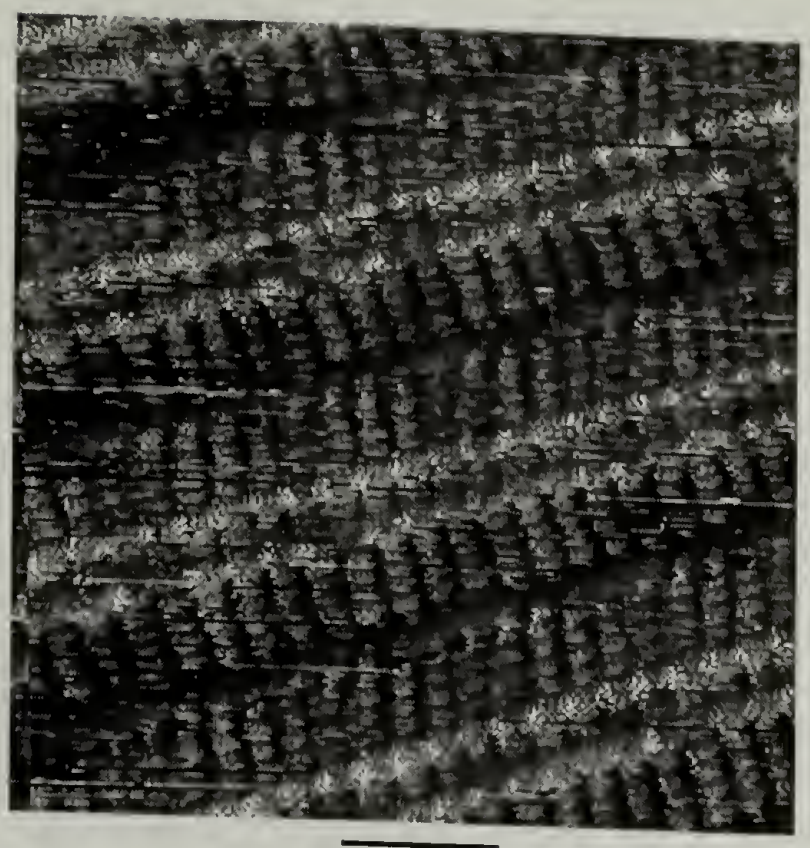

2 nm

(a)

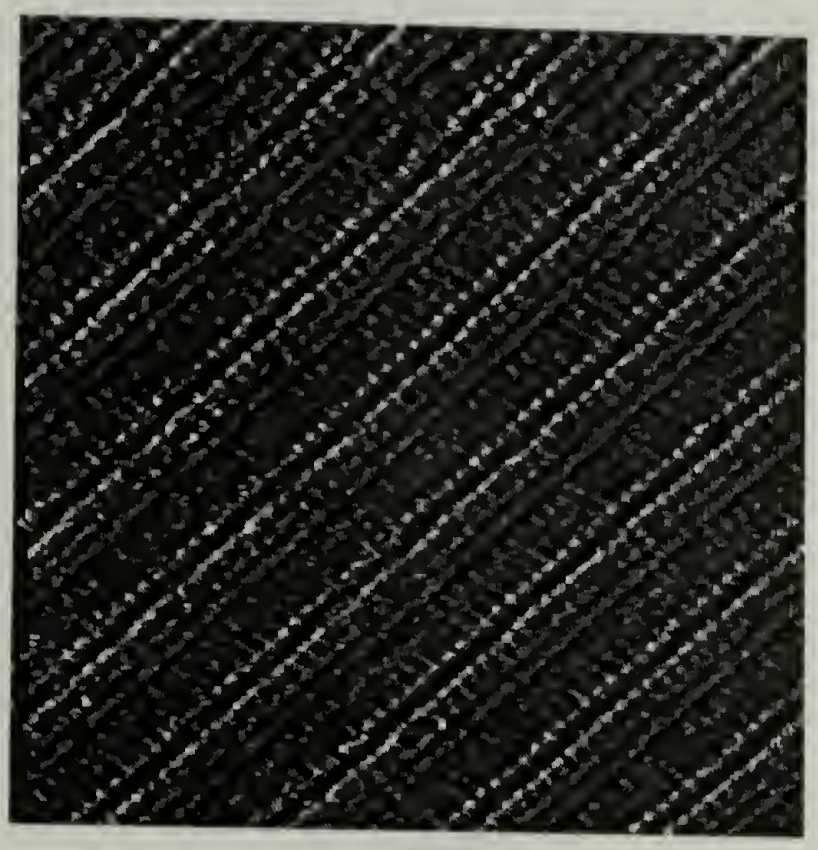

4 nm

(b)

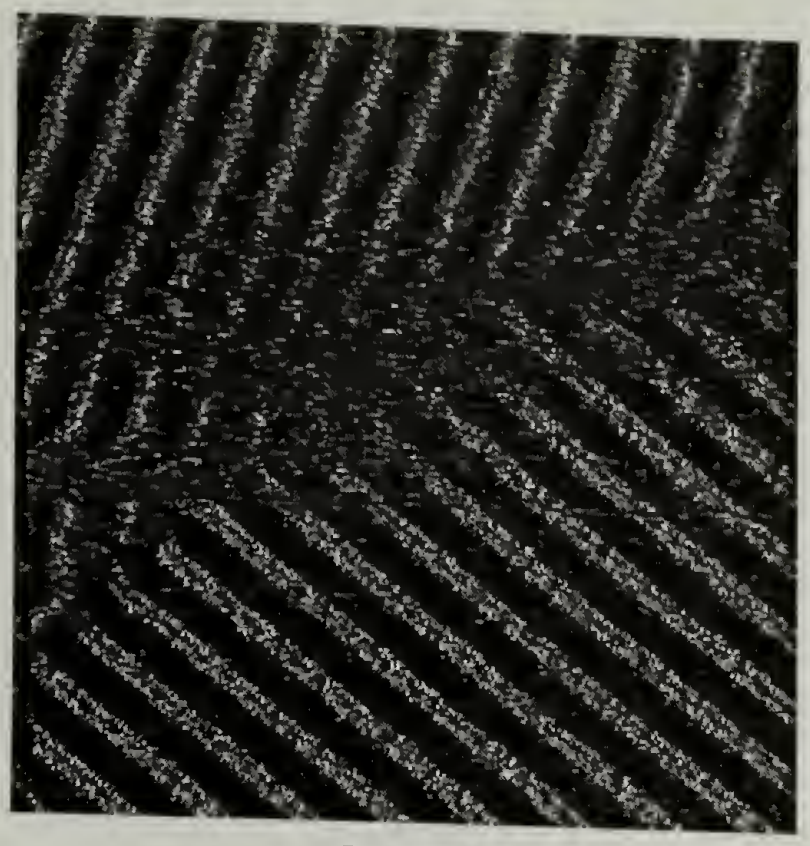

(c)

Figure 6.2. STM Images of the 1,29(2S)-Diol: (a) 10 nm, (b) 20 nm, and (c) 50 nm.

However, the LSP values (Table 6.1) as determined by SAXS (see Section 3.3.2.4) of the melt-crystallized, long-chain m,n-polyurethanes were much larger than the theoretical values, indicating that the desired chain-folding did not occur. The theoretical values were derived assuming adjacent re-entry chain-folding of all *trans* chains (109° bond angle) with bond lengths of C-C = 1.54 Å, C-N = 1.47 Å, and C-O = 1.43 Å.[20] It is important to note that the SAXS results reflect the length of the tilted chain, and they correlate to the length of the crystalline and amorphous regions combined. If certain experimental values (sample thickness, beam area, etc.) are known, a complicated mathematical treatment can be employed to derive the thickness of the crystal and amorphous regions separately (although the researcher must arbitrarily decide which value corresponds to each region).[21,22]

Table 6.1. Experimental and Theoretical LSP of the Melt-Crystallized, Long-Chain m,n-Polyurethanes.

m,n-Polymer	Observed LSP (Å)	Theoretical Long Period (Å)
12,4	104	27.0
12,6	108	29.5
12,8	119	32.0
12,12	134	37.0
22,4	149	39.5
22,6	102	42.0
22,8	136	44.5
22,12	139	49.5
32,4	182	52.0
32,6	137	54.5
32,8	130	57.0
32,12	131	62.0
46,6	130	72.0

In order to determine the length of the straight, crystalline chain length (and not the crystalline and amorphous length), TEM was employed. As discussed in Chapter 3, the TEM images of ruthenium oxide-stained, melt-crystallized 22,n-polyurethanes gave LSP values (crystalline and amorphous length) of ~ 100 to 150 Å, which was consistent with that found using SAXS. The stain preferentially complexed with the amorphous regions (thus making them darker in the TEM) and allowed for the visualization of the lamellar morphology of the polymers. Measurement of the lighter, crystalline regions gave straight, crystalline chain lengths of ~ 30 to 70 Å. However, these values are only approximate values as the staining technique is not perfect. Depending on the thickness of the sample and on the staining time, the stain may not have penetrated to all the amorphous regions (giving too high a value) or may have also complexed with the crystalline regions (giving too low a value).

In an attempt to more accurately determine the length of the straight crystalline chain length, low frequency (5 to 200 cm^{-1}) Raman spectroscopy was used to try and locate longitudinal acoustic (or accordion) modes (LAMs). LAMs are the result of longitudinal vibrations associated with the length of the entire extended chain. The LAM frequency ν can be related to the straight chain length L by Equation 6.1 where m = mode order, c = speed of light, E = elastic modulus, and ρ = single chain density.[23]

$$\nu_m = (m/2cL)\cdot(E/\rho)^{-1/2} \qquad \text{(Eq. 6.1)}$$

LAMs were first observed in *n*-paraffins in 1949 by Mizushima and Shimanouchi.[24] Since then, LAMs have been experimentally found for several polyethylene-like polymers including: polytetrafluoroethylene,[25] isotactic polypropylene,[26,27] poly(oxymethylene),[27] poly(ethylene oxide),[28,29] and several linear, aliphatic polyesters.[30-33] However, LAMs have never been experimentally found in polymers containing hydrogen-bonds such as polypeptides.[34,35] It is believed that hydrogen-bonds perturb the chains affecting both the intensity and frequency of the LAMs. To date, no LAMs have been found using low frequency Raman spectroscopy for the m,n-polyurethanes in this study.

6.3.2 Monomer Synthesis

6.3.2.1 Overview of Synthetic Methods

Diisocyanates with a stronger driving force (e.g. sterically hindered branches or 1,3-disubstituted cyclics) to form chain-folds than just hydrogen-bonding were desired. Le Fevere de Ten Hove[22] showed that propyl branches could not be accommodated into the crystalline regions of long-chain, aliphatic polyesters. It was desired to see if branched diisocyanates would likewise be excluded from the crystalline regions of the long-chain m,n-polyurethanes.

The synthesis of 1,1-dimethylisocyanatobutane $CH_3CH_2CH_2CH(CH_2\text{-}N{=}C{=}O)_2$ has not been reported in the literature. In theory, it should be possible to synthesize this branched diisocyanate from the corresponding acid (3-*n*-propylglutaric acid $CH_3CH_2CH_2CH(CH_2\text{-}CO_2H)_2$) via the general diisocyanate synthetic methods discussed in Chapter 4. Although the synthesis of 1,3-diisocyanatopropane $O{=}C{=}N\text{-}(CH_2)_3\text{-}N{=}C{=}O$ (the non-branched equivalent of 1,1-dimethylisocyanatobutane) has been reported in the literature,[36-40] the global yield and purity of the short-chain diisocyanate are typically low. In general, the synthesis and purification of 1,3-diisocyanates are hampered by the formation of stable, cyclic urea byproducts.[40-42]

Until very recently, 3-*n*-propylglutaric acid was commercially available from Lancaster. Since Lancaster stopped selling the branched diacid, there has been no commercial source for the diacid. However, there are several multi-step, literature methods discussing the synthesis of 3-*n*-propylglutaric acid in global yields ranging from very low to quantitative. Most of the early work[43,44] resulted in a mixture of products that

required conversion to the corresponding anhydride for purification reasons. However, in 1920, Day and Thorpe[1] published a procedure for the synthesis of pure 3-*n*-propylglutaric acid via the condensation of cyanoacetamide and butyraldehyde followed by hydrolysis. Boots et al.[45] reported a modification of this procedure where the cyanoacetamide was replaced with diethyl propylmalonate. I. G. Farbenindustrie[46] patented an alternative procedure in 1952 based on the hydrolysis of the corresponding dinitrile. Modifications of this procedure have also been reported.[2,47]

6.3.2.2 Attempted Synthesis of 1,1-Dimethylisocyanatobutane

3-*n*-Propylglutaric acid (**31**) was synthesized by the method originally proposed by Day and Thorpe[1] (Scheme 6.1). Using this method, α,α'-dicyano-β-propylglutaramide (**30**) $CH_3CH_2CH_2CH(CH(C{\equiv}N)\text{-}C(O)NH_2)_2$ was synthesized from the base-catalyzed condensation of butyraldehyde $CH_3CH_2CH_2\text{-}C(O)H$ and cyanoacetamide $N{\equiv}C\text{-}CH_2\text{-}C(O)NH_2$. Acid-catalyzed hydrolysis of the dicyano-propylglutaramide produced 3-*n*-propylglutaric acid (**31**) in a global yield of 69%.

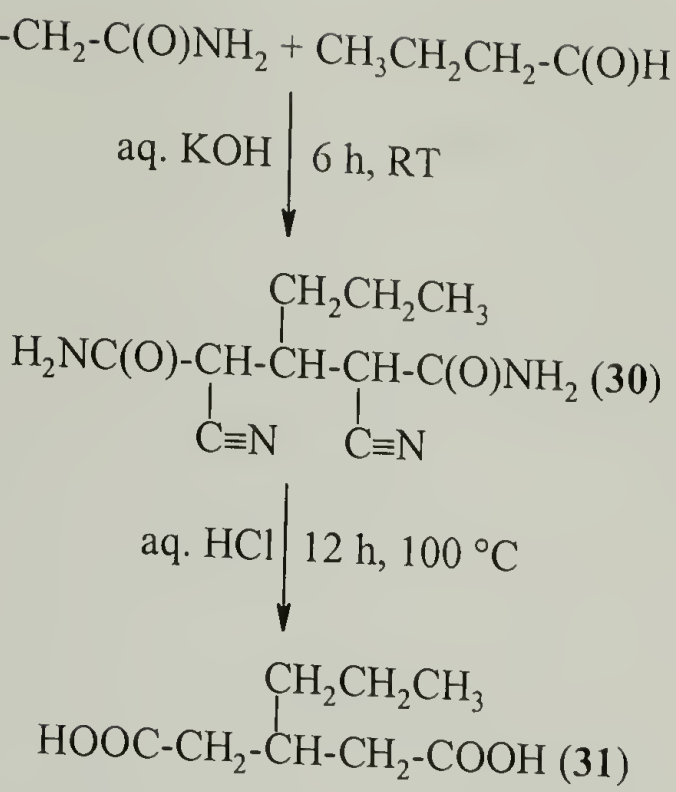

Scheme 6.1. Synthesis of 3-*n*-Propylglutaric Acid (**31**).

The synthesis of 1,1-dimethylisocyanatobutane (**34**) was attempted using the multi-step Curtius rearrangement of 3-*n*-propylglutaric acid. 3-*n*-Propylglutaric acid (**31**) was esterified under acidic conditions to the branched diethylester (**32**) $CH_3CH_2CH_2CH(CH_2\text{-}CO_2CH_2CH_3)_2$. The diester was then treated with hydrazine monohydrate in an attempt to synthesize the branched dihydrazide (**33**) $CH_3CH_2CH_2CH(CH_2\text{-}C(O)NHNH_2)_2$. Although a trace amount of 3-*n*-propylglutaric dihydrazide was synthesized, the majority of the product was a yellowish-orange solid that did not dissolve in any common, organic solvents. It is believed that this solid was some sort of cyclic byproduct.

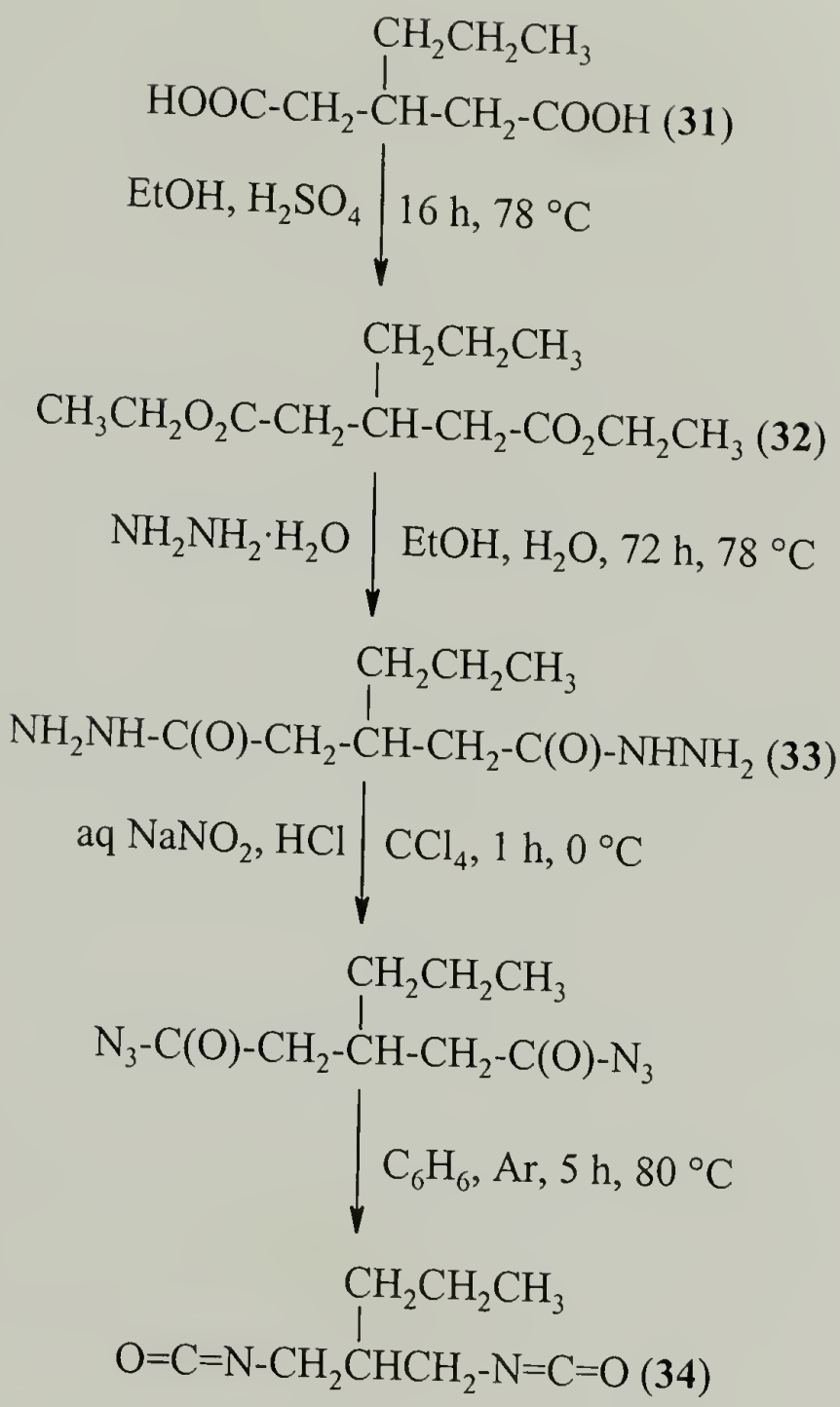

Scheme 6.2. Synthesis of 1,1-Dimethylisocyanatobutane (**34**) from the Corresponding Branched Diacid via a Curtius Rearrangement.

6.4 Conclusions

Attempts to chemically engineer the lamellar thickness of the long-chain m,n-polyurethanes are ongoing. STM showed that the long-chain α,ω-diols used to synthesize the polymers could self-organize to form layered structures consisting of the aliphatic chains aligned parallel to each other. However, the LSP values of the resulting m,n-polyurethanes as determined by SAXS were much larger than the theoretical values,

indicating that the chain-folding was not controlled. This failure could be the result of several factors including too short an aliphatic length, the existence of intermolecular hydrogen-bonding, or that intramolecular hydrogen-bonding was not a strong enough driving force.

The LSP values determined by SAXS included the length of the crystalline and amorphous regions. Mathematical treatments to determine the individual lengths of each region are underway. In an attempt to determine the straight chain length of the crystalline region, TEM imaging on ruthenium oxide-stained samples was performed. However, the staining method is imprecise, and the values obtained are only an approximation. In order to obtain more precise values, low-frequency Raman spectroscopy was used to try to locate LAMs. However, most probably as a result of the interference caused by the hydrogen-bonds to the intensity and frequency of the LAMs, to date no LAMs have been experimentally detected.

Chain-folding of the m,n-polyurethanes should be controllable by factors (e.g. sterics and mimicking of the fold) other than hydrogen-bonding. Due to the successful results with branched polyesters reported by Le Fevere de Ten Hove,[22] it was decided to use branches that should not be able to be accommodated into the crystalline regions. The synthesis of 3-*n*-propylglutaric acid was accomplished in high yield. However, the Curtius rearrangement of this branched diacid to the corresponding diisocyanate did not prove successful due to the formation of cyclic side products.

6.5 References

(1) Day, J. N. E.; Thorpe, J. F. *J. Chem. Soc.* **1920**, *117*, 1465.

(2) Irwin, A. J.; Lok, K. P.; Huang, K. W.-C.; Jones, J. B. *J. Chem. Soc. Perkin Trans. 1* **1978**, 1636.

(3) Jeffery; Vogel *J. Chem. Soc.* **1939**, *117*, 1471.

(4) Gaudemar-Bardone, F.; Gaudemar, M. *Bull. Soc. Chim. Fr.* **1968**, *7*, 3065.

(5) Dreyfuss, P.; Keller, A.; Willmouth, F. M. *J. Polym. Sci., Part A: Polym. Chem.* **1972**, *10*, 857.

(6) Atkins, E. D. T.; Keller, A.; Sadler, D. M. *J. Polym. Sci., Part A: Polym. Chem.* **1972**, *10*, 863.

(7) Burmester, A. F.; Dreyfuss, P.; Geil, P. H.; Keller, A. *J. Polym. Sci., Polym. Lett. Ed.* **1972**, *10*, 769.

(8) McGrath, K. P.; Fournier, M. J.; Mason, T. L.; Tirrell, D. A. *J. Am. Chem. Soc.* **1992**, *114*, 727.

(9) Wang, J.; Parkhe, A. D.; Tirrell, D. A.; Thompson, L. K. *Macromolecules* **1996**, *29*, 1548.

(10) Winningham, M. J.; Sogah, D. Y. *Polym. Mater. Sci. Eng.* **1997**, *76*, 156.

(11) Hessel, V.; Ringsdorf, H. *Makromol. Chem., Rapid Commun.* **1993**, *14*, 707.

(12) Lokey, R. S.; Iverson, B. L. *Nature* **1995**, *375*, 303.

(13) Lindsay, G. A.; Stenger-Smith, J. D.; Henry, R. A.; Hoover, J. M.; Nissan, R. A. *Macromolecules* **1992**, *25*, 6075.

(14) Magagnini, P. L.; Tassi, E. L.; Andruzzi, F.; Paci, M. *Polym. Sci.* **1994**, *36*, 1502.

(15) Weissbuch, I.; Lahav, M.; Leiserowitz, L.; Lederer, K.; Godt, A.; Wegner, G.; Howes, P. B.; Kjaer, K.; Als-Nielsen, J. *J. Phys. Chem.* **1998**, *102*, 6313.

(16) Schmidt, R.; Decher, G.; Muller, P.; Mésini, P. *Polym. Mater. Sci. Eng.* **1999**, *80*, 93.

(17) Ulman, A. *Chem. Rev.* **1996**, *96*, 1533.

(18) Padowitz, D. F.; Messmore, B. W. *J. Phys. Chem. B* **2000**, *104*, 9943.

(19) Padowitz, D. F.; Sada, D. M.; Kemer, E. L.; Dougan, M. L.; Xue, W. A. *J. Phys. Chem. B* **2002**, *106*, 593.

(20) Allen, F. H.; Kennard, O.; Watsun, D. G.; Brammer, L.; Orpen, A. G.; Taylor, R. *J. Chem. Soc. Perkin Trans. 2* **1987**, S1.

(21) Goderis, B.; Reynaers, H.; J., K. M. H.; Mathot, V. B. F. *J. Polym. Sci., Part B: Polym. Phys.* **1999**, *37*, 1715.

(22) Le Fevere de Ten Hove, C. Controlling Solid-State Microstructure of Semi-Crystalline Polymers Through Chemical Design of Chains: A Study of Model Polyesters. Ph.D. Thesis, Université Catholique de Louvain, Louvain-la-Neuve, 2001.

(23) Hsu, S. L.; Ford, G. W.; Krimm, S. *J. Polym. Sci., Part B: Polym. Phys.* **1977**, *15*, 1769.

(24) Mizushima, S. I.; Shimanouchi, T. *J. Am. Chem. Soc.* **1949**, *71*, 1320.

(25) Rabolt, J. F.; Fanconi, B. *Polymer* **1977**, *18*, 1258.

(26) Hsu, S. L.; Krimm, S.; Krause, S.; Yeh, G. S. Y. *J. Polym. Sci., Polym. Lett. Ed.* **1976**, *14*, 195.

(27) Rabolt, J. F.; Fanconi, B. *J. Polym. Sci., Polym. Lett. Ed.* **1977**, *15*, 121.

(28) Hartley, A.; Leung, Y. K.; Booth, C.; Shepherd, I. W. *Polymer* **1976**, *17*, 354.

(29) Song, K.; Krimm, S. *J. Polym. Sci., Part B: Polym. Phys.* **1990**, *28*, 63.

(30) Folkes, M. J.; Keller, A.; Stejny, J.; Goggin, P. L.; Fraser, G. V.; Hendra, P. J. *Colloid Polym. Sci.* **1975**, *253*, 354.

(31) Wang, Y. K.; Shu, P. H. C.; Stein, R. S.; Hsu, S. L. *J. Polym. Sci., Part B: Polym. Phys.* **1980**, *18*, 2287.

(32) Chang, C.; Wang, Y. K.; Waldman, D. A.; Hsu, S. L. *J. Polym. Sci., Part B: Polym. Phys.* **1984**, *22*, 2185.

(33) Berrill, S. A.; Heatley, F.; Collett, J. H.; Attwood, D.; Booth, C.; Fairclough, J. P. A.; Ryan, A. J.; Viras, K.; Dutton, A. J.; Blundell, R. S. *J. Mater. Chem.* **1999**, *9*, 1059.

(34) Rabolt, J. F. *J. Polym. Sci., Part B: Polym. Phys.* **1979**, *17*, 1457.

(35) Chien, B. T.-W.; Hsu, S. L.; Stidham, H. D. *Macromolecules* **1996**, *29*, 4247.

(36) Siefken, W. *Liebigs Ann. Chem.* **1949**, *562*, 122.

(37) King, C. *J. Am. Chem. Soc.* **1964**, *86*, 437.

(38) Upjohn Company. U.S. Patent 3,410,887, 1965.

(39) Ulrich, H.; Sayigh, A. A. R. *Angew. Chem.* **1966**, *78*, 761.

(40) Peerlings, H. W. I.; Meijer, E. W. *Tetrahedron Lett.* **1999**, *40*, 1021.

(41) Kurita, K.; Matsumura, T.; Iwakura, Y. *J. Org. Chem.* **1976**, *41*, 2670.

(42) Gilman, J. W.; Otonari, Y. A. *Synth. Commun.* **1993**, *23*, 335.

(43) Farmer, E. H.; Mehta, T. N. *J. Chem. Soc.* **1930**, 1610.

(44) Linstead; Noble; Boorman *J. Chem. Soc.* **1933**, 559.

(45) Boots, M. R.; Yeh, Y.-M.; Boots, S. G. *J. Pharm. Sci.* **1980**, *69*, 506.

(46) I. G. Farbenindustrie. German Patent DE 924,386, 1952.

(47) Arnarp, J.; Enzell, C.; Petersson, K.; Pettersson, T. *Acta Chem. Scand., Ser. B* **1986**, *40*, 839.

CHAPTER 7. CONCLUSIONS AND PERSPECTIVES

7.1 Synthesis of Long-Chain, Functionalized, Monodisperse Monomers

Semi-crystalline polymers, which make up the majority (by volume) of commercialized polymers, have physical, thermal, and mechanical properties that are strongly influenced by their crystallization. The crystallization of these polymers depends on both structural variables (e.g. chemical repeat, molecular architecture, and stereochemistry) as well as the crystallization conditions (e.g. cooling rate, melting temperature, pressure, presence of orientation, and additives). To date, disagreements exist in the scientific community over crucial aspects of polymer crystallization models.

In order to help elucidate the relationship between structural variables (e.g. nature, size, distribution, and regularity of functionalities along a polymer backbone), model polymers with functionalities placed at periodic and controlled locations along the backbone would be useful. Step-growth polymerizations (e.g. ADMET polycondensation or polyesterification) of long-chain monomers containing the structural defects (functionality) have been used by other researchers as a means to meet this synthetic objective. However, this polymerization method is currently limited by the aliphatic length of the functionalized monomers used.

This study examined and modified several literature procedures to synthesize a range of long-chain, monodisperse α,ω-diols. 1,22-Docosanediol (**3**) HO-$(CH_2)_{22}$-OH was synthesized by a modified and optimized Wurtz-coupling method in both higher yield (59%) and shorter time (3.5 hours) than literature methods. Difficulties in purification of the resulting diol limited the use of this method in synthesizing even

longer diols. Instead, a modified enamine-coupling procedure originally developed to synthesize long-chain α,ω-diacids was used to prepare 1,32-dotriacontanediol (**9**) HO-$(CH_2)_{32}$-OH and 1,46-hexatetracontanediol (**19**) HO-$(CH_2)_{46}$-OH. Although the purification of these long-chain, aliphatic α,ω-diols was easily achievable, the use of these diols is limited by their extremely low global yields (12 and 1%, respectively). Long-chain, monodisperse α,ω-diols containing heteroatoms were also synthesized and investigated to determine whether they could be used as an affordable alternative to the purely aliphatic, long-chain α,ω-diols. 12,18-Dithianonacosanediol (**26**) HO-$(CH_2)_{11}$-S-$(CH_2)_5$-S-$(CH_2)_{11}$-OH, 12,18-dithia-15-oxanonacosanediol (**27**) HO-$(CH_2)_{11}$-S-$(CH_2)_2$-O-$(CH_2)_2$-S-$(CH_2)_{11}$-OH, and 12,21-dithia-15,18-dioxadotriacontanediol (**28**) HO-$(CH_2)_{11}$-S-$(CH_2)_2$-O-$(CH_2)_2$-O-$(CH_2)_2$-S-$(CH_2)_{11}$-OH were synthesized by a one-step, free-radical telomerization in global yields of > 80%.

7.2 Influence of Hydrogen-Bonding and Heteroatoms on the Physical, Thermal, and Morphological Properties of Long-Chain m,n-Polyurethanes

Step-growth polyadditions of the long-chain, aliphatic α,ω-diols with an equimolar ratio of commercially available, aliphatic α,ω-diisocyanates produced a series of increasingly aliphatic m,n-polyurethanes that had the general structure [O-$(CH_2)_m$-O-C(O)-NH-$(CH_2)_n$-NH-C(O)]$_n$ (**20**). The polymerizations were performed under mild conditions and produced polyurethanes of relatively low polydispersity (PDI ~2) and reasonable molecular weight (~ 3000 to 80,000 g·mol^{-1}). By carefully controlling the polymerization conditions (e.g. presence of water, temperature, and ratio of monomers), side reactions were avoided, and the polyurethanes synthesized were of high purity.

Increasing the length of the α,ω-diol employed decreased the density of hydrogen-bonding in the resulting m,n-polyurethanes. This dilution in hydrogen-bonding density dramatically influenced the physical and thermal properties of the polymers resulting in a polyethylene-like behavior. As the aliphatic length of the polyurethanes was increased, the polymers had decreasing solubility in solvents typically used to break up hydrogen-bonding (e.g. *m*-cresol, DMF, DMSO, formic acid, and sulfuric acid) and increasing solubility in *o*-dichlorobenzene, a solvent typically used to dissolve HDPE. Both the melting temperature and enthalpy of the increasingly aliphatic m,n-polyurethanes approached that of HDPE. The longest polymer, the 46,6-polyurethane, had a melting temperature of 135 °C, which is the approximate value obtained for chain-folded HDPE (133 to 138 °C). Unlike typical polyurethanes of higher hydrogen-bonding density, the m,n-polyurethanes in this study had LSP values of at least 100 Å, a behavior more typical of polyethylene (110 to 140 Å).

However, the crystallization behavior (e.g. crystal structure, morphology, annealing behavior, and kinetics) of the increasingly aliphatic m,n-polyurethanes was not affected by the dilution in hydrogen-bonding density. All of the polyurethanes had triclinic packing (characteristic WAXS reflections at *d*-spacings 4.7 to 4.5 Å (d_{100}) and 3.8 to 3.7 Å (d_{010} and d_{110})) and a varying amount of pseudohexagonal packing (characteristic WAXS reflection at *d*-spacing 4.2 to 4.1 Å (d_{110})) similar to that observed for polyurethanes and polyamides of higher hydrogen-bonding density. As with polyamides, the long-chain polyurethanes had lath-shaped crystals that aggregated to form sheaves. Unlike polyethylene, which can undergo a continuous increase in lamellar thickness under annealing conditions, the polyurethane crystals did not anneal. The

polyurethanes also had percent crystallinity values and hydrogen-bonding strengths typical of polyamides of higher hydrogen-bonding densities.

Heteroatom-containing m,n-polyurethanes of the general structure $[O\text{-}(CH_2)_{11}\text{-}S\text{-}(CH_2)_2\text{-}X\text{-}(CH_2)_2\text{-}S\text{-}(CH_2)_{11}\text{-}O\text{-}C(O)\text{-}NH\text{-}(CH_2)_6\text{-}NH\text{-}C(O)]_n$ (**29**) were also synthesized under equivalent conditions and had PDI values and molecular weights similar to the purely aliphatic polyurethanes. Most probably as a result of the increased flexibility in the polymer chains, the introduction of heteroatoms (oxygen and sulfur) resulted in a decrease in the melting temperatures of ~20 to 40 °C compared to the analogous aliphatic polyurethanes. However, neither the decomposition temperature nor crystal packing was influenced by the heteroatoms.

7.3 Chemical Engineering of the Crystal Thickness

Chemical engineering of the crystal thickness in the m,n-polyurethanes requires that the aliphatic segments are long enough to crystallize, and that the defects (carbamate esters) are not incorporated into the crystalline regions. Based on the melting temperature and self-assembling of *n*-alkanes, the first requirement should be met if the aliphatic segment is at least 20 methylene units long. STM of the long-chain diols synthesized for this study showed that they in fact self-organized to form layered structures.

However, the second requirement appears not to have been met. The lamellar stacking periodicity was much larger than the theoretical length (assuming adjacent re-entry and tight hairpin turns). The experimental evidence indicated that intramolecular hydrogen-bonding did not pre-organize the polymers to form tight hairpin turns.

However, since the LSP values included the length of the crystalline as well as the amorphous regions, it was difficult to get a true picture of the chain-folding. With the low degree of crystallinity, it is possible that the m,n-polyurethanes have crystalline regions of only 1 repeat unit. TEM imaging of the ruthenium oxide-stained samples indicated that the crystalline regions actually contained 1 to 2 repeat units. A more accurate value for the length of the crystalline region was desired. Low-frequency Raman spectroscopy was employed to try to locate the LAMs, which are proportional to the length of the crystalline chain, but to date none have been observed. Instead, a mathematical treatment of the SAXS is underway to determine the length of both the crystalline and amorphous regions.

7.4 Perspectives

Due to the multi-step synthesis and low global yields of the long-chain, aliphatic α,ω-diols, the model polyurethanes synthesized in this study can only be employed for academic purposes (e.g. examination of the crystallization behavior) and not for industrial applications (e.g. use as a blend-compatibilizer for hydrogen-bonded polymer-polyolefin blends). Additionally, due to the low amount of polymer sample available, examination of the mechanical properties with existing technologies is not feasible. This problem could be overcome by eliminating the monodisperse nature of the long-chain α,ω-monomers. Polydisperse, long-chain α,ω-diols can be abstracted from natural products. Additionally, polyethylene can be etched with nitric acid to create polydisperse, long-chain α,ω-diacids, which depending on their solubility could (as in this work) be reduced to the corresponding α,ω-diol. Another possibility is to maintain

the monodisperse nature of the long-chain α,ω-monomers but eliminate the purely aliphatic requirement. The heteroatom-containing α,ω-diols synthesized in this study were inexpensive to make, had better thermal properties than similar, commercially available polydisperse diols (e.g. polytetrahydrofuran), and lowered the melting temperature of the resulting polyurethanes thus making their processing easier.

The aliphatic, long-chain m,n-polyurethanes synthesized and examined in this study provided an excellent opportunity to examine the influence of hydrogen-bonding on the crystallization of polyethylene-like polymers. Other functionalities (e.g. dipole-dipole interactions) could be used. For example, a model LLDPE with perfectly regularly placed methyl branches could be imagined and synthesized by a combination of a polycondensation method such as ADMET and long-chain α,ω-monomers similar to the ones synthesized in this study (in the case of an ADMET chemistry, the long-chain monomers would need to have terminal double bonds and a methyl branch somewhere along its backbone). The importance of the regularity of the backbone functionality could be determined by polymerizing 2 α,ω-diols of different length (e.g. 1,22- and 1,46-diols) with a diisocyanate and comparing the resulting properties with a polyurethane synthesized with the 1,32-diol and the same diisocyanate.

This study unsuccessfully attempted to force chemical turns by using intramolecular hydrogen-bonding. However, other perturbations or defects could be imagined that would create this turn either through the geometry of the specific bond orientations (e.g. cis double bonds or 1,2-disubstituted aromatic or cyclic groups) or by simple sterics that could not be accommodated into the crystalline region (e.g. branching or bulky groups). The synthesis of such α,ω-diisocyanates proved difficult due to the

high reactivity of the isocyanato groups. However, the corresponding α,ω-diamines could be easily synthesized and in some cases are already commercially available. By reacting these diamines in the melt with the long-chain α,ω-diols, long-chain polyamides could be synthesized. Unfortunately, the ease of synthesizing these hydrogen-bonding, polyethylene-like polymers is balanced out by the more difficult task of characterizing these polymers. In particular, the melting temperature of polyamides are considerably higher than that of the corresponding polyurethanes. Even with the decrease in melting temperature with increase in aliphatic length, these polyamides might have a melting temperature higher than the upper use limit of the high-temperature IR spectrometer, making the examination of the crystallization process impossible by this technique. Perhaps through a combination of the commercial availability of α,ω-diamines containing different perturbations and the lower melting temperatures of the heteroatom-containing, long-chain α,ω-diols, long-chain polyethylene-like polymers containing hydrogen-bonds could be synthesized (in gram amounts rather than the current milligram amounts). These polyamides could then be used for academic purposes (e.g. to examine the influence of hydrogen-bonds on crystallization) as well as for commercial applications (e.g. as a compatibilizer for blends of polyethylene and polyamides).

Bibliography

Adams, K. R.; Bonnett, R. *Phytochemistry* **1971**, *10*, 1885.

Alamo, R. G.; Chan, E. K. M.; Mandelkern, L. *Macromolecules* **1993**, *26*, 5740.

Allcock, H. A.; Lampe, F. W. *Contemporary Polymer Chemistry*; 2nd ed.; Prentice Hall: New Jersey, 1990.

Allen, F. H.; Kennard, O.; Watsun, D. G.; Brammer, L.; Orpen, A. G.; Taylor, R. *J. Chem. Soc. Perkin Trans. 2* **1987**, S1.

Allen, J.; Drewitt, J. G. *Chem. Abstr.* **1948**, *42*, 4603h.

Améduri, B.; Berrada, K.; Boutevin, B.; Bowden, R. D. *Phosphorus, Sulfur Silicon Relat. Elem.* **1993**, *74*, 477.

Améduri, B.; Berrada, K.; Boutevin, B.; Bowden, R. D. *Phosphorus, Sulfur Silicon Relat. Elem.* **1993**, *83*, 39.

Améduri, B.; Berrada, K.; Boutevin, B.; Bowden, R. D. *Polym. Bull. (Berlin)* **1992**, *28*, 389.

Améduri, B.; Berrada, K.; Boutevin, B.; Bowden, R. D. *Polym. Bull. (Berlin)* **1992**, *28*, 497.

Améduri, B.; Berrada, K.; Boutevin, B.; Melas, M.; Bowden, R. D. *Makromol. Chem.* **1993**, *194*, 3001.

Améduri, B.; Boutevin, B.; Khamlichi, M.; Robin, J. J.; Elidrissi, A.; Ramdani, A. *Macromol. Chem. Phys.* **1994**, *195*, 3425.

Améduri, B.; Khamlichi, M.; Robin, J. J.; Elidrissi, A.; Ramdani, A. *Phosphorus, Sulfur Silicon Relat. Elem.* **1993**, *82*, 109.

Armistead, K.; Goldbeck-Wood, G.; Keller, A. *Adv. Polym. Sci.* **1992**, *100*, 219.

Arnarp, J.; Enzell, C.; Petersson, K.; Pettersson, T. *Acta Chem. Scand., Ser. B* **1986**, *40*, 839.

Atkins, E. D. T.; Hill, M.; Hong, S. K.; Keller, A.; Organ, S. *Macromolecules* **1992**, *25*, 917.

Atkins, E. D. T.; Keller, A.; Sadler, D. M. *J. Polym. Sci., Part A: Polym. Chem.* **1972**, *10*, 863.

Austin, P. W.; Seshadri, T. R.; Sood, M. S. *Indian J. Chem.* **1969**, *7*, 43.

Bamford, C. H.; Dyson, R. W.; Eastmond, G. C. *Polymer* **1969**, *10*, 885.

Bamford, C. H.; Eastmond, G. C.; Whittles, D. *Polymer* **1969**, *10*, 771.

Barham, P. J. Crystallization and Morphology of Semicrystalline Polymers. In *Materials Science and Technology: Structure and Properties of Polymers*; Thomas, E. L., Ed.; John Wiley & Sons: New York, 1993; Vol. 12.

BASF. German Patent DE 801,993, 1948.

Bassett, D. C.; Block, S.; Piermarina, S. *Jpn. J. Appl. Phys.* **1974**, *45*, 4146.

Bayer, O. *Angew. Chem.* **1947**, *59 A*, 275.

Bayer, O.; Rinke, H.; Siefken, W.; Orthner, L.; Schild, H. German Patent DE 728,981, 1942.

Beletskaya, I. P.; Artamkina, G. A.; Reutov, O. A. *Russ. Chem. Rev. (Engl. Transl.)* **1976**, *45*, 330.

Berrill, S. A.; Heatley, F.; Collett, J. H.; Attwood, D.; Booth, C.; Fairclough, J. P. A.; Ryan, A. J.; Viras, K.; Dutton, A. J.; Blundell, R. S. *J. Mater. Chem.* **1999**, *9*, 1059.

Bierer, D. E.; Gerber, R. E.; Jolad, S. D.; Ubillas, R. P.; Randle, J.; Nauka, E.; Latour, J.; Dener, J. M.; Fort, D. M.; Kuo, J. E.; Inman, W. D.; Dubenko, L. G.; Ayala, F.; Ozioko, A.; Obialor, C.; Elisabetsky, E.; Carlson, T.; Truong, T.; C., B. R. *J. Org. Chem.* **1995**, *60*, 7022.

Blackwell, J.; Gardner, K. H. *Polymer* **1979**, *20*, 13.

Blackwell, J.; Ross, M. *J. Polym. Sci., Polym. Lett. Ed.* **1979**, *17*, 447.

Bloch, D. R. Solvents and Non Solvents for Polymers. In *Polymer Handbook*; 4th ed.; Brandrup, J., Immergut, E. H., Grulke, E. A., Eds.; John Wiley & Sons: New York, 1999.

Boerio, F. J.; Koenig, J. L. *J. Chem. Phys.* **1970**, *52*, 3425.

Boldyrev, V. V. *J. Chim. Phys.* **1986**, *83*, 821.

Boots, M. R.; Yeh, Y.-M.; Boots, S. G. *J. Pharm. Sci.* **1980**, *69*, 506.

Borchert, W. Z. *Angew. Chem.* **1951**, *63*, 31.

Born, L.; Crone, J.; Hespe, H.; Müller, E. H.; Wolf, K. H. *J. Polym. Sci., Part B: Polym. Phys.* **1984**, *22*, 63.

Boutevin, B.; Elidrissi, A.; Parisi, J. P. *Makromol. Chem.* **1990**, *191*, 445.

Bower, D. I.; Maddams, W. F. *The Vibrational Spectroscopy of Polymers*; Cambridge University: Cambridge, 1989.

Brill, R. *Z. Phys. Chem. (Munich)* **1943**, *1353*, 61.

Broadhurst, M. G. *J. Res. Natl. Bur. Stand., Sect. A.* **1962**, *66*, 241.

Brooke, G. M.; Burnett, S.; Mohammed, S.; Proctor, D.; Whiting, M. C. *J. Chem. Soc. Perkin Trans. 1* **1996**, 1635.

Brzezinska, K. R.; Wagener, K. B. *Macromolecules* **1992**, *25*, 2049.

Buchta, E.; Huhn, C. *Liebigs Ann. Chem.* **1966**, *695*, 42.

Bunn, C. W.; Alcock, T. C. *Trans. Faraday Soc.* **1945**, *41*, 317.

Bunn, C. W.; Garner, E. V. *Proc. Roy. Soc. (London), Part A* **1947**, *189*, 39.

Bunn, C. W. *Trans. Faraday Soc.* **1939**, *35*, 482.

Burk Jr., E. H.; Carlos, D. D. U.S. Patent 3,423,449, 1969.

Burmester, A. F.; Dreyfuss, P.; Geil, P. H.; Keller, A. *J. Polym. Sci., Polym. Lett. Ed.* **1972**, *10*, 769.

Buysch, H.; Hünig, S. *Angew. Chem.* **1966**, *78*, 145.

Cahours; Hoffman *Ann.* **1857**, *102*, 291.

Champetier, G.; Aélion, R. *Bull. Soc. Chim. Fr.* **1948**, 683.

Chang, C.; Wang, Y. K.; Waldman, D. A.; Hsu, S. L. *J. Polym. Sci., Part B: Polym. Phys.* **1984**, *22*, 2185.

Cheng, S. Z. D.; Wunderlich, B. *J. Polym. Sci., Part B: Polym. Phys.* **1986**, *24*, 557.

Cheng, S. Z. D.; Wunderlich, B. *J. Polym. Sci., Part B: Polym. Phys.* **1986**, *24*, 595.

Chien, B. T.-W.; Hsu, S. L.; Stidham, H. D. *Macromolecules* **1996**, *29*, 4247.

Cho, I.; Lee, K. *Macromol. Chem. Phys.* **1997**, *198*, 861.

Chuit, P. *Helv. Chim. Acta* **1926**, *12*, 264.

Chum, S. P.; Knight, G. W.; Ruiz, J. M.; Phillips, P. J. *Macromolecules* **1994**, *27*, 656.

Culbertson, B. M.; Sedor, E. A.; Slagel, R. C. *Macromolecules* **1968**, *1*, 254.

Damle, S. B. *Chem. Eng. News* **1993**, 4.

Day, J. N. E.; Thorpe, J. F. *J. Chem. Soc.* **1920**, *117*, 1465.

Dictionary of Natural Products; 1st ed.; Buckingham, J., Ed.; Chapman & Hall: London, 1994.

Dieter Jr., J. A.; Kutts, H. W.; Wolgenuth, L. B. U.S. Patent 3,531,425, 1970.

DiMarzio, E. A.; Guttman, C. M. *J. Appl. Phys.* **1982**, *53*, 6581.

Downing, D. T.; Kranz, Z. H.; Murray, K. E. *Aust. J. Chem.* **1961**, *14*, 619.

Drake, N. L.; Carhart, H. W.; Mozingo, R. *J. Am. Chem. Soc.* **1941**, *63*, 617.

Dreyfuss, P. *J. Polym. Sci., Polym. Phys. Ed.* **1973**, *11*, 201.

Dreyfuss, P.; Keller, A. *J. Macromol. Sci., Phys.* **1970**, *4*, 811.

Dreyfuss, P.; Keller, A. *J. Polym. Sci., Part B: Polym. Phys.* **1970**, *8*, 253.

Dreyfuss, P.; Keller, A.; Willmouth, F. M. *J. Polym. Sci., Part A: Polym. Chem.* **1972**, *10*, 857.

Duhamel, L. *Ann. Chim. (Paris)* **1963**, *8*, 315.

DuPont de Nemours & Co. U.S. Patent 2,374,340, 1940.

Ehrenstein, M.; Dellsperger, S.; Kocher, C.; Stutzmann, N.; Weder, C.; Smith, P. *Polymer* **2000**, *41*, 3531.

Einhorn, C.; Einhorn, J.; Luche, J. *Synthesis* **1989**, *11*, 787.

Fakirov, S.; Fischer, E. W.; Hoffmann, R.; Schmidt, G. F. *Polymer* **1977**, *18*, 1121.

Farlow *Org. Synth.* **1951**, *31*, 63.

Farmer, E. H.; Mehta, T. N. *J. Chem. Soc.* **1930**, 1610.

Fischer, E. W.; Fakirov, S. *J. Mater. Sci.* **1976**, *11*, 1041.

Flory, P. J. *J. Am. Chem. Soc.* **1962**, *84*, 2858.

Flory, P. J.; Vrij, A. *J. Am. Chem. Soc.* **1963**, *85*, 3548.

Folkes, M. J.; Keller, A.; Stejny, J.; Goggin, P. L.; Fraser, G. V.; Hendra, P. J. *Colloid Polym. Sci.* **1975**, *253*, 354.

Franco, L.; Cooper, S. J.; Atkins, E. D. T.; Hill, M. J.; Jones, N. A. *J. Polym. Sci., Part B: Polym. Phys.* **1998**, *36*, 1153.

Frisch, K. C.; Klempner, D. K. Polyurethanes. In *Comprehensive Polymer Science*; Pergamon: Oxford, 1989; Vol. 5, p 413.

Fuller, C. S. *Chem. Rev.* **1940**, *26*, 143.

Fuller, C. S.; Frosch, C. J. *J. Am. Chem. Soc.* **1939**, *61*, 2575.

Furukawa, A.; Shoji, H.; Nakaya, T.; Imoto, M. *Makromol. Chem.* **1987**, *188*, 265.

Gaudemar-Bardone, F.; Gaudemar, M. *Bull. Soc. Chim. Fr.* **1968**, *7*, 3065.

Gen. Aniline & Film Corp. U.S. Patent 2,847,440, 1956.

Gerum, W.; Hohne, G. W. H.; Wilke, W.; Arnold, M.; Wegner, T. *Macromol. Chem. Phys.* **1995**, *196*, 3797.

Gilman, J. W.; Otonari, Y. A. *Synth. Commun.* **1993**, *23*, 335.

Goderis, B.; Reynaers, H.; J., K. M. H.; Mathot, V. B. F. *J. Polym. Sci., Part B: Polym. Phys.* **1999**, *37*, 1715.

Goodrich Co. U.S. Patent 2,642,449, 1953.

Grechishnikova, I. V.; Johansson, L. B.-Å.; Molotkovsky, J. G. *Chem. Phys. Lipids* **1996**, *81*, 87.

Guth, E.; James, H. M.; Mark, H. *Advances in Colloid Science*; Interscience: New York, 1946; Vol. II.

Han, B. H.; Boudjouk, P. *Tetrahedron Lett.* **1981**, *22*, 2757.

Hartley, A.; Leung, Y. K.; Booth, C.; Shepherd, I. W. *Polymer* **1976**, *17*, 354.

Hellmuth; Wunderlich, B. *J. Appl. Phys.* **1965**, *36*, 3039.

Hentschel, W. *Ber.* **1884**, *17*, 1284.

Hessel, V.; Ringsdorf, H. *Makromol. Chem., Rapid Commun.* **1993**, *14*, 707.

Hill, R.; Walker, E. E. *J. Polym. Sci.* **1948**, *3*, 609.

Hinrichsen, G. *Makromol. Chem.* **1973**, *166*, 291.

Hoffman, J. D.; Guttman, C. M.; DiMarzio, E. A. *Discuss. Faraday Soc.* **1979**, *68*, 177.

Hoffman, J. D.; Miller, R. L. *Macromolecules* **1989**, *21*, 3038.

Hoffman, J. D. *Polymer* **1983**, *24*, 3.

Hoffman, J. D.; Weeks, J. J. *J. Chem. Phys.* **1965**, *42*, 4301.

Hollingsworth, M. D. *Chem. Eng. News* **1992**, *70*, 4.

Hsu, S. L.; Ford, G. W.; Krimm, S. *J. Polym. Sci., Part B: Polym. Phys.* **1977**, *15*, 1769.

Hsu, S. L.; Krimm, S.; Krause, S.; Yeh, G. S. Y. *J. Polym. Sci., Polym. Lett. Ed.* **1976**, *14*, 195.

Hünig, S.; Buysch, H. *Chem. Ber.* **1967**, *100*, 4017.

I. G. Farbenindustrie. German Patent DE 844,896, 1944.

I. G. Farbenindustrie. German Patent DE 870,097, 1942.

I. G. Farbenindustrie. German Patent DE 924,386, 1952.

I. G. Farbenindustrie. German Patent DE 947,471, 1956.

Imp. Chem. Ind. U.S. Patent 2,379,948, 1943.

Irwin, A. J.; Lok, K. P.; Huang, K. W.-C.; Jones, J. B. *J. Chem. Soc. Perkin Trans. 1* **1978**, 1636.

Israelachvili, J. N. *Intermolecular and Surface Forces*; 2nd ed.; Academic: New York, 1992.

Jeffery; Vogel *J. Chem. Soc.* **1939**, *117*, 1471.

Jones, A. T. *J. Polym. Sci.* **1962**, *62*, 553.

Jones, N. A.; Atkins, E. D. T.; Hill, M. J.; Cooper, S. J.; Franco, L. *Macromolecules* **1996**, *29*, 6011.

Jones, N. A.; Atkins, E. D. T.; Hill, M. J.; Cooper, S. J.; Franco, L. *Macromolecules* **1997**, *30*, 3569.

Keller, A. *Philos. Mag.* **1957**, *2*, 1171.

Keller, A. *Rep. Prog. Phys.* **1968**, *31*, 623.

Khoury, F.; Passaglia, E. In *Treatise on Solid State Chemistry*; Hannay, N. B., Ed.; Plenum: New York, 1976; Vol. 3.

Kimura, K.; Takahashi, M.; Tanaka, A. *Chem. Pharm. Bull.* **1960**, *8*, 1059.

King, C. *J. Am. Chem. Soc.* **1964**, *86*, 437.

Kinoshita, Y. *Makromol. Chem.* **1959**, *33*, 21.

Kirrmann, A.; Duhamel, L. *Hebd. Seances Acad. Sci.* **1962**, *254*, 1303.

Kobayashi, H.; Nakamura, N. *Cryst. Res. Technol.* **1995**, *30*, 495.

Kolattukudy, P. E.; Agrawal, V. P. *Lipids* **1974**, *9*, 682.

Kurita, K.; Matsumura, T.; Iwakura, Y. *J. Org. Chem.* **1976**, *41*, 2670.

Lash, T. D.; Berry, D. *J. Chem. Educ.* **1985**, *62*, 85.

Lauritzen, J. I.; Hoffman, J. D. *J. Appl. Phys.* **1973**, *44*, 4340.

Lauritzen, J. I.; Hoffman, J. D. *J. Res. Natl. Bur. Stand., Sect. A.* **1960**, *64*, 73.

Lee, K.-S.; Wagner, G.; Hsu, S. L. *Polymer* **1987**, *28*, 889.

Le Fevere de Ten Hove, C. Controlling Solid-State Microstructure of Semi-Crystalline Polymers Through Chemical Design of Chains: A Study of Model Polyesters. Ph.D. Thesis, Université Catholique de Louvain, Louvain-la-Neuve, 2001.

Le Fevere de Ten Hove, C.; Jonas, A.; Penelle, J. *Polym. Prepr. (Am. Chem. Soc. Div. Polym. Chem.)* **1998**, *39*, 156.

Lesiak, T.; Seyda, K. *J. Prakt. Chem.* **1979**, *321*, 161.

Lewis, H. F.; Tryon, M. *J. Chem. Educ.*, *7*, 2712.

Lindsay, G. A.; Stenger-Smith, J. D.; Henry, R. A.; Hoover, J. M.; Nissan, R. A. *Macromolecules* **1992**, *25*, 6075.

Linstead; Noble; Boorman *J. Chem. Soc.* **1933**, 559.

Lokey, R. S.; Iverson, B. L. *Nature* **1995**, *375*, 303.

Lotz, B. *Eur. Phys. J. E* **2000**, *3*, 185.

Loudon, G. M. *Organic Chemistry*; 2nd ed.; Benjamin/Cummings: Menlo Park, 1988.

Lukes, R.; Havlickova, L.; Dudek, V. *Collect. Czech. Chem. Commun.* **1961**, *26*, 1719.

MacKnight, W. J.; Yang, M.; Kajiyama, T. *Polym. Prepr. (Am. Chem. Soc. Div. Polym. Chem.)* **1968**, *9*, 860.

Magagnini, P. L.; Tassi, E. L.; Andruzzi, F.; Paci, M. *Polym. Sci.* **1994**, *36*, 1502.

Magill, J. H.; Girolamo, M.; Keller, A. *Polymer* **1981**, *22*, 43.

Maglio, G.; Marchetta, C.; Botta, A.; Palumbo, R.; Pracella, M. *Eur. Polym. J.* **1979**, *15*, 695.

Mandelkern, L.; Alamo, R. G. Polyethylene, Linear High-Density. In *Polymer Data Handbook*; Mark, J. E., Ed.; Oxford University: New York, 1999; p 493.

Mandelkern, L. In *Physical Properties of Polymers*; Mark, J. E., Ed.; American Chemical Society: Washington, D. C., 1984.

Mansfield, M. L. *Polym. Commun.* **1990**, *31*, 283.

Mansfield, M. L. *Polymer* **1988**, *29*, 1755.

Mashio, F.; Nomachi, T. *Kogyo Kagaku Zasshi* **1953**, *56*, 289.

Mason, T. J.; Luche, J. L. Ultrasound as a New Tool for Synthetic Chemists. In *Chemistry Under Extreme or Non-Classical Conditions*; van Eldik, R., Hubbard, C. D., Eds.; John Wiley & Sons: New York, 1997.

Mayer, A.; Magne, H.; Plantefol, L. *Compt. Rend.* **1921**, *172*, 136.

Mazliak, P. *Phytochemistry* **1962**, *1*, 79.

McGrath, K. P.; Fournier, M. J.; Mason, T. L.; Tirrell, D. A. *J. Am. Chem. Soc.* **1992**, *114*, 727.

Menges, G. University of Massachusetts, Amherst. Unpublished work, 2002.

Miller, R. L. Crystallographic Data and Melting Points for Various Polymers. In *Polymer Handbook*; 4th ed.; Brandrup, J., Immergut, E. H., Grulke, E. A., Eds.; John Wiley & Sons: New York, 1999.

Miyaki, Y.; Ozaki, S.; Hirata, Y. *J. Polym. Sci., Part A: Polym. Chem.* **1969**, *7*, 899.

Mizushima, S. I.; Shimanouchi, T. *J. Am. Chem. Soc.* **1949**, *71*, 1320.

Morton, A. A.; Davidson, J. B.; Best, R. J. *J. Am. Chem. Soc.* **1942**, *64*, 2239.

Moss, R. A.; Fujita, T.; Okumura, Y. *Langmuir* **1991**, *7*, 2415.

Murray, K. E.; Schoenfeld, R. *Aust. J. Chem.* **1955**, *8*, 432.

Murray, K. E.; Schoenfeld, R. *Aust. J. Chem.* **1955**, *8*, 437.

Musgrave, O. C.; Stark, J.; Spring, F. S. *J. Chem. Soc.* **1952**, 4393.

Muthukumar, M. *Eur. Phys. J. E* **2000**, *3*, 199.

Nakajima, A.; Hamada, F. *Kolloid Z. Z. Polym.* **1965**, *205*, 55.

Navarro, E.; Aleman, C.; Subirana, J. A.; Puiggali, J. *Macromolecules* **1996**, *29*, 5406.

Navarro, E.; Franco, L.; Subirana, J. A.; Puiggali, J. *Macromolecules* **1996**, *28*, 8742.

Nuyken, O.; Hofinger, M. *Polym. Bull. (Berlin)* **1981**, *4*, 343.

Nuyken, O.; Völker, T. *Makromol. Chem.* **1990**, *191*, 2465.

Nylon Plastics Handbook; Kohan, M. I., Ed.; Hanser: Munich, 1995.

Odian, G. *Principles of Polymerization*; 3rd ed.; John Wiley & Sons: New York, 1991.

O'Gara, J. E.; Portmess, J. D.; Wagener, K. B. *Macromolecules* **1993**, *26*, 2837.

Ogawa, Y.; Nakamura, N. *Bull. Chem. Soc. Jpn.* **1999**, *72*, 943.

Okabayashi, H.; Izawa, K.; Yamamoto, T.; Masuda, H.; Nishio, E.; O'Conner, C. J. *Colloid Polym. Sci.* **2002**, *280*, 135.

Osakada, K.; Takenaka, Y.; Yamaguchi, I.; Yamamoto, T. *Bull. Chem. Soc. Jpn.* **1998**, *71*, 1477.

Ozaki, S. *Chem. Rev.* **1972**, *72*, 457.

Padowitz, D. F.; Messmore, B. W. *J. Phys. Chem. B* **2000**, *104*, 9943.

Padowitz, D. F.; Sada, D. M.; Kemer, E. L.; Dougan, M. L.; Xue, W. A. *J. Phys. Chem. B* **2002**, *106*, 593.

Parodi, F. Isocyanate-Derived Polymers. In *Comprehensive Polymer Science*; Allen, G., Bevington, J. C., Eds.; Pergamon: Oxford, 1989; Vol. 5, p 387.

Patil, R.; Reneker, D. H. *Polymer* **1994**, *35*, 1909.

Patwardhan, S. A. *Org. Prep. Proced. Int.* **1994**, *26*, 645.

Peerlings, H. W. I.; Meijer, E. W. *Tetrahedron Lett.* **1999**, *40*, 1021.

Penelle, J.; Le Fevere de Ten Hove, C.; Schall, J.; Jonas, A.; Hu, W.; Schmidt-Rohr, K.; Waddon, A. J. *Polym. Prepr. (Am. Chem. Soc. Div. Polym. Chem.)* **1999**, *40*, 617.

Pestman, J. M.; Engberts, J. B. F. N.; de Jong, F. *Recl. Trav. Chim. Pays-Bas* **1994**, *113*, 533.

Point, J. J. *Discuss. Faraday Soc.* **1978**, *68*.

Point, J. J.; Kovacs, A. J. *Macromolecules* **1980**, *13*, 399.

Point, J. J. *Macromolecules* **1979**, *12*, 770.

Polyurethanes. In *Polymer Synthesis*; 2 ed.; Sandler, S. T., Karo, W., Eds.; Academic: San Diego, 1994; Vol. 1, p 232.

Popovitz-Biro, R.; Majewski, J.; Margulis, L.; Cohen, S.; Leiserowitz, L.; Lahav, M. *J. Phys. Chem.* **1994**, *98*, 4970.

Posner, T. *Ber. Dtsch. Chem. Ges.* **1905**, *38*, 646.

Prasad, A. Polyethylene, Linear Low-Density. In *Polymer Data Handbook*; Mark, J. E., Ed.; Oxford University: New York, 1999; p 508.

Prasad, A. Polyethylene, Low-Density. In *Polymer Data Handbook*; Mark, J. E., Ed.; Oxford University: New York, 1999; p 518.

Prasad, A. Polyethylene, Metallocene Linear Low-Density. In *Polymer Data Handbook*; Mark, J. E., Ed.; Oxford University: New York, 1999; p 529.

Price, G. J. Applications of High Intensity Ultrasound in Polymer Chemistry. In *Chemistry Under Extreme or Non-Classical Conditions*; van Eldik, R., Hubbard, C. D., Eds.; John Wiley & Sons: New York, 1997.

Puiggali, J.; Aceituno, J. E.; Navarro, E.; Campos, J. L.; Subirana, J. A. *Macromolecules* **1996**, *29*.

Quirk, R. P.; Alsamarraie, M. A. A. Physical Constants of Polyethylene. In *Polymer Handbook*; 3rd ed.; Brandrup, J., Immergut, E. H., Eds.; John Wiley & Sons: New York, 1989.

Rabolt, J. F.; Fanconi, B. *J. Polym. Sci., Polym. Lett. Ed.* **1977**, *15*, 121.

Rabolt, J. F.; Fanconi, B. *Polymer* **1977**, *18*, 1258.

Rabolt, J. F. *J. Polym. Sci., Part B: Polym. Phys.* **1979**, *17*, 1457.

Ramesh, C.; Keller, A.; Eltink, S. J. E. A. *Polymer* **1994**, *35*, 2483.

Rinke, H.; Schlid, H.; Siefken, W. U.S. Patent 2,511,544, 1950.

Rusanova, E. E.; Sebyakin, Y. L.; Volkova, L. V.; Evstigneeva, R. P. *Zh. Org. Khim. (Engl. Transl.)* **1984**, *20*, 279.

Saito, Y.; Hara, K.; Kinoshita, S. *Polym. J. (Tokyo)* **1982**, *14*, 19.

Saito, Y.; Nansai, S.; Kinoshita, S. *Polym. J. (Tokyo)* **1972**, *3*, 113.

Saotome, K.; Komoto, H. *J. Polym. Sci., Part A: Polym. Chem.* **1967**, *5*, 119.

Saotome, K.; Komoto, H.; Yamazaki, T. *Bull. Chem. Soc. Jpn.* **1966**, *39*, 480.

Schall, J. D. Condensation Polymers with Regularly-Spaced, Strongly-Segregating Functionalities. Ph.D. Thesis, University of Massachusetts, Amherst, 2001.

Schill, G.; Bechmann, W.; Vetter, W. *Chem. Ber.* **1980**, *113*, 941.

Schill, G.; Merkel, C. *Chem. Ber.* **1978**, *111*, 1446.

Schmidt, F. *Chem. Ber.* **1922**, *55*, 1584.

Schmidt, R.; Decher, G.; Muller, P.; Mésini, P. *Polym. Mater. Sci. Eng.* **1999**, *80*, 93.

Schneider, J. P.; Kelly, J. W. *Chem. Rev.* **1995**, *95*, 2169.

Schultz, J. M.; Scott, R. D. *J. Polym. Sci., Part A: Polym. Chem.* **1969**, *7*, 659.

Seto, T.; Hara, T.; Tanaka, T. *Jpn. J. Appl. Phys.* **1968**, *7*, 31.

Siefken, W. *Liebigs Ann. Chem.* **1949**, *562*, 122.

Signer, R.; Sprecher, P. *Helv. Chim. Acta* **1947**, *30*, 1001.

Sigurdsson, S. T.; Seeger, B.; Kutzke, U.; Eckstein, F. *J. Org. Chem.* **1996**, *61*, 3883.

Sikorski, P.; Atkins, E. D. T. *Macromolecules* **2001**, *34*, 4788.

Silverstein, R. M.; Webster, F. X. *Spectrometric Identification of Organic Compounds*; 6th ed.; John Wiley & Sons: New York, 1998.

Singh, H.; Hutt, J. W.; Williams, M. E. Eur. Pat. Appl. 81,305,695.9, 1981.

Skrovanek, D. J.; Painter, P. C.; Coleman, M. M. *Macromolecules* **1986**, *19*, 699.

Slezak, F. B.; Stallings, J. P.; Wagner, D. H.; Wotiz, J. H. *J. Org. Chem.* **1961**, *26*, 3137.

Smith, D. W., Jr.; Wagener, K. B. *Macromolecules* **1991**, *24*, 6073.

Smith, D. W., Jr.; Wagener, K. B. *Macromolecules* **1993**, *26*, 3533.

Smith, J. A.; Brzezinska, K. R.; Valenti, D. J.; Wagener, K. B. *Macromolecules* **2000**, *33*, 3781.

Smith, M. B.; March, J. *March's Advanced Organic Chemistry: Reactions, Mechanism, and Structure*; 5th ed.; John Wiley & Sons: New York, 2001.

Smith, P. A. S. The Curtius Reaction. In *Organic Reactions*; Adams, R., Ed.; John Wiley & Sons: New York, 1942; Vol. 3.

Song, K.; Krimm, S. *J. Polym. Sci., Part B: Polym. Phys.* **1990**, *28*, 63.

Statton, W. O.; Geil, P. H. *J. Appl. Polym. Sci.* **1960**, *3*, 357.

Stolov, A. A.; Borisover, M. D.; Solomonov, B. N. *J. Phys. Org. Chem.* **1996**, *9*, 241.

Strobl, G. R. *Eur. Phys. J. E* **2000**, *3*, 165.

Strobl, G. R. *The Physics of Polymers: Concepts for Understanding Their Structure and Behavior*; 2nd ed.; Springer: Berlin, 1997.

Subirana, J. A.; Aceituno, J. E. *Macromol. Symp.* **1996**, *102*, 317.

Sugeta, H.; Go, A.; Miyazawa, T. *Chem. Lett.* **1972**, 83.

Tashiro, K.; Sasaki, S.; Kobayashi, M. *Macromolecules* **1996**, *29*, 7460.

Thakkar, S. M.; Deshmukh, V. K.; Saoji, A. N.; Duragkar, N. J. *J. Indian Chem. Soc.* **1986**, *63*, 619.

Toda, A. *Polymer* **1991**, *32*, 771.

Trifan, D. S.; Terenzi, J. F. *J. Polym. Sci.* **1958**, *28*, 443.

Tsubomura, H. *J. Chem. Phys.* **1956**, *24*, 927.

Tsuruda, M.; Arimoto, H.; Ishibashi, M. *Chem. High Polym. (Japan)* **1958**, *15*, 619.

Twitchett, H. J. *Chem. Soc. Rev.* **1974**, *3*, 209.

Ulman, A. *Chem. Rev.* **1996**, *96*, 1533.

Ulrich, H.; Sayigh, A. A. R. *Angew. Chem.* **1966**, *78*, 761.

Ungar, G.; Zeng, K. B. *Chem. Rev.* **2001**, *101*, 4157.

Upjohn Company. U.S. Patent 3,410,887, 1965.

Valenti, D. J.; Wagener, K. B. *Macromolecules* **1998**, *31*, 2764.

Veda, S.; Kimura, T. *Chem. High Polym. (Japan)* **1958**, *15*, 243.

Vogelsong, D. C. *J. Polym. Sci., Part A* **1963**, *1*, 1055.

Wagener, K. B.; Patton, J. T.; Boncella, J. M. *Macromolecules* **1992**, *25*, 3862.

Wagener, K. B.; Patton, J. T. *Macromolecules* **1993**, *26*, 249.

Wagener, K. B.; Tao, D. *Macromolecules* **1994**, *28*, 1281.

Wagener, K. B.; Valenti, D. J.; Hahn, S. F. *Macromolecules* **1997**, *30*, 6688.

Wang, J.; Parkhe, A. D.; Tirrell, D. A.; Thompson, L. K. *Macromolecules* **1996**, *29*, 1548.

Wang, Y. K.; Shu, P. H. C.; Stein, R. S.; Hsu, S. L. *J. Polym. Sci., Part B: Polym. Phys.* **1980**, *18*, 2287.

Weissbuch, I.; Lahav, M.; Leiserowitz, L.; Lederer, K.; Godt, A.; Wegner, G.; Howes, P. B.; Kjaer, K.; Als-Nielsen, J. *J. Phys. Chem.* **1998**, *102*, 6313.

White, E. V.; Tsuboyama, S.; McCloskey, J. A. *J. Am. Chem. Soc.* **1971**, *92*, 6340.

Williams, D. H.; Westwell, M. S. *Chem. Rev.* **1998**, *27*, 57.

Winningham, M. J.; Sogah, D. Y. *Polym. Mater. Sci. Eng.* **1997**, *76*, 156.

Wittbecker, E. L.; Katz, M. *J. Polym. Sci.* **1959**, *20*, 367.

Wittbecker, E. L.; Morgan, P. W. *J. Polym. Sci.* **1959**, *40*, 289.

Wittmann, J. C.; Lotz, B. *J. Polym. Sci., Part B: Polym. Phys.* **1985**, *23*, 205.

Wunderlich, B. *Crystal Melting*; Academic: New York, 1980; Vol. 3.

Wunderlich, B. *Crystal Nucleation, Growth, Annealing*; Academic: New York, 1976; Vol. 2.

Wunderlich, B. *Crystal Structure, Morphology, Defects*; Academic: New York, 1973; Vol. 1.

Wunderlich, B.; Mellilo, J. *Macromol. Chem.* **1968**, *118*, 250.

Wunderlich, B.; Poland, D. *J. Polym. Sci., Part A* **1963**, *1*, 357.

Yasuniwa, F.; Enoshito, R.; Takemura, T. *Jpn. J. Appl. Phys.* **1970**, *15*, 142.

Young, R. J.; Lovell, P. A. *Introduction to Polymers*; 2nd ed.; Chapman & Hall: London, 1991.

Zahn, H.; Kohler, K. *Kolloid-Z.* **1950**, *118*, 115.

Zahn, H.; Winter, V. *Kolloid-Z.* **1952**, *128*, 142.

Ziabicki, A.; Kedzierska, A. *J. Appl. Polym. Sci.* **1959**, *2*, 14.

Ziabicki, A. *Kolloid-Z.* **1960**, *167*, 132.